

Characterization of Acyltransferases in Neutral Lipid Synthesis

Dissertation

for the award of the degree

“Doctor rerum naturalium”

of the Georg-August-Universität Göttingen

within the doctoral program

“Microbiology and Biochemistry”

of the Georg-August University School of Science (GAUSS)

submitted by

Katharina Vollheyde

from Salzgitter (Germany)

Göttingen 2020

Thesis Committee

Prof. Dr. Ivo Feußner, Department for Plant Biochemistry, Albrecht-von-Haller Institute for Plant Science, University of Göttingen

Prof. Dr. Ralf Ficner, Department for Molecular Structural Biology, Institute for Microbiology and Genetics, University of Göttingen

Prof. Dr. Andrea Polle, Department of Forest Botany and Tree Physiology, Buesgen Institute, University of Göttingen

Members of the Examination Board

Referee: Prof. Dr. Ivo Feußner, Department for Plant Biochemistry, Albrecht-von-Haller Institute for Plant Science, University of Göttingen

2nd Referee: Prof. Dr. Ralf Ficner, Department for Molecular Structural Biology, Institute for Microbiology and Genetics, University of Göttingen

Further Members of the Examination Board

PD Dr. Till Ischebeck, Department for Plant Biochemistry, Albrecht-von-Haller Institute for Plant Science, University of Göttingen

Prof. Dr. Christiane Gatz, Department for Plant Molecular Biology and Physiology, Schwann-Schleiden-Research-Center for Molecular Cellbiology, University of Göttingen

PD Dr. Thomas Teichmann, Department of Plant Cell Biology, Schwann-Schleiden-Research-Center for Molecular Cellbiology, University of Göttingen

Date of oral examination: 17.12.2020

AFFIDAVIT

I hereby confirm that I have written the dissertation “Characterization of acyltransferases in neutral lipid synthesis” on my own and that I have not used other sources than those that have been specified.

Katharina Vollheyde, Göttingen 2020

TABLE OF CONTENTS

ABSTRACT	1
1 INTRODUCTION	3
1.1 WE properties and characteristics	3
1.2 WE in nature.....	5
1.3 WE in industry	6
1.4 WE biosynthesis in plants.....	6
1.5 WE biosynthesis in bacteria	10
1.6 Fatty alcohol synthesizing enzymes (FAR).....	11
1.6.1 Arabidopsis FAR.....	12
1.6.2 Marinobacter FAR.....	13
1.7 WE synthesizing enzymes (WSD)	14
1.7.1 <i>A. baylyi</i> WSD1	17
1.7.2 <i>Marinobacter</i> WSD1	19
1.7.3 <i>Marinobacter</i> WSD2	21
1.7.4 <i>Marinobacter</i> WSD5	22
1.8 WE production in transgenic plants: current achievements.....	22
1.9 Thesis objectives.....	26
2 ARTICLE I	28
2.1 The Fifth WS/DGAT Enzyme of the Bacterium <i>Marinobacter aquaeolei</i> VT8	28
2.2 Additional work to manuscript Article I	52
3 ARTICLE II	55
3.1 The crystal structure of the bifunctional wax synthase 1 from <i>Acinetobacter baylyi</i> (AbWSD1) reveals a conformational change upon substrate binding.....	55
3.2 Additional work to manuscript Article II	121
4 ARTICLE III	127
4.1 Plastidial localized wax ester biosynthesis results in the formation of shorter and more saturated wax esters	127
5 DISCUSSION	155
5.1 Overview about results obtained in this work	155
5.2 WS(D) catalyze a repertoire of diverse acyl transfer reactions.....	156
5.3 WS(D) crystal structures as a basis to improve and design enzymes.....	159
5.3.1 Change of substrate specificities.....	160
5.3.2 Change in enzymatic activity	161
5.3.3 Change in localization.....	164

5.3.4 WSD structures as a general WS concept?.....	165
5.4 Influence of substrate availability on WE formation.....	166
5.4.1 The role of promoter choice on substrate availability	166
5.4.2 The role of metabolic regulation and fatty acid export on substrate availability.....	168
5.5 Influence of WE storage on WE accumulation.....	169
5.5.1 The influence of WE packing on WE accumulation.....	170
5.5.2 The influence of WSD localization on WE accumulation.....	172
5.6 Future strategies for transgenic WE production: summary, conclusions and open research questions	173
REFERENCES	176
ACKNOWLEDGEMENTS	186
CURRICULUM VITAE	189

ABSTRACT

Wax ester (WE) are neutral lipids, which consist of a fatty acid and a fatty alcohol moiety connected by an ester bond. WE are synthesized via two reactions from acyl-coenzyme A (CoA)/acyl carrier protein (ACP) substrates. In a first step, fatty acyl reductases (FAR) reduce acyl-CoA/ACP to form fatty alcohols. In the second step, fatty alcohols are esterified to another acyl-CoA/ACP by wax synthases (WS) to yield WE. Reflecting the diversity of acyl-chain substrates, a huge variety of WE exist in nature. Dependent on the chain length and further modifications such as desaturation of the acid and alcohol moieties, WE have diverse physicochemical properties, supporting their various functions in nature. WE may be deposited in the plant cuticle or on the human skin as protection agents and accumulate in bacteria and seeds of the desert shrub jojoba as carbon storage compounds. Due to their diverse properties, WE are used in various industrial applications. They are part of cosmetics, lubricants or candles. Until the banning of whale hunting, industrially used WE were obtained from spermaceti oil. Nowadays, WE are expensively extracted from jojoba seeds or are synthesized chemically from fossil fuels or plant oils. Attempts to cost-efficiently and environmentally-friendly synthesize tailor-made WE in suitable crop plants are made. However, further improvements regarding enzyme use, substrate availability and storage capacities of the sink tissue are necessary.

With the aim to improve tailor-made WE production in plants in terms of enzyme use and substrate availability, three main projects were conducted within this thesis. The first project dealt with the characterization of the fifth WS/acyl-CoA:diacylglycerol acyl transferase (WSD) from the bacterium *Marinobacter aquaeolei* (MaWSD5). Experiments revealed that the enzyme is a suitable candidate for WE production in plants. *In vitro* substrate specificity assays showed a broad substrate range of the enzyme and confirmed the lack of a side reaction towards TAG formation. Expression in *Arabidopsis thaliana* seeds together with a FAR from the same bacterium resulted in the production of WE consisting of long chain monoenoic moieties.

In the second project, a detailed structure-function analysis on the basis of the recently obtained crystal structure of WSD1 from the bacterium *Acinetobacter baylyi* (AbWSD1) was conducted. The identification of the diacylglycerol binding site and potential CoA binding residues provide now a basis for future protein engineering in order to generate WE producing enzymes with altered substrate specificities. A comparison of the AbWSD1 structure, co-crystallized with bound myristic acid, and the structure of WSD1 from *Marinobacter aquaeolei* revealed a structural rearrangement upon substrate binding and lead to the development of a substrate-binding model for WSD.

In the third project, the effect of cellular WE biosynthesis location was studied and a change in localization was established as a suitable tool to alter substrate availability in WE producing plants. Expression of different constructs consisting of FAR, WSD2 or WSD5 from *Marinobacter aquaeolei* with and without plastidial localization tag in *A. thaliana* seeds resulted in the formation of shorter and more saturated WE in plastids compared to cytosolic WE synthesis.

1 INTRODUCTION

Wax ester (WE) belong to the class of neutral lipids as triacylglycerols (TAG) also do. They are formed by the esterification of a fatty alcohol to a fatty acid (Patel *et al.*, 2001). Dependent on the fatty acid and fatty alcohol moieties, WE have diverse physicochemical properties including melting temperature and oxidation stability (Hagemann & Rothfus, 1979; Patel *et al.*, 2001). Given their diverse properties, WE occur in organisms distributed over the whole tree of life fulfilling different functions. As protection agents, they are located on our skin or are part of the plants cuticle (Jacobsen *et al.*, 1985; Samuels *et al.*, 2008). They are found as carbon storage compounds in bacteria and the slow-growing desert shrub jojoba (*Simmondsia chinensis*) (Miwa, 1971; Fixter *et al.*, 1986). Additionally, they are used as structural components in honeycombs or are discussed to be needed for buoyancy in sperm whale (Clarke, 1970; Aichholz & Lorbeer, 2000; Miller *et al.*, 2004).

Due to their diverse physicochemical properties and application spectra, WE attracted attention in industry as well. Nowadays, WE are used in cosmetics, as candles, coatings packaging and lubricants (Wei, 2012; Vanhercke *et al.*, 2013). Before banning of whale hunting in 1986, large amounts of WE were obtained from spermaceti oil (Rowland & Domergue, 2012; Vanhercke *et al.*, 2013). Today, WE are either synthesized chemically from fossil fuel or plant-derived TAG or are expensively extracted from jojoba seeds or carnauba leaves (Hills, 2003; Al-Obaidi *et al.*, 2017; de Freitas *et al.*, 2019). In order to develop a suitable and cost-efficient alternative, attempts to establish tailor-made WE biosynthesis in feasible crop plants are made (Iven *et al.*, 2016; Zhu *et al.*, 2016; Ivarson *et al.*, 2017; Ruiz-Lopez *et al.*, 2017; Yu *et al.*, 2018). To achieve this, it is important to understand WE biosynthesis in detail, including all enzymes involved, their structural requirements as well as the surrounding metabolic network including the available substrate pool provided by the chosen host plant.

1.1 WE properties and characteristics

WE are obtained by the esterification of fatty alcohols to fatty acids. Conventional nomenclature describes WE by their fatty alcohol and fatty acid moieties (alcohol moiety/acid moiety) (Figure 1.1). Fatty alcohols and fatty acids are further characterized by the number of carbon atoms and the number of double bonds they contain (number carbon atoms:number double bonds). Hence, a WE named 16:0/18:1, consists of a saturated 16 carbon long alcohol moiety and a 18 carbon long acid part with one double bond. Reflecting the diversity of fatty alcohols and fatty acids in nature or industrially produced, a huge number of different WE exists. Dependent on the length as well as the desaturation degree of the acyl and alcohol

moieties, WE can have diverse physical and chemical properties, which influence their biological function and range of application.

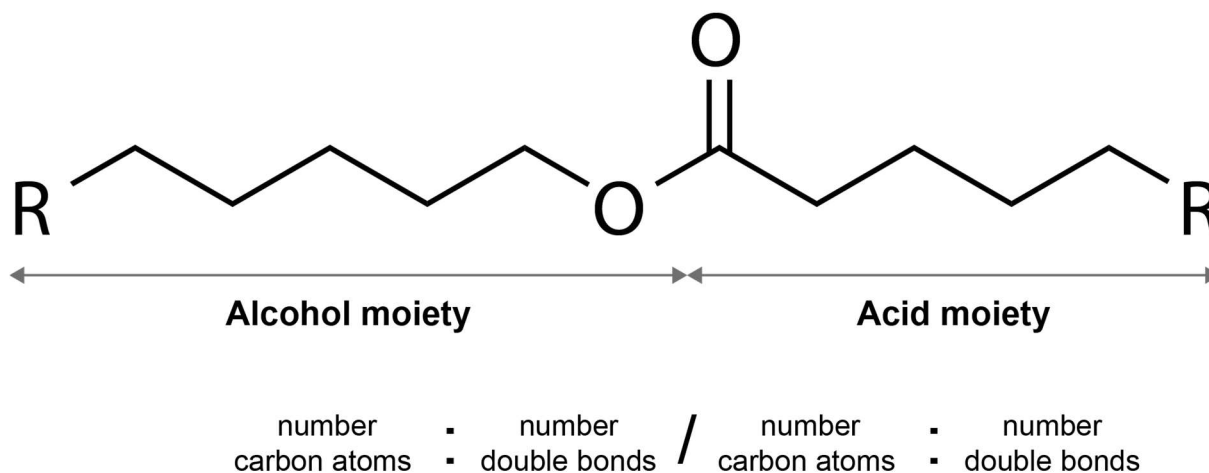


Figure 1.1. WE structure and nomenclature.

WE are formed upon the esterification of a fatty alcohol to a fatty acid. The conventional nomenclature describes WE by the alcohol and acid moiety. Both moieties are further typified by the number of carbon atoms and double bonds.

The biological functions or industrial applications of WE are highly affected by melting temperatures, as they determine the aggregate state of WE. The aggregate state of a substance at a certain temperature is the result of the packing of its molecules and the interaction strength between them. Irregular molecule packing, e.g. caused by double bonds in acyl chains that lead to the formation of kinks in the chain, results in lower melting points. Patel *et al.* (2001) conducted a comprehensive study on the influence of straight chain fatty alcohols and fatty acids on melting temperatures of different WE. The authors showed, that the melting temperature of WE is influenced by the total number of carbon atoms, the desaturation degree as well as the position of the ester bond. Melting temperatures of saturated WE decrease with decreasing numbers of carbon atoms. A reduction of one carbon atom results in a decrease of 1-2 °C. The presence of double bonds reduces the melting temperature as well. Interestingly, the authors observed, that desaturation at the alcohol moiety has a larger influence on the melting temperature than desaturation of the acid moiety. Whereas 18:0/18:1 melts at around 35 °C, 18:1/18:0 already becomes liquid at around 25 °C. An additive effect was observed by the authors upon introduction of double bonds on both moieties. Differences in melting temperature of 1-5 °C were detected by Patel *et al.* (2001) upon changes of the ester bond position in analyzed WE species with the same number of carbons. Highest melting temperatures were measured for symmetric WE, which consist of alcohol and acid moieties with the same chain lengths. Upon moving of the ester bond towards the methyl ends of either the alcohol or the acid moieties, melting temperatures decreased.

This is different to what was observed for double bonds and methyl branches. Melting temperatures decrease for phospholipids with double bonds at more internal positions (Stubbs & Smith, 1984). Likewise, lower melting temperatures are observed for hydrocarbons with methyl groups at more central positions (Gibbs, 1995).

Apart from suitable melting temperatures, high oxidation stability is especially for industrially used WE an important quality criterion. Double bonds present in WE are potential points for oxidation events (Hagemann & Rothfus, 1979). Oxidation of acyl and alcohol moieties of WE cannot only change the physicochemical properties of WE and with this their suitability for certain applications, but can also lead to degradation of the WE molecules.

1.2 WE in nature

WE are ubiquitously found in all kind of species, ranging from bacteria to plants and mammals. Given their diverse properties, WE fulfill different functions in nature. Two main functions of WE are protection and carbon storage.

In plants, WE are part of a physical barrier on the outside of leaves and stems. Together with other waxy compounds, WE help to protect the plants against desiccation, UV radiation and pathogen attack (Post-Beittenmiller, 1996; Samuels *et al.*, 2008). In humans, WE are secreted via sebaceous glands on the skin (Jacobsen *et al.*, 1985) and are also responsible for the evaporation retarding effect of the eye's tear film helping to reduce tear evaporation rates (Craig & Tomlinson, 1997; Rantamäki *et al.*, 2013).

Similar to TAG, WE are used as carbon storage compounds. For instance, WE accumulation was observed under nitrogen limiting conditions in *Acinetobacter* (Fixter *et al.*, 1986; Wältermann *et al.*, 2005). In this connection, WE do not only serve as carbon reservoir for conditions, when nitrogen is available again, but it is also speculated, that upon carbon chain oxidation WE degradation provides water for the cells under harsh conditions (Wältermann & Steinbuchel, 2005a). As energy reservoir for germination, the slow-growing desert shrub jojoba stores up to 50 % oil in its seeds, which consists mainly of WE (Miwa, 1971; Busson-Breyse *et al.*, 1994; Sturtevant *et al.*, 2020).

In conjunction with insects, WE are not only found on the insect's surface where they prevent water loss (Jackson & Baker, 1970; Nelson *et al.*, 2001), but WE are also used as structural components in honey combs of bees (Tulloch, 1970; Blomquist *et al.*, 1980; Aichholz & Lorbeer, 2000). An interesting function is assigned to WE in sperm whale. A 13 m long sperm whale stores about 1450 kg spermaceti oil, which is discussed to be important for buoyancy (Clarke, 1970; Miller *et al.*, 2004). The spermaceti oil is predominantly composed of WE and

lower amounts of TAG (Morris, 1973). Interestingly, ratios of WE and TAG vary upon different locations in the spermaceti organ.

1.3 WE in industry

We encounter WE in our daily life. They are e.g. part of candles, coatings, packaging and cosmetics and are used as lubricants (Wei, 2012; Vanhercke *et al.*, 2013). In former times, WE were obtained from the spermaceti organs of sperm whale. As stated above, sperm whales contain large amounts of WE in their spermaceti oil (Morris, 1973). Due to its excellent properties, sperm whale WE were extensively used as high-pressure and high-temperature lubricant (Vanhercke *et al.*, 2013). Their extensive hunting and nearly extinction lead to a banning of whale hunting in 1986. Since then, most WE are generated either chemically from fossil fuel or from fatty acids of plant-derived TAG (Hills, 2003). As jojoba accumulates also large amounts of WE in its seeds, it became a natural provider for industrial used WE (Al-Obaidi *et al.*, 2017). Nevertheless, jojoba is a slow-growing desert shrub, which is not easy to cultivate (Al-Obaidi *et al.*, 2017), and accumulates WE with 36-46 carbons in chain length, which are longer than those of sperm whale, which only have 25-38 carbons in chain length (Challinor *et al.*, 1969; Tada *et al.*, 2014). Due to that, jojoba WE are comparably expensive and have different physicochemical properties and are therefore mostly used in cosmetics. Other natural WE providers are bee wax and carnauba palm (*Copernicia prunifera*) (Tada *et al.*, 2014). Carnauba wax has the highest melting point of commercially used natural waxes (de Freitas *et al.*, 2019). It contains WE of 50-62 carbons chain length and is widely used in food industry e.g. as glazing agent, acidity regulator, anticaking agent and carrier agent (Tada *et al.*, 2014; de Freitas *et al.*, 2019). Due to its shiny properties, it is also used for polishes, car waxes and as additives in cosmetics (Rowland & Domergue, 2012).

Besides their industrial usage as whole molecules, WE can also serve as fatty acid provider and feedstock for other chemical compounds (Vanhercke *et al.*, 2013). Compared to TAG, WE have the advantage to not contain a glycerol backbone and can be used therefore completely after hydrolysis of the ester bond. Obtained monounsaturated fatty acids can then either be used directly due to their comparatively high oxidation stabilities or can be cleaved at their double bonds to generate smaller compounds demanded in industry.

1.4 WE biosynthesis in plants

In plants, WE are found mostly outside the cell in the cuticle to protect plants from desiccation, UV radiation or pathogen attack (Post-Beittenmiller, 1996; Samuels *et al.*, 2008). However,

jojoba uses WE additionally as storage compounds in its seeds (Miwa, 1971). In this case, WE are stored within the cell in lipid droplets (Sturtevant *et al.*, 2020).

The two building blocks of WE are acyl-coenzyme A (CoA)/acyl carrier protein (ACP) and fatty alcohols. As fatty alcohols are synthesized from acyl-CoA/ACP by the reduction of the carboxyl group, acyl-CoA/ACP are the overall precursors of WE. In plants, acyl-CoA/ACP are synthesized by *de novo* fatty acid synthesis (Ohlrogge & Jaworski, 1997; Hölzl & Dörmann, 2019). As Figure 1.2 depicts, two cellular compartments are involved in this biosynthetic pathway. In plastids, fatty acids of mainly 16 and 18 carbons chain length are synthesized from acetyl-CoA in successive rounds of reactions adding C2 units to a growing acyl chain. Exported from plastids, endoplasmic reticulum (ER)-localized enzymes elongate and modify fatty acids in form of acyl-CoA derivatives or glycerolipid bound.

The first and highly regulated step in fatty acid synthesis is the formation of malonyl-CoA from acetyl-CoA and CO₂, in form of hydrogen carbonate. The reaction is catalyzed by the membrane associated multi subunit acetyl-CoA carboxylase (ACCase) (Alban *et al.*, 1994; Konishi *et al.*, 1996; Roesler *et al.*, 1996). Subsequent to this, the CoA group of malonyl-CoA is exchanged to ACP by malonyl-CoA:ACP transacylase yielding malonyl-ACP, the actual molecule required for the transfer of C2 units to the growing fatty acid chains. As C-C bond formations are energetically not favorable, the condensation reactions are driven by CO₂ release when malonyl-ACP reacts with acyl-ACP. Four consecutive reaction steps repeated in successive rounds enable the elongation of acyl chains. In the first step, malonyl-ACP reacts with acyl-ACP of diverse chain length to form 3-ketoacyl-ACP. The condensation reaction, catalyzed by 3-ketoacyl-ACP synthase (KAS), transfers two carbon units to the carboxyl terminus of the increasing acyl chain. Subsequently, the keto group present at the C3 atom of 3-ketoacyl-ACP is reduced to a hydroxyl group by 3-ketoacyl-ACP reductase. A dehydration of the formed 3-hydroxyacyl-ACP by 3-hydroxyacyl-ACP dehydratase yields trans- Δ^2 -enoyl-ACP, which is further reduced to acyl-ACP by 2,3-trans-enoyl-ACP reductase during the fourth and last reaction step. The KAS enzymes, catalyzing the condensation of C2 units on elongating acyl chains, are chain length specific regarding the acyl-ACP substrate. Plastids harbor three different KAS enzymes: KAS III is specific for the reaction of malonyl-ACP with acetyl-CoA, which is the first condensation reaction in fatty acid biosynthesis and yields 4:0 ACP (Clough *et al.*, 1992; Jaworski *et al.*, 1993). KAS I catalyzes the following condensation reactions obtaining up to 16:0 ACP and KAS II is specific for 16:0 ACP and catalyzes the condensation to form 18:0 ACP (Shimakata & Stumpf, 1982).

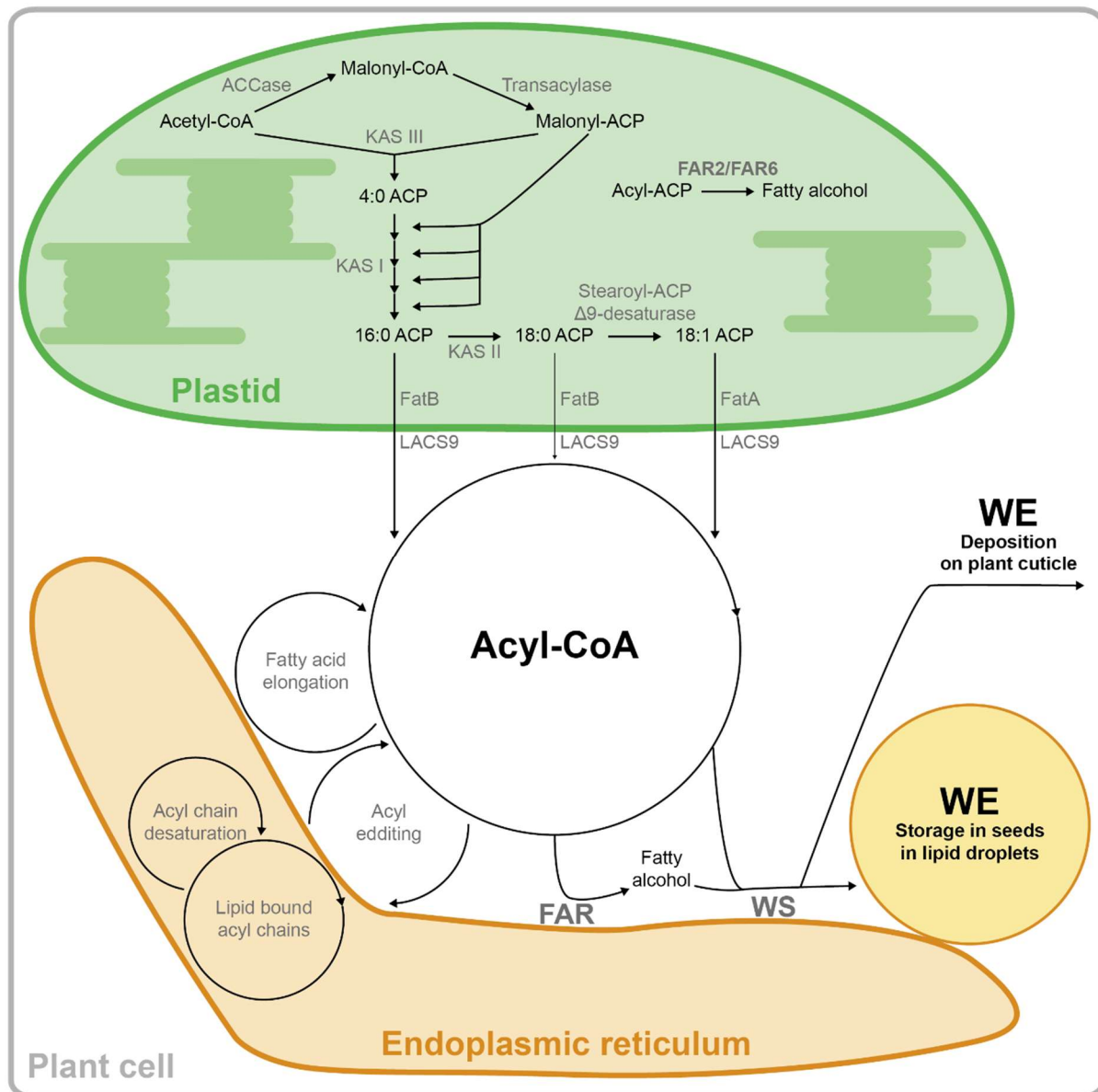


Figure 1.2. WE biosynthesis in plants.

WE biosynthesis in plants takes place in two cellular compartments. Long chain fatty acids are synthesized via *de novo* fatty acid synthesis in plastids. They enter as CoA derivatives the cytosolic acyl-CoA pool. Endoplasmic reticulum-localized enzymes introduce further modifications such as elongation directly on the acyl chains of acyl-CoA or such as desaturation on glycerolipid bound fatty acids, which are connected with the acyl-CoA pool via acyl editing reactions. In order to synthesize WE for deposition in the plant cuticle or in seeds as storage molecules in lipid droplets, fatty acyl-CoA reductases (FAR) enzymes catalyze the formation of fatty alcohols, which are subsequently esterified to activated fatty acids by wax synthases (WS) to form WE. Enzymes or enzyme catalyzed reaction steps are depicted in grey. CoA: coenzyme A, ACP: acyl carrier protein, ACCase: acetyl-CoA carboxylase, KAS: 3-ketoacyl-ACP synthase, FatA/FatB: acyl-ACP thioesterase, LACS: long-chain acyl-CoA synthetase, FAR: fatty acyl-CoA reductase, WS: wax synthase, WE: wax ester.

Termination of fatty acid biosynthesis is influenced by diverse reactions acting on synthesized acyl-ACP, such as transesterification of acyl moieties to glycerolipids, desaturation of acyl-ACP or hydrolysis of ACP from acyl chains inducing fatty acid export from plastids (Ohlrogge

& Jaworski, 1997). The desaturation of 18:0 ACP is catalyzed by the soluble stearyl-ACP Δ^9 -desaturase (Jacobson *et al.*, 1974; Shanklin & Somerville, 1991). The cleavage of ACP from acyl-ACP is achieved by the action of acyl-ACP thioesterases (Dörmann *et al.*, 1995; Jones *et al.*, 1995). The reaction yields fatty acids, which are subsequently exported from plastids. By the action of long-chain acyl-CoA synthetase (LACS) 9, which is located at the outer plastid envelope, the fatty acids are esterified to CoA and enter the cytosolic acyl-CoA pool (Jessen *et al.*, 2015). Plastidial thioesterases, inducing fatty acid export, are divided into two groups: FatA thioesterase is specific to 18:1 ACP (Dörmann *et al.*, 1995). Thioesterases of the FatB group act on saturated acyl-ACP and a FatB thioesterase mainly active on 16:0 ACP is ubiquitous in plants (Jones *et al.*, 1995). FatB thioesterases from diverse plants specific for medium chain acyl-ACP, enable an export of shorter chain fatty acids from the plastid, too (Pollard *et al.*, 1991; Davies, 1993; Dörmann *et al.*, 1993).

Plastidial *de novo* fatty acid synthesis yields mainly 16:0 ACP, 18:0 ACP and 18:1 ACP. Elongation of these fatty acids, as well as modifications, preferentially in form of desaturation are catalyzed by ER-localized enzymes (Hölzl & Dörmann, 2019). Elongation of fatty acids by ER membrane enzymes is similar to plastidial fatty acid elongation and achieved by the four above described reaction steps, too. However, acyl intermediates and malonate are bound to CoA instead of ACP. Desaturation of fatty acids occurs on lipid-bound acyl chains. Diverse acyl editing reactions facilitate a constant exchange of acyl chains between several lipid-bound acyl pools and the cytosolic acyl-CoA as well as the plastidial acyl-ACP pool. Acyl-CoA desaturase-like (ADS) enzymes are discussed to desaturate acyl-CoA directly (Smith *et al.*, 2013).

Fatty acids in form of acyl-CoA/ACP are precursors for diverse lipids such as glycerolipids, which are synthesized by the esterification of acyl chains to a glycerol backbone and include membrane-forming phospholipids or the storage lipid TAG, or such as WE, which are obtained upon the esterification of an acyl chain to a fatty alcohol. In plants, WE formation for cuticular WE takes place in epidermis cells (Kunst & Samuels, 2003). Via the acyl reduction pathway, the carboxyl groups of activated very long chain fatty acids are reduced by fatty acyl-CoA reductases (FAR) to form primary alcohols (Vioque & Kolattukudy, 1997). Wax synthases (WS) catalyze the esterification of fatty alcohols to activated long chain fatty acids to yield WE, which are transported to the cuticle (Li *et al.*, 2008). WE formation in jojoba seeds takes place through a similar pathway (Lardizabal *et al.*, 2000; Metz *et al.*, 2000), resulting in the accumulation of mainly WE in seed oil consisting of 36-46 carbon chain length that is deposited in lipid droplets in the cytosol (Miwa, 1971; Busson-Breyse *et al.*, 1994; Tada *et al.*, 2014; Sturtevant *et al.*, 2020).

1.5 WE biosynthesis in bacteria

Most bacteria use polyhydroxyalkanoates as energy storage compounds, nevertheless, some species accumulate TAG and WE (Wältermann & Steinbuchel, 2005a). WE as storage compounds were detected in several genera (Wältermann & Steinbuchel, 2005b) e.g. in *Acinetobacter* (Gallagher, 1971; Fixter & Fewson, 1974; Fixter & McCormack, 1976; Scott & Finnerty, 1976), *Moraxella* (Bryn *et al.*, 1977), *Micrococcus* (Russell & Volkman, 1980), *Fundibacter* (Bredemeier *et al.*, 2003), *Corynebacterium* (Bacchin *et al.*, 1974), *Mycobacterium* (Wang *et al.*, 1972), *Nocardia* (Raymond & Davis, 1960) and *Marinobacter* (Rontani *et al.*, 1999; Holtzapple & Schmidt-Dannert, 2007). Whereas WE in plants are mostly synthesized and deposited to build a protection barrier or to form a carbon reservoir for the development of the next generation, bacteria store WE under environmentally unfavorable conditions. WE accumulation was observed in *Acinetobacter* and in *Marinobacter* under nitrogen limiting growth conditions (Fixter *et al.*, 1986; Wältermann *et al.*, 2005; Barney *et al.*, 2012). Under these conditions, carbon is stored in form of neutral lipids, until nitrogen is available again for the formation of biomolecules.

The two WE building blocks, activated fatty acids and fatty alcohols, can be synthesized in bacteria from various carbon sources (Alvarez, 2016). From carbon sources, which can be used to generate acetyl-CoA, acyl-CoA can be synthesized by successive rounds of *de novo* fatty acid synthesis and fatty alcohols can be generated by the reduction of acyl-CoA or acyl-ACP as described for plants (see above) (Alvarez, 2016). Besides that, bacteria can also produce WE when grown on hydrocarbons, n-alkanols, fatty acids and phytol derivatives as carbon source (Rontani, 2010). WE production is described from related carbon sources such as n-alkanes (Ishige *et al.*, 2002), phytane (Silva *et al.*, 2007), squalene (Rontani *et al.*, 2003), oleic acid (Kaneshiro *et al.*, 1996) and phytol (Rontani *et al.*, 1999). Upon diverse oxidation and/or reduction reactions, terminal carboxyl and hydroxyl functional groups can be introduced into the different carbon backbones or carboxyl and hydroxyl groups can be converted into each other. Successive rounds of β -oxidation allow additionally chain length shortening of the precursors.

As in other organisms, WE formation in bacteria is only possible, when the organism encodes a WS. WS found in bacteria belong to the class of bifunctional WS/acyl-CoA:diacylglycerol acyltransferases (WS/DGAT, WSD) (see below). The term bifunctional indicates the ability of several WSD enzymes to not only catalyze the formation of WE, but also the production of TAG from diacylglycerol (DAG) and acyl-CoA/ACP (Kalscheuer & Steinbüchel, 2003; Daniel *et al.*, 2004; Holtzapple & Schmidt-Dannert, 2007; Kalscheuer *et al.*, 2007; Alvarez *et al.*, 2008; Kaddor *et al.*, 2009; Lázaro *et al.*, 2017; Zhang *et al.*, 2017; Petronikolou & Nair, 2018). This

ability is discussed to allow the bacteria to accumulate different neutral lipids depending on available carbon sources (Alvarez, 2016).

WE are stored in bacterial cells in lipid inclusions similar to lipid droplets described for plant cells. These lipid inclusions were found in diverse shapes. *Acinetobacter baylyi* ADP1 accumulates WE in spherical inclusions (Wältermann & Steinbuchel, 2005a). In *Acinetobacter* sp. strain HO1-N, WE are stored in small rectangular inclusions (Singer *et al.*, 1985) and in *Acinetobacter* sp. strain M1, WE inclusions have the form of disc-shaped structures (Ishige *et al.*, 2002). In contrast to lipid droplet formation described in plants, WE inclusions are not formed upon the accumulation of neutral lipids between the two phospholipid leaflets of a bilayer membrane, but their biogenesis is proposed to happen in a membrane associated manner (Wältermann *et al.*, 2005). Wältermann *et al.* (2005) could show that WE biosynthesis takes place at the cytoplasmic side of the plasma membrane in *A. baylyi* ADP1. The authors proposed the following model for the neutral lipid inclusion formation in this bacterium: WSD associate with the plasma membrane and synthesize WE, which accumulate in small lipid droplets. Several of WSD associated small lipid droplets form an oleogenous layer at the plasma membrane and start to conglomerate. Conglomerated small lipid droplets are released to the cytosol as a lipid-prebody with a phospholipid monolayer. Upon coalescence of the small lipid droplets, mature lipid droplets arise.

1.6 Fatty alcohol synthesizing enzymes (FAR)

FAR catalyze the formation of fatty alcohols upon the reduction of acyl substrates (Rowland & Domergue, 2012). Fatty alcohols can be either synthesized from activated fatty acids (acyl-CoA or acyl-ACP) via a four-electron-reaction and an aldehyde intermediate or from fatty aldehydes via a two-electron-reaction (Figure 1.3). Dependent on the enzyme, nicotinamide adenine dinucleotide (NADH) or NADH phosphate (NADPH) provides the electrons necessary for the reaction.

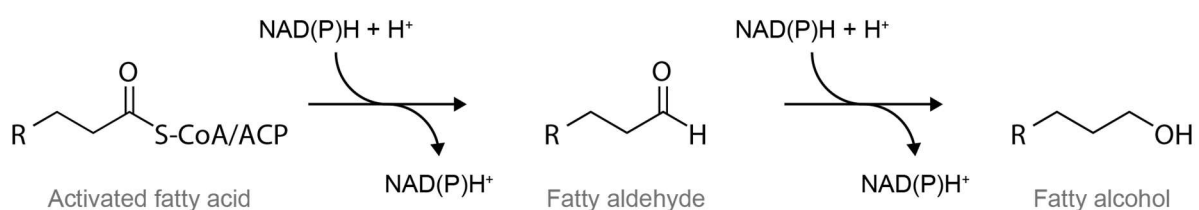


Figure 1.3. FAR reaction.

The reduction of activated fatty acids to fatty aldehydes and further to fatty alcohols is catalyzed by FAR enzymes. Each reduction step requires two electrons provided by NAD(P)H (nicotinamide adenine dinucleotide phosphate).

Proteins belonging to the fatty acyl-CoA reductase family (the term acyl-CoA is misleading here, as some members of this family can also use acyl-ACP as substrates) have two conserved domains (Rowland & Domergue, 2012): At the N-terminus a conserved Rossman fold is located, which harbors the NAD(P)H binding motif. The C-terminus is formed by the fatty acyl-CoA reductase (FAR_C) domain, which is also known as sterile or male sterile domain due to its identification in the *A. thaliana* enzyme MALE STERILITY 2 (AtFAR2) (Aarts *et al.*, 1993).

The purification and cloning of the *S. chinensis* FAR (ScFAR) in 2000 (Metz *et al.*, 2000) paved the way for the identification of related enzymes (Rowland & Domergue, 2012), e. g. eight FAR in *A. thaliana* (Aarts *et al.*, 1993; Aarts *et al.*, 1997; Rowland *et al.*, 2006; Doan *et al.*, 2009; Domergue *et al.*, 2010; Chen *et al.*, 2011), two mouse FAR (Cheng & Russell, 2004a) and two FAR in *Marinobacter aquaeolei* (Wahlen *et al.*, 2009; Hofvander *et al.*, 2011; Willis *et al.*, 2011).

1.6.1 Arabidopsis FAR

The genome of *A. thaliana* encodes eight FAR. *A. thaliana* FAR can be divided into groups of predicted ER-localized FAR (AtFAR1, AtFAR3, AtFAR4, AtFAR5, AtFAR7, AtFAR8), which are predicted to have transmembrane domains and plastid-localized FAR (AtFAR2, AtFAR6) which are not predicted to have transmembrane domains (Figure 1.2) (Rowland & Domergue, 2012).

AtFAR1, AtFAR4 and AtFAR5 were identified to be expressed in root endodermal cells (Domergue *et al.*, 2010). Upon deletion of either of the proteins, suberin composition in roots and seed coats changed, suggesting an involvement of the enzymes in suberin synthesis. AtFAR3, also well known as eceriferum (CER) 4, was found to be important for cuticular wax biosynthesis in stems and leaves (Rowland *et al.*, 2006). Fluorescence protein-tagged AtFAR3 expressed in yeast was found to localize to the ER.

AtFAR2 was first identified as MALE STERILITY 2 (Aarts *et al.*, 1993). Further analysis of the protein showed its involvement in male gametogenesis and its sequence similarity to a jojoba FAR (Aarts *et al.*, 1997). A detailed characterization of the enzyme revealed, that AtFAR2 is important for pollen wall development and that the protein localizes to plastids (Chen *et al.*, 2011). Purified protein showed high activity with 16:0 ACP and trace activity with 18:0 ACP. No activity was observed with 14:0 ACP, 16:1 ACP and 18:1 ACP. Acyl-CoA substrates are not accepted by the enzyme. The enzyme can use NADPH and NADH as cofactors, but shows higher activity with NADPH. AtFAR6 is the second *A. thaliana* FAR localizing to plastids (Doan *et al.*, 2009). In contrast to AtFAR2, AtFAR6 was found to use acyl-CoA and acyl-ACP as substrates. However, as cofactor only NADPH is accepted and no significant activity was

detected with NADH. The purified enzyme showed a strong preference for 16:0 CoA and a release of fatty aldehydes and free fatty acids could be observed in parallel to full reduction of the substrate yielding fatty alcohol.

1.6.2 *Marinobacter* FAR

M. aquaeolei possesses two enzymes capable to synthesize fatty alcohols from activated fatty acid substrates (Maqu_2220 and Maqu_2507) (Wahlen *et al.*, 2009; Hofvander *et al.*, 2011; Willis *et al.*, 2011). Both enzymes were found to be sufficient to synthesize fatty alcohols for WE biosynthesis in *M. aquaeolei* (Lenneman *et al.*, 2013). However, while Maqu_2507 was found to be expressed mainly during exponential growth and only to a lesser extent during WE accumulation, Maqu_2220 was found to be highly expressed under WE accumulating conditions and at lower levels during exponential growth (Lenneman *et al.*, 2013).

Maqu_2507 was identified and characterized in 2011 (Willis *et al.*, 2011). As the protein could be purified within two steps via 8x histidine (His)- and maltose binding protein (MBP)-tag, a detailed *in vitro* characterization of the protein was possible. The authors showed, that Maqu_2507 is able to catalyze the formation of fatty alcohols from acyl-CoA substrates in one step using NADPH as electron donor. As it was not possible to trap any fatty aldehyde intermediate, it was suggested, that it stays bound to the enzyme. Although no release of aldehyde intermediates could be detected, Maqu_2507 is able to synthesize fatty alcohols from acyl-CoA and fatty aldehydes, showing an even higher activity with the latter ones. The enzyme generates fatty alcohols from saturated and unsaturated acyl-CoA substrates ranging from 8 to 20 carbon chain length, favoring 16:0 CoA and 16:1 CoA. The protein furthermore is able to reduce saturated and unsaturated aldehydes ranging from 2 to 16 carbons in chain length preferring decanal and dodecanal. Using 16:0 CoA as substrate with increasing concentration, a sigmoidal curve was obtained suggesting allosterism or cooperativity.

Maqu_2220 was first described as a fatty aldehyde reductase (Wahlen *et al.*, 2009). The protein was identified upon BLAST search with the coding sequence of *A. thaliana* CER4/FAR3. A fusion to MBP-tag allowed the purification of the protein, which remained otherwise associated to cell debris. *In vitro* experiments revealed, that Maqu_2220 is able to catalyze the reduction of aldehydes to fatty alcohols in a NADPH dependent manner. The reduction of oleic acid was not detected and neither was the oxidation of fatty alcohols to fatty aldehydes. Maqu_2220 was found to use octanal, decanal, dodecanal and *cis*-11-hexadecenal as substrates. No apparent activity was detected in the study with butanal, hexanal and the aromatic benzaldehyde. The authors observed product inhibition by probing dodecanol. Inhibition was observed as well with dithionite, which, according to the authors, might indicate

the presence of an active site residue or cofactor prone to reduction. As only moderate inhibition was detected with two metal chelators, the authors suggested that transition metals, if present, are not easily accessible. A second characterization of Maqu_2220 was published in 2011, showing, that the enzyme is able to catalyze fatty alcohol formation from activated fatty acids, using acyl-CoA and acyl-ACP (Hofvander *et al.*, 2011). Purified enzyme produced fatty alcohols from 16:0 CoA, 18:0 CoA, 18:1 CoA, 20:0 CoA, 22:1 CoA, ricinoleoyl-CoA and 16:0 ACP. 18:1 CoA was clearly favored by the enzyme and alcohol production was slightly decreased using 16:0 ACP instead of 16:0 CoA as substrate in this study.

As only Maqu_2220 is important for the rest of this thesis, the protein is referred to as MaFAR from here on, as done by other publications as well.

1.7 WE synthesizing enzymes (WSD)

The formation of WE is catalyzed by WS. WS enzymes belong to the class of acyltransferases, which facilitate the transfer of acyl donors to appropriate acyl acceptors, carrying a free hydroxyl group (Röttig & Steinbüchel, 2013a). Dependent on their protein sequence and resembling their evolutionary origin, WS are divided into three classes (Röttig & Steinbüchel, 2013a): The first class of WS enzymes is formed by acyl-CoA:diacylglycerol acyltransferase (DGAT) 1-like WS. These proteins harbor six to nine transmembrane domains, which are distributed over the whole amino acid chain and share sequence homologies with DGAT1 proteins. The WS from *S. chinensis*, which is responsible for WE formation in jojoba seeds, is classified as DGAT1-like WS (Röttig & Steinbüchel, 2013a). The second group contains WS proteins of the group of DGAT2-like WS. WS of this group have one to two transmembrane domains at their N-terminus. The third group of WS consists of enzymes of bifunctional WSD proteins. This enzyme class was proposed in 2003 by the identification of a WS in the bacterium *A. baylyi* (AbWSD1) (Kalscheuer & Steinbüchel, 2003). As the amino acid sequence of the newly identified WS did not match with sequences of other published WS, it was proposed, that the protein is part of a new class of WS enzymes, named WSD. The term bifunctional, as well as the name affix DGAT, accounts for the ability of AbWSD1 to catalyze the formation of TAG from DAG and acyl-CoA/ACP in addition to the formation of WE from acyl-CoA/ACP and fatty alcohols (Figure 1.4a). Up to now, WSD enzymes were identified in several other bacteria (Daniel *et al.*, 2004; Holtzapple & Schmidt-Dannert, 2007; Kalscheuer *et al.*, 2007; Alvarez *et al.*, 2008; Arabolaza *et al.*, 2008; Kaddor *et al.*, 2009; Barney *et al.*, 2012; Shi *et al.*, 2012; Lázaro *et al.*, 2017; Zhang *et al.*, 2017), as well as in a few plants (King *et al.*, 2007; Li *et al.*, 2008; Shalini & Martin, 2020). Whereas several WSD were also characterized as bifunctional enzymes, being able to catalyze WE and TAG formation (Kalscheuer & Steinbüchel, 2003; Daniel *et al.*, 2004; Holtzapple & Schmidt-Dannert, 2007;

Kalscheuer *et al.*, 2007; Li *et al.*, 2008; Lázaro *et al.*, 2017; Zhang *et al.*, 2017; Petronikolou & Nair, 2018; Shalini & Martin, 2020), some WSD only harbor WS (Kalscheuer *et al.*, 2007; King *et al.*, 2007) and some only DGAT activity (Daniel *et al.*, 2004; Arabolaza *et al.*, 2008).

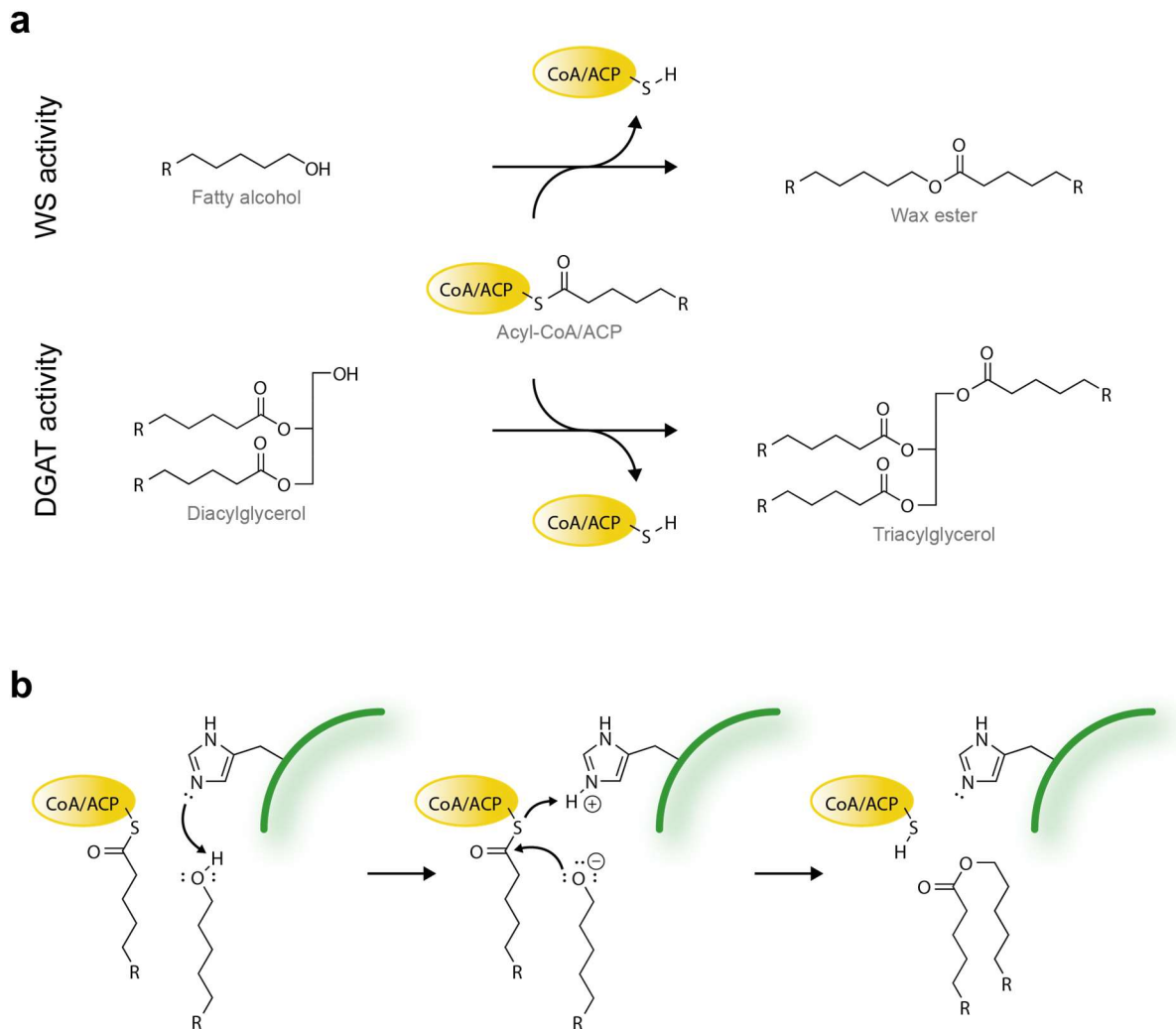


Figure 1.4. WSD reaction.

(a) Bifunctional WSD enzymes can catalyze the formation of WE from fatty alcohols and acyl-CoA/ACP (wax synthase (WS) activity) and they can further catalyze the formation of TAG from DAG and acyl-CoA/ACP (acyl-CoA:diacylglycerol acyltransferase (DGAT) activity). **(b)** The acyltransferase reaction is proposed to function via a catalytic active histidine (Stöveken *et al.*, 2009). The histidine abstracts the hydrogen from the hydroxyl group of the fatty alcohol. Subsequently, the negatively charged oxyanion attacks the thioester bond of the activated fatty acid. The thioester bond is cleaved upon the nucleophilic attack and a new oxoester bond is formed. Protonated CoA/ACP-SH and WE are released from the enzyme. CoA: coenzyme A, ACP: acyl carrier protein, WS: wax synthase, DGAT: acyl-CoA:diacylglycerol acyltransferase.

Besides AbWSD1, WSD from *Marinobacter* are extensively characterized, especially WSD of *M. aquaeolei* and *Marinobacter hydrocarbonoclasticus* (Holtzapple & Schmidt-Dannert, 2007; Barney *et al.*, 2012; Shi *et al.*, 2012; Villa *et al.*, 2014; Röttig *et al.*, 2015; Röttig *et al.*, 2016; Miklaszewska *et al.*, 2018; Petronikolou & Nair, 2018). A study from 2005 revealed, that both

species are the same, which should be classified under the same name as well (Márquez & Ventosa, 2005). Nevertheless, in research studies dealing with the characterization of WSD, both species names are still used and due to different isolation locations and different evolutionary events, that occurred in the genome of both strains, corresponding WSD proteins are not identical on the amino acid level (Röttig & Steinbüchel, 2013a). It should be noted, that the differentiation between *M. aquaeolei* and *M. hydrocarbonoclasticus* WSD will be also made in this thesis to allow an easier comparison with published research studies on WSD from both strains and to refer easier to differences in amino acid sequences of corresponding WSD from both strains if needed. Until now, four WSD enzymes are described in *M. hydrocarbonoclasticus* (MhWS1-4) (Holtzapfle & Schmidt-Dannert, 2007) and five in *M. aquaeolei* (MaWSD1-5) (Barney *et al.*, 2012; Yu, 2016; Knutson *et al.*, 2017).

Characteristic for WSD is a catalytic motif, consisting of two histidine residues, an aspartate and a glycine residue separated by three amino acids (HHxxxDG) (Kalscheuer & Steinbüchel, 2003). Amino acid substitutions of both histidines alone and together in AbWSD1 and MaWSD2 led to a reduction in enzymatic activity (Stöveken *et al.*, 2009; Villa *et al.*, 2014). As enzymatic activity was more reduced upon mutation of the second histidine and the position of the first histidine in the crystal structure of MaWSD1 indicated a rather structural role of the residue, the second histidine is proposed to be the catalytic active residue (Stöveken *et al.*, 2009; Villa *et al.*, 2014; Petronikolou & Nair, 2018). Stöveken *et al.* (2009) proposed a reaction mechanism for WSD enzymes based on the action of a histidine residue (Figure 1.4b). The catalytic active histidine abstracts the hydrogen of the hydroxyl group of the acyl acceptor. By this, a negatively charged oxyanion is generated, which attacks the carboxyl carbon of the thioester bond of the activated acyl donor. Upon the nucleophilic attack, the thioester bond is cleaved and a new oxoester bond is formed. The released CoA/ACP is protonated by the catalytic histidine to generate CoA/ACP-SH, which is released from the enzyme as the WE also is.

In order to get a deeper understanding of the function of WSD enzymes, several amino acid substitution studies were conducted within the last years (Stöveken *et al.*, 2009; Barney *et al.*, 2013; Röttig & Steinbüchel, 2013b; Villa *et al.*, 2014; Barney *et al.*, 2015; Petronikolou & Nair, 2018). A lack of a WSD crystal structure however, made it difficult to assign particular functions for structural integrity, substrate binding or catalysis to certain amino acids. In addition to mutations of the catalytic motif amino acids in AbWSD1 and MaWSD2 (Stöveken *et al.*, 2009; Villa *et al.*, 2014), Villa *et al.* (2014) generated and analyzed amino acid exchange mutants in MaWSD2 of residues of three other conserved WSD motifs (PLW, ND, R). Although reduced enzyme activities were observed for the mutated enzyme variants, it could only be speculated about certain roles assigned to the residues. Similar held true for amino acids of AbWSD1, mutated via a random mutagenesis conducted by Röttig and Steinbüchel (2013b). In 2013 and

2015, Barney and co-workers (Barney *et al.*, 2013; Barney *et al.*, 2015) identified amino acids in AbWSD1 and MaWSD1, whose substitution with other amino acids resulted in changes in the alcohol selectivity of the two enzymes. The results indicated that the mutated residues might be involved in alcohol binding. The publication of the MaWSD1 crystal structure in 2018 (Petronikolou & Nair, 2018) could finally help to assign an alcohol binding pocket supported by the positions of the amino acid residues identified by Barney and co-workers (Barney *et al.*, 2013; Barney *et al.*, 2015). Petronikolou and Nair (2018) furthermore allocated the acyl-CoA binding site of MaWSD1 to a second pocket. Amino acid exchange mutants introduced around the cavity resulted in changes in the acyl-CoA preference of the enzyme. Shortly before work regarding this thesis started, the crystal structure of AbWSD1 was obtained, containing the electron density of a co-crystallized myristic acid (Dr. Karin Kühnel, unpublished data).

1.7.1 A. *baylyi* WSD1

A. *baylyi* AbWSD1 (also known as Ac1, AtfA or WS/DGAT) was identified in 2003 as a novel type of WS and led to the introduction of the class of WSD proteins (Kalscheuer & Steinbüchel, 2003). Characterized by many scientific research studies since then (Kalscheuer *et al.*, 2004; Stöveken *et al.*, 2005; Uthoff *et al.*, 2005; Barney *et al.*, 2012; Shi *et al.*, 2012; Barney *et al.*, 2013; Röttig & Steinbüchel, 2013b; Röttig *et al.*, 2015; Röttig *et al.*, 2016), AbWSD1 became a model enzyme for the class of WSD proteins and led to the identification of WSD in other bacteria and some plants (Daniel *et al.*, 2004; Holtzapfel & Schmidt-Dannert, 2007; Kalscheuer *et al.*, 2007; King *et al.*, 2007; Alvarez *et al.*, 2008; Arabolaza *et al.*, 2008; Li *et al.*, 2008; Kaddor *et al.*, 2009; Barney *et al.*, 2012; Shi *et al.*, 2012; Lázaro *et al.*, 2017; Zhang *et al.*, 2017; Shalini & Martin, 2020).

The 458 amino acids encoding AbWSD1 was identified as a bifunctional enzyme exhibiting WS and to an about 10 fold lesser extent DGAT activity *in vivo* and *in vitro* (Kalscheuer & Steinbüchel, 2003). *In vivo* and *in vitro* acyl donor and acyl acceptor specificities revealed a broad substrate range of the enzyme (Kalscheuer & Steinbüchel, 2003; Kalscheuer *et al.*, 2004; Barney *et al.*, 2012; Shi *et al.*, 2012; Röttig *et al.*, 2015; Röttig *et al.*, 2016). Even the formation of thio WE, originating from fatty acids and thiols instead of alcohols, was observed for AbWSD1 *in vitro* and *in vivo* (Uthoff *et al.*, 2005).

A detailed biochemical characterization of AbWSD1 was published in 2005 (Stöveken *et al.*, 2005). The authors managed to purify the protein near to homogeneity by a three-step purification protocol consisting of cation-exchange, hydrophobic-interaction and anion-exchange chromatography. Gel filtration chromatography results proposed the purification of AbWSD1 mainly as homodimer. Incubation of AbWSD1 with either 16:0 OH or di-16:0-DAG

with increasing concentrations of 16:0 CoA revealed, that WS activity follows Michaelis-Menten kinetics, whereas DGAT activity could not be fitted with Michaelis-Menten nor cooperative kinetics. Interestingly, the authors observed a concentration-dependent inhibition of the WS activity by free CoA and an inhibition of DGAT activity at high 16:0 CoA concentrations. The broad substrate range of AbWSD1 already detected before (Kalscheuer & Steinbüchel, 2003) was further confirmed by the study of Stöveken *et al.* (2005). The enzyme showed the ability to produce WE with a large range of linear acyl-CoA *in vitro*, preferring mid and long chain acyl donors. Similar held true for the alcohol specificity. AbWSD1 catalyzed the formation of WE from linear fatty alcohols of various chain length *in vitro* and preferred mid chain and long chain substrates. The study revealed furthermore, that the enzyme especially favors terminal hydroxyl groups by showing a larger activity with 1-decanol than with 2- or 4-decanol. Similar to that, *sn*-1 and/or *sn*-3 positions were preferably more acylated by AbWSD1 in acyl acceptors such as 1-16:0-monoacylglycerol (MAG), 2-16:0-MAG, 3-16:0-MAG, 1,2-di-16:0-DAG and 1,3-di-16:0-DAG compared to the *sn*-2 position. Apart from linear fatty alcohols and acylglycerols, AbWSD1 is able to acylate a large range of additional acyl acceptors. *In vitro* enzymatic activity was observed using cyclohexanol, cyclohexandiol, 2-cyclohexylethanol, cyclododecanol, cyclohexanone oxime, phenol and phenylethanol. Cellular localization studies in *A. baylyi* ADP1 using immunogold labelling showed, that AbWSD1 is mainly associated with the plasma membrane and lipid inclusions, but also localizes in the cytoplasm. The authors observed the partial soluble character of the protein also during purification, as 40-50 % of AbWSD1 was present in the soluble fraction before purification.

Upon the characterization of substrate specificities of five bacterial WSD, including AbWSD1, Barney *et al.* (2012) observed differences in obtained WS activities dependent on the order of substrate addition. For all analyzed enzymes, higher activities were obtained, when adding the acyl-CoA last (pre-incubation of the enzyme with fatty alcohol). For AbWSD1, the detected WS activity when the fatty alcohol added last was only 5 % of the WS activity, when acyl-CoA was added last. The authors assumed an allosteric control of enzyme activity by cellular substrate levels.

Besides the characterization of the wild type AbWSD1 enzyme, several mutant variants of the protein were generated and analyzed regarding changes in overall enzymatic activity and changes in substrate specificities (Stöveken *et al.*, 2009; Barney *et al.*, 2013; Röttig & Steinbüchel, 2013b; Kawelke, 2014). To analyze the role in catalysis of the proposed active site residues of the catalytic motif (HHxxxDG), Stöveken *et al.* (2009) introduced amino acid substitutions at the corresponding positions. Whereas alanine substitutions of aspartate and glycine did not result in changes in enzymatic activity, leucine substitutions of either one or both histidine residues led to drastic decreases in enzymatic activities. A larger decrease in enzymatic activity was observed upon mutation of the second histidine. Upon random

mutagenesis, Röttig and Steinbüchel (2013b) obtained 17 single amino acid substitution or truncation AbWSD1 variants with altered enzymatic activities compared to the wild type protein. Except for one mutation, all variants had a lower activity compared to wild type AbWSD1. Barney *et al.* (2013) published the exchange of AbWSD1-G355 towards isoleucine. The introduced mutation resulted in a change in substrate selectivity of the protein towards shorter alcohols. A higher affinity towards shorter substrates of AbWSD1-G355I compared to wild type AbWSD1 was also observed by Röttig *et al.* (2016). Expressed in *Escherichia coli*, AbWSD1-G355I was not able to produce TAG *in vivo*, indicating an involvement in DGAT activity as well (Röttig *et al.*, 2015). The generation of an AbWSD1 amino acid substitution variant, in which the two isoleucine residues at position 358 and 359 were exchanged to serine residues, resulted in an enzyme variant that was more stable after purification via a hexahistidine (His₆) tag than the wild type enzyme (Kawelke, 2014).

Kawelke (2014) published first experiments to crystallize AbWSD1 in cooperation with Dr. Karin Kühnel and Dr. Felix Lambrecht. The protein was expressed with a N-terminal His₆-tag and trigger factor (TF) fusion (His₆-TF-AbWSD1), supporting folding of fused AbWSD1 during translation. The fusion protein was purified by ion metal affinity chromatography followed by size exclusion chromatography and diffracting crystals were obtained. However, at first the structure could not be solved. Before work regarding this thesis was started, it was finally possible to solve the structure of AbWSD1 with a resolution of 2.1 Å (Dr. Karin Kühnel, unpublished work). The protein consists of 11 α -helices and 15 β -sheets. Interestingly, a myristic acid co-crystallized with the protein with the carboxyl group of the molecule facing towards the proposed active site of the enzyme.

1.7.2 *Marinobacter* WSD1

MaWSD1 (also referred to as Ma1 and Ma-WS/DGAT) and MhWS1 are 455 amino acids long proteins. Except for two residues (MaWSD1-194G/MhWS1-194D, MaWSD1-321E/MhWS1-321G), both enzymes share the same amino acid sequence (Röttig & Steinbüchel, 2013a). With 45-46 % sequence identity, both enzymes are the closest *Marinobacter* WSD homologs to AbWSD1 (Röttig & Steinbüchel, 2013a; Yu, 2016).

The identification and a detailed characterization of MhWS1 was published in 2007 by Holtzapple and Schmidt-Dannert (2007). The authors managed to purify the enzyme and observed *in vitro* WE formation by MhWS1 with various short, mid and long chain fatty acids in the range of ten to 20 carbon chain length and phytanic acid, as well as short and mid chain fatty alcohols ranging from ten to 16 carbon chain length and isoprenoid alcohols. Similar to AbWSD1, MhWS1 exhibits WS and DGAT activity *in vivo* and *in vitro* (Holtzapple & Schmidt-

Dannert, 2007; Röttig *et al.*, 2015). In 2012, a detailed characterization of MaWSD1 was published showing a broad substrate range of the enzyme as well (Barney *et al.*, 2012). Barney *et al.* (2012) observed, that purified MaWSD1 synthesizes WE from 16:0 CoA and fatty alcohols ranging from 8:0 OH to 18:0 OH, with a preference of the enzyme for 11:0 OH and 12:0 OH. WE formation of MaWSD1 was detected additionally with isoamyl alcohol, 6:0 OH and phenyl ethanol. When 12:0 OH was provided, MaWSD1 produced WE with acyl-CoA ranging from 8:0 CoA to 16:0 CoA favoring 14:0 CoA and 16:0 CoA. Consistent with AbWSD1, Barney *et al.* (2012) observed different WS activities influenced by the order of substrate addition for MaWSD1, too. The WS activity when fatty alcohol was added last was only 12 % of the WS activity when acyl-CoA was added last.

Together with AbWSD1, the mutation of an amino acid residue in MaWSD1 was published, that influenced the fatty alcohol selectivity of the protein (Barney *et al.*, 2013). Upon the exchange of alanine 360 to larger residues such as valine, isoleucine and phenylalanine, the enzyme variants preferred the incorporation of shorter alcohols. A second study published two years later identified two more residues in MaWSD1 (MaWSD1-L356, MaWSD1-M405), that showed altered alcohol selectivity upon mutation (Barney *et al.*, 2015).

In 2018, Petronikolou and Nair (2018) published the crystal structure of MaWSD1. The protein crystallized as dimer and the structure was solved with 2.4 Å resolution. The authors identified two pockets within the enzyme that are connected with the proposed active site motif. The amino acid residues whose mutations by Barney and co-workers (Barney *et al.*, 2013; Barney *et al.*, 2015) resulted in altered alcohol selectivities are located around pocket 2 and supported the assignment of pocket 2 as alcohol binding site (Petronikolou & Nair, 2018). Petronikolou and Nair (2018) furthermore proposed pocket 1 as acyl-CoA binding site. The authors suggested a binding of acyl-CoA with the acyl chain in pocket 1, the pantetheine part extended into the active site and the phosphoadenosine part exposed to the solvent. Amino acid exchange studies, substituting adjacent amino acids of pocket 1, resulted in altered acyl-CoA preferences of the mutants. MaWSD1-G25V and MaWSD1-A144F favored the synthesis of WE with 6:0 CoA over 16:0 CoA. Changes in fatty alcohol preferences were not observed analyzing the mutants.

Upon expression of MaWSD1 in *Saccharomyces cerevisiae* strain H1246, which is deficient in TAG and steryl ester biosynthesis, MaWSD1 synthesized three unknown compounds in addition to WE and TAG ((Yu, 2016). An identification of the unknown compounds could not be achieved.

1.7.3 *Marinobacter* WSD2

MaWSD2 (also referred to as Ma2 and MaWS2) and MhWS2 are 473 long proteins that are similar well characterized as MaWSD1 and MhWS1 (Holtzapple & Schmidt-Dannert, 2007; Barney *et al.*, 2012; Shi *et al.*, 2012; Villa *et al.*, 2014; Röttig *et al.*, 2015; Yu, 2016; Miklaszewska *et al.*, 2018). MaWSD2 and MhWS2 only differ in one amino acid residue (MaWSD2-395D/MhWS2-395G). Both enzymes have 37-39 % sequence identity to AbWSD1 (Röttig & Steinbüchel, 2013a; Yu, 2016).

Holtzapple and Schmidt-Dannert (2007) identified and characterized MhWS2 in the same research study as MhWS1. *In vitro* assays revealed a broad substrate range for MhWS2 accepting various fatty acids, including phytanic acid, and fatty alcohols and isoprenoid alcohols. A higher preference for long chain fatty alcohols compared to MhWS1 was observed. A broad substrate range for MhWS2 was also detected in a study published in 2018 (Miklaszewska *et al.*, 2018). WS activities for 204 different acyl acceptor and acyl donor combinations were analyzed *in vitro*. The enzyme was able to catalyze WE formation with the majority of the tested substrate combinations. Highest activities were obtained with 14:0 CoA, followed by 12:0 CoA. Decreased activities were observed with acyl-CoA longer than 18 carbon chain length as well as with polyunsaturated acyl-CoA with 18 carbon chain length. For combinations with fatty alcohols having more than 16 carbon chain length, reduced WS activities were detected as well. Interestingly, higher WS activities were observed with corresponding unsaturated fatty alcohols.

In contrast to AbWSD1 and MaWSD1, no DGAT activity was detected for MhWS2 *in vitro* by Holtzapple and Schmidt-Dannert (2007). Miklaszewska *et al.* (2018) detected as well no TAG formation for MhWS2 *in vitro* and *in vivo* upon expression in yeast. These data were additionally supported by a similar observation (Yu, 2016). Upon expression of MaWSD2 in yeast, the enzyme only produced WE. However, minor DGAT activity of MhWS2 was detected *in vivo* in *E. coli* (Röttig *et al.*, 2015) and *in vitro* TAG formation was observed for MaWSD2 as well (Villa *et al.*, 2014).

Providing saturating 16:0 CoA and increasing 16:0 OH concentrations, WS activity of MhWS2 followed Michaelis-Menten kinetics (Holtzapple & Schmidt-Dannert, 2007). Similar to AbWSD1 and MaWSD1, Barney *et al.* (2012) observed an influence of the order of substrate addition on WS activity for MaWSD2. Nevertheless, for MaWSD2 the difference in activity comparing fatty alcohol and acyl-CoA addition as last compound was much smaller. WS activity was only reduced to 79 % in MaWSD2 when fatty alcohol was added last.

Before the crystal structure of MaWSD1 was published, Villa *et al.* (2014) modelled the structure of MaWSD2 using the acyltransferase tyrocidine synthase as template. A structure

consisting of two domains connected via a helical linker was predicted. The two domain structure was verified via limited proteolysis and the authors observed additionally, that co-expressed N- and C-terminal domains reconstitute to a functional protein, that can be purified and has WS and DGAT activity accounting to around 70-80 % of wild type activity. Upon generation and analysis of amino acid exchange mutants, Villa *et al.* (2014) observed reduced WS and DGAT activities for MaWSD2 alanine variants of amino acids corresponding to the proposed active site motif as well as to the three identified motifs PLW, ND and R.

1.7.4 *Marinobacter* WSD5

A putative fifth WSD was identified in the genome of *M. aquaeolei* only recently (Yu, 2016; Knutson *et al.*, 2017). The 452 amino acid long protein shares about 19 % sequence identity with AbWSD1 and between 23 % and 33 % with MaWSD1-4 (Yu, 2016).

Acyltransferase activity of MaWSD5 was confirmed *in vivo* and *in vitro* (Yu, 2016). Upon expression of the protein in the TAG and steryl ester deficient *S. cerevisiae* H1246 strain, WE formation, but no TAG formation was detected for MaWSD5 suggesting the protein to be a monofunctional WSD (Yu, 2016). A purification of C-terminally His₆-tagged MaWSD5 was possible using ion metal affinity chromatography and yielded active enzyme. Active protein was also obtained after subsequent size exclusion chromatography. However, to reduce the amount of aggregated protein, the purification buffer had to be supplemented with detergent (Yu, 2016).

1.8 WE production in transgenic plants: current achievements

After the banning of whale hunting, jojoba attracted notice as potential WE provider for industrial applications (Zhu *et al.*, 2016). Nevertheless, jojoba is a slow-growing desert shrub, which is not easy to cultivate in industrial needed scales (Al-Obaidi *et al.*, 2017). In order to produce industrial desired WE in large amounts and sustainable ways, the idea arose to establish WE biosynthesis in crop plants. The perspective of generating plants with modifiable WE synthesis for tailor-made WE production spurred research even more. Up to now, several studies have been published dealing with the generation of transgenic WE producing plants and their analysis regarding WE amount and composition (Lardizabal *et al.*, 2000; Heilmann *et al.*, 2012; Aslan *et al.*, 2014; Aslan *et al.*, 2015a; Aslan *et al.*, 2015b; Iven *et al.*, 2016; Zhu *et al.*, 2016; Ivarson *et al.*, 2017; Ruiz-Lopez *et al.*, 2017; Yu *et al.*, 2018).

In 2000, Lardizabal *et al.* (2000) published the identification of a WS from *S. chinensis* (ScWS). In conjunction with the identification of the jojoba FAR (ScFAR) in the same year (Metz *et al.*,

2000) it was possible to establish WE biosynthesis in *A. thaliana* seeds (Lardizabal *et al.*, 2000). Upon seed specific expression of ScFAR, ScWS and a β -ketoacyl-CoA synthase from *Lunaria annua*, WE formation was detected in seeds. The analysis of WE by ^{13}C -nuclear magnetic resonance revealed up to 70 % (by weight) WE in oil of some seeds, consisting mostly of fatty acids and fatty alcohols with chain lengths longer than 18 carbons.

Zhu *et al.* (2016) analyzed the usage of three *Brassicaceae* oilseed species for their feasibility as jojoba-like WE production hosts via metabolic engineering of seed neutral lipid formation. Different transgenic *Crambe abyssinica*, *Brassica carinata* and *Camelina sativa* lines expressing ScFAR and ScWS with and without additional fatty acid metabolism modifying enzymes such as the *S. chinensis* fatty acid elongase (FAE, ScFAE) 1-like 3-ketoacyl-CoA synthase, *L. annua* FAE2 or fatty acid desaturase (FAD) 2 RNAi constructs, were generated. WE amounts of 15-30 % of total seed oil were obtained by the different approaches, with single seeds exceeding 50 % WE content in some *C. abyssinica* lines. Especially in *B. carinata* and *C. sativa*, the expression of a FAE resulted in the formation of longer WE. The blocking of fatty acid polyunsaturation by RNAi constructs was successful in generating more WE with monounsaturated moieties. A field trial with ScFAR/ScWS and ScFAR/ScWS/ScFAE1 *C. abyssinica* lines showed WE formation also under natural conditions, nevertheless, the seed yield, oil content and germination rate was reduced in the transgenic lines and to a higher extent in the line expressing three genes.

In order to test, whether the wild oil species field cress (*Lepidium campestre*) is suitable as a WE producing oil crop, transgenic *L. campestre* plants were generated, expressing either ScFAR/ScWS or ScFAR/ScWS/ScFAE1 (Ivarson *et al.*, 2017). The expression of both constructs resulted in seed WE formation where co-expression of ScFAE1 resulted in longer WE, as seen before by Zhu *et al.* (2016). Interestingly, Ivarson *et al.* (2017) detected different compartmentation of some generated WE species that preferentially accumulated in the seed coat rather than in the embryo. Additionally, they observed disrupted neutral lipid organization in cells of seeds with high WE amounts. As seeds with high WE content did not germinate, the authors speculated, that low germination rate might be associated with neutral lipid packaging disruption or alcohol accumulation.

Besides establishing the jojoba WE biosynthesis in diverse plants, studies were also published analyzing the suitability of WS(D) and FAR enzymes from other organisms for transgenic WE production, sometimes in combination with other fatty acid metabolism modifying enzymes as well.

Heilmann *et al.* (2012) expressed different versions of mouse FAR1 and WS (MmFAR1, MmWS) in *A. thaliana* and obtained a WE content of ca. 20 $\mu\text{g}/\text{mg}$ seed. It was possible to double seed WE amount by deleting a peroxisomal targeting signal from the C-terminus of

MmFAR1 and by fusing either MmFAR1 Δ c or MmFAR1 Δ c and MmWS to the lipid droplet protein oleosin 3. Analysis of the formed WE species revealed that mainly polyunsaturated WE were produced by the tested enzyme combinations. Especially polyunsaturated 18 carbon chain length fatty acids were incorporated.

The expression of MmFAR1 Δ c/MmWS, MmFAR1 Δ c/ScWS and MaFAR/ScWS in *A. thaliana* and *C. sativa* by Iven *et al.* (2016) allowed the direct comparison of different WE producing enzyme combinations. Compared to the two other constructs, an about five and four times higher WE content was obtained in MaFAR/ScWS *A. thaliana* and *C. sativa* lines, respectively. WE production reached WE amounts of 89-108 mg/g seed in *A. thaliana* and of 33-47 mg/g seed in *C. sativa* plants expressing MaFAR/ScWS. The expression of ScWS instead of MmWS resulted in the incorporation of mainly 20 carbon monounsaturated fatty acids, instead of polyunsaturated 18 carbon moieties. A shift towards monounsaturated alcohol moieties was observed upon expression of MaFAR together with ScWS compared to the MmFAR1 Δ c/ScWS construct.

Iven *et al.* (2016) was not only testing eukaryotic WE producing enzymes, but also expressed the bacterial MaFAR. Other studies tested the suitability of several bacterial WE producing enzyme combinations as well (Aslan *et al.*, 2014; Aslan *et al.*, 2015a; Aslan *et al.*, 2015b; Ruiz-Lopez *et al.*, 2017; Yu *et al.*, 2018). Ruiz-Lopez *et al.* (2017) transformed *C. sativa* plants with combinations of WS(D) originating from *M. hydrocarbonoclasticus* (MhWS2), mouse, *A. baylyi* (AbWSD1) and *Tetrahymena thermophile* as well as FAR originating from *M. aquaeolei* and *T. thermophile*. Additionally, fatty acid metabolism modifying enzymes such as different thioesterases or a fatty acid hydroxylase were expressed. Interestingly, compared to the expression of the other WS, upon the expression of MmWS a smaller range of WE were produced, consisting mainly of 36 and 38 carbon chain length. The expression of 14:0 ACP thioesterase from *Cuphea palustris* resulted in the formation of shorter WE. As observed before (Heilmann *et al.*, 2012; Iven *et al.*, 2016), MmWS constructs favored the incorporation of polyunsaturated and 18 carbon acyl moieties (Ruiz-Lopez *et al.*, 2017). MhWS2 expressing constructs produced WE with mainly saturated and monounsaturated acyl moieties of 18 or 20 carbon chain length (Ruiz-Lopez *et al.*, 2017). Regarding the alcohol specificities, no large differences were observed between the different constructs. All favored 20 and 18 carbon chain length and monoenoic and saturated alcohol moieties.

Yu *et al.* (2018) analyzed WE formation in transgenic *A. thaliana* expressing different MaFAR/ScWS and MaFAR/ScWS fusion constructs. Additionally, the authors tested the expression of MaFAR/MaWSD2 and several MaFAR/AbWSD1 constructs. For all constructs expressing ScWS, higher WE contents were detected compared to when bacterial WSD were expressed. However, expression of MaFAR and ScWS fusion constructs lowered WE content

in comparison to the separately expressed enzymes. As seen previously (Iven *et al.*, 2016), all MaFAR/ScWS constructs favored the incorporation of monoenoic 18 and 20 carbon fatty acids and fatty alcohols (Yu *et al.*, 2018). The MaFAR/MaWSD2 and diverse MaFAR/AbWSD1 constructs mainly produced WE from 18:1 and 18:2 fatty alcohol and 18:0 and 18:1 fatty acid substrates.

Due to its excellent lubrication properties, researchers aim for high levels of 18:1/18:1 WE. Although several of the above described enzyme combinations synthesized WE from long chain monoenoic substrates, no enzyme combination was so far identified, that predominantly produced 18:1/18:1 WE. A reason for that are the broad substrate specificities of WS(D) enzymes (see above). An approach to overcome this drawback is to provide a limited substrate pool to WE synthesizing enzymes allowing the formation of only certain WE species. Heilmann *et al.* (2012), Iven *et al.* (2016) and Yu *et al.* (2018) expressed several FAR/WS constructs in *A. thaliana fae1 fad2* mutant plants. The plants lack FAE1 and FAD2, which are needed for the elongation of fatty acids beyond 18 carbon chain length and for the introduction of double bonds in monounsaturated fatty acids in seeds (Kunst *et al.*, 1992; Okuley *et al.*, 1994). By this approach 18:1/18:1 WE contents of around 60 mol% of total WE were obtained independent of which FAR or WS were expressed. The expression of MaFAR/ScWS in high oleate *C. sativa* plants resulted in the formation of around 30 mol% 18:1/18:1 WE, too (Yu *et al.*, 2018). Although reduced overall WE contents were observed in these plants, WE quality consisting of mainly one WE species drastically increased by this approach.

The above described studies aimed for WE production in oil seed seeds as this tissue is specialized for high levels of neutral lipid synthesis. As total plant biomass is often higher than seed yield per land area, engineering of plants for the production of industrial valuable lipids in green tissue is discussed as well (Carlsson *et al.*, 2011; Chapman *et al.*, 2013; Aslan *et al.*, 2014). Aslan and co-workers (Aslan *et al.*, 2014; Aslan *et al.*, 2015a; Aslan *et al.*, 2015b) produced WE in stable and transiently transformed *Nicotiana benthamiana* leaves. Chloroplasts were chosen for WE formation because of their role in carbon metabolism in form of starch accumulation and degradation as well as fatty acid synthesis. Upon transient expression of different combinations of plastid localized *A. thaliana* FAR6 (AtFAR6) and phytol ester synthase 2 (AtPES2) as well as AtFAR6 transit peptide tagged MhWS2 and MaFAR, WE formation was detected for all constructs (Aslan *et al.*, 2014). Except for AtFAR6/AtPES2, WE content could not be increased upon expression of *A. thaliana* wrinkled (AtWRI) 1, which is known to induce *de novo* fatty acid synthesis (Focks & Benning, 1998; Ma *et al.*, 2013). Upon plastidial WE formation, AtFAR6 constructs favored the incorporation of 16:0 OH and MaFAR constructs produced WE with mainly 16:0 OH and 18:0 OH. On the acyl side, AtPES2 preferred to form WE from 12:0 and 14:0 acyl substrates, whereas MhWS2 favored the incorporation of longer acyl moieties, mainly 16:0 and 18:0. Using transmission electron microscopy,

aggregation bodies containing WE were observed in chloroplasts of transformed leaves. In a follow-up publication, Aslan *et al.* (2015b) generated stable transgenic *N. benthamiana* plants expressing a plastid localized fusion protein made up from MaFAR and MhWS2. The transgenic plants displayed a stunted growth, chlorotic leaves and stems. The authors assumed a negative effect of accumulating free fatty alcohols. Consistent with this, the authors also observed lower WE levels in % dry weight in stable transformed plants compared to transiently transformed plants (Aslan *et al.*, 2014) with the same construct. As a reason for this, a counter-selection for strong transgene expression was suggested.

1.9 Thesis objectives

As stated above, several studies have been published within the past years establishing WE production for industrial usage in transgenic (crop) plants. Although WE formation was achieved by the diverse approaches, it became apparent, that further work regarding enzyme use, substrate availability and storage capacities is needed in order to obtain large amounts of WE consisting predominantly of desired WE species.

Aim of this thesis is to further improve tailor-made WE production regarding enzyme use and substrate availability. The aspect enzyme use will be investigated within two projects. First, it will be studied, whether the recently identified MaWSD5 is a suitable candidate for transgenic WE production by characterization of the protein and expression of the enzyme in *A. thaliana*. Second, it is aimed to identify substrate binding sites in the recently solved AbWSD1 crystal structure by the generation of amino acid exchange mutants, as this establishes the basis for the generation of WSD variants with altered substrate preferences. In a third project, the aspect substrate availability will be studied by expressing different MaFAR, MaWSD2 and MaWSD5 combinations with and without plastidial localization tag under the control of different promoters. A detailed comparison of plastidial and cytosolic as well as seed and leaf WE biosynthesis will be conducted to study whether a change of WE synthesis location is a suitable tool to alter substrate availability and to analyze whether seed plastids are an appropriate organelle for WE production.

For the first project, the characterization of the recently identified fifth WSD from *M. aquaeolei* (MaWSD5) (Yu, 2016; Knutson *et al.*, 2017) is planned. As a purification of the protein is established, the *in vitro* characterization of fatty alcohol and acyl-CoA specificities of the enzyme is possible. As it was shown, that MaWSD5 lacks DGAT activity *in vivo* (Yu, 2016), it is furthermore intended to test for DGAT activity of MaWSD5 *in vitro* with several substrates. Additionally, it will be tested, whether MaWSD5 is suited for WE formation in *A. thaliana* seeds.

Upon co-expression with MaFAR, WE amount and generated WE species are planned to be analyzed.

The second project deals with the identification of substrate binding sites in the recently solved structure of the bacterial AbWSD1 from *A. baylyi*. As cavities can be predicted in the structure connecting the proposed catalytic motif of the protein with the outside, the generation of amino acid exchange mutants is planned, substituting residues located around these tunnels. Substrate specificity analyses of the enzyme variants will be conducted to test for changes in substrate specificities caused by the mutation hinting towards the involvement of mutated residues in substrate binding. A detailed comparison of the AbWSD1 structure, carrying a co-crystallized myristic acid, with the structure of MaWSD1 (Petronikolou & Nair, 2018), which was published while working on this thesis, aims furthermore for the identification of conserved structural parts in WSD proteins and the identification of potential structural rearrangements upon substrate binding.

In order to compare different substrate pools within the cell and the entire plant, aim of the third project is to analyze the influence of plastidial localized WE biosynthesis on the WE amount and formed WE species and studying whether a subcellular change of WE biosynthesis is a suitable tool for altering substrate availability. It is planned to generate transgenic *A. thaliana* plants expressing different MaFAR/MaWSD2 and MaFAR/MaWSD5 constructs with and without plastidial localization signal. The constructs will allow a direct comparison between cytosolic and plastidial WE biosynthesis in terms of WE amount and formed WE species, as well as a comparison between MaWSD2 and MaWSD5 catalyzed WE formation. To study additionally alterations between WE biosynthesis in transgenic leaves and seeds, the generation of constructs is planned expressing the enzymes under the control of seed specific promoters or ubiquitous 35S promoter.

The planned experiments of the three projects aim together for a more detailed understanding of WE biosynthesis, including the analysis of different WE producing enzymes, structural prerequisites of WSD and the influence of host metabolism of transgenic plants.

2 ARTICLE I

2.1 The Fifth WS/DGAT Enzyme of the Bacterium *Marinobacter aquaeolei* VT8

This manuscript was published online 20 May 2020 in Lipids (American Oil Chemists' Society (AOCS)). Katharina Vollheyde and Dan Yu are shared first authors. Supporting information are appended to the manuscript in the order of appearance. A list of the corresponding figure legends and the table heading is inserted before the supporting information.

The manuscript can be found under the following web link:

<https://doi.org/10.1002/lipd.12250>

Katharina Vollheyde established the gravity flow purification protocol for MaWSD5, performed and analyzed the *in vitro* bifunctionality assay and the DTNB-based *in vitro* substrate specificity assay. She cloned the constructs and generated the transgenic *A. thaliana* plants. She prepared the samples for the nanoESI-MS/MS WE measurement of transgenic *A. thaliana* MaFAR/MaWSD5 seeds and processed, analyzed, displayed and discussed the obtained WE data. Katharina Vollheyde wrote the first draft of the manuscript corresponding to Figures 1, 3, 4 and supplemental Figures S2-S4 as well as the discussion and part of the introduction.



The Fifth WS/DGAT Enzyme of the Bacterium *Marinobacter aquaeolei* VT8

Katharina Vollheyde^{1†} · Dan Yu^{1†} · Ellen Hornung¹ · Cornelia Herrfurth^{1,2} · Ivo Feussner^{1,2,3}

Received: 23 December 2019 / Revised: 9 April 2020 / Accepted: 30 April 2020

© 2020 The Authors. *Lipids* published by Wiley Periodicals, Inc. on behalf of American Oil Chemists' Society

Abstract Wax esters (WE) belong to the class of neutral lipids. They are formed by an esterification of a fatty alcohol and an activated fatty acid. Dependent on the chain length and desaturation degree of the fatty acid and the fatty alcohol moiety, WE can have diverse physicochemical properties. WE derived from monounsaturated long-chain acyl moieties are of industrial interest due to their very good lubrication properties. Whereas WE were obtained in the past from spermaceti organs of the sperm whale, industrial WE are nowadays mostly produced chemically from fossil fuels. In order to produce WE more sustainably, attempts to produce industrial WE in transgenic plants are

steadily increasing. To achieve this, different combinations of WE producing enzymes are expressed in developing *Arabidopsis thaliana* or *Camelina sativa* seeds. Here we report the identification and characterization of a fifth wax synthase from the organism *Marinobacter aquaeolei* VT8, MaWSD5. It belongs to the class of bifunctional wax synthase/acyl-CoA:diacylglycerol *O*-acyltransferases (WSD). The protein was purified to homogeneity. *In vivo* and *in vitro* substrate analyses revealed that MaWSD5 is able to synthesize WE but no triacylglycerols. The protein produces WE from saturated and monounsaturated mid- and long-chain substrates. *Arabidopsis thaliana* seeds expressing a fatty acid reductase from *Marinobacter aquaeolei* VT8 and MaWSD5 produce WE. Main WE synthesized are 20:1/18:1 and 20:1/20:1. This makes MaWSD5 a suitable candidate for industrial WE production *in planta*.

Supporting information Additional supporting information may be found online in the Supporting Information section at the end of the article.

✉ Ivo Feussner
ifeussn@uni-goettingen.de

¹ Department for Plant Biochemistry, Albrecht-von-Haller-Institute for Plant Sciences, University of Goettingen, 37077, Goettingen, Germany

² Service Unit for Metabolomics and Lipidomics, Goettingen Center for Molecular Biosciences (GZMB), University of Goettingen, D-37077, Goettingen, Germany

³ Department for Plant Biochemistry, Goettingen Center for Molecular Biosciences (GZMB), University of Goettingen, 37077, Goettingen, Germany

[†]Katharina Vollheyde and Dan Yu contributed equally to this work.

This is an open access article under the terms of the Creative Commons Attribution License, which permits use, distribution and reproduction in any medium, provided the original work is properly cited.

Keywords *Marinobacter aquaeolei* VT8 · Neutral lipids · Seed oil · Storage lipids · Wax ester · Wax synthase/acyl CoA:diacylglycerol *O*-acyltransferase

Lipids (2020) 55: 479–494.

Abbreviations

<i>A. baylyi</i>	<i>Acinetobacter baylyi</i>
<i>A. calcoaceticus</i>	<i>Acinetobacter calcoaceticus</i> , nowadays: <i>Acinetobacter baylyi</i>
<i>A. thaliana</i>	<i>Arabidopsis thaliana</i>
aa	amino acids
AbWSD1	<i>Acinetobacter baylyi</i> WSD1, Ac1, AtfA
ACP	acyl carrier protein
ATP	adenosine triphosphate
<i>C. sativa</i>	<i>Camelina sativa</i>

CFP	cyan fluorescent protein	
CHAPS	3-[(3-cholamidopropyl)dimethylammonio]-1-propanesulfonate	
CoA	coenzyme A	
DGAT	acyl-CoA:diacylglycerol acyltransferase	<i>O</i> -
DMSO	dimethyl sulfoxide	
DNA	deoxyribonucleic acid	
DTNB	5,5'-dithiobis-(2-nitrobenzoic acid)	
<i>E. coli</i>	<i>Escherichia coli</i>	
EV	empty vector	
FAR	fatty acyl reductase	
FFA	free fatty acid	
GC	gas chromatography	
GC-MS	gas chromatography coupled to mass spectrometry	
his ₆ -tag	hexahistidine tag	
IMAC	ion metal affinity chromatography	
<i>M. aquaeolei</i>	<i>Marinobacter aquaeolei</i>	
<i>M. hydrocarbonoclasticus</i>	<i>Marinobacter hydrocarbonoclasticus</i>	
MaFAR	<i>Marinobacter aquaeolei</i> FAR	
MaWSD1	<i>Marinobacter aquaeolei</i> WSD1, Ma1, Ma-WS/DGAT	
MaWSD2	<i>Marinobacter aquaeolei</i> WSD2, Ma2	
MaWSD3-5	<i>Marinobacter aquaeolei</i> WSD3-5	
MhWS1-4	<i>Marinobacter hydrocarbonoclasticus</i> WS1-4	
MmWS	<i>Mus musculus</i> WS	
nanoESI-MS/MS	nano-electrospray ionization tandem mass spectrometry	
OD ₆₀₀	optical density at 600 nm	
PMSF	phenylmethane sulfonyl fluoride	
<i>S. cerevisiae</i>	<i>Saccharomyces cerevisiae</i>	
<i>S. chinensis</i>	<i>Simmondsia chinensis</i>	
ScFar	<i>Simmondsia chinensis</i> FAR	
ScWS	<i>Simmondsia chinensis</i> WS	
SDS-PAGE	sodium dodecyl sulfate—polyacrylamide gel electrophoresis	
SEC	size exclusion chromatography	
STD	standard	
TAG	triacylglycerol	
TLC	thin layer chromatography	
U1-4	unknown compound 1–4	
WE	wax ester	
WS	wax synthase	
WSD	wax synthase/acyl diacylglycerol <i>O</i> -acyltransferase	CoA:

YFP yellow fluorescent protein

Introduction

Like triacylglycerols (TAG), wax esters (WE) belong to the class of neutral lipids and consist of a fatty alcohol esterified to a fatty acid moiety (Athenstaedt and Daum, 2006; Röttig and Steinbüchel, 2013). WE occur in nearly all groups of organisms having different functions *e.g.* as energy storage compounds or as part of protective layers (Bagge et al., 2012; Barney et al., 2012; Blomquist et al., 1972; Cheng and Russell, 2004; Duncan et al., 1974; Miklaszewska et al., 2013; Razeq et al., 2014; Rottler et al., 2013; Santala et al., 2014; Yeats and Rose, 2013). Accompanied with their various functions, WE have diverse physicochemical properties (Patel et al., 2001). Properties like melting temperature and oxidation stability are influenced by the type of fatty acid and fatty alcohol being incorporated into WE (Patel et al., 2001).

Due to their different chemical properties, WE are of great industrial interest. They are part of coatings and cosmetics and are widely used as industrial lubricants (Rontani, 2010; Wei, 2012). Due to their low melting temperatures and high-oxidation stabilities, WE consisting of monounsaturated long-chain acyl moieties are of interest as industrial lubricants (Carlsson et al., 2011). In early times, those WE were obtained from spermaceti organs of sperm whale (Röttig and Steinbüchel, 2013). Since the banning of whale hunting, WE are industrially produced from fossil fuel or plant-derived TAG or are extracted from the expensive seeds of the slow-growing desert plant jojoba (*Simmondsia chinensis*, *S. chinensis*) (Sturtevant et al., 2020). Nowadays, attempts to produce WE in transgenic plants in an industrial scale are steadily increasing (Heilmann et al., 2012; Iven et al., 2016; Lardizabal et al., 2000; Ruiz-Lopez et al., 2017; Yu et al., 2018).

The two building blocks of WE are coenzyme A (CoA) or acyl carrier protein (ACP) activated fatty acids and fatty alcohols (Samuels et al., 2008). Acyl-CoA/ACP are ubiquitously found in living cells. They are synthesized through the repeating reaction steps of fatty acid biosynthesis or are set free from esterified acyl-containing molecules during acyl editing or degradation processes (Lands, 1958). Fatty alcohols are synthesized from acyl-CoA/ACP upon the reduction of the acyl group to an alcohol group. The reduction is catalyzed by fatty acyl reductases (FAR) in a NAD (P)H-dependent one- or two-step reaction (Hofvander et al., 2011; Reiser and Somerville, 1997). WE are then formed by the esterification of acyl-CoA/ACP and fatty

alcohol. The esterification is catalyzed by wax synthases (WS) (Samuels et al., 2008). WS enzymes can be found in all kingdoms of life and can be - dependent on their evolutionary origin - classified into three major classes (Röttig and Steinbüchel, 2013). Acyl-CoA:diacylglycerol *O*-acyltransferase (DGAT) isoform 1-like WS are transmembrane proteins with six to nine transmembrane domains distributed over the whole protein. DGAT2-like WS are classified as membrane-bound proteins, too. However, they contain only one or two transmembrane domains at their N-terminus. In 2003, a third class of WS was introduced, due to the identification of a new type of WS in the bacterium *Acinetobacter baylyi* (*A. baylyi* former known as *A. calcoaceticus*) (Kalscheuer and Steinbüchel, 2003). This enzyme was characterized as a bifunctional enzyme exhibiting WS and DGAT activity. Proteins of the third class of WS are named WS/DGAT (WSD) enzymes. WSD1 from *A. baylyi* (AbWSD1, also known as WS/DGAT, Ac1 or AtfA, respectively) was found to be a soluble protein that can be purified to homogeneity (Barney et al., 2012; Stöveken et al., 2005). Nevertheless, localization studies conducted within the bacterium itself also revealed that a large portion of AbWSD1 is membrane associated (Stöveken et al., 2005). The identification of AbWSD1 paved the way for the identification of WSD in other bacteria and in plants (Alvarez et al., 2008; Arabolaza et al., 2008; Barney et al., 2012; Daniel et al., 2004; Holtzapple and Schmidt-Dannert, 2007; Kaddor et al., 2009; Kalscheuer et al., 2007; King et al., 2007; Lázaro et al., 2017; Li et al., 2008; Zhang et al., 2017). All WSD share a conserved catalytic motif (HHxxxDG), from which the second histidine is proposed to be important for catalyzing the ester bond formation by the enzyme (Petronikolou and Nair, 2018; Stöveken et al., 2009; Villa et al., 2014).

Besides AbWSD1, WSD from the bacterium *Marinobacter* belong to the best characterized ones. In 2007, the identification and characterization of four WSD (MhWS1-4) in *Marinobacter hydrocarbonoclasticus* DSM 8798 (*M. hydrocarbonoclasticus*) were published (Holtzapple and Schmidt-Dannert, 2007). MhWS1 was found to exhibit WS and DGAT activity similar to AbWSD1 (Holtzapple and Schmidt-Dannert, 2007). In contrast to that, experiments revealed that MhWS2 has only WS activity but no DGAT activity *in vitro* (Holtzapple and Schmidt-Dannert, 2007). However, upon expression of MhWS2 in *Escherichia coli* (*E. coli*) trace amounts of TAG were synthesized *in vivo* (Röttig et al., 2015). For MhWS3 neither WS nor DGAT activity was detected and MhWS4 was identified as a pseudogene, harboring a stop codon that truncates the open reading frame (Holtzapple and Schmidt-Dannert, 2007).

In addition to WSD from *M. hydrocarbonoclastius* DSM 8798, WSD from *M. aquaeolei* VT8 were characterized in several studies (Barney et al., 2012; Barney et al., 2013;

Barney et al., 2015; Röttig et al., 2016). Although identified as two different species, it is nowadays assumed that *M. hydrocarbonoclasticus* and *M. aquaeolei* are the same organism (Márquez and Ventosa, 2005). However, due to different places of discovery of both strains and accompanied with the occurrence of different evolutionary events, the genomes of both strains are not identical. Hence, there are also differences in the amino acid sequences of WSD from *M. hydrocarbonoclasticus* DSM 8798 and *M. aquaeolei* VT8. Between MhWS1 and MaWSD1 (also referred to as Ma1 and Ma-WS/DGAT) as well as between MhWS2 and MaWSD2 (also referred to as Ma2 and MaWS2) only a small number of amino acid substitutions are present: MhWS1-194D/MaWSD1-194G, MhWS1-321G/MaWSD1-321E, and MhWS2-395G/MaWSD2-395D. In contrast to that, MhWS3/MaWSD3 and MhWS4/MaWSD4 differ in a larger number of amino acids. MaWSD3 differs from MhWS3 in nine amino acids and is a bit shorter due to a four amino acid deletion in the N-terminus of the protein. The largest difference occurs between MhWS4 and MaWSD4. Both proteins do not only differ in eight amino acids, MhWS4 also encodes for a stop codon at position 350. Due to that, MhWS4 was identified as a pseudogene whereas the open reading frame of MaWSD4 is intact (Holtzapple and Schmidt-Dannert, 2007). MaWSD1 and MaWSD2 were characterized by several studies regarding substrate specificities and overall performance (Barney et al., 2012; Barney et al., 2013; Barney et al., 2015; Petronikolou and Nair, 2018; Röttig et al., 2016; Villa et al., 2014). In contrast to MhWS2, MaWSD2 exhibits DGAT activity *in vitro* (Holtzapple and Schmidt-Dannert, 2007; Villa et al., 2014). MaWSD1 is the first crystallized WSD from this class of enzymes (Petronikolou and Nair, 2018). The analysis of different amino acid exchange mutants allowed the assignment of the acyl-CoA and fatty alcohol binding sites to two large pockets present within the structure (Barney et al., 2013; Barney et al., 2015; Petronikolou and Nair, 2018).

In order to avoid the production of industrial WE from limiting fossil fuel resources, attempts to synthesize WE in plant seeds are steadily increasing (Heilmann et al., 2012; Iven et al., 2016; Lardizabal et al., 2000; Ruiz-Lopez et al., 2017; Yu et al., 2018). In the beginning eukaryotic FAR (jojoba FAR (ScFAR) and mouse FAR (MmFAR)) in combination with eukaryotic DGAT1-like or DGAT2-like WS (jojoba WS (ScWS) and mouse WS (MmWS)) were expressed in the seeds of the model plant *Arabidopsis thaliana* (*A. thaliana*) and revealed a successful WE production (Heilmann et al., 2012; Lardizabal et al., 2000). In 2011, a detailed characterization of the bacterial *M. aquaeolei* VT8 FAR (MaFAR) revealed, that the enzyme favors to produce 18:1 and 20:0 fatty alcohols *in vitro* (Hofvander et al., 2011). Due to that, MaFAR was also tested in combination with ScWS in *A. thaliana* and *Camelina sativa* (*C. sativa*) (Iven

et al., 2016). In 2017 and 2018, two studies were published, successfully synthesizing WE in *A. thaliana* and *C. sativa* seeds when using the soluble bacterial WSD AbWSD1, MaWSD2, and MhWS2 in combination with different FAR enzymes (Ruiz-Lopez et al., 2017; Yu et al., 2018).

In the present study, the identification and characterization of a fifth WSD from *M. aquaeolei* (MaWSD5) is reported. The protein belongs due to its protein sequence to the class of WSD enzymes, but exhibits only WS activity *in vivo* and *in vitro*. *In vitro* substrate specificity analyses revealed that MaWSD5 is able to produce WE from saturated and unsaturated mid- and long-chain acyl-CoA and fatty alcohols. Expression of MaWSD5 in combination with MaFAR in *A. thaliana* seeds resulted in the synthesis of WE mainly derived from monounsaturated long-chain fatty acids and fatty alcohols and identifies MaWSD5 as a suitable candidate enzyme for the synthesis of WE *in planta*.

Materials and Methods

Gene Identification and Cloning into Yeast and *E. coli* Expression Vectors

The protein sequence of the WSD from *A. baylyi* ADP1 (AbWSD1, accession number: Q8GGG1) was used to perform a BLAST homology search on the *M. aquaeolei* VT8 genome sequence in the NCBI database. The search identified putative wax synthases. The corresponding genes were amplified from the genomic deoxyribonucleic acid (DNA) of *M. aquaeolei* VT8 using gene-specific primers with *HindIII/XhoI* or *HindIII/SacI* restriction sites. For protein purification, the coding sequence of MaWSD5 was cloned into *E. coli* expression vector pET28b (Novagen, Darmstadt, Germany) using the *HindIII/XhoI* restriction site, resulting in production of protein fused to a C-terminal hexahistidine-tag (his₆-tag). For expression in *Saccharomyces cerevisiae* (*S. cerevisiae*), the DNA sequences of the five MaWSD genes were cloned into pYES2/CT (Thermo Fisher Scientific) vector. For primer sequences see Table S1.

Cultivation of *E. coli* Expression Cultures and Cell Harvesting

BL21 Star™ (DE3) cells (Thermo Fisher Scientific) transformed with the pET28-MaWSD5-his₆ plasmid were cultivated for protein expression in YYP-5052 rich medium for auto-induction (Studier, 2005). Pre-cultures were set up in 20 mL lysogeny broth medium supplemented with kanamycin (25 µg/mL) and were shaken over night at 37 °C.

Main cultures were prepared by supplementing 1 L of YYP-5052-rich medium for auto-induction with kanamycin (25 µg/mL) and 5 mL pre-culture. The main cultures were shaken for 2 h to 2.5 h at 37 °C and were subsequently transferred to 16 °C, where the cultures were shaken for another 2 days. Cells were harvested by centrifugation (4000g, 25 min, 4 °C). Cell pellets were stored at -20 °C to be used for protein extraction.

Protein Purification

A cell pellet, harvested from 500 mL expression culture, was thawed and resuspended in 30 mL ion metal affinity chromatography (IMAC) buffer A (20 mM Tris pH 8.0, 150 mM NaCl, 1 mL/L 1 M phenylmethane sulfonyl fluoride (PMSF) dissolved in isopropanol, 0.1% (w/v) 3-[(3-cholamidopropyl)dimethylammonio]-1-propanesulfonate (CHAPS)). After the addition of lysozyme (Fluka Analytical, Steinheim, Germany) and DNaseI (Sigma, Germany), the cell suspension was incubated on ice for 1 h. Afterward, the solution was divided into two aliquots and each aliquot was filled up to a total volume of 25 mL with IMAC buffer A. Both aliquots were sonicated for 15 min (pulsed sonication, 40% duty cycle, output control: 4 (micro)), with an alternation of sonication phase and resting phase of 1 min. To remove cell debris, the samples were centrifuged for at least 25 min at 10,000g and 4 °C. The supernatant was used either for the two-step purification using an automated pump system or the cobalt ion-based gravity flow purification.

For the two-step purification, MaWSD5 was purified *via* its his₆-tag binding to immobilized Ni²⁺ ions. The previously obtained supernatant was applied to a prepacked 5 mL column Ni²⁺-NTA column (HisTrap™ HP Column, GE Healthcare) using an automated pump system (Äktaprime™ Plus System, GE Healthcare). The whole purification was executed with a constant flow rate of 1 mL/min. Column-bound protein was washed with IMAC buffer A after loading, followed by two additional washing steps consisting of IMAC adenosine triphosphate (ATP) buffer (20 mM Tris pH 8.0, 150 mM NaCl, 0.1% (w/v) CHAPS, 5 mM ATP, 5 mM MgCl₂) and IMAC buffer A. All washing steps were executed until the UV absorption remained stable. Loosely bound proteins were eluted from the column with a mixture consisting of 95% IMAC buffer A and 5% IMAC buffer B (20 mM Tris pH 8.0, 150 mM NaCl, 0.5 M imidazole, 0.1% (w/v) CHAPS). MaWSD5-his₆ eluted from the column by applying a mixture of 60% IMAC buffer A and 40% IMAC buffer B. The combined elution fractions, containing MaWSD5-his₆ were concentrated using a Corning® Spin-X® UF concentrator (10 kDa molecular weight cut-off, Merck KGaA) and were applied to a size exclusion chromatography (SEC) column to separate MaWSD5-his₆ from aggregates and contaminating

proteins. The chromatography was carried out using a HiLoad™ 26/60 Superdex™ S200 column (GE Healthcare) on an automated pump system (Äkta FPLC™ system, GE Healthcare). The whole purification was executed with a constant flow rate of 1 mL/min of SEC buffer (50 mM sodium phosphate pH 7.0, 150 mM NaCl, 2% (v/v) glycerol).

The cobalt ion-based gravity flow purification was adopted from the IMAC protocol of the two-step purification. The obtained supernatant was applied to a 1 mL talon metal affinity resin (Takara Clontech). After loading, the column-bound proteins were washed with 10 mL IMAC buffer A, 10 mL IMAC ATP buffer, 10 mL IMAC buffer A and 10 mL of a mixture consisting of 95% IMAC buffer A and 5% IMAC buffer B. MaWSD5-his₆ was eluted from the column with 10 times 1 mL of a mixture consisting of 60% IMAC buffer A and 40% IMAC buffer B. Elution fractions 2 and 3 were combined and used for enzymatic activity assays.

Protein concentrations were determined by Bradford assay (Bradford, 1976). Protein purity of MaWSD5-his₆ was assayed by sodium dodecyl sulfate polyacrylamide gel electrophoresis (SDS-PAGE) and western blot analysis using the tetra-His antibody (diluted 1:1000, Qiagen) followed by the anti-Mouse IgG (whole molecule)—Alkaline Phosphatase (diluted 1:15,000, Sigma).

Cultivation of *S. cerevisiae*

The quadruple mutant *S. cerevisiae* strain H1246 (Sandager et al., 2002) was used for expressing the five MaWSD. For cultivation, 20 mL single drop out medium lacking uracil and supplemented with 2% (w/v) galactose were inoculated with an overnight culture to a final optical density at 600 nm (OD₆₀₀) of 0.05. For some experiments, the cultures were supplemented with 18:1 OH (stock: 500 mM in ethanol) reaching a final concentration of 1 mM. The cultures were incubated at 30 °C for 3 days while shaking at 180 rpm. For neutral lipid analysis, 50 OD₆₀₀ units were harvested by centrifugation.

In vitro Bifunctionality Assay

The assay was modified from Stöveken et al. (Stöveken et al., 2005). Fatty alcohols and acyl-CoA were purchased from Sigma if not stated differently.

For the bifunctionality analysis, the assay was carried out with cobalt ion-based gravity flow purified protein. The reaction mixture consisted of 20 μM 16:1 OH or di-6:0-DAG, respectively (Cayman Chemical) (20 μL of 1 mM stock solution in dimethyl sulfoxide (DMSO)), 12.5 μL acyl-CoA (stock solutions in 20 mM phosphate buffer, pH 7.34) (12:0 CoA (Larodan AB): stock concentration: 0.65 mM, 16:1 CoA: stock concentration: 0.85 mM, 20:0 CoA (Avanti Polar Lipids): stock concentration: 0.53 mM; stock) and

20 μL of a 1 μg/μL protein solution in a total volume of 1 mL enzymatic activity reaction buffer (50 mM sodium phosphate buffer, pH 7.4, 150 mM NaCl). The reaction samples were incubated for 1 h at room temperature (22–25 °C). The reactions were stopped by shock-freezing the samples in liquid nitrogen and the samples were stored at –20 °C until neutral lipid extraction was performed.

Thin Layer Chromatography–Based *in vitro* Substrate Specificity Assay

The assay was modified from Stöveken et al. (2005). Fatty alcohols and acyl-CoA were purchased from Sigma if not stated differently.

For the *in vitro* substrate specificity assay, the assay was carried out with IMAC purified protein. Each reaction mixture consisted of 20 μM alcohol (40 μL of 1 mM stock solution in DMSO) (4:0 (J.T. Baker), 6:0, 8:0, 10:0, 12:0, 14:0, 16:0, 18:0, 18:1, 20:0, 22:0, 24:0, 26:0, 30:0), 25 μL acyl-CoA (stock solutions in 20 mM phosphate buffer pH 7.34) (2:0 CoA (Larodan AB): stock concentration: 1.05 mM, 4:0 CoA (Larodan AB): stock concentration: 0.89 mM, 6:0 CoA (Larodan AB): stock concentration: 0.69 mM, 8:0 CoA (Larodan AB): stock concentration: 0.94 mM, 12:0 CoA (Larodan AB): stock concentration: 0.65 mM, 14:0 CoA: stock concentration: 1.05 mM, 16:0 CoA: stock concentration: 0.27 mM, 16:1 CoA: stock concentration: 0.85 mM, 18:0 CoA (Avanti Polar Lipids): stock concentration: 0.62 mM, 18:1 CoA: stock concentration: 0.62 mM, 20:0 CoA (Avanti Polar Lipids): stock concentration: 0.53 mM) and 40 μL protein solution in a total volume of 2 mL enzymatic activity reaction buffer (50 mM sodium phosphate buffer pH 7.4, 150 mM NaCl). To analyze acyl-CoA specificities of MaWSD5-his₆, the enzyme was incubated with 18:1 OH and saturated and desaturated acyl-CoA. To analyze fatty alcohol specificities, the protein was incubated with 18:1 CoA and saturated and desaturated fatty alcohols. The reaction samples were incubated for 1 h at room temperature (20–25 °C). The reactions were stopped by shock-freezing the samples in liquid nitrogen and the samples were stored at –20 °C until neutral lipid extraction was performed.

5,5'-Dithiobis-(2-Nitrobenzoic Acid)–Based *in vitro* Substrate Specificity Assay

The assay was performed according to Barney et al. (Barney et al., 2012) while applying minor changes to the protocol. Fatty alcohols and acyl-CoA were purchased from Sigma if not stated differently.

For this assay, cobalt ion-based gravity flow purified protein was used. The reaction mixture consisted of 20 μM alcohol (20 μL of 1 mM stock solution in DMSO) (2:0 (Nordbrand Nordhausen GmbH), 4:0 (J.T. Baker), 6:0, 8:0, 10:0, 12:0, 14:0, 16:0, 16:1, 18:0, 18:1, 20:0, 22:0, 24:0, 26:0, 30:0),

12.5 μL acyl-CoA (stock solutions in 20 mM phosphate buffer pH 7.34) (2:0 CoA (Larodan AB): stock concentration: 1.05 mM, 4:0 CoA (Larodan AB): stock concentration: 0.89 mM, 6:0 CoA (Larodan AB): stock concentration: 0.69 mM, 8:0 CoA (Larodan AB): stock concentration: 0.94 mM, 12:0 CoA (Larodan AB): stock concentration: 0.65 mM, 14:0 CoA: stock concentration: 1.05 mM, 16:0 CoA: stock concentration: 0.27 mM, 16:1 CoA: stock concentration: 0.85 mM, 18:0 CoA (Avanti Polar Lipids): stock concentration: 0.62 mM, 18:1 CoA: stock concentration: 0.62 mM, 20:0 CoA (Avanti Polar Lipids): stock concentration: 0.53 mM), 10 μL of a 1 $\mu\text{g}/\mu\text{L}$ protein solution and 10 μL of 5,5'-dithiobis-(2-nitrobenzoic acid) (DTNB) (stock solution: 20 mg/mL in DMSO) in a total volume of 1 mL enzymatic activity reaction buffer (50 mM sodium phosphate buffer, pH 7.4, 150 mM NaCl). To analyze acyl-CoA specificities of gravity flow purified MaWSD5-his₆, the DTNB assay was carried out by analyzing the WE production rate of the enzyme with 18:1 OH and saturated and desaturated acyl-CoA. Alcohol specificities of MaWSD5-his₆ was analyzed in an analogous manner to the acyl-CoA specificities testing the incorporation of saturated and desaturated fatty alcohols when 18:1 CoA was provided. Except for the acyl-CoA, all components were added to a spectrophotometer cuvette and were mixed vigorously by vortexing. The reaction, performed at room temperature (22–25 °C), was started by adding acyl-CoA and mixing again vigorously by vortexing. Subsequently, absorption of the sample at 412 nm was recorded using a Cary 100 Bio spectrophotometer (Agilent Technologies). The initial slope of the obtained curve was analyzed and used to calculate WS activity *via* Lambert–Beer–Law using an extinction coefficient for DTNB of 13,600 $\text{L}/(\text{M}\cdot\text{cm})$ (Ellman, 1959). Each substrate combination was measured in triplicates (technical replicates) to determine mean values. Each substrate specificity experiment was repeated three times with freshly purified protein (biological replicates). Mean values of the biological replicates were calculated from normalized values (for the acyl-CoA specificity WS activity for 14:0 CoA was set to 1 and for the alcohol specificity WS activity for 16:1 alcohol was set to 1). Different control measurements revealed that only a WS activity above 10 nmol/(mg*min) is distinct for enzymatic catalysis. Therefore, WS activities below 10 nmol/(mg*min) were considered as background and were set to 0 nmol/(mg*min). When only one technical replicate as well as one biological repetition showed zero activity for one substrate combination the mean value for all measurements of this substrate combination was set to zero.

Neutral Lipid Extraction

For neutral lipid extraction from yeast cells, 50 OD₆₀₀ units of cell pellets were resuspended in 1 mL methanol and

vortexed with 0.5 mm glass beads for 15 min. Then, additional 2 mL hexane was added and the sample was again vortexed for 15 min. The polar and nonpolar phases of the sample were separated by centrifugation for 10 min. The upper nonpolar phase was transferred to a new vial and solvent was evaporated under a nitrogen stream. The sample was resolved in 200 μL hexane for further analysis by thin layer chromatography (TLC).

For samples derived from the *in vitro* bifunctionality assay and the TLC-based *in vitro* substrate specificity assay, neutral lipids including WE and TAG were extracted from the aqueous solution using a methanol/chloroform-based extraction according to Bligh and Dyer (Bligh and Dyer, 1959). To 1 mL reaction mixture, 1 mL of methanol and 1 mL of chloroform were added, as well as an internal extraction standard. For the *in vitro* bifunctionality assay, 5 μg WE or 5 μg cholesterol was used as internal standard for the respective samples (di-17:0-WE or cholesterol, stock solutions: 1 mg/mL in chloroform). For the TLC-based *in vitro* substrate specificity assay, 12 μg TAG was used as an internal standard (tri-15:0-TAG, stock solution: 0.4 mg/mL in toluol). The samples were shaken for 15 min at 4 °C. After a centrifugation step (10 min, 450g, 4 °C), the lower chloroform phase was transferred to a new vial and again 1 mL chloroform was added to the remaining upper phase. The samples were shaken a second time for 15 min at 4 °C and were centrifuged (10 min, 450g, 4 °C) subsequently. The obtained lower chloroform phase was combined with the first lower phase and chloroform was evaporated under a nitrogen stream. The extracted neutral lipids were resolved in 50 μL hexane to perform TLC.

Thin Layer Chromatography

For TLC analysis of yeast samples, 50 μL of yeast lipid extracts were applied on TLC silica plate (TLC Silica gel 60, 20 × 20 cm, Merck Millipore) with the assistance of an automatic TLC sampler (CAMAG). For the TLC-based *in vitro* substrate specificity assay, 25 μL lipid extract was applied on the TLC plate with the assistance of the TLC sampler. For samples from the *in vitro* bifunctionality assay, 50 μL lipid extracts were spotted on the TLC silica plate by hand. The TLC plates were developed with hexane/diethyl ether/acetic acid (80:20:1, v/v/v) as running solvent. Bands of neutral lipids were visualized by dipping the plate into a CuSO₄ solution (10% (w/v) CuSO₄, 6.8% (v/v) phosphoric acid) and subsequent heating of the plate to up to 190 °C.

Generation of Transgenic *A. thaliana* Plants

For simultaneous transformation of MaFAR and MaWS5 into *A. thaliana*, a binary transformation vector was generated using Gateway technology (Thermo Fisher Scientific) as described before (Heilmann et al., 2012).

A gene construct consisting of the MaFAR sequence (Accession Number: WP_011785687.1) optimized for *E. coli* codon usage and N-terminally fused to the coding sequence of yellow fluorescent protein (YFP) and myc tag was cloned into a pENTRY B vector carrying a β -conglycinin promoter (pENTRYB- β con::YFP::myc::MaFAR) via *SalI/BamHI* restriction sites. A gene construct consisting of the MaWSD5 sequence (Accession Number: ABM20482.1) N-terminally fused to the coding sequence of cyan fluorescent protein (CFP) and flag tag was cloned into a pENTRY C vector carrying a glycinin promoter (pENTRYC-gly::CFP::flyg::MaWSD5) via *XhoI/BglIII* restriction sites. For primer sequences, see Table S1. After performing the clonase reaction with the pENTRY B and C vectors together with an empty pENTRY A vector and a destination vector (pCAMBIA33) the binary vector MaFAR/MaWSD5: pCAMBIA33- β con::YFP::myc::MaFAR/gly::CFP::flyg::MaWSD5 was obtained.

Transgenic *A. thaliana* plants were generated through *Agrobacterium tumefaciens*-mediated transformation of *A. thaliana* ecotype Col-0 via floral dipping. Selection of transgenic plants was performed by herbicide treatment (Basta, Bayer CropScience).

Screening of Transgenic *A. thaliana* Plants

Screening of transgenic *A. thaliana* plants was performed as described previously (Iven et al., 2013). Neutral lipids extracted from seeds and separated by TLC were visualized by dipping the plate into a CuSO₄ solution (10% (w/v) CuSO₄, 6.8% (v/v) phosphoric acid) and subsequent heating of the plate to up to 190 °C.

Analysis of WE Species by Nano-Electrospray Ionization Tandem Mass Spectrometry (nanoESI-MS/MS)

WE analysis was performed by nanoESI-MS/MS with a 6500 QTRAP[®] tandem mass spectrometer (AB Sciex) as previously described (Iven et al., 2013).

Results

M. aquaeolei VT8 Possesses a Fifth WSD

To identify new WSD enzymes in the bacterium *M. aquaeolei* VT8, a BLAST homology search on the genome of *M. aquaeolei* VT8 using the amino acid sequence of AbWSD1 was performed. In addition to the four already known and partly characterized WSD MaWSD1, MaWSD2, MaWSD3, and MaWSD4 (Barney et al., 2012, 2013, 2015; Petronikolou and Nair, 2018; Röttig et al., 2016; Villa et al., 2014), a

putative fifth WSD (MaWSD5, Maqu_3411) was identified. While characterizing MaWSD5, the existence of the protein was also mentioned in a book chapter (Knutson et al., 2017).

The MaWSD5 gene encodes for a 452 amino acids long protein, which shares around 19% sequence identity with AbWSD1 and 23–24% sequence identity with MaWSD1, MaWSD2, and MaWSD3 (Table 1). MaWSD5's closest homolog is MaWSD4, sharing 33% sequence identity. The conserved catalytic HHxxxDG motif of WSD enzymes is present in MaWSD5 (H123 H124 C125 Y126 A127 D128 G129) as well as the three conserved regions identified by Villa and co-workers (PLW, ND, R) (Villa et al., 2014). However, in MaWSD5 the leucine of the PLW motif is exchanged to an arginine (P102 R103 W104, N259 D260, and R295).

His₆-Tagged MaWSD5 Can Be Purified to Homogeneity

Most bacterial WSD are most likely soluble but membrane-associated proteins (Stöveken et al., 2005). Successful purifications are published for several WSD, including AbWSD1, MaWSD1 and MaWSD2 (Barney et al., 2012; Holtzapfle and Schmidt-Dannert, 2007; Petronikolou and Nair, 2018; Röttig et al., 2016; Stöveken et al., 2005; Villa et al., 2014). An analysis of MaWSD5 with the public available online tool TMHMM Server, v. 2.0 (Krogh et al., 2001; Sonnhammer et al., 1998) revealed, that the protein does not contain any hydrophobic regions similar to MaWSD1 and in contrast to MaWSD2, MaWSD3, and MaWSD4 (Fig. S1).

Using the pET28 expression system, it was possible to express MaWSD5 heterologously in the *E. coli* expression strain BL21 Star[™] (DE3) with a C-terminally his₆-tag. Although MaWSD5 is predicted to harbor no transmembrane domains or hydrophobic regions, a predominant portion of the protein remained in the pellet after cell lyses and centrifugation. Nevertheless, the supernatant contained reasonable amounts of MaWSD5-his₆ to perform protein purification. By applying a two-step purification protocol consisting of IMAC and SEC, it was possible to purify MaWSD5-his₆ to homogeneity (Fig. 1). Best purification results were obtained, when IMAC buffers were supplemented with 0.1% (w/v) of the detergent CHAPS and when 2% (v/v) glycerol was added to the SEC buffer. By performing an additional IMAC washing step with 5 mM ATP and 5 mM MgCl₂ the purity of MaWSD5-his₆ could be increased even more. The usage of ATP and MgCl₂ to remove chaperons from linker regions or unfolded parts of resin-bound fusion proteins was described by Rial and Ceccarelli before (Rial and Ceccarelli, 2002).

SDS-PAGE analyses revealed that MaWSD5-his₆ can be enriched to a high degree by IMAC and can be further purified by SEC (Fig. 1c). From the elution volume of

Table 1 Multiple sequence alignment of AbWSD1 and the five MaWSD

Enzyme	AbWSD1	MaWSD1	MaWSD2	MaWSD3	MaWSD4	MaWSD5
AbWSD1 ^{aa}	100	—	—	—	—	—
MaWSD1 ^{bb}	45.2	100	—	—	—	—
MaWSD2 ^{cc}	37.2	38.0	100	—	—	—
MaWSD3 ^{dd}	27.1	28.4	30.5	100	—	—
MaWSD4 ^{ee}	20.4	23.8	24.1	22.5	100	—
MaWSD5 ^{ff}	18.9	22.9	24.1	24.0	32.7	100

The numbers show the peptide sequence identity (% ID) to related enzymes. The analysis was conducted using multiple sequence alignment MUSCLE online service (Madeira et al., 2019).

^aGenBank: AAO17391.1, 458 amino acids.

^bGenBank: ABM17275.1 (Maqu_0168), 455 amino acids.

^cGenBank: ABM20141.1 (Maqu_3067), 473 amino acids.

^dGenBank: ABM17947.1 (Maqu_0851), 504 amino acids.

^eGenBank: ABM20442.1 (Maqu_3371), 472 amino acids.

^fGenBank: ABM20482.1 (Maqu_3411), 452 amino acids.

MaWSD5-his₆ (51.2 kDa) of 200 mL it was assumed, that the protein eluted as a dimer. The activity of the purified protein was tested. Purified MaWSD5-his₆ is able to produce WE from stearidonyl alcohol (18:0 OH) and oleyl-CoA (18:1 CoA) (data not shown). Unfortunately, the enzymatic activity of MaWSD5-his₆ decreased upon and shortly after purification, making the two-step purification protocol not suitable for obtaining protein for enzymatic activity assays. Therefore, a shorter purification protocol was established consisting of IMAC only. By switching from the automated pump system-based purification to gravity flow purification and a smaller column volume, the time required to perform IMAC decreased. The shorter protocol is suitable to enrich MaWSD5-his₆ compared to lysate and to obtain active protein, which can be used for enzymatic activity analyses directly after purification (SDS-PAGE gravity flow purification, Fig. S2).

MaWSD5 Is a Monofunctional Enzyme

WSD enzymes are described as bifunctional enzymes, being able to catalyze the formation of WE and TAG. However, within the class of WSD enzymes not all characterized proteins are bifunctional. Some enzymes are only able to produce WE (Kalscheuer et al., 2007; King et al., 2007) and some enzymes can only catalyze the formation of TAG (Arabolaza et al., 2008; Daniel et al., 2004).

To analyze WS and DGAT activity of MaWSD5 and compare the enzyme with the other four MaWSD, all five MaWSD were heterologously expressed in *S. cerevisiae* H1246 (Sandager et al., 2002). This strain is deficient in TAG and steryl ester biosynthesis. For the assay, yeast cells expressing the proteins were cultivated in the presence or

absence of oleyl alcohol (18:1 OH) since *S. cerevisiae* H1246 is not able to synthesize fatty alcohols. 18:1 OH was chosen, since it is the second most abundant fatty alcohol present in the neutral lipid fraction of *M. aquaeolei* VT8 and more soluble in ethanol compared to the slightly more abundant palmitoyl alcohol (16:0 OH) (Barney et al., 2012). After 3 days of cultivation, the cells were harvested and neutral lipid extraction was performed. Fig. 2 depicts, WE formation was observed for MaWSD1, MaWSD2, and MaWSD5 when the media was supplemented with 18:1 OH. TAG formation however was only detected for MaWSD1. For MaWSD3 no activity was observed upon expression in yeast. In addition to WE and TAG, other reaction products of MaWSD were visible on the TLC plates. In MaWSD1 expressing yeast cells, three unknown substances (U1, U2, and U3) were synthesized independently from supplementing the media with fatty alcohol or not. In the MaWSD4 sample, U3 was formed only when the media was not supplemented with fatty alcohol. MaWSD5 forms a fourth unknown substance (U4) in the presence of exogenous fatty alcohol. Further analysis of the unknown compounds by gas chromatography coupled to mass spectrometry (GC-MS) revealed no conclusive results.

The yeast experiment revealed that MaWSD5 is able to synthesize WE. However, *in vivo* TAG production was neither observed in cultures with nor without supplemented fatty alcohol. To investigate further, whether MaWSD5 lacks DGAT activity *in vitro* as well, an *in vitro* bifunctionality assay was performed. Gravity flow purified MaWSD5-his₆ was incubated for 1 h with palmitoleyl alcohol (16:1 OH) or di-hexanoyl-diacylglycerol (di-6:0-DAG) and with acyl-CoA of different chain lengths and unsaturation degree. Fig. 3 depicts that only WE production but no TAG formation was observed.

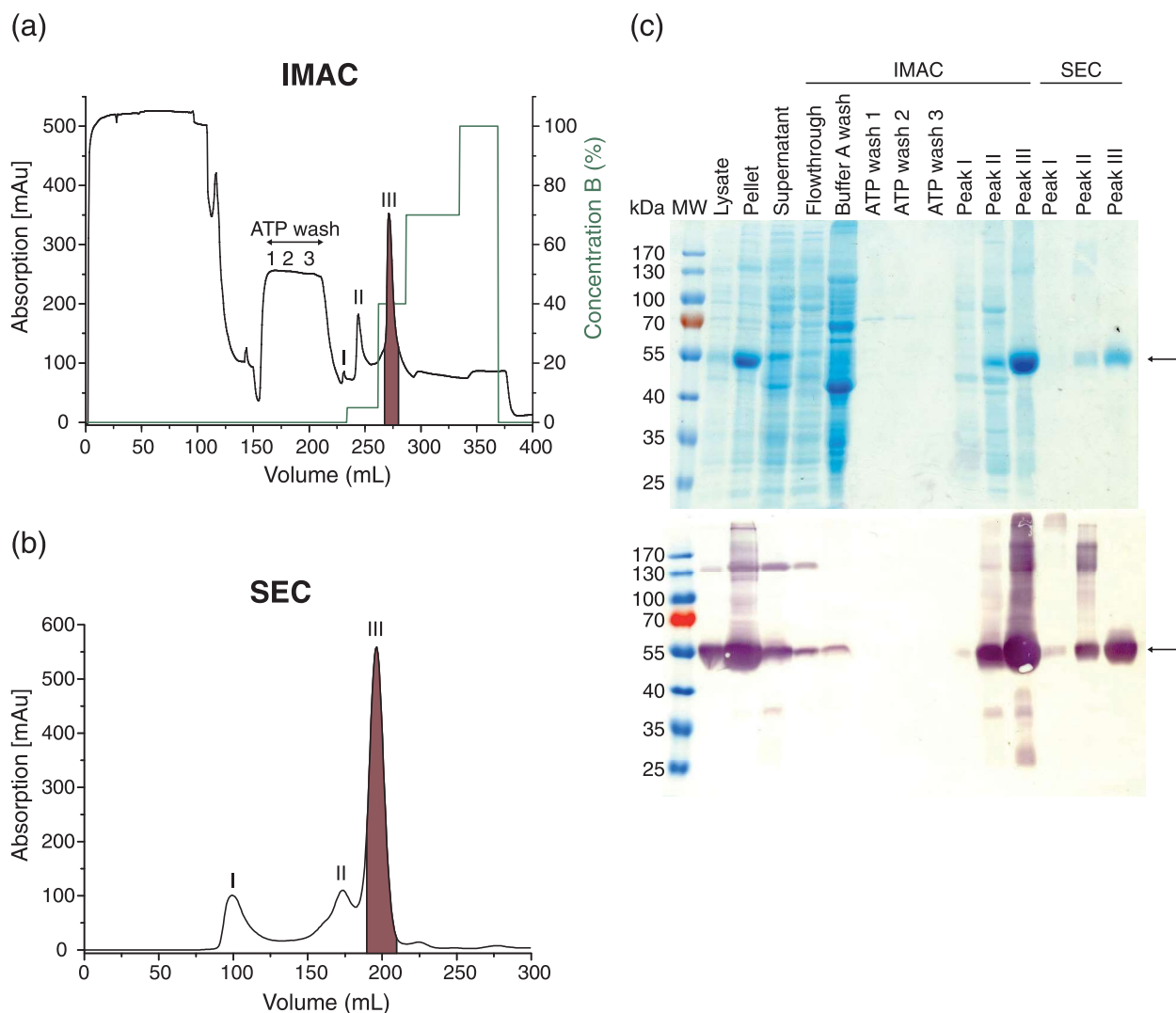


Fig 1 Two-step purification of his₆-tagged MaWSD5. (a) To purify MaWSD5, BL21 Star™ (DE3) cells expressing C-terminally his₆-tagged MaWSD5 were lysed in IMAC buffer A (20 mM Tris pH 8.0, 150 mM NaCl, 1 mL/L PMSF, 0.1% CHAPS) by using lysozyme and sonication. The soluble fraction was applied to the IMAC column (HisTrap™ HP, 5 mL, GE Healthcare) after centrifugation. Before elution, the column was washed with IMAC buffer A and IMAC ATP buffer (20 mM Tris pH 8.0, 150 mM NaCl, 0.1% CHAPS, 5 mM ATP, 5 mM MgCl₂). Contaminating proteins were eluted from the column with 5% IMAC buffer B (20 mM Tris pH 8.0, 150 mM NaCl, 0.5 M imidazole, 0.1% CHAPS) (peak I and II). MaWSD5-his₆ was finally eluted with 40% IMAC buffer B (peak III, highlighted in purple). (b) The combined and concentrated MaWSD5-his₆ IMAC fractions were subsequently applied to the SEC column (HiLoad™ 26/60 Superdex™ S200, GE Healthcare) to separate MaWSD5-his₆ (peak III, highlighted in purple) from aggregates (peak I) and contaminating protein (peak II) (SEC buffer: 50 mM sodium phosphate buffer pH 7.0, 150 mM NaCl, 2% (v/v) glycerol). (c) Different fractions of the two-step purification were analyzed by SDS-PAGE and western blot analysis: 3 μL pre-stained protein ladder (MW: molecular weight, size of the protein standards in kDa), 7.5 μL 1:50 (v/v) diluted lysate, 7.5 μL 1:100 (v/v) diluted pellet, 7.5 μL 1:2 (v/v) diluted supernatant, 7.5 μL 1:2 (v/v) diluted flowthrough, 7.5 μL 1:2 (v/v) diluted IMAC buffer A wash and 6 μL of all other analyzed fractions were applied to the gel. All samples were mixed with 4× Laemmli buffer before loading on the gel (2.5 and 2 μL, respectively). Bands corresponding to MaWSD5-his₆ (51.2 kDa) are marked by black arrows. The figures are representative for two purifications

MaWSD5 Prefers to Produce WE from Monounsaturated Long-Chain Acyl Substrates

There are two studies published within the last years investigating the usage of bacterial WSD to produce industrial lubricants in plants (Ruiz-Lopez et al., 2017; Yu et al., 2018). Researchers are especially interested to

identify combinations of WE synthesizing enzymes that produce WE consisting of long chain monounsaturated fatty acid and fatty alcohol moieties. Those WE have favorable lubrication properties.

To investigate whether MaWSD5 is suitable for industrial WE production and is able to synthesize the requested WE species, two *in vitro* substrate specificity assays were

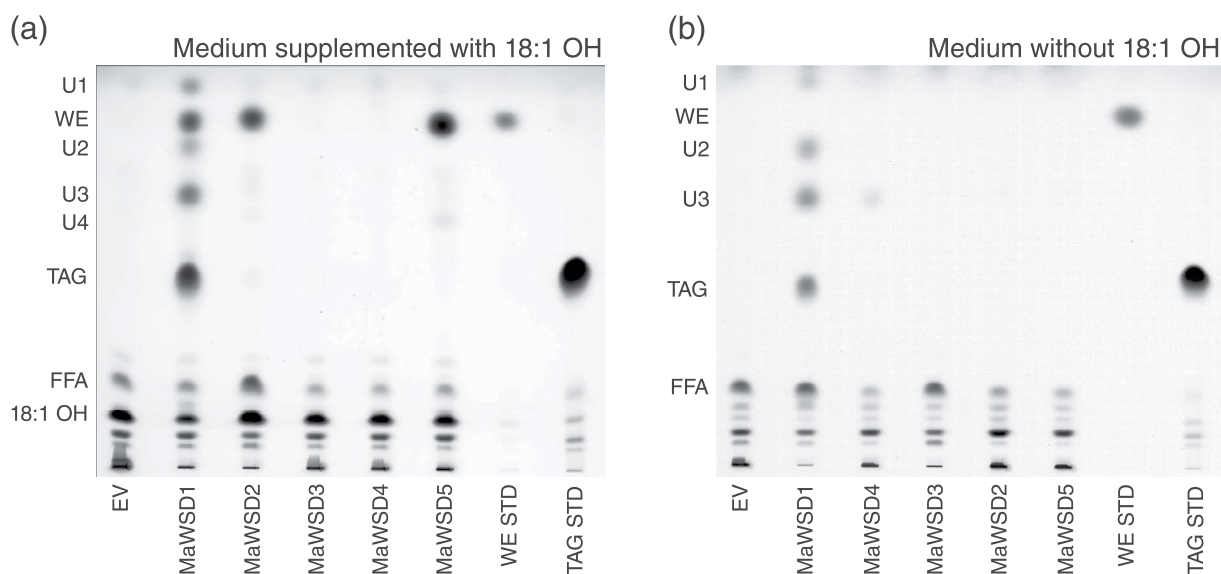


Fig 2 Accumulation of neutral lipids in *S. cerevisiae* H1246 expressing five different MaWSD. *S. cerevisiae* H1246 cells expressing either one of the MaWSD or empty vector (EV) were grown for 3 days either in medium supplemented with 18:1 OH (a) or medium without 18:1 OH (b). Neutral lipids extracted from the harvested yeast cells were separated by TLC. The TLC plates are representative for three experiments yielding the same results. FFA, free fatty acids; TAG, triacylglycerol; TAG STD, olive oil; U1–U4, unknown compound; WE, wax ester; WE STD, di-17:0-WE standard

performed to analyze acyl-CoA and fatty alcohol specificities of the enzyme. For the first assay, a TLC-based *in vitro* substrate specificity assay, IMAC purified MaWSD5-his₆ was incubated for 1 h with different combinations of acyl-CoA and fatty alcohols. Subsequent to that neutral lipids were extracted from the reaction mix, and then separated and visualized on a TLC plate (Fig. S3). Second, a DTNB-based *in vitro* substrate specificity assay was performed as already used for the characterization of other WSD (Fig. S4) (Barney et al., 2012). The assay is based on the spectrophotometric measurement of the released CoA-SH, which is generated upon WE production. Both performed *in vitro* substrate specificity assays revealed that MaWSD5-his₆ is able to incorporate saturated acyl-CoA from 4:0 to 20:0, as well as palmitoleyl-CoA (16:1 CoA) and 18:1 CoA into WE. The protein can also synthesize WE with fatty alcohols from 6:0 to 18:0, as well as using 16:1 OH and 18:1 OH.

Since the *in vitro* substrate specificity assays revealed that MaWSD5-his₆ can use saturated and monounsaturated mid- and long-chain acyl-CoA and fatty alcohols as substrates, the capability of the enzyme to produce WE in *A. thaliana* seeds, was tested.

Transgenic *A. thaliana* plants were generated expressing N-terminally YFP- and myc-tagged MaFAR under the control of the seed specific β -conglycin promoter together with N-terminally CFP- and flag-tagged MaWSD5 under the

control of the glycinin promoter (MaFAR/MaWSD5). MaFAR (Maqu_2220) (Hofvander et al., 2011) was already successfully used in combination with other WS(D) to produce WE in *A. thaliana* and *C. sativa* seeds (Iven et al., 2016; Ruiz-Lopez et al., 2017; Yu et al., 2018).

Transgenic MaFAR/MaWSD5 *A. thaliana* plants were screened *via* TLC for high WE content in seeds (data not shown). Five independent transgenic lines, showing the highest WE amounts on TLC plate, were further investigated by nanoESI-MS/MS regarding the WE amounts and the WE species that were produced. Fig. 4a shows that seeds of MaFAR/MaWSD5 line 4 contained most WE of all five lines with 19.8 ± 0.7 mg/g seed followed by line 7 with $14.2 \pm 1.2 \times$ mg/g seed. For lines 2, 5 and 10, WE amounts of 9.4 ± 0.2 , 6.9 ± 0.1 and 4.7 ± 0.4 mg/g seed, respectively, were determined.

Fig. 4b depicts the top 20 WE species that were synthesized in transgenic MaFAR/MaWSD5 seeds. The two main WE generated are 20:1/18:1 (fatty alcohol moiety / fatty acid moiety) and 20:1/20:1 with 11 and 10 mol %, respectively. A closer look at the top 20 produced WE species revealed that the used MaFAR/MaWSD5 combination favors to synthesize WE from monounsaturated long chain fatty alcohols and activated fatty acids (Fig. 4c and Fig. 4d). On the site of the fatty alcohol moiety, chains with 20 carbons as well as chains with one double bond are favored. On the site of the fatty acid moiety acyl chains with 18

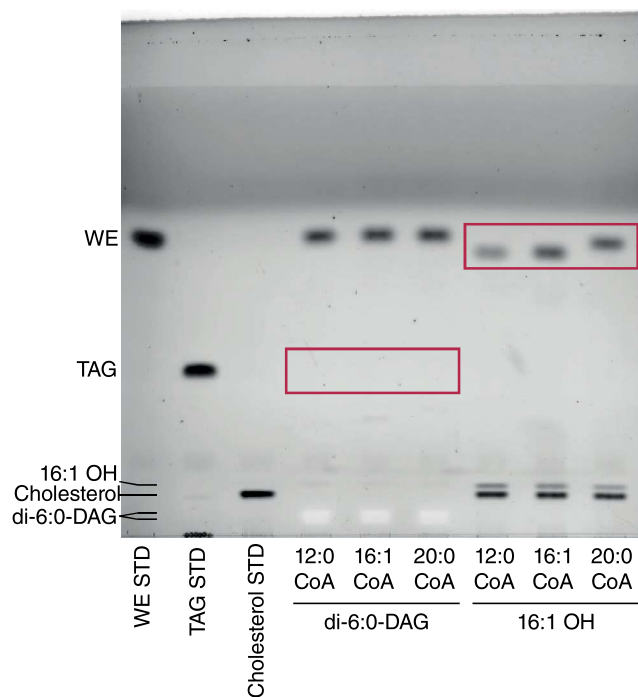


Fig 3 *In vitro* bifunctionality assay of his₆-tagged MaWSD5. Gravity flow purified recombinant MaWSD5-his₆ was used to analyze the capability of the enzyme to produce WE and TAG *in vitro*. Each reaction was carried out with 20 μg purified MaWSD5-his₆, 20 μM 16:1 OH or di-6:0-DAG and 12.5 μL acyl-CoA (for exact concentration see Materials and Methods section) in a total volume of 1 mL reaction buffer (50 mM sodium phosphate buffer pH 7.4, 150 mM NaCl). The reaction samples were incubated for 1 h at room temperature. After stopping the reaction by shock-freezing in liquid nitrogen, the samples were stored at −20 °C. Neutral lipid extraction was performed as described in the Materials and Methods section, followed by separation *via* TLC. To assign bands on the TLC plate, 10 μg of each standard (TAG (triacylglycerol, tri-15:0-TAG), WE (wax ester, di-17:0-WE), and cholesterol) were also spotted on the plate. Red boxes mark the positions of WE and TAG bands. The assay was performed once

carbons are preferred to be incorporated into WE as well as monounsaturated acyl chains.

Discussion

In the present study, a fifth WSD was identified in the bacterium *M. aquaeolei* VT8. The protein shares between 23% to 33% sequence identity to other MaWSD and can be purified to homogeneity. Expression of MaWSD5 in yeast and a performed *in vitro* bifunctionality assay revealed that the enzyme is monofunctional, being only able to catalyze the formation of WE and not of TAG *in vivo* and *in vitro*. *In vitro* substrate specificity assays showed that MaWSD5-his₆ favors saturated and monounsaturated mid and long-chain

acyl-CoA and fatty alcohols making the enzyme an excellent candidate for WE production *in planta*. First analyses of transgenic *A. thaliana* seeds expressing MaFAR and MaWSD5 displayed that the produced WE mainly derived from monounsaturated long-chain fatty acids and fatty alcohols.

MaWSD5 is predicted to be a soluble protein. An analysis with the TMHMM Server, v 2.0 revealed neither transmembrane domains nor hydrophobic regions in MaWSD5 (Fig. S1). The TMHMM analysis showed a similar result for MaWSD1. In contrast to that, hydrophobic regions were identified in MaWSD2, MaWSD3, and MaWSD4. However, although no hydrophobic regions were identified in MaWSD5 and the enzyme can be purified to homogeneity when fused to a his₆-tag, a large portion of the protein remained in the cell pellet after cell lyses and centrifugation, pointing toward a hydrophobic character of MaWSD5. Similar to that, a hydrophobic character was also observed for MaWSD1 despite of no identification of hydrophobic regions by the TMHMM analysis (Barney et al., 2012; Knutson et al., 2017). Purification of MaWSD1 could be improved by protein fusion to solubility enhancing tags (Barney et al., 2012; Knutson et al., 2017). AbWSD1 is another soluble protein with hydrophobic character (Stöveken et al., 2005). Upon purification of AbWSD1, only 40–50% of the protein remained in the soluble fraction after cell lysis and centrifugation (Stöveken et al., 2005). Analysis of subcellular fractions and localization studies of AbWSD1 within *A. baylyi* cells revealed furthermore that the enzyme is soluble to some extent and present in the cytosol, but is predominantly membrane associated or localizes to lipid inclusions (Stöveken et al., 2005). The soluble but hydrophobic nature of WSD is advantageous for the proteins having in mind the amphipathic nature of the substrates and products of WSD. Due to the large CoA or ACP part, acyl-CoA/ACP are soluble in the cytosol. However, long-chain fatty alcohols are insoluble and therefore localize to membranes, while WSD reaction products, WE and TAG, are stored in lipid droplets (Nettebrock and Bohnert, 2020).

The sequence identities of MaWSD5 to AbWSD1 and other MaWSD as well as the presence of the conserved catalytic HHxxDG motif in MaWSD5 assigned the protein to the group of bifunctional WSD enzymes. MaWSD5 is able to synthesize WE when expressed in yeast and during *in vitro* activity assays. Although exhibiting WS activity, MaWSD5 lacks DGAT activity *in vivo* and *in vitro*. This strongly suggests that MaWSD5 is a monofunctional enzyme similar to AtFA2 from *Alcanivorax borkumensis* SK2 (Kalscheuer et al., 2007) and WS1 from *Petunia hybrid* (King et al., 2007). The here performed yeast experiment revealed that MaWSD2 is a monofunctional WSD as well. This is in contrast to observations made by Villa and

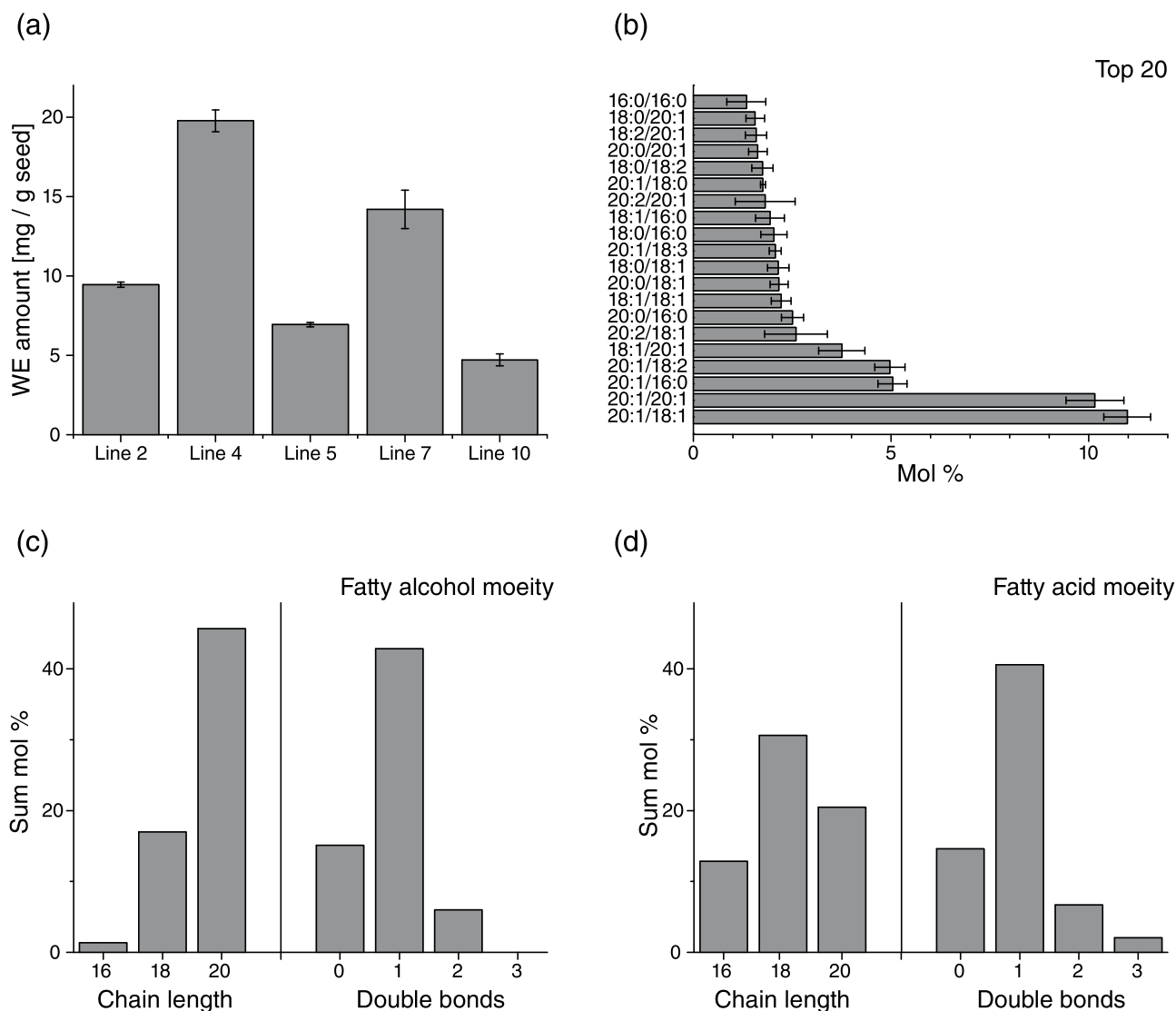


Fig 4 Analysis of synthesized molecular WE species in MaFAR/MaWSD5 *A. thaliana* seeds. Neutral lipids were extracted from seeds of five independent *A. thaliana* MaFAR/MaWSD5 lines. WE were separated from other extracted neutral lipids by TLC and molecular WE species were analyzed by nanoESI-MS/MS. (a) WE amount in mg/g seed in the different independent *A. thaliana* MaFAR/MaWSD5 lines. Error bars represent SD of three nanoESI-MS/MS measurements of one extraction. (b) Top 20 WE species (fatty alcohol moiety / fatty acid moiety) according to their occurrence in mol %. Error bars represent SD of five independent plant lines. The experiment was conducted once. (c) Chain length and desaturation specificity on the fatty alcohol moiety. Values were obtained by summing up the average mol % of the individual top 20 WE species (shown in b) having the depicted chain length (left panel) or desaturation degree (right panel) in the fatty alcohol moiety. As average values from five independent plant lines were summed up, no error bars are shown. (d) Chain length and desaturation specificity on the fatty acid moiety. Values were obtained by summing up the average mol % of the individual top 20 WE species (shown in b) having the depicted chain length (left panel) or desaturation degree (right panel) in the fatty acid moiety. As average values from five independent plant lines were summed up, no error bars are shown.

co-workers, who reported *in vitro* DGAT activity for MaWSD2 (Villa et al., 2014). Differences between *in vivo* and *in vitro* activities were also observed for WS2 from *M. hydrocarbonoclasticus* DSM 8798 (Holtzapfel and Schmidt-Dannert, 2007; Röttig et al., 2015). The enzyme, which only differs from MaWSD2 in one amino acid, lacked DGAT activity *in vitro* but was able to produce trace

amounts of TAG upon expression in *E. coli*. Similar holds true for WSD1 from *A. thaliana* (Li et al., 2008). The enzyme was able to produce WE and TAG *in vitro*. But expression of the protein in *S. cerevisiae* H1246 did not lead to TAG production in detectable amounts.

In contrast to MaWSD5 and MaWSD2, TAG production was observed for MaWSD1 upon expression in yeast in

this study. The result is in line with other publications describing MaWSD1 and MhWS1 as bifunctional WSD (Barney et al., 2012; Holtzaple and Schmidt-Dannert, 2007; Petronikolou and Nair, 2018). MaWSD3 did not show any activity when expressed in *S. cerevisiae* H1246. Holtzaple and co-workers reported no WS or DGAT activity for MhWS3 as well (Holtzaple and Schmidt-Dannert, 2007). The same study described a truncated open reading frame for MhWS4, whereas the open reading frame for MaWSD4 was found to be intact (Holtzaple and Schmidt-Dannert, 2007). Although MaWSD4 did not produce WE or TAG in the here conducted experiments, to our knowledge this study is the first one showing activity for MaWSD4, producing an unknown compound (U3).

The ability to produce compounds apart from WE or TAG upon expression in yeast was observed for MaWSD1 and MaWSD5, too. Analysis of the unknown substances using GC-MS remained inconclusive and was not further pursued. Other WSD were shown to use additional substrates beside acyl-CoA/ACP, fatty alcohol and DAG (Barney et al., 2015; Holtzaple and Schmidt-Dannert, 2007; Miklaszewska et al., 2018; Stöveken et al., 2005). The reported substrates are hydroxylated or isoprenoid CoA esters as acyl donors and hydroxylated, cyclic, aromatic, or isoprenoid alcohols as well as isoamyl alcohol or monoacylglycerol as acyl acceptors (Holtzaple and Schmidt-Dannert, 2007; Stöveken et al., 2005). The term “bifunctional” for WSD referring to the ability to produce WE and TAG seems therefore rather narrow for a class of enzymes that catalyzes the acylation of different organic substances.

The here performed *in vitro* substrate specificity assays revealed that MaWSD5-his₆ can use saturated and desaturated mid- and long-chain acyl-CoA and fatty alcohols as substrates for WE synthesis. Polyunsaturated substrates were not tested. The usage of saturated and desaturated mid- and long-chain acyl-CoA and fatty alcohol substrates is a common feature of characterized WSD; however, not in all analyses polyunsaturated substrates were tested (Barney et al., 2012, 2013; Holtzaple and Schmidt-Dannert, 2007; Shi et al., 2012; Stöveken et al., 2005). Stöveken and co-workers reported that AbWSD1 favors saturated fatty alcohols ranging from 12 to 18 carbons in chain length and also showed a high preference for 18:1 OH in *in vitro* activity assays using 16:0 CoA as acyl donor (Stöveken et al., 2005). On the acyl-CoA site, the protein had highest WS activity using 14:0, 16:0, 16:1, and 18:0 CoA in combination with 16:0 OH (Stöveken et al., 2005). MhWS2 preferred saturated alcohols ranging from 10 to 16 carbons in chain length as well as 16:0, 18:0, 18:3, and 20:0 CoA to incorporate into WE (Holtzaple and Schmidt-Dannert, 2007). It has to be noted that the specificity for 18:0 and 18:3 CoA was similar (Holtzaple and Schmidt-Dannert, 2007). A detailed substrate specificity analyses on yeast microsomal MhWS2 that also included polyunsaturated

substrates with 18 carbon in chain length, revealed that the enzyme favors to synthesize WE from saturated acyl-CoA of carbon chain length 12–18 and 18:1 CoA (Miklaszewska et al., 2018). On the fatty alcohol site, MhWS2 preferred the synthesis of WE using fatty alcohols ranging from 10 to 18 carbons in chain length and including also the unsaturated fatty alcohols 16:1 OH, 18:1 OH, 18:2 OH, and 18:3 OH as acyl acceptors (Miklaszewska et al., 2018). Interestingly, the authors of the study observed clear differences in the specificity of MhWS2 between saturated and corresponding desaturated fatty alcohols of 18 carbons and longer chain length (Miklaszewska et al., 2018). Thus, the specific activity of MhWS2 was higher with 18:1 OH, 18:2 OH, or 18:3 OH compared to 18:0 OH and WS activities with fatty alcohols longer than 18 carbons in chain length were predominately observed with monounsaturated fatty alcohols and almost not with the corresponding saturated ones (Miklaszewska et al., 2018). A similar specificity was observed in the here presented study. MaWSD5-his₆ had a higher WS activity with 18:1 OH compared to 18:0 OH and no WS activity was observed for saturated fatty alcohols of 20 carbons chain length or longer. This observation might be either explained by a different solubility of saturated and desaturated fatty alcohols which can affect the accessibility of the substrate for the enzyme or by spatial limitations of the fatty alcohol binding site (Barney et al., 2013, 2015; Petronikolou and Nair, 2018). The binding site might allow only the binding of fatty alcohols with a certain chain length. Longer monounsaturated acyl chains might still bind, as they are not as rigid as saturated ones due to their kinked structure and higher flexibility in their acyl chain orientation. A comparison of fatty alcohol specificities of a mouse WS and four different WSD (AbWSD1, MhWS2, WS from *Rhodococcus opacus* PD630 and WS from *Psychobacter articus* 273–4) revealed that the analyzed WSD had a preference for mid- and long-chain fatty alcohols (AbWSD1: 12:0 OH—18:0 OH, MhWS2: 8:0 OH—18:0 OH, WS from *Rhodococcus opacus* PD630: 8:0 OH—18:0 OH, WS from *Psychobacter articus* 273–4: 10:0 OH—18:0 OH) when saturated substrates were tested (Shi et al., 2012). Another study comparing substrate specificities of five WSD (MaWSD1, MaWSD2, AbWSD1, Ps1 from *Psychobacter cryohalolentis* K5, and Rh1 from *Rhodococcus jostii* RHA1) was described by Barney and co-workers (Barney et al., 2012). Analyzing the incorporation of saturated substrates into WE, the tested enzymes had a preference for 16:0 and 14:0 CoA, as well as for 12:0 CoA in case of MaWSD2 and 12:0 and 10:0 CoA in case of Ps1. On the fatty alcohol site, all enzymes favored fatty alcohols ranging from 10 to 14 carbons chain length. The low WE production with 16:0, 17:0, and 18:0 OH, which was also observed by Barney and co-workers in another study of AbWSD1 and MaWSD1 is in contrast to the before mentioned studies (Barney et al., 2013). However, observed differences in substrate specificities

might be due to different experimental set-ups. Whereas in the first mentioned studies WS activities were tested by providing a substrate combinations consisting only of one acyl donor and one acyl acceptor, the two studies of Barney and co-workers analyzed the substrate specificities when providing one acyl donor and several acyl acceptors or *vice versa* at the same time.

Due to its preference for mid- and long-chain substrates, MaWSD5 was expressed in combination with MaFAR in developing *A. thaliana* seeds in order to analyze, whether this WSD might be a suitable candidate for the synthesis of industrial lubricants *in planta*. Especially WE formed from monounsaturated long-chain substrates are requested as industrial lubricants due to their excellent melting temperature and oxidation stability. One highly desired candidate is the 18:1/18:1 WE that was obtained mostly from sperm whale in former times (Heilmann et al., 2012). First analysis of transgenic *A. thaliana* seeds expressing MaFAR and MaWSD5 revealed that indeed WE can be produced by the enzyme combination and that the synthesized WE mainly derived from monounsaturated long-chain fatty acids and fatty alcohols. The main WE species that were produced are 20:1/18:1 and 20:1/20:1. Both species account to more than one fifth of all molecular WE species.

When evaluating the suitability of enzyme combinations for industrial WE production, two major points are taken into consideration: the WE species, that are produced and the overall amount of formed WE.

Evaluating the WE species synthesized by the different enzyme combinations, the substrate specificities of both enzymes have to be taken into consideration. While the preference to use certain acyl-CoA/ACP is only influenced by the WS(D), the preference to incorporate certain fatty alcohols into WE is also influenced by the FAR expressed. The FAR displays the bottle neck being important for which fatty alcohols are provided to the WS(D). The here tested MaFAR/MaWSD5 combination expressed in *A. thaliana* favors to incorporate monoenoic fatty alcohols with 20 carbon chain length and monoenoic fatty acids with 18 carbon chain length. This is in accordance with other tested FAR/WS(D) combinations expressed either in *A. thaliana* or *C. sativa* seeds, which resulted in similar fatty acid and fatty alcohol specificities (Iven et al., 2016; Ruiz-Lopez et al., 2017; Yu et al., 2018). With the exception for FAR and WS from mouse, in most cases, monoenoic fatty alcohols with 18 or 20 carbon chain length are preferred (Iven et al., 2016; Ruiz-Lopez et al., 2017; Yu et al., 2018). On the acyl site, monoenoic fatty acids with 18 or 20 carbons chain length are preferred (Iven et al., 2016; Ruiz-Lopez et al., 2017; Yu et al., 2018).

Although WE from monounsaturated long-chain fatty acids are preferably produced by the so far tested FAR/WS(D) combinations, those WE are not exclusively produced.

A large amount of other WE species is also formed. A promising approach to push the synthesis of WE to the almost exclusive formation of one WE species, namely 18:1/18:1 WE, is achieved by providing only a narrow pool of substrates. It was successfully shown by three different studies that expressing FAR/WS(D) combinations in the *A. thaliana fad2fae1* mutant (Smith et al., 2003) almost all WE produced were 18:1/18:1, no matter which FAR/WS(D) combination was analyzed (Heilmann et al., 2012; Iven et al., 2016; Yu et al., 2018). FAE1 elongates fatty acids beyond 18 carbon chain length, and FAD2 introduces double bonds to monounsaturated fatty acids (Kunst et al., 1992; Okuley et al., 1994). When both enzymes are lacking, 18:1 CoA/ACP are the predominant acyl-CoA/ACP species. This approach might be also worth trying with MaFAR/MaWSD5 in order to promote the synthesis of 18:1/18:1 WE.

Besides for high levels of specific 18:1/18:1 WE, transgenic WE producing plants are also screened for high WE amounts. Seeds of transgenic *A. thaliana* MaFAR/MaWSD5 lines analyzed in this study contained WE amounts from around 5 mg/g seeds to up to nearly 20 mg/g seeds. These amounts are comparable to WE amounts in transgenic *A. thaliana* MaFAR/AbWSD1, MaFAR/PCOAbWSD1 (PCO: first 20 amino acids plant codon optimized) and MaFAR/MaWS2 (MaWS2 refers to MaWSD2) of 4 mg/g seeds, 12 mg/g seeds, and 14 mg/g seeds, respectively (Yu et al., 2018). Highest WE amounts in transgenic *A. thaliana* lines reached so far around 100 mg/g seeds when MaFAR and ScWS were coexpressed (Iven et al., 2016; Yu et al., 2018). However, a comparison of different FAR/WS(D) combinations for WE production has to be done with care as not only the enzymatic activities but also the expression levels of the enzymes have to be taken into account. In MaFAR/AbWSD1, MaFAR/PCOAbWSD1, MaFAR/MaWS2, and MaFAR/ScWS *A. thaliana* lines described before enzymes were all expressed under the control of the seed specific napin promoter (Iven et al., 2016; Yu et al., 2018). In contrast to that MaFAR and MaWSD5 expression was controlled by the seed specific β -conglycinin and glycinin promoters in this study. Since studies of WE producing enzymes in transgenic plants using these promoters are missing so far, only FAR/WS(D) combinations that used the same promoters can be compared in detail in terms of WE amounts.

The here presented analysis of MaFAR/MaWSD5 plants shows that MaWSD5 is a suitable candidate for industrial WE production *in planta*. A combination of MaFAR and MaWSD5 synthesizes the requested WE derived from monounsaturated long-chain fatty acid substrates. Obtained WE amounts in seeds are comparable with other published MaFAR/WS(D) combinations; however, higher amounts are desired. Screening of more transgenic MaFAR/MaWSD5

lines might identify lines with higher WE seed content. Besides that it will be interesting to determine the ratio of produced WE to TAG, since seeds with high WE and low TAG amounts are favored.

Acknowledgements The authors are grateful to Prof. Ed Cahoon for providing us with the seed-specific promoters from soybean and Kevin Schlabach for expert technical assistance. K.V. was supported by the GGNB Program Microbiology and Biochemistry and D.Y. was supported by the GAUSS Program Bionutz. I.F. acknowledges funding by the Deutsche Forschungsgemeinschaft (INST 186/822-1).

Conflict of Interest The authors declare that they have no conflict of interest.

References

- Alvarez, A. F., Alvarez, H. M., Kalscheuer, R., Waltermann, M., & Steinbüchel, A. (2008) Cloning and characterization of a gene involved in triacylglycerol biosynthesis and identification of additional homologous genes in the oleaginous bacterium *Rhodococcus opacus* PD630. *Microbiology*, **154**:2327–2335.
- Arabolaza, A., Rodriguez, E., Altabe, S., Alvarez, H., & Gramajo, H. (2008) Multiple pathways for triacylglycerol biosynthesis in *Streptomyces coelicolor*. *Applied and Environmental Microbiology*, **74**:2573–2582.
- Athenstaedt, K., & Daum, G. (2006) The life cycle of neutral lipids: Synthesis, storage and degradation. *Cellular and Molecular Life Sciences*, **63**:1355–1369.
- Bagge, L. E., Koopman, H. N., Rommel, S. A., McLellan, W. A., & Pabst, D. A. (2012) Lipid class and depth-specific thermal properties in the blubber of the short-finned pilot whale and the pygmy sperm whale. *The Journal of Experimental Biology*, **215**:4330–4339.
- Barney, B. M., Mann, R. L., & Ohlert, J. M. (2013) Identification of a residue affecting fatty alcohol selectivity in wax ester synthase. *Applied and Environmental Microbiology*, **79**:396–399.
- Barney, B. M., Ohlert, J. M., Timler, J. G., & Lijewski, A. M. (2015) Altering small and medium alcohol selectivity in the wax ester synthase. *Applied Microbiology and Biotechnology*, **99**:9675–9684.
- Barney, B. M., Wahlen, B. D., Garner, E., Wei, J., & Seefeldt, L. C. (2012) Differences in substrate specificities of five bacterial wax ester synthases. *Applied and Environmental Microbiology*, **78**:5734–5745.
- Bligh, E. G., & Dyer, W. J. (1959) A rapid method of total lipid extraction and purification. *Canadian Journal of Biochemistry and Physiology*, **37**:911–917.
- Blomquist, G. J., Soliday, C. L., Byers, B. A., Brakke, J. W., & Jackson, L. L. (1972) Cuticular lipids of insects: V. Cuticular wax esters of secondary alcohols from the grasshoppers *Melanoplus packardii* and *Melanoplus sanguinipes*. *Lipids*, **7**:356–362.
- Bradford, M. M. (1976) A rapid and sensitive method for the quantitation of microgram quantities of proteins utilizing the principle of protein-dye binding. *Analytical Biochemistry*, **72**:248–254.
- Carlsson, A. S., Yilmaz, J. L., Green, A. G., Stymne, S., & Hofvander, P. (2011) Replacing fossil oil with fresh oil—With what and for what? *European Journal of Lipid Science and Technology*, **113**:812–831.
- Cheng, J. B., & Russell, D. W. (2004) Mammalian wax biosynthesis: II. Expression cloning of wax synthase cDNAs encoding a member of the acyltransferase enzyme family. *Journal of Biological Chemistry*, **279**:37798–37807.
- Daniel, J., Deb, C., Dubey, V. S., Sirakova, T. D., Abomoelak, B., Morbidoni, H. R., & Kolattukudy, P. E. (2004) Induction of a novel class of diacylglycerol acyltransferases and triacylglycerol accumulation in *Mycobacterium tuberculosis* as it goes into a dormancy-like state in culture. *Journal of Bacteriology*, **186**:5017–5030.
- Duncan, C. C., Yermanos, D. M., Kumamoto, J., & Levesque, C. S. (1974) Rapid ethanolsis procedure for jojoba wax analysis by gas liquid chromatography. *Journal of the American Oil Chemists Society*, **51**:534–536.
- Ellman, G. L. (1959) Tissue sulfhydryl groups. *Archives of Biochemistry and Biophysics*, **82**:70–77.
- Heilmann, M., Iven, T., Ahmann, K., Hornung, E., Stymne, S., & Feussner, I. (2012) Production of wax esters in plant seed oils by oleosomal cotargeting of biosynthetic enzymes. *Journal of Lipid Research*, **53**:2153–2161.
- Hofvander, P., Doan, T. T. P., & Hamberg, M. (2011) A prokaryotic acyl-CoA reductase performing reduction of fatty acyl-CoA to fatty alcohol. *FEBS Letters*, **585**:3538–3543.
- Holtzapfel, E., & Schmidt-Dannert, C. (2007) Biosynthesis of isoprenoid wax ester in *Marinobacter hydrocarbonoclasticus* DSM 8798: Identification and characterization of isoprenoid coenzyme A synthetase and wax ester synthases. *Journal of Bacteriology*, **189**:3804–3812.
- Iven, T., Herrfurth, C., Hornung, E., Heilmann, M., Hofvander, P., Stymne, S., ... Feussner, I. (2013) Wax ester profiling of seed oil by nano-electrospray ionization tandem mass spectrometry. *Plant Methods*, **9**:24.
- Iven, T., Hornung, E., Heilmann, M., & Feussner, I. (2016) Synthesis of oleyl oleate wax esters in *Arabidopsis thaliana* and *Camelina sativa* seed oil. *Plant Biotechnology Journal*, **14**:252–259.
- Kaddor, C., Biermann, K., Kalscheuer, R., & Steinbüchel, A. (2009) Analysis of neutral lipid biosynthesis in *Streptomyces avermitilis* MA-4680 and characterization of an acyltransferase involved herein. *Applied Microbiology and Biotechnology*, **84**:143–155.
- Kalscheuer, R., & Steinbüchel, A. (2003) A novel bifunctional wax ester synthase/acyl-CoA:Diacylglycerol acyltransferase mediates wax ester and triacylglycerol biosynthesis in *Acinetobacter calcoaceticus* ADP1. *Journal of Biological Chemistry*, **278**:8075–8082.
- Kalscheuer, R., Stoveken, T., Malkus, U., Reichelt, R., Golyshin, P. N., Sabirova, J. S., ... Steinbüchel, A. (2007) Analysis of storage lipid accumulation in *Alcanivorax borkumensis*: Evidence for alternative triacylglycerol biosynthesis routes in bacteria. *Journal of Bacteriology*, **189**:918–928.
- King, A., Nam, J.-W., Han, J., Hilliard, J., & Jaworski, J. (2007) Cuticular wax biosynthesis in petunia petals: Cloning and characterization of an alcohol-acyltransferase that synthesizes wax-esters. *Planta*, **226**:381–394.
- Knutson, C. M., Lenneman, E. M., & Barney, B. M. (2017) *Marinobacter* as a model organism for wax ester accumulation in bacteria. In O. Geiger (Ed.), *Biogenesis of fatty acids, lipids and membranes* (pp. 1–22). Cham, Switzerland: Springer International.
- Krogh, A., Larsson, B., von Heijne, G., & Sonnhammer, E. L. L. (2001) Predicting transmembrane protein topology with a hidden Markov model: Application to complete genomes. *Journal of Molecular Biology*, **305**:567–580.
- Kunst, L., Taylor, D. C., & Underhill, E. W. (1992) Fatty acid elongation in developing seeds of *Arabidopsis thaliana*. *Plant Physiology and Biochemistry*, **30**:425–434.
- Lands, W. E. M. (1958) Metabolism of glycerolipides: A comparison of lecithin and triglyceride synthesis. *Journal of Biological Chemistry*, **231**:883–888.
- Lardizabal, K. D., Metz, J. G., Sakamoto, T., Hutton, W. C., Pollard, M. R., & Lassner, M. W. (2000) Purification of a jojoba embryo wax synthase, cloning of its cDNA, and production of high levels of wax in seeds of transgenic *Arabidopsis*. *Plant Physiology*, **122**:645–656.

- Lázaro, B., Villa, J. A., Santín, O., Cabezas, M., Milagre, C. D. F., de la Cruz, F., & Moncalián, G. (2017) Heterologous expression of a thermophilic diacylglycerol acyltransferase triggers triglyceride accumulation in *Escherichia coli*. *PLoS One*, **12**:e0176520.
- Li, F., Wu, X., Lam, P., Bird, D., Zheng, H., Samuels, L., ... Kunst, L. (2008) Identification of the wax ester synthase/acyl-coenzyme A: Diacylglycerol acyltransferase WSD1 required for stem wax ester biosynthesis in arabidopsis. *Plant Physiology*, **148**:97–107.
- Madeira, F., Park, Y. M., Lee, J., Buso, N., Gur, T., Madhusoodanan, N., ... Lopez, R. (2019) The EMBL-EBI search and sequence analysis tools APIs in 2019. *Nucleic Acids Research*, **47**:W636–W641.
- Márquez, M. C., & Ventosa, A. (2005) *Marinobacter hydrocarbonoclasticus* Gauthier et al. 1992 and *Marinobacter aquaeoli* Nguyen et al. 1999 are heterotypic synonyms. *International Journal of Systematic and Evolutionary Microbiology*, **55**:1349–1351.
- Miklaszewska, M., Dittrich-Domergue, F., Banaś, A., & Domergue, F. (2018) Wax synthase MhWS2 from *Marinobacter hydrocarbonoclasticus*: Substrate specificity and biotechnological potential for wax ester production. *Applied Microbiology and Biotechnology*, **102**:4063–4074.
- Miklaszewska, M., Kawinski, A., & Banas, A. (2013) Detailed characterization of the substrate specificity of mouse wax synthase. *Acta Biochimica Polonica*, **60**:209–215.
- Nettebrock, N. T., & Bohnert, M. (2020) Born this way—Biogenesis of lipid droplets from specialized ER subdomains. *Biochimica et Biophysica Acta*, **1865**:158448.
- Okuley, J., Lightner, J., Feldmann, K., Yadav, N., Lark, E., & Browse, J. (1994) Arabidopsis *FAD2* gene encodes the enzyme that is essential for polyunsaturated lipid synthesis. *The Plant Cell*, **6**:147–158.
- Patel, S., Nelson, D. R., & Gibbs, A. G. (2001) Chemical and physical analyses of wax ester properties. *Journal of Insect Science*, **1**:4.
- Petronikolou, N., & Nair, S. (2018) Structural and biochemical studies of a biocatalyst for the enzymatic production of wax esters. *ACS Catalysis*, **8**:6334–6344.
- Razeq, F. M., Kosma, D. K., Rowland, O., & Molina, I. (2014) Extracellular lipids of *Camelina sativa*: Characterization of chloroform-extractable waxes from aerial and subterranean surfaces. *Phytochemistry*, **106**:188–196.
- Reiser, S., & Somerville, C. (1997) Isolation of mutants of *Acinetobacter calcoaceticus* deficient in wax ester synthesis and complementation of one mutation with a gene encoding a fatty acyl coenzyme a reductase. *Journal of Bacteriology*, **179**:2969–2975.
- Rial, D. V., & Ceccarelli, E. A. (2002) Removal of DnaK contamination during fusion protein purifications. *Protein Expression and Purification*, **25**:503–507.
- Rontani, J.-F. (2010) Production of wax esters by bacteria. In K. N. Timmis (Ed.), *Handbook of hydrocarbon and lipid microbiology* (pp. 459–470). Berlin, Heidelberg, Germany: Springer.
- Röttig, A., & Steinbüchel, A. (2013) Acyltransferases in bacteria. *Microbiology and Molecular Biology Reviews*, **77**:277–321.
- Röttig, A., Wolf, S., & Steinbüchel, A. (2016) In vitro characterization of five bacterial WS/DGAT acyltransferases regarding the synthesis of biotechnologically relevant short-chain-length esters. *European Journal of Lipid Science and Technology*, **118**:124–132.
- Röttig, A., Zurek, P. J., & Steinbüchel, A. (2015) Assessment of bacterial acyltransferases for an efficient lipid production in metabolically engineered strains of *E. coli*. *Metabolic Engineering*, **32**:195–206.
- Rottler, A.-M., Schulz, S., & Ayasse, M. (2013) Wax lipids signal nest identity in bumblebee colonies. *Journal of Chemical Ecology*, **39**:67–75.
- Ruiz-Lopez, N., Broughton, R., Usher, S., Salas, J. J., Haslam, R. P., Napier, J. A., & Beaudoin, F. (2017) Tailoring the composition of novel wax esters in the seeds of transgenic *Camelina sativa* through systematic metabolic engineering. *Plant Biotechnology Journal*, **15**:837–849.
- Samuels, L., Kunst, L., & Jetter, R. (2008) Sealing plant surfaces: Cuticular wax formation by epidermal cells. *Annual Review of Plant Biology*, **59**:683–707.
- Sandager, L., Gustavsson, M. H., Stahl, U., Dahlqvist, A., Wiberg, E., Banas, A., ... Stymne, S. (2002) Storage lipid synthesis is non-essential in yeast. *Journal of Biological Chemistry*, **277**:6478–6482.
- Santala, S., Efimova, E., Koskinen, P., Karp, M. T., & Santala, V. (2014) Rewiring the wax ester production pathway of *Acinetobacter baylyi* ADP1. *ACS Synthetic Biology*, **3**:145–151.
- Shi, S., Octavio, V.-R. J., Khoomrung, S., Siewers, V., & Nielsen, J. (2012) Functional expression and characterization of five wax ester synthases in *Saccharomyces cerevisiae* and their utility for biodiesel production. *Biotechnology for Biofuels*, **5**:7.
- Smith, M., Moon, H., Chowrira, G., & Kunst, L. (2003) Heterologous expression of a fatty acid hydroxylase gene in developing seeds of *Arabidopsis thaliana*. *Planta*, **217**:507–516.
- Sonnhammer, E., von Heijne, G., & Krogh, A. (1998) A hidden Markov model for predicting transmembrane helices in protein sequences. *Proceedings on the International Conference on Intelligent Systems Molecular Biology*, **6**:175–182.
- Stöveken, T., Kalscheuer, R., Malkus, U., Reichelt, R., & Steinbüchel, A. (2005) The wax ester synthase/acyl coenzyme a: Diacylglycerol acyltransferase from *Acinetobacter* sp. strain ADP1: Characterization of a novel type of acyltransferase. *Journal of Bacteriology*, **187**:1369–1376.
- Stöveken, T., Kalscheuer, R., & Steinbüchel, A. (2009) Both histidine residues of the conserved HHXXXDG motif are essential for wax ester synthase/acyl-CoA:Diacylglycerol acyltransferase catalysis. *European Journal of Lipid Science and Technology*, **111**:112–119.
- Studier, F. W. (2005) Protein production by auto-induction in high-density shaking cultures. *Protein Expression and Purification*, **41**:207–234.
- Sturtevant, D., Lu, S., Zhou, Z.-W., Shen, Y., Wang, S., Song, J.-M., ... Guo, L. (2020) The genome of jojoba (*Simmondsia chinensis*): A taxonomically isolated species that directs wax ester accumulation in its seeds. *Science Advances*, **6**:eaay3240.
- Villa, J. A., Cabezas, M., de la Cruz, F., & Moncalián, G. (2014) Use of limited proteolysis and mutagenesis to identify folding domains and sequence motifs critical for wax ester synthase/acyl coenzyme A: Diacylglycerol acyltransferase activity. *Applied and Environmental Microbiology*, **80**:1132–1141.
- Wei, H. (2012) An overview of wax production, requirement and supply in the world market. *European Chemical Bulletin*, **1**:266–268.
- Yeats, T. H., & Rose, J. K. C. (2013) The formation and function of plant cuticles. *Plant Physiology*, **163**:5–20.
- Yu, D., Hornung, E., Iven, T., & Feussner, I. (2018) High-level accumulation of oleyl oleate in plant seed oil by abundant supply of oleic acid substrates to efficient wax ester synthesis enzymes. *Biotechnology for Biofuels*, **11**:53.
- Zhang, N., Mao, Z., Luo, L., Wan, X., Huang, F., & Gong, Y. (2017) Two bifunctional enzymes from the marine protist *Thraustochytrium roseum*: Biochemical characterization of wax ester synthase/acyl-CoA:Diacylglycerol acyltransferase activity catalyzing wax ester and triacylglycerol synthesis. *Biotechnology for Biofuels*, **10**:185.

SUPPORTING INFORMATION

The Fifth WS/DGAT Enzyme of the Bacterium *Marinobacter aquaeolei* VT8

Fig. S1 Schematic illustration of the five MaWSD

The gray boxes depict the five MaWSD schematically. The length of each gray box visualizes the size of each protein in accordance to the number of amino acids (aa). Dark red boxes highlight hydrophobic regions predicted with the online TMHMM Server, v. 2.0 (Krogh et al., 2001; Sonnhammer et al., 1998). Vertical arrows mark the position of the catalytic motif (HHxxxDG). Black characters correspond to conserved parts of the catalytic motif; gray characters visualize non-conserved residues.

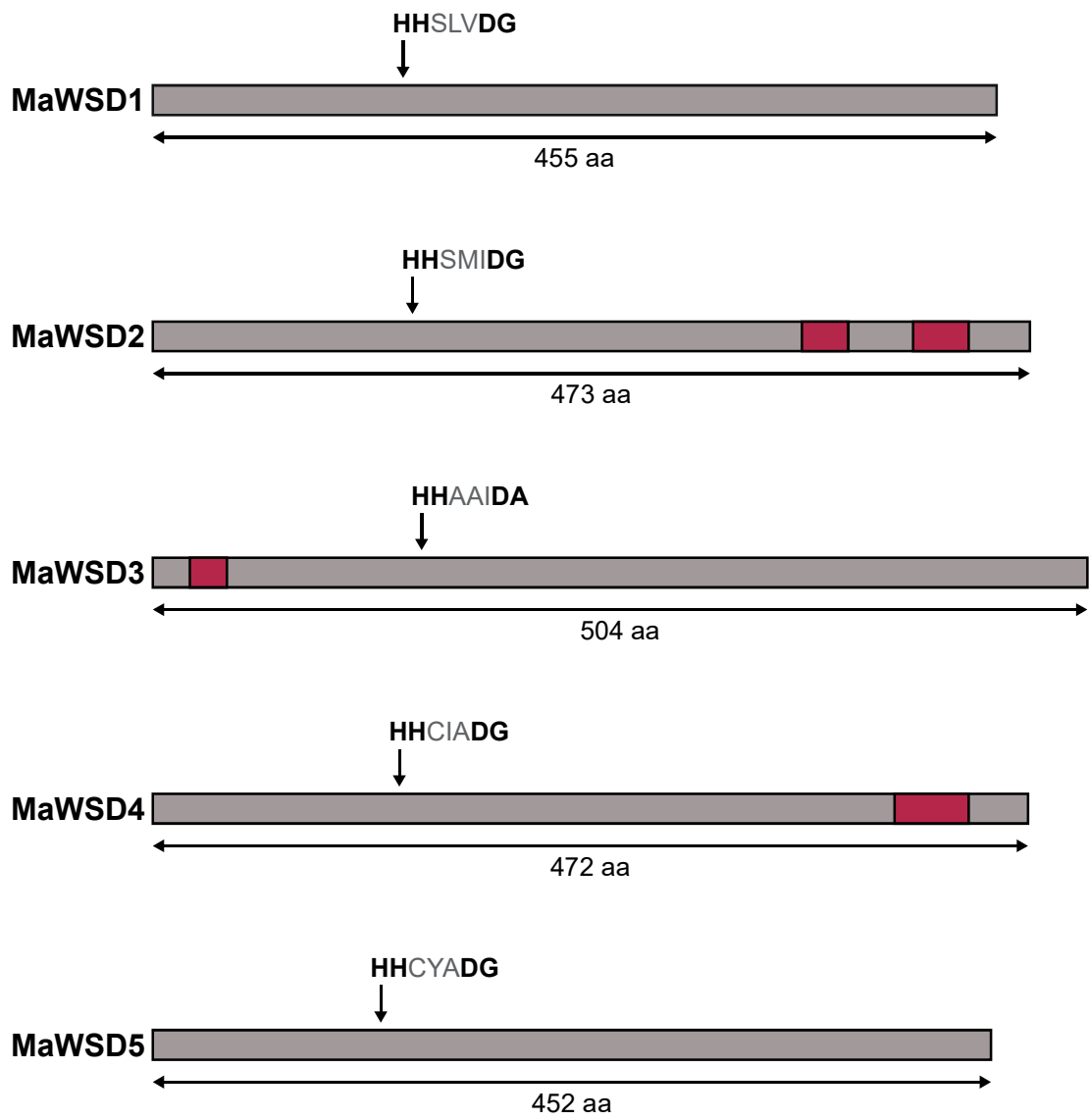
Fig. S2 Gravity flow purification of his₆-tagged MaWSD5

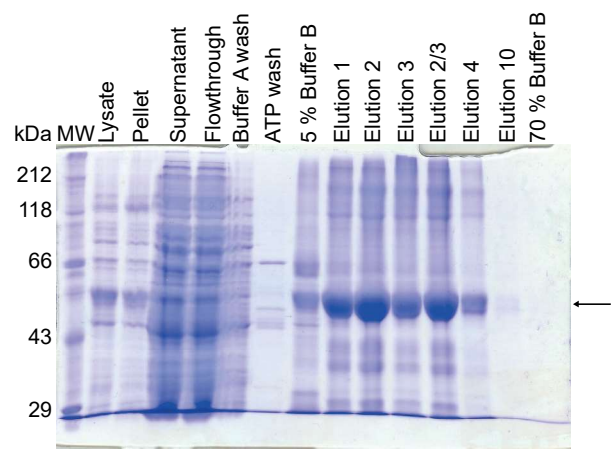
For the gravity flow purification of MaWSD5-his₆, cell lysis was performed identical to the cell lysis of the two-step purification. The soluble proteins were applied to a 1 mL talon metal affinity resin (Clontech). Column-bound proteins were washed with 10 mL IMAC buffer A, 10 mL IMAC ATP buffer, 10 mL IMAC buffer A and 10 mL of a mixture consisting of 95% IMAC buffer A and 5% IMAC buffer B. MaWSD5-his₆ was eluted from the column with 10 times 1 mL of a mixture consisting of 60% IMAC buffer A and 40% IMAC buffer B. Different fractions of the purification were analyzed by SDS-PAGE: 10 μ L protein ladder (MW: molecular weight, size of the protein standards in kDa), 7.5 μ L 1:50 (v/v) diluted lysate, 7.5 μ L 1:100 (v/v) diluted pellet, 7.5 μ L 1:2 (v/v) diluted supernatant, 7.5 μ L 1:2 (v/v) diluted flow through, 7.5 μ L 1:2 (v/v) diluted IMAC buffer A washing and 7.5 μ L of all other analyzed fractions were applied to the gel. All samples were mixed with 2.5 μ L 4 \times Laemmli buffer before loading on the gel. Bands corresponding to MaWSD5-his₆ (51.2 kDa) are marked by a black arrow. The gravity flow purification was performed nine times showing the same results.

Fig. S3 Determination of substrate specificities of his₆-tagged MaWSD5 by thin layer chromatography (TLC)-based *in vitro* substrate specificity assay. To analyze the substrate specificities of MaWSD5-his₆, IMAC purified protein was used for a TLC-based *in vitro* substrate specificity assay. Each reaction was carried out with 40 μ L protein solution in a total reaction volume of 2 mL reaction buffer (50 mM sodium phosphate buffer, pH 7.4, 150 mM NaCl) supplemented with 20 μ M fatty alcohol and 25 μ L acyl-CoA (for exact concentrations see [Materials and Methods](#) section). Acyl-CoA specificities were analyzed by setting up reactions with 18:1 OH and acyl-CoA of different chain length and desaturation degree (a). Alcohol specificities were studied by setting up reactions with 18:1 CoA and alcohols of different chain length and desaturation degree (FA OH: fatty alcohols) (b). The reaction samples were incubated for 1 h at room temperature before stopping the reaction by shock-freezing the samples in liquid nitrogen. Neutral lipid extraction was performed as described in the [Materials and Methods](#) section using 12 μ g tri-15:0-TAG as internal extraction standard. To assign bands on the TLC plates, di-17:0-WE and tri-15:0-TAG were spotted on the TLC plates as standards (STD). The assay was performed twice with similar results.

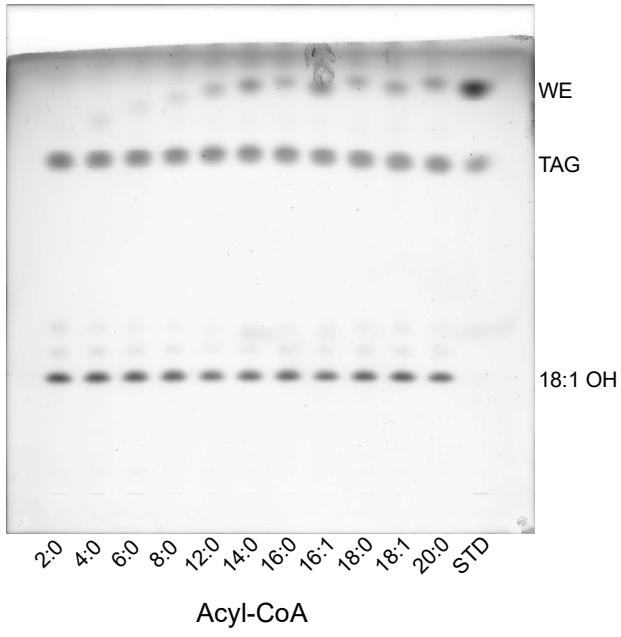
Fig. S4 Determination of substrate specificities of his₆-tagged MaWSD5 by 5,5'-dithiobis-(2-nitrobenzoic acid) (DTNB)-based *in vitro* substrate specificity assay. To analyze the substrate specificities of MaWSD5-his₆, gravity flow purified protein was used for a DTNB-based *in vitro* substrate specificity assay. Each reaction was carried out with 10 µg total protein of the combined elution fractions two and three in a total reaction volume of 1 mL reaction buffer (50 mM sodium phosphate buffer, pH 7.4, 150 mM NaCl) supplemented with 0.2 mg DTNB, 20 µM fatty alcohol and 12.5 µL acyl-CoA (for exact concentrations see [Materials and Methods](#) section). Acyl-CoA specificities were analyzed by monitoring the reactions of 18:1 OH with acyl-CoA of different chain length and desaturation degree (a). Alcohol specificities were studied by setting up reactions with 18:1 CoA and alcohols of different chain length and desaturation degree (b). Each reaction was started by adding the acyl-CoA to the reaction mix in the cuvette. Subsequently, the absorption change at 412 nm was recorded. By using Lambert–Beer-Law, the WS activities were calculated from the slopes of the gained curves. Both experiments were performed three times by measuring each time three technical replicates for every substrate combination. Mean values of the biological replicates were calculated from normalized values (for the acyl-CoA specificity WS activity for 14:0 CoA was set to 1 and for the alcohol specificity WS activity for 16:1 OH was set to 1). WS activities below 10 nmol/(mg*min) were considered as background and were therefore set to 0 nmol/(mg*min). Error bars represent SD of the biological replicates.

Table. S1 Primer sequences

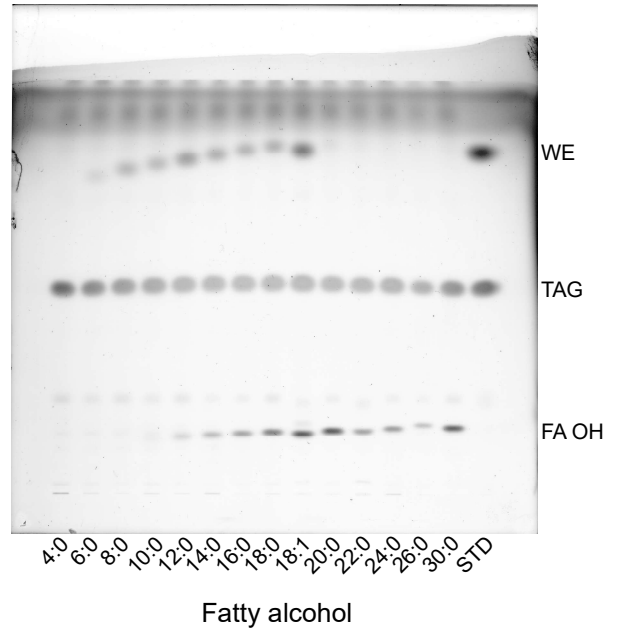


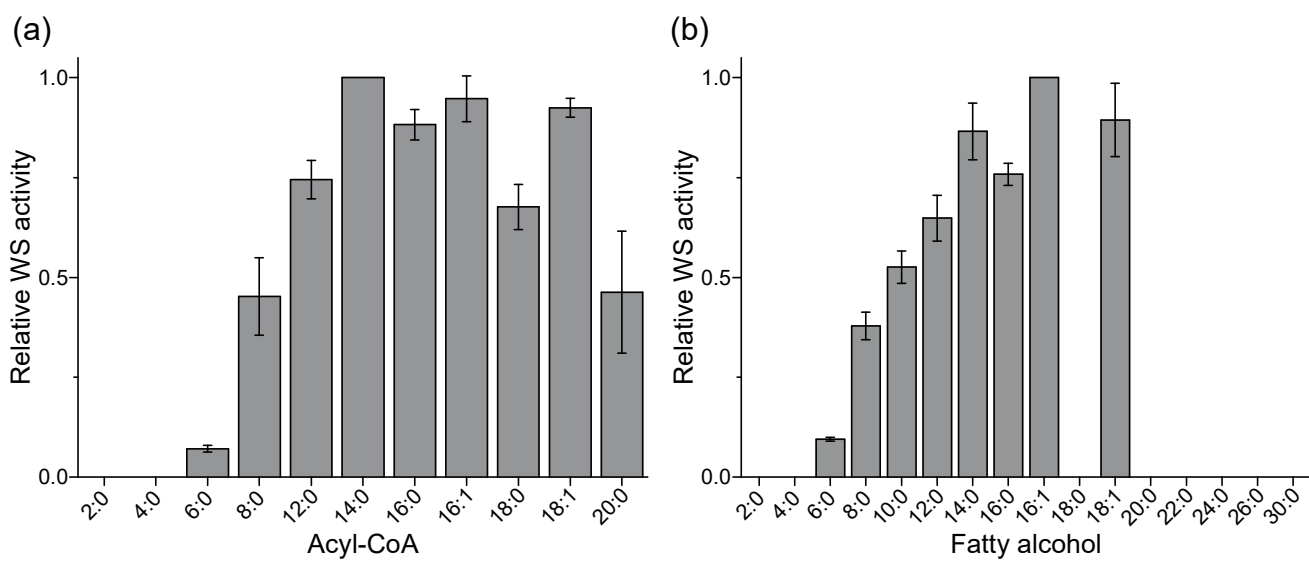


(a)



(b)





Tab. S1 Primer sequences

Primer Name	Primer Sequence (5` -> 3`)
Primers for yeast and <i>E. coli</i> constructs	
MaWSD1_For_HindIII	ACGAAGCTTATGACGCCCCTGAATCCCCTG
MaWSD1_Rev_XhoI	ACGCTCGAGCAGACCGGCGTTGAGCTCCAG
MaWSD2_For_HindIII	ACGAAGCTTATGAAACGTCTCGGAACCCTGGA
MaWSD2_Rev_XhoI	ACGCTCGAGCTTGCGGGTTCTGGGCGCGCTT
MaWSD3_For_HindIII	ACGAAGCTTATGCGTCAGCTGTCGGAACCTGGA
MaWSD3_Rev_XhoI	ACGCTCGAGCCTTCTGAATTTGCCAGCCCAC
MaWSD4_For_HindIII	ACGAAGCTTATGTCAGCAAACGGACGGCCAT
MaWSD4_Rev_SacI	ACGGAGCTCGGAGGCCTGGCGGAAACCGC
MaWSD5_For_HindIII	ACGAAGCTTATGCTGCCTTCGGATTCAGCCTG
MaWSD5_Rev_XhoI	ACGCTCGAGGTCCAGCTGATCCAGTTCGCC
Primers for <i>A. thaliana</i> constructs	
YFP_For_SalI	ACTGTCGACATGGTGAGCAAGGGCGAGGAG
MaFAR_Rev_BamHI	GCGGATCCTCATGCCGCTTTTTTACG
CFP_For_XhoI	ACTCTCGAGATGGTGAGCAAGGGCGAGGAG
MaWSD5_Rev_BglII	GCAGATCTTCAGTCCAGCTGATCCAGTTCGCC

2.2 Additional work to manuscript Article I

Katharina Vollheyde prepared the samples for the nanoESI-MS/MS measurement, processed, analyzed, displayed and discussed the obtained data. She generated the MaWSD5 mutant variant and performed the bifunctionality assay. The nanoESI-MS/MS samples were measured by Dr. Cornelia Herrfurth from the Department for Plant Biochemistry (Georg-August-University, Göttingen).

MaWSD5 and AbWSD1 have similar substrate preferences

In order to compare fatty alcohol and acyl-CoA preferences of MaWSD5 with those of AbWSD1, a nano-electrospray ionization tandem mass spectrometry (nanoESI-MS/MS) competition assay (Article II) was performed. The nanoESI-MS/MS method was optimized to detect plant WE with 32 carbons or more (Iven *et al.*, 2013). The competition assay can be used for a direct comparison of *in vitro* substrate preferences of WE producing enzymes. The assay was performed in parallel with *E. coli* lysate expressing his₆-tagged AbWSD1 and MaWSD5 (for materials and methods see manuscript of Article II). As depicted in Figure 2.5, MaWSD5 and AbWSD1 share similar acyl-CoA and fatty alcohol preferences *in vitro*.

DGAT activity cannot be established in MaWSD5 upon mutation

MaWSD5 was characterized as a monofunctional WSD, showing no DGAT activity *in vivo* and *in vitro* (see section 2.1 (Article I)). In AbWSD1, two amino acid residues (AbWSD1-V139, AbWSD1-I303) were identified within the scope of this thesis, which influence DGAT activity of AbWSD1 (Article II). Upon mutation of AbWSD1-V139 towards alanine, phenylalanine or tryptophan, DGAT activity was reduced compared to AbWSD1 WT. The double mutant AbWSD1-V139W-I303W was not able to produce TAG. In order to test, whether MaWSD5 can be converted into a bifunctional WSD, residue MaWSD5-L130, which corresponds to AbWSD1-V139 was mutated towards a valine residue (quick change site-directed mutagenesis see section 3.1 (Article II), primer sequences (5'→3'): MaWSD5-L130V-for ctgttacgccgatggtGTTccctgctgggtatTTTTgacc, MaWSD5-L130V-rev cccagcaggaAACcaccatcggcgtaacagtgatgc). WS and DGAT activities of MaWSD5 WT and MaWSD5-L130V were analyzed *in vitro*. According to the *in vitro* bifunctionality assay (see section 2.1 (Article I)), *E. coli* lysate expressing either his₆-tagged MaWSD5 WT or MaWSD5-L130V corresponding to 20 µg total protein was incubated with 20 µM 16:0 OH or di-16:0-DAG

and 12.5 μL 18:1 CoA (stock concentration: 0.62 mM) for one hour. Extraction, separation and visualization of neutral lipids from the reaction mix revealed, that MaWSD5-L130V exhibits WS activity similar to MaWSD5 WT. The amino acid substitution did not lead to an establishment of DGAT activity in MaWSD5.

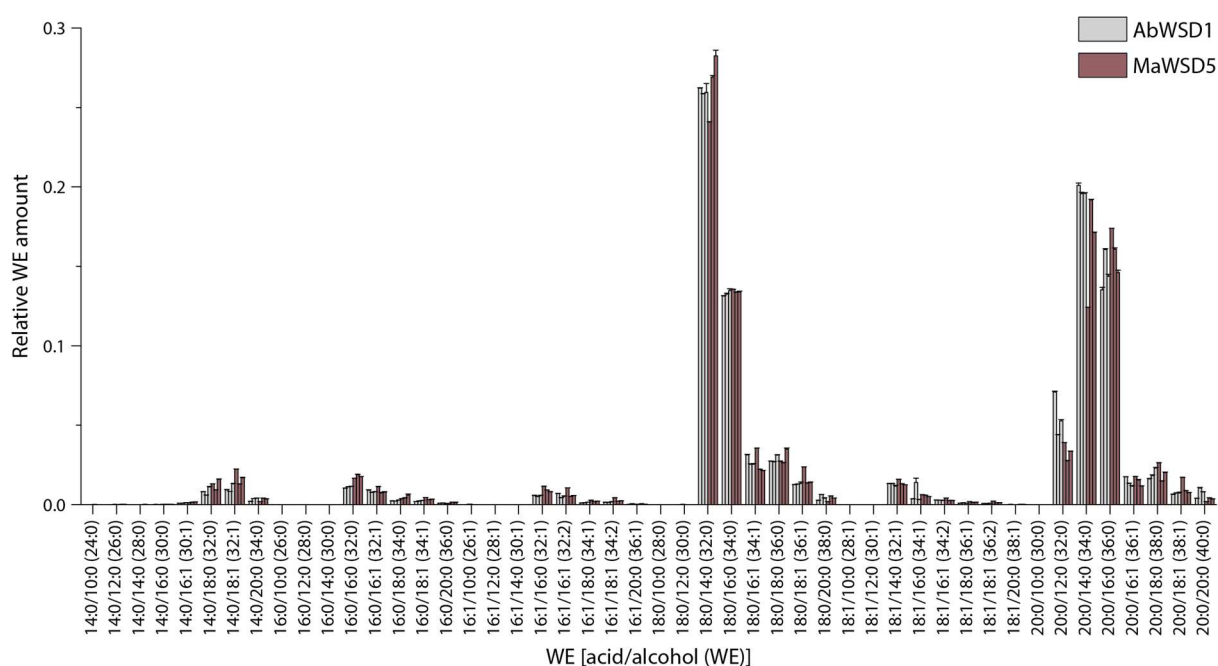


Figure 2.5. WE profiles of MaWSD5 and AbWSD1.

E. coli lysate expressing his₆-tagged MaWSD5 (purple) and AbWSD1 (grey) was incubated with six different acyl-CoA and eight different fatty alcohols. The produced WE species were analyzed by nanoESI-MS/MS. The method was optimized for the detection of WE species with 32 carbons or more (Iven *et al.*, 2013). Each bar represents the mean of three measurements of one biological replicate + standard deviation. Bars of the same color depict different biological replicates. For a better comparison of both enzymes, the data for AbWSD1, which are presented in Article II, are displayed again.

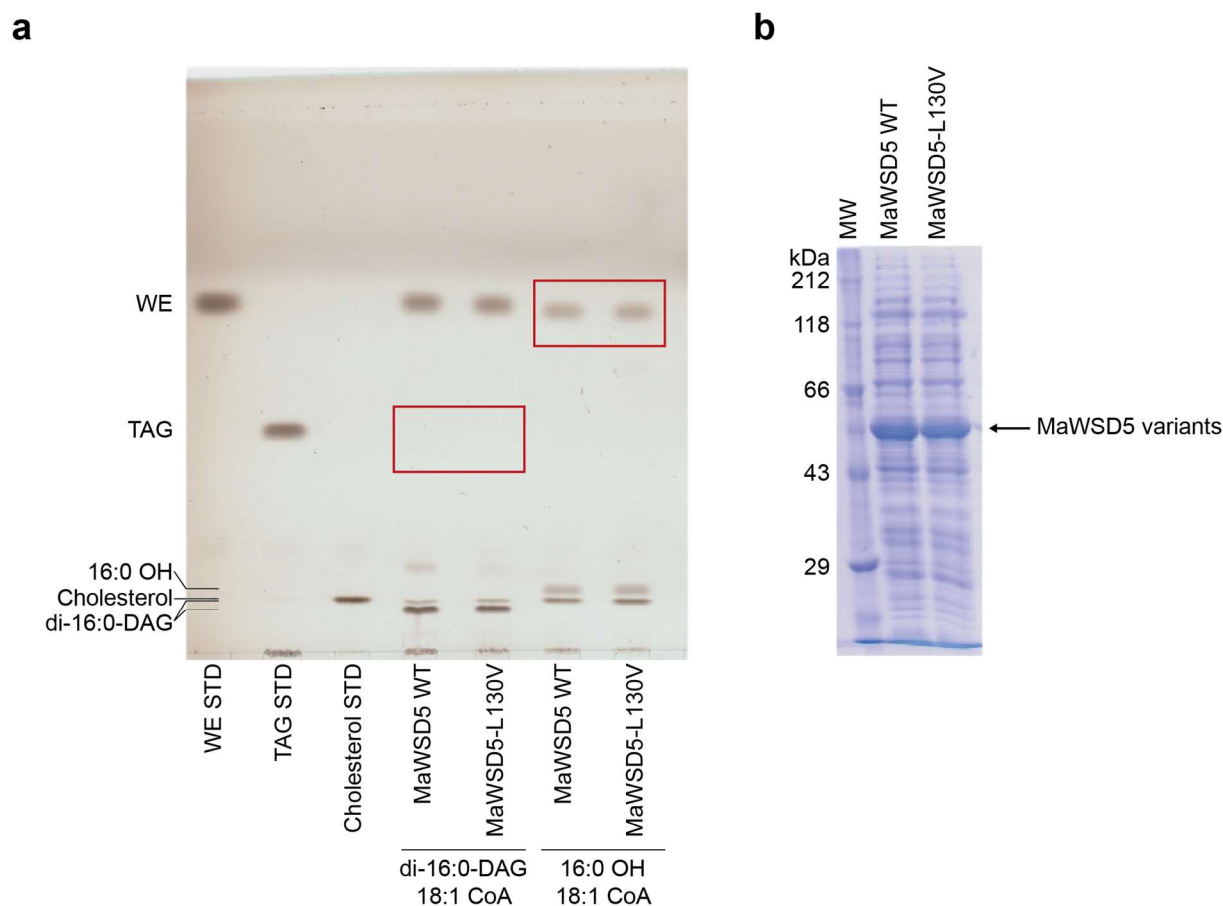


Figure 2.6. Analysis of WS and DGAT activity of his₆-tagged MaWSD5 WT and MaWSD5-L130V. **(a)** *E. coli* lysate expressing either his₆-tagged MaWSD5 WT or his₆-tagged MaWSD5-L130V was incubated with 20 μM 16:0 OH or di-16:0-DAG and 12.5 μL 18:1 CoA (stock concentration: 0.62 mM) for one hour at room temperature. After neutral lipid extraction, lipids were separated and visualized by thin layer chromatography. The assay was performed once. **(b)** SDS-PAGE of *E. coli* lysate expressing the MaWSD5 variants. 7.5 μg total protein were loaded on the gel for each sample. The assay was performed once.

3 ARTICLE II

3.1 The crystal structure of the bifunctional wax synthase 1 from *Acinetobacter baylyi* (AbWSD1) reveals a conformational change upon substrate binding

The manuscript is ready for submission. Katharina Vollheyde and Karin Kühnel are shared first authors.

Except for the AbWSD1 mutants AbWSD1-S148A, AbWSD1-L149A, AbWSD-S148A-L149A, AbWSD1-S148A-I343F, AbWSD1-I343F, AbWSD1-I343Y, AbWSD1-I343W, AbWSD1-S347F, AbWSD1-S347Y, AbWSD1-S374W, Katharina Vollheyde generated the AbWSD1 amino acid substitution variants within the scope of her thesis. She performed and analyzed the TLC-based activity assay and the DTNB-based enzymatic activity assay. She prepared the samples for the nanoESI-MS/MS competition assay and processed, analyzed, displayed and discussed the obtained data. Katharina Vollheyde generated the multiple sequence alignment, analyzed and discussed it regarding prediction of DGAT activity of the enzymes based on amino acid residues. She conducted the detailed comparison and interpretation of similarities and differences of the AbWSD1 and MaWSD1 crystal structures. She modeled acyl-CoA into the structure of AbWSD1, interpreted the results and proposed the substrate-binding model of WSD proteins. Except for the crystallization part, Katharina Vollheyde wrote the first draft of the manuscript.

The crystal structure of the bifunctional wax synthase 1 from *Acinetobacter baylyi* (AbWSD1) reveals a conformational change upon substrate binding

Katharina Vollheyde^{1‡}, Karin Kühnel^{2‡}, Felix Lambrecht¹, Steffen Kawelke¹, Cornelia Herrfurth^{1,3}, Ivo Feussner^{1,3,4*}

¹University of Goettingen, Albrecht-von-Haller-Institute for Plant Sciences, Department for Plant Biochemistry, D-37077 Goettingen, Germany

²Max Planck Institute for Biophysical Chemistry, Department of Neurobiology, D-37077 Goettingen, Germany

³University of Goettingen, Goettingen Center for Molecular Biosciences (GZMB), Service Unit for Metabolomics and Lipidomics, D-37077 Goettingen, Germany

⁴University of Goettingen, International Center for Advanced Studies of Energy Conversion (ICASEC) and Goettingen Center for Molecular Biosciences (GZMB), D-37077 Goettingen, Germany

‡These authors contributed equally.

Keywords

Acinetobacter baylyi, AbWSD1, amino acid exchange mutants, bifunctional wax synthase/acyl-CoA:diacylglycerol acyltransferase, conformational change, induced fit model, structure function analysis, triacylglycerol, wax ester

Abstract

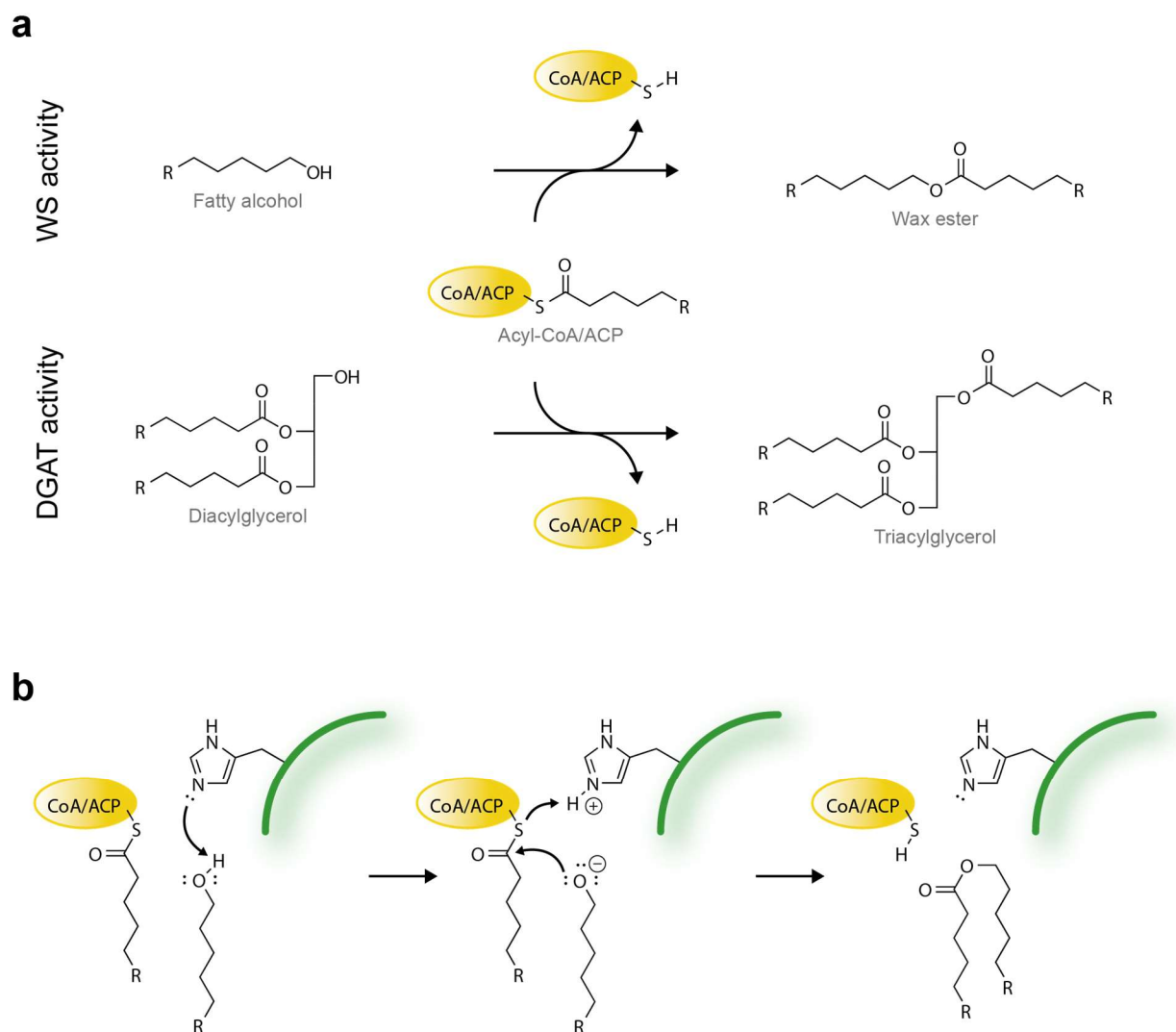
Wax ester (WE) belong to the class of neutral lipids. They are formed by transesterification of an activated fatty acyl moiety to a fatty alcohol. They exhibit diverse physicochemical properties, which are of great industrial interest. In order to facilitate a sustainable WE production, attempts to produce WE in bacteria and plants are steadily increasing. However, for tailor-made WE production a detailed understanding of the catalytic mechanism of WE forming enzymes and the structural determinants influencing substrate specificity are necessary. A class of well-studied WE producing enzymes are bifunctional bacterial wax synthases/acyl-coenzyme A (CoA):diacylglycerol acyltransferases (WSD). Here we report the 2.1 Å crystal structure of *Acinetobacter baylyi* WSD1 (AbWSD1), which is the first WSD structure with a fatty acid molecule bound in the active site. The location of a co-crystallized myristic acid confirms the position of an earlier proposed acyl-CoA binding site. Mutagenesis studies identified two amino acids, which are crucial for the acyl-CoA:diacylglycerol O-acyltransferase (DGAT) activity of the enzyme. Three other residues influence the acyl-CoA specificity of AbWSD1. A comparison of the AbWSD1 and *Marinobacter aquaeolei* WSD1 (MaWSD1) structures revealed a rearrangement in the C-terminal part of AbWSD1, which might be induced upon substrate binding. This conformational change leads to the formation of a potential coenzyme A binding site. Structural comparison of AbWSD1 and MaWSD1 together with an evaluation of published amino acid substitution studies yields a deeper understanding on how WSD catalyze acyl transfer reactions and the structural determinants for substrate specificity. These findings will help to generate WSD variants for tailor-made WE production in bacteria and plants.

Introduction

Wax ester (WE) belong to the class of neutral lipids, similar as triacylglycerol (TAG) (Athenstaedt & Daum, 2006). They can be found throughout the whole tree of life, fulfilling different functions (Blomquist *et al.*, 1972; Duncan *et al.*, 1974; Cheng & Russell, 2004b; Bagge *et al.*, 2012; Barney *et al.*, 2012; Miklaszewska *et al.*, 2013; Rottler *et al.*, 2013; Yeats & Rose, 2013; Razeq *et al.*, 2014; Santala *et al.*, 2014). WE are formed by the transesterification of an

activated fatty acyl-coenzyme A (CoA) ester and a fatty alcohol. Physicochemical properties of WE are dependent on the number of carbon atoms and the number of double bonds of the fatty acid and the fatty alcohol moiety (Patel *et al.*, 2001). Due to their properties, WE are of great interest as industrial lubricants and they are also used for the production of cosmetics, packing and coatings (Rontani, 2010; Wei, 2012). Before the banning of whale hunting in the 1980s, WE mostly derived from sperm whale; nowadays, they are predominantly either generated chemically from fossil fuels and plant-derived TAG or they are expensively extracted from jojoba seeds (Lardizabal *et al.*, 2000; Hills, 2003; Röttig & Steinbüchel, 2013a). Attempts to produce WE in bacteria or plants are steadily increasing (Lardizabal *et al.*, 2000; Kalscheuer *et al.*, 2006a; Kalscheuer *et al.*, 2006b; Heilmann *et al.*, 2012; Iven *et al.*, 2016; Ruiz-Lopez *et al.*, 2017; Yu *et al.*, 2018). However, to produce tailor-made WE it is important to fully understand the biosynthesis of WE as well as structure determinants for substrate specificities of WE-producing enzymes.

The esterification of a CoA or acyl carrier protein (ACP) activated fatty acid with a fatty alcohol is catalyzed by wax synthases (WS), which belong to the class of acyltransferases (Röttig & Steinbüchel, 2013a). WS enzymes can be divided into three subclasses: acyl-CoA:diacylglycerol *O*-acyltransferase (DGAT) 1-like WS, DGAT2-like WS and WS/DGAT (WSD) which are mostly found in bacteria (Röttig & Steinbüchel, 2013a). In contrast to DGAT1- and DGAT2-like WS, bacterial WSD are predicted to have no transmembrane domains; however, they were still found to have a hydrophobic character or even to be membrane associated (Stöveken *et al.*, 2005; Barney *et al.*, 2012; Knutson *et al.*, 2017; Vollheyde *et al.*, 2020). Besides the formation of WE from acyl-CoA/ACP and fatty alcohol, most WSD enzymes are also able to catalyze the production of TAG from acyl-CoA/ACP and diacylglycerol (DAG, Scheme 3.1a) (Daniel *et al.*, 2004; Stöveken *et al.*, 2005; Holtzapple & Schmidt-Dannert, 2007; Kalscheuer *et al.*, 2007; Alvarez *et al.*, 2008; Li *et al.*, 2008; Kaddor *et al.*, 2009; Villa *et al.*, 2014; Röttig *et al.*, 2015; Lázaro *et al.*, 2017; Zhang *et al.*, 2017; Petronikolou & Nair, 2018). All WSD share a conserved HHxxxDG motif, which is proposed to be the catalytic motif (Kalscheuer & Steinbüchel, 2003; Wältermann *et al.*, 2007; Röttig & Steinbüchel, 2013a). The catalytic mechanism of WSD is hypothesized to function via a histidine residue (Scheme 3.1b) (Stöveken *et al.*, 2009). It is assumed, that the histidine abstracts the proton of the hydroxyl group of the fatty alcohol or DAG. The originated negatively charged oxyanion acts as a nucleophile and attacks the carbonyl carbon atom of acyl-CoA/ACP. This leads to a cleavage of the thioester bond and to the formation of a new oxo ester bond. The obtained CoA/ACP-S⁻ is protonated by the histidine and released from the enzyme together with the produced WE or TAG.



Scheme 3.1. WSD reaction.

Reaction catalyzed by WSD (**a**) and proposed reaction mechanism of WSD (based on Stöveken *et al.* (2009)) (**b**).

The first identified WSD was AbWSD1 from *Acinetobacter baylyi* (former known as *A. calcoaceticus*) ADP1 (Kalscheuer & Steinbüchel, 2003). Studied for more than 15 years, AbWSD1 (also known as WS/DGAT, Ac1 or AtfA) became a well characterized model enzyme for bifunctional WSD (Stöveken *et al.*, 2005; Stöveken *et al.*, 2009; Barney *et al.*, 2012; Shi *et al.*, 2012; Barney *et al.*, 2013; Röttig & Steinbüchel, 2013b; Röttig *et al.*, 2015; Röttig *et al.*, 2016). Due to its lack of transmembrane domains, it is possible to purify the enzyme almost to homogeneity (Stöveken *et al.*, 2005). *In vitro* substrate specificity analyses of the WT enzyme revealed broad acyl-CoA and fatty alcohol specificities (Stöveken *et al.*, 2005). Whereas WS activity of the protein was shown to follow Michaelis-Menten kinetics, DGAT activity did neither apply to Michaelis-Menten nor to cooperative kinetics (Stöveken *et al.*, 2005). Mutagenesis studies identified one amino acid residue of AbWSD1 that is important for the alcohol specificity

of the enzyme, as well as several residues, whose substitution resulted in reduced enzymatic activity (Barney *et al.*, 2013; Röttig & Steinbüchel, 2013b).

The identification of AbWSD1 resulted in the identification of WSD in other organisms. They were mostly identified in bacteria, but there are also plant WSD described (Daniel *et al.*, 2004; Holtzapple & Schmidt-Dannert, 2007; Kalscheuer *et al.*, 2007; King *et al.*, 2007; Alvarez *et al.*, 2008; Arabolaza *et al.*, 2008; Li *et al.*, 2008; Kaddor *et al.*, 2009; Barney *et al.*, 2012; Shi *et al.*, 2012; Villa *et al.*, 2014; Lázaro *et al.*, 2017; Zhang *et al.*, 2017; Vollheyde *et al.*, 2020). Besides AbWSD1, the best-characterized WSD are those from the bacterium *Marinobacter*. There are studies available, dealing with the characterization of WSD from *Marinobacter aquaeolei* (MaWSD1-5) and *Marinobacter hydrocarbonoclasticus* (MhWS1-4) (Holtzapple & Schmidt-Dannert, 2007; Barney *et al.*, 2012; Barney *et al.*, 2013; Villa *et al.*, 2014; Barney *et al.*, 2015; Röttig *et al.*, 2015; Petronikolou & Nair, 2018; Vollheyde *et al.*, 2020). A phylogenetic analysis from 2005 revealed, that both *Marinobacter* species are actually the same, which should be, according to the rules of priority, named *M. hydrocarbonoclasticus* (Márquez & Ventosa, 2005). Nevertheless, the genomes of both strains are not hundred percent identical as both strains were discovered at different places. Hence, corresponding WSD from *M. hydrocarbonoclasticus* and *M. aquaeolei* differ slightly from each other.

MhWS1 and MaWSD1 (also referred to as Ma1 and Ma-WSD/DGAT) differ only in two amino acids (MhWS1-194D/MaWSD1-194G, MhWS1-321G/MaWSD1-321E). Besides WS activity, MhWS1 and MaWSD1 exhibit DGAT activity similar to AbWSD1 (Holtzapple & Schmidt-Dannert, 2007; Petronikolou & Nair, 2018). Amino acid substitution studies identified amino acid residues of MaWSD1 which are important for the alcohol specificity (Barney *et al.*, 2013; Barney *et al.*, 2015). MhWS2 and MaWSD2 (also referred to as Ma2) vary in only one residue (MhWS2-395G/MaWSD2-395D). MhWS2 showed WS but no DGAT activity in *in vitro* activity tests (Holtzapple & Schmidt-Dannert, 2007). Nevertheless, upon expression of the protein in *Escherichia coli* a small portion of *in vivo* TAG production was observed (Röttig *et al.*, 2015). For MaWSD2 however, *in vitro* DGAT activity was observed (Villa *et al.*, 2014). Mutagenesis studies in MaWSD2 revealed several residues whose substitution led to reduced enzymatic activity (Villa *et al.*, 2014). MhWS3 and MaWSD3 differ in more regions than the two WSD pairs described above. Besides a four amino acid long N-terminal deletion in MaWSD3, nine amino acid substitutions can be found between both proteins. So far no enzymatic activity was observed for any of these proteins (Holtzapple & Schmidt-Dannert, 2007; Vollheyde *et al.*, 2020). Amino acid sequences of MhWS4 and MaWSD4 vary not only in eight positions, in addition MhWS4 encodes for a stop codon at position 350, which results in a MhWS4 pseudogene in contrast to an intact open reading frame of MaWSD4 (Holtzapple & Schmidt-Dannert, 2007). Although WS and DGAT activity were not detected for MaWSD4, the formation of an unknown compound upon expression in yeast was observed (Vollheyde *et al.*, 2020). A

fifth WSD in *M. aquaeolei* was only characterized recently (Vollheyde *et al.*, 2020). The enzyme was identified to only exhibit WS activity and lacks DGAT activity *in vitro* and *in vivo* (Vollheyde *et al.*, 2020).

In 2018, the crystal structure of MaWSD1 was published as the first WSD structure (Petronikolou & Nair, 2018). Supported by already published amino acid exchange mutants and based on further amino acid substitution studies, the fatty alcohol and the acyl-CoA binding sites were assigned by the authors (Barney *et al.*, 2013; Barney *et al.*, 2015; Petronikolou & Nair, 2018).

Here we present the crystal structure of AbWSD1, which is the first WSD structure with a bound fatty acid. The co-crystallized myristic acid aligns with the proposed acyl-CoA binding site. A structural alignment of AbWSD1 and MaWSD1 revealed structural differences between both enzymes especially in one part of the alignment. We hypothesize that this conformational rearrangement might be the consequence of substrate binding by an induced fit mechanism. Amino acid substitution studies resulted furthermore in the identification of residues, which may be important for the correct positioning of acyl-CoA, as well as residues, which are crucial for the DGAT activity of AbWSD1. A detailed structural comparison of AbWSD1 and MaWSD1 together with a further analysis of earlier published WSD mutants, yields a more detailed understanding of structural determinants for enzyme catalysis and substrate specificities. This knowledge is especially important for tailor-made WE production using bacterial WSD.

Materials and Methods

Cloning and generation of mutant variants

A synthetic and for *E. coli* codon optimized AbWSD1 (accession number: Q8GGG1) (Kalscheuer & Steinbüchel, 2003) gene was purchased from WIZ-GEN.

For crystallization, the AbWSD1 gene was amplified from the synthetic plasmid using gene-specific primers with *Bam*HI/*Eco*RI restriction sites. The amplified sequence was cloned into *E. coli* expression vector pCOLD (Takara Bio) with a N-terminal hexahistidine (His₆) tag and a trigger factor (TF) (pCOLD-His₆-TF-AbWSD1).

For enzyme characterization and mutant generation, the AbWSD1 gene was amplified from the synthetic plasmid using gene-specific primers with *Bam*HI/*Hind*III restriction sites. The amplified sequence was cloned into *E. coli* expression vector pET28a (Novagen) with an N-terminal His₆-tag (pET28a-His₆-AbWSD1).

To generate amino acid substitution mutants of AbWSD1, quick change site-directed mutagenesis was performed to introduce nucleobase exchanges on pET28a-His₆-AbWSD1. Primer sequences for AbWSD1 cloning and mutant generation can be found in Table S3.1.

Crystallization

pCold-His₆-TF-AbWSD1 was transformed into *E. coli* BL21 StarTM (DE3) cells (Thermo Fisher Scientific). Bacteria were expressed in lysogeny broth (LB) medium or minimal medium was used for the incorporation of selenomethionine into the protein (Van Duyne *et al.*, 1993). After induction with 1 mM isopropyl β -D-1-thiogalactopyranoside (IPTG) cultures were grown overnight at 25 °C. Bacteria were harvested and resuspended into buffer A (30 mM imidazole, 10 % glycerol, 150 mM NaCl, 50 mM TRIS pH 7.6) and directly processed without freezing them. Cells were lysed with a microfluidizer M-110L (Microfluidics Corporation, Westwood, MA) and spun at 20000 *g* for 1 h at 4 °C. Supernatant was applied onto a 1 mL HisTrap column (Sigma) and protein was eluted with a gradient from 0 % to 100 % buffer B composed of 500 mM imidazole, 10 % glycerol, 150 mM NaCl, 50 mM TRIS pH 7.6. Pooled fractions were diluted with the same volume gel filtration buffer (150 mM NaCl, 10 % glycerol, 30 mM glycine pH 10.0) and kept overnight at 4 °C.

The protein sample was then concentrated and applied onto a Superdex 200 HiLoad 16/60 column (Sigma). Fractions were pooled and concentrated to 20 mg/mL, aliquoted, frozen in liquid nitrogen and stored at -80 °C.

Crystals were grown by *in situ* proteolysis with trypsin. Trypsin was added in a 1:200 (*w/w*) ratio to 20 mg/mL native His₆-TF-AbWSD1 before set up of the crystallization screens. 100 nL precipitant (17.3 % ethanol, 0.2 M MgCl₂, 0.1 M TRIS pH 8.0) were added to 200 nL protein using 96-well plates with a Cartesian pipetting robot (Zinsser Analytic). Plates were stored at 4 °C. Crystals were transferred into a cryoprotectant consisting of mother liquor supplemented with 30 % ethylene glycol and then flash cooled in liquid nitrogen.

Trypsin was added in a 1:1000 ratio (*w/w*) to 15 mg/mL selenomethionine-labelled His₆-TF-AbWSD1. Sitting drops consisting of 100 nL protein and 100 nL precipitant (14.1 % ethanol, 0.1 M MgCl₂, 0.1 M HEPES pH 7.5) were pipetted with a Gryphon robot (Art Robbins Instruments). The 96-well plates were stored at 4 °C. For cryoprotection of the crystals, 2-methyl-2,4-pentanediol was added to the crystallization drop by transferring it five times with a 0.4 mm LithoLoop (Molecular Dimensions) at 4 °C. Crystals were then harvested from the drop and flash-cooled in liquid nitrogen.

X-ray diffraction data were collected at SLS beamlines X06SA and X10SA at 100 K. Data were processed with the XDS software package (Kabsch, 1993). The structure was determined by single-wavelength anomalous diffraction phasing using the data collected from the selenomethionine incorporated crystals. Eleven Se-sites were identified with SHELXD/HKL2MAP with an overall correlation coefficient of 51.4 % (Pape & Schneider, 2004; Sheldrick, 2008). Subsequent phasing and density modification with SHELXE/HKL2MAP yielded an interpretable electron density map. ArpWarp was used for automatic model building (Perrakis *et al.*, 1999). Subsequent manual model building was done with COOT (Emsley & Cowtan, 2004). The higher resolution native data set was used for refinement with PHENIX (Adams *et al.*, 2010). Figures were prepared with PYMOL (Schrodinger, 2006; Schrodinger, 2010; Schrodinger, 2015). Ligand protein interactions were visualized with LigPlot+ (Wallace *et al.*, 1995).

***E. coli* expression cultures for enzymatic activity test**

pET28a-His₆-AbWSD1 was transformed into BL21 StarTM (DE3) and cells were cultivated for protein expression in ZYP-5052 rich medium for auto-induction (Studier, 2005) as described by Vollheyde *et al.* (2020). For protein purification, cells from 500 mL culture were harvested by centrifugation (4000 *g*, 25 min, 4 °C) and combined to one pellet. For enzymatic activity assays for which only *E. coli* lysate was needed, cells from 10 mL expression culture were harvested by centrifugation (3220 *g*, 20 min, 4 °C) and were combined to one pellet. Cell pellets were stored at -20 °C for further use.

Gravity flow purification of AbWSD1 and variants

To a cell pellet harvested from 500 mL expression culture 30 mL of ion metal affinity chromatography (IMAC) buffer A (50 mM Tris pH 7.5, 150 mM NaCl, 30 mM imidazole, 10 mM *n*-octyl- β -D-glucopyranoside (OGP)) were added. The pellet was thawed on ice and meanwhile resuspended in the buffer by pipetting up and down and vortexing. A spatula tip of each lysozyme (Fluka analytical) and DNaseI (Sigma) were added to the resuspended cell pellet and the solution was incubated on ice for 1 h. Afterwards, the solution was split into two aliquots, from which each was filled up with IMAC buffer A to a total volume of 25 mL. To each of the two aliquots, 125 μ L phenyl methane sulfonyl fluoride (PMSF) (stock: 200 mM in isopropanol) were added and the samples were immediately sonicated for 15 min (pulsed sonication, 40 % duty cycle, output control: 4 (micro)), with an alternation of sonication phase and resting phase of 1 min. Afterwards, the samples were centrifuged for at least 25 min at

10000 g and 4 °C to spin down cell debris. For further protein purification steps the supernatant was used.

IMAC was used to purify the His₆-tagged AbWSD1 and mutant variants via tag binding to immobilized Co²⁺ ions. The purification was carried out using 1 mL Talon metal affinity resin (Takara Clontech). After loading the before obtained supernatant on the column, impurities were washed from the column with 10 mL IMAC buffer A, 10 mL IMAC adenosine triphosphate (ATP) buffer (50 mM Tris pH 7.5, 150 mM NaCl, 30 mM imidazole, 10 mM OGP, 5 mM ATP, 5 mM MgCl₂) and 10 mL IMAC buffer A. Elution of His₆-tagged protein was done with ten times 1 mL of a mixture consisting of 50 % IMAC buffer A and 50 % IMAC buffer B (50 mM Tris pH 7.5, 150 mM NaCl, 0.5 M imidazole, 10 mM OGP). Elution fraction 3 was used for further experiments or in case more protein was needed, elution fractions 2 and 3 were combined for further use.

Protein concentrations were determined either by Bradford assay (Bradford, 1976) or by using a Nanodrop™ 2000 Spectrophotometer (Thermo Scientific). Protein purity was assayed by sodium dodecyl sulfate polyacrylamide gel electrophoresis (SDS-PAGE).

Cell lysis for enzymatic activity assays

For each sample a cell pellet harvested from 10 mL expression culture was used. The pellet was thawed on ice and meanwhile resuspended in 6 mL IMAC buffer A (50 mM Tris pH 7.5, 150 mM NaCl, 30 mM imidazole, 10 mM OGP). 30 µL PMSF (stock: 200 mM in isopropanol) were added and the cells were immediately lysed by sonicating five times for 30 s (pulsed sonication, 40 % duty cycle, output control: 4 (micro)) with a resting phase of 1 min after each sonication phase. Total protein concentration of the lysate sample was determined by Bradford assay (Bradford, 1976) and lysate samples were diluted with IMAC buffer A to the desired protein concentration.

Nano-electrospray ionization tandem mass spectrometry (nanoESI-MS/MS) competition assay

The nanoESI-MS/MS measurement was performed as described by Iven *et al.* (2013). Enzymatic reaction conditions were chosen according to Barney *et al.* (2012) by applying changes to the protocol. If not stated differently, fatty alcohols and acyl-CoA were purchased from Sigma.

Reaction mixtures were set up consisting of 20 μ L *E. coli* lysate (corresponding to 20 μ g total protein), 4 μ L of each of the eight fatty alcohols (1 mM stock solution in dimethyl sulfoxide (DMSO); used fatty alcohols: 10:0 OH, 12:0 OH, 14:0 OH, 16:0 OH, 16:1 OH, 18:0 OH, 18:1 OH, 20:0 OH) and 2.5 μ L of each of the six acyl-CoA (stock solutions in 20 mM phosphate buffer pH 7.34; used acyl-CoA: 14:0 CoA (stock: 1.05 mM), 16:0 CoA (stock: 0.27 mM), 16:1 CoA (stock: 0.85 mM), 18:0 CoA (stock: 0.73 mM), 18:1 CoA (stock: 0.62 mM), 20:0 CoA (Avanti Polar Lipids, stock: 0.53 mM)) in a total volume of 800 μ L reaction buffer (50 mM sodium phosphate buffer pH 7.4, 150 mM NaCl). To determine the signal background of the nanoESI-MS/MS measurement, a control sample with lysate from *E. coli* expressing an empty vector was also prepared. Samples were incubated for 30 min at room temperature before stopping the reactions by shock-freezing the samples in liquid nitrogen. Until neutral lipid extraction was performed, samples were stored at -20 °C.

Neutral lipid extraction was performed as described by Vollheyde *et al.* (2020) for the *in vitro* bifunctionality assay using 800 μ L solvents instead of 1 mL and without adding internal extraction standards. The extracted neutral lipids were spotted on a thin layer chromatography (TLC) silica plate (TLC Silica gel 60, 20 x 20 cm, Merck Millipore). The TLC plate was developed with hexane/diethyl ether/acetic acid (80:20:1, v/v/v) as running solvent. Afterwards, the plate was sprayed with 8-anilino-1-naphthalene sulfonic acid (0.2 %, w/v) and lipid bands were marked under UV light. WE-containing bands were scraped from the plate and WE were extracted from the silica with hexane. For that, 1 mL hexane was added to the silica of each sample and the samples were vortexed. The samples were either stored overnight at -20 °C with argon or processed further immediately. After centrifugation (10 min, 800 g), the hexane phase was transferred to a new vial and another 1 mL hexane was added to the silica. After vortexing and centrifuging (10 min, 800 g), the hexane phase was combined with the first hexane phase. To remove remaining small silica particles, 500 μ L ultrapure water were added to the combined hexane phase, the sample was vortexed and centrifuged (10 min, 800 g). The upper hexane phase was transferred to a new vial and either stored overnight at -20 °C with argon or processed further immediately. The hexane was evaporated under a nitrogen stream and WE were dissolved in 50 μ L methanol:chloroform (2:1, v/v) containing 5 mM ammonium acetate for the nanoESI-MS/MS measurement. Each sample was measured three times. From all three empty vector controls, the signal areas of each transition of the multiple reaction monitoring (MRM) were averaged and these data were considered as background signals. Therefore, these means were subtracted from the signal area of the corresponding MRM transition of each sample measurement. Resulted negative values were set to zero. Relative amounts of all WE species in one measurement were calculated and mean values and standard deviations were calculated from the three measurements for each WE species of each sample.

TLC-based enzymatic activity assay

The assay, modified from Stöveken *et al.* (2005) using enzymatic reaction conditions chosen according to Barney *et al.* (2012), was performed as described by Vollheyde *et al.* (2020). Fatty alcohol, DAG and acyl-CoA were purchased from Sigma if not stated differently.

The assay was performed with *E. coli* lysate. The reactions were set up with 20 μ M 18:1 OH or di-16:0-DAG (20 μ L of 1 mM stock solution in DMSO), 12.5 μ L 18:1 CoA (stock solution of 0.62 mM in 20 mM phosphate buffer pH 7.34) and 20 μ L protein solution (corresponding to 20 μ g total protein from lysate samples) in a total volume of 1 mL enzymatic activity reaction buffer (50 mM sodium phosphate buffer pH 7.4, 150 mM NaCl).

Neutral lipid extraction and TLC were performed as described by Vollheyde *et al.* (2020) for the *in vitro* bifunctionality assay.

Results

AbWSD1 crystallized with a bound myristic acid

A fusion protein of *E. coli* TF and *A. baylyi* bifunctional AbWSD1 was crystallized through *in situ* proteolysis with trypsin (Table S3.2). Crystals diffracted up to 2.1 Å resolution. The structure was determined by single-wavelength anomalous diffraction phasing using selenomethionine labelled crystals. The structure revealed that AbWSD1 crystallized without the TF.

AbWSD1 consists of two subdomains and each subdomain is composed of an α/β fold with a mixed β -sheet (Figure 3.1a). The stretch comprising residues 166-217, which connects both subdomains is missing from the structure. The AbWSD1 structure contains 384 from 458 residues. There are crossovers between the two subdomains with strands β 12 and β 13 completing the N-terminal β -sheet and strand β 13 interacts with strand β 1. Furthermore, strands β 7 and β 8 interact with strand β 15 in the β -sheet of the C-terminal subdomain. The electrostatic potential of the protein revealed mostly negatively charged residues on the surface of the N-terminal part of the enzyme and more positively charged residues on the surface of the C-terminal part (Figure 3.1b).

AbWSD1 belongs to the superfamily of CoA-dependent acyltransferases (Murzin *et al.*, 1995). A DALI search revealed that the structure of MaWSD1 (PDB accession code 6CHJ) is the most similar structure to AbWSD1 in the Protein Data Bank (Petronikolou & Nair, 2018; Holm, 2020). AbWSD1 and MaWSD1 structures share 47 % sequence identity and superimpose with a root

mean square deviation (r.m.s.d.) of 1.9 Å for 355 aligned residues in case of MaWSD1 chain A and 356 aligned residues in case of MaWSD1 chain B.

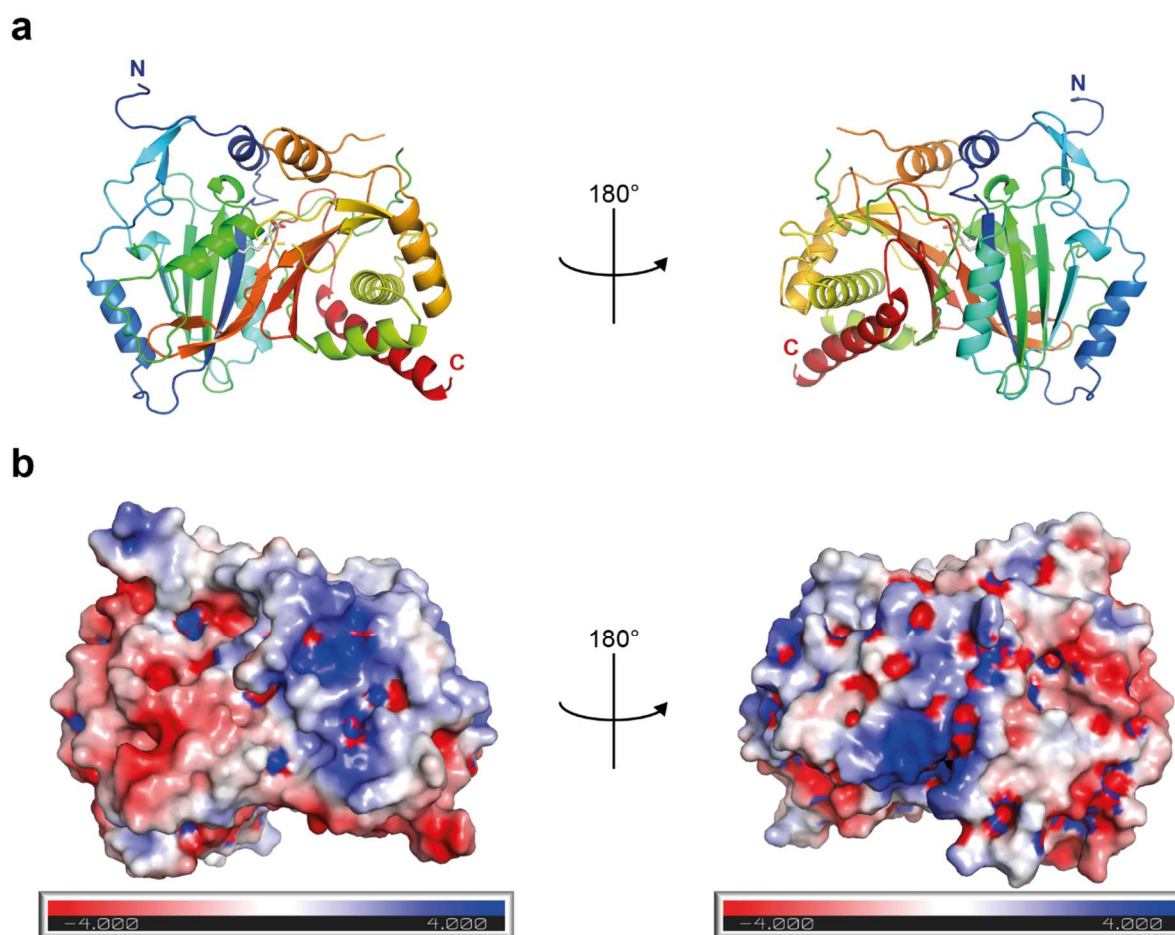


Figure 3.1. Crystal structure of AbWSD1.

(a) Rainbow representation of AbWSD1. The polypeptide chain and secondary structure elements are colored from dark blue (N-terminus) to red (C-terminus). The co-crystallized myristic acid is depicted in grey with red oxygen atoms. A detailed view of the fatty acid is shown in Figure 3.2a. **(b)** Electrostatic potential of AbWSD1. The electrostatic potential of the surface was depicted using the APBS Tools Pymol plugin (Baker *et al.*, 2001; Dolinsky *et al.*, 2004; Lerner & Carlson, 2006). Red color marks areas with positively charged residues, blue highlights regions with negatively charged residues, grey depicts neutral amino acids.

The AbWSD1 structure contains a myristic acid (14:0, the number in front of the colon displays the number of carbon atoms, the number behind the colon displays the number of double bonds) that most likely bound during *E. coli* expression (Figure 3.1a and 3.2). The aliphatic chain of the saturated fatty acid forms hydrophobic interactions with the β -sheet and helix α_6 in the N-terminal subdomain (Figure 3.2). The carboxylate group is localized in the active center of the enzyme at the interface of both subdomains. The conserved HHxxxDG motif is

localized in the loop connecting strand $\beta 6$ and helix $\alpha 6$ (Figure 3.2a). A part of the motif is arranged in a short α -helical turn ($\alpha 5$). The second histidine AbWSD1-H133 of the motif and AbWSD1-D137 are pointing towards the active site. The carboxylate group of myristic acid forms a hydrogen bond with the amide nitrogen of AbWSD1-G138 (Figure 3.2b).

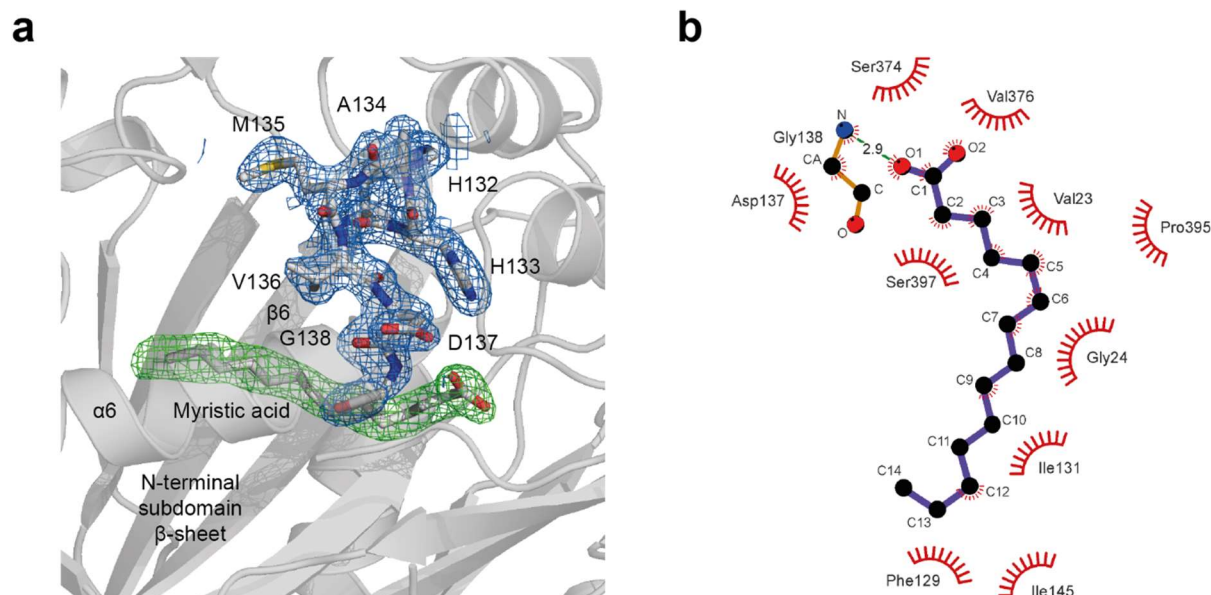


Figure 3.2. Active site.

(a) The conserved motif HHAMVDG is shown with the 2.1 Å resolution 2mFo-DFc electron density map contoured at $\sigma=1.3$. The bound ligand myristic acid is shown with the omit difference electron density map contoured at $\sigma=+2.5$. Oxygen atoms are depicted in red, nitrogen atoms in blue and sulfur in yellow. (b) The schematic view shows the interactions between myristic acid and AbWSD1. Oxygen atoms are depicted in red, the nitrogen atom is depicted in blue. The figure was prepared with LigPlot+ (Wallace *et al.*, 1995).

AbWSD1 and MaWSD1 crystal structures differ in two distinct areas

The recently crystallized MaWSD1 is the closest homolog of AbWSD1 in *Marinobacter* (Holtzapfle & Schmidt-Dannert, 2007; Petronikolou & Nair, 2018). A structural comparison of both MaWSD1 chains with AbWSD1 shows that the two proteins share a nearly identical tertiary structure (Figure 3.3a, Figure S3.1). The second histidine of the catalytic motif (HHxxxDG) of both enzymes is located at a similar position. However, MaWSD1-H136 is slightly twisted in both chains compared to AbWSD1-H133.

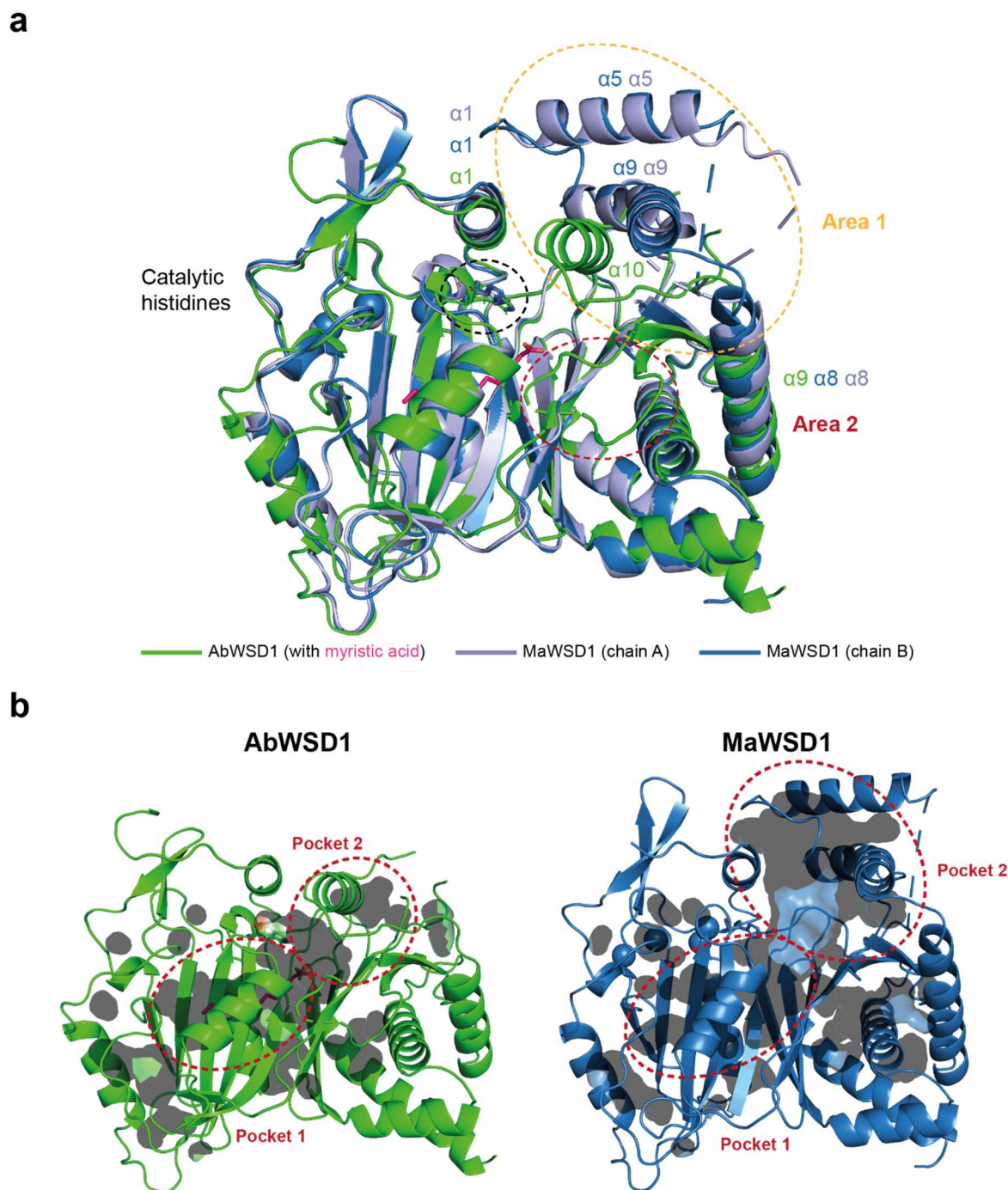


Figure 3.3. Structural alignment of AbWSD1 and MaWSD1.

(a) The structures of AbWSD1 (green) and MaWSD1 chain A (purple) and chain B (dark blue) were superimposed using Pymol 2.2.0a0 (Schrodinger, 2015). The yellow and red dashed ellipses highlight areas that structurally differ between AbWSD1 and MaWSD1. The black dashed ellipse marks the proposed catalytic histidines. The co-crystallized myristic acid in AbWSD1 is depicted in pink with red oxygen atoms. (b) Inner surfaces of AbWSD1 and MaWSD1 chain B. The red dashed ellipses mark putative substrate binding sites (Pocket 1: acyl-CoA; Pocket 2: fatty alcohol) proposed by Petronikolou and Nair (2018).

Although AbWSD1 and MaWSD1 are structurally very similar, they differ in two areas (Figure 3.3a). Area 1 consists of the region C-terminal of helix $\alpha 9$ and $\alpha 10$ from AbWSD1 as well as $\alpha 5$, the C-terminal part of $\alpha 8$ and $\alpha 9$ (and a small α -helix only present in chain A) from MaWSD1. Helix $\alpha 5$ from MaWSD1 was described as a helical linker region between the N- and C-terminal domain of the protein (Petronikolou & Nair, 2018). The helix is positioned on top of the C-terminal part of $\alpha 9$. Both helices interact with each other through hydrophobic interactions between alanine, leucine, isoleucine and phenylalanine residues. The corresponding region of AbWSD1 is missing in the crystal structure.

Helix $\alpha 9$ from MaWSD1 and the corresponding helix $\alpha 10$ from AbWSD1 differ not only in position, but also in length. Whereas $\alpha 10$ from AbWSD1 is shorter and shifted towards $\alpha 1$, $\alpha 9$ is longer and kinked and shifted towards the outer part of the protein. Due to the inward position of $\alpha 10$ in AbWSD1, the C-terminal part of $\alpha 9$ is shortened in the protein compared to MaWSD1 $\alpha 8$. Petronikolou and Nair (2018) identified two potential substrate binding pockets in MaWSD1, which were proposed to harbor the acyl-CoA and the fatty alcohol during WE production. Whereas pocket 1 can be found in a similar position and also with a comparable size in AbWSD1, pocket 2 is much smaller (Figure 3.3b). The reduction in size of pocket 2 in AbWSD1 is caused by the shift of $\alpha 10$ towards $\alpha 1$. This conformational difference results in the closure of pocket 2 on top of the active site.

Area 2 depicts a second region with structural differences between AbWSD1 and MaWSD1 (Figure 3.3a). This area consists of a loop region that is present in AbWSD1 but not displayed in the structure of MaWSD1. The loop region is located on the outside of the protein, covering the region beneath the entrance towards the active site of the enzyme.

The co-crystallized myristic acid aligns with the proposed acyl-CoA binding site

Petronikolou and Nair (2018) assigned pocket 1 of MaWSD1 as the potential acyl-CoA binding site. This assignment is confirmed by our finding that the co-crystallized myristic acid aligns perfectly with pocket 1 of AbWSD1 (Figure 3.3b). Furthermore, Petronikolou and Nair (2018) could show that mutations of the pocket aligning residues MaWSD1-G25 and MaWSD1-A144 towards valine and phenylalanine, respectively, change the acyl-CoA preference of MaWSD1, but not the fatty alcohol specificity. These mutations shorten pocket 1 and only allow the binding of C6-CoA and C7-CoA in a fully extended form. A structural alignment of AbWSD1 and MaWSD1 shows that MaWSD1-G25 and MaWSD1-A144 are both located as such that an interaction with an acyl chain positioned like the co-crystallized myristic acid is possible (Figure 3.4a, c, e). Within the alignment, the side chain of MaWSD1-A144 even interacts with

the carbons C8 and C9 of myristic acid within a distance of 3.5 Å. This shows, that a mutation of both residues towards larger amino acids closes the cavity and results in a preference for shorter acyl chains.

In order to obtain more evidence for the binding of acyl-CoA in pocket 1 upon WE production, amino acid exchange mutants were generated for AbWSD1. Residues AbWSD1-V23 and AbWSD1-G24 were chosen for mutations towards tryptophan. Both residues are located on the β -strand β 1 like MaWSD1-G25, but compared to MaWSD1-G25 and MaWSD1-A144, both amino acids are closer positioned towards the proposed catalytic histidine (Figure 3.4a, b, d). A LigPlot+ analysis depicts that AbWSD1-V23 and AbWSD1-G24 both show hydrophobic interactions with carbon C3 and C5 as well as C6 and C8 of myristic acid (Figure 3.2b). However, as neither WE nor TAG formation was detected for the generated double mutant AbWSD1-V23W-G24W by the TLC-based enzymatic activity assay, a more detailed analysis for changes in substrate specificities was not possible (Figure 3.5a, Figure S3.2, Table S3.3).

Attempts to extend pocket 1 by generating the mutants AbWSD1-S148A, AbWSD1-L149A and AbWSD1-S148A-L149A, resulted in less active protein in case of the AbWSD1-L149 mutants and no changes in acyl-CoA specificity for AbWSD1-S148A (data not shown). All generated amino acid exchange mutants are summarized in Table S3.3. The AbWSD1 structure with all marked amino acids that were substituted is shown in Figure S3.3.

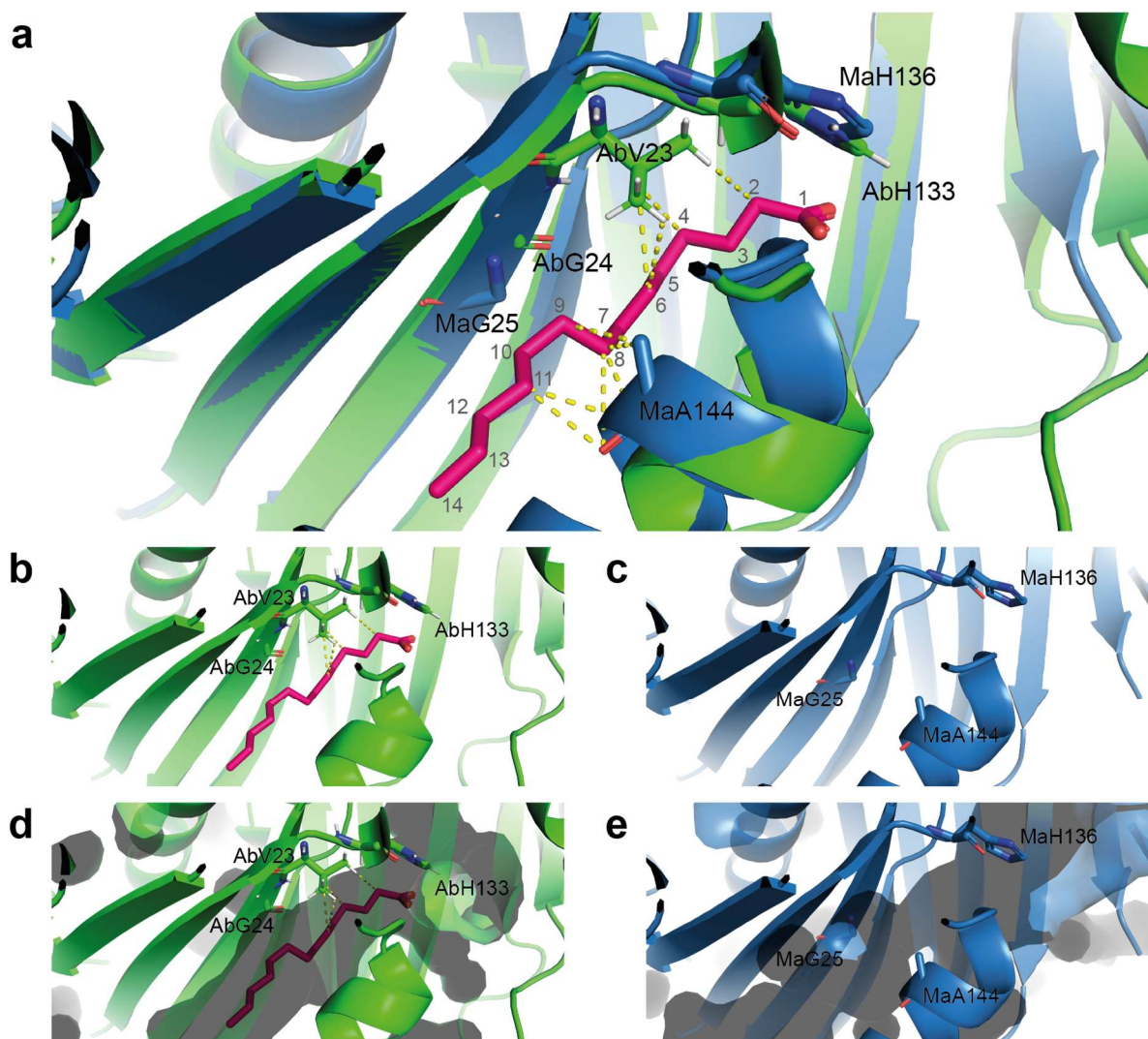


Figure 3.4. Acyl-CoA binding pocket.

(a) Superimposition of AbWSD1 (green) with co-crystallized myristic acid (pink) and MaWSD1 chain B (blue) (b) AbWSD1 alone (c) MaWSD1 chain B alone (d) inner surface of AbWSD1 (e) inner surface of MaWSD1 chain B. The proposed catalytic histidines are depicted as well as mutated residues around the acyl-CoA binding site in AbWSD1 (this study) and in MaWSD1 (Petronikolou & Nair, 2018). Yellow dashed lines mark interactions between atoms within 3.5 Å. Oxygen atoms are depicted in red, nitrogen atoms in blue.

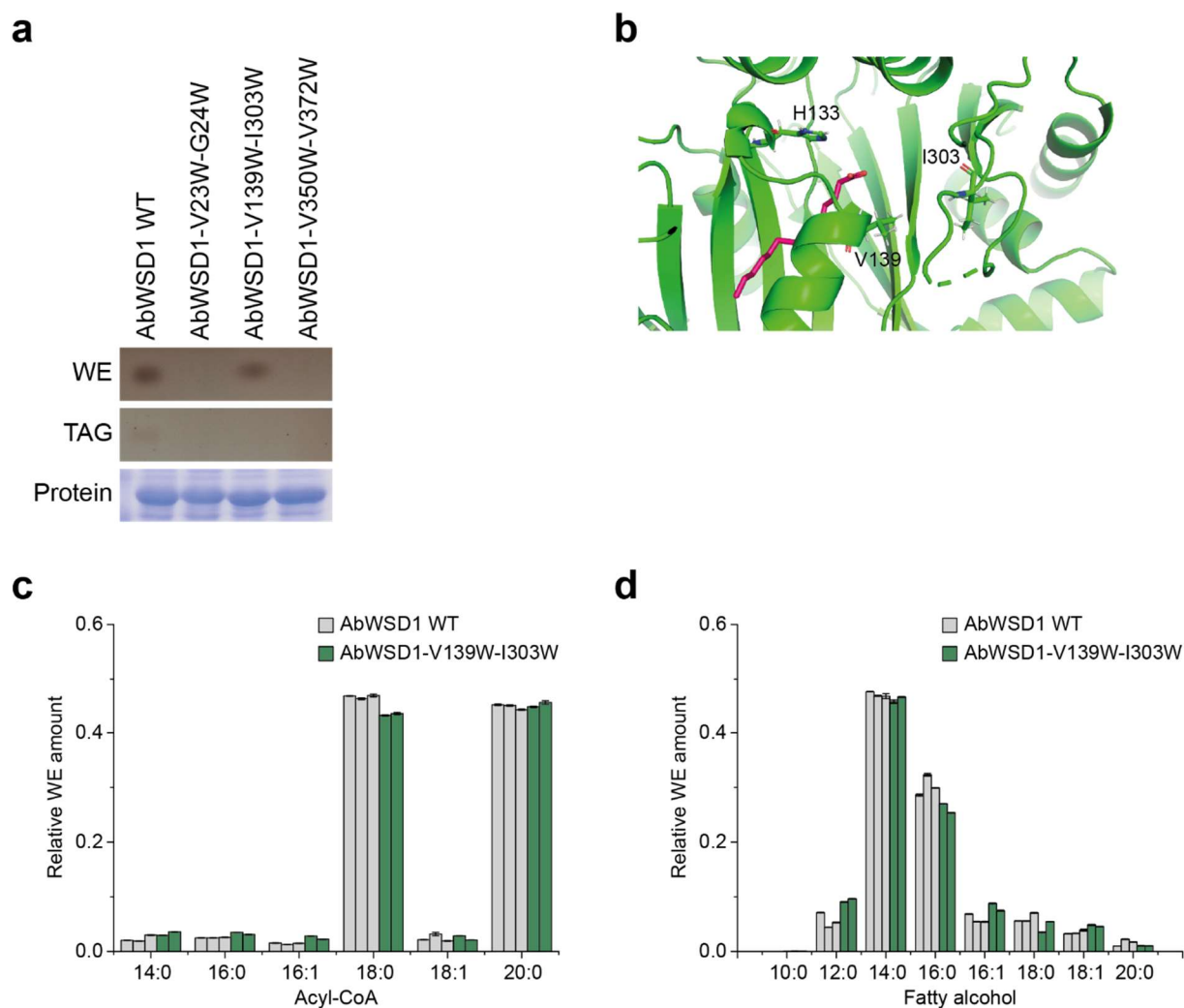


Figure 3.5. Analysis of the DAG binding pocket.

(a) Analysis of WS and DGAT activities of different AbWSD1 variants. *E. coli* lysate of cells expressing AbWSD1 WT or the generated amino acid exchange mutants was incubated for one hour at room temperature either with 18:1 CoA and 18:1 OH to test for WS activity or 18:1 CoA and di-16:0-DAG to test for DGAT activity. Neutral lipids were extracted from the reaction mix and separated by TLC. **(b)** Close up of the DAG binding cavity. The mutated residues are depicted as well as the proposed catalytic histidine. Oxygen atoms are depicted in red, nitrogen atoms in blue. **(c)** **(d)** WE competition assay. *E. coli* lysate expressing the enzyme variants was incubated with six different acyl-CoA and eight different fatty alcohols. The produced WE species were analyzed by nanoESI-MS/MS. The method is optimized for the detection of WE species with 32 carbons or more (Iven *et al.*, 2013). To determine enzyme specificities, detected WE species were grouped by the incorporated acyl-CoA **(c)** and fatty alcohol species **(d)**. Each bar represents the mean of three measurements of one biological replicate \pm standard deviation. Bars of the same color depict different biological replicates. For a better comparison of AbWSD1 WT and AbWSD1-V139W-I303W, the data for AbWSD1 WT, which is the same presented in Figure 3.6, is displayed again.

The β -strand β 11 is important for right acyl-CoA positioning

The LigPlot+ analysis shows an interaction of AbWSD1-S374 and AbWSD1-V376 with the carboxylate group of myristic acid, too (Figure 3.2b). Both residues are located on the β -strand β 11 (Figure 3.6a, Figure S3.4). Amino acids forming this β -strand are quite conserved in WSD (Figure S3.5). The β -strand forms the curvature opposite to the active site. Except for AbWSD1-S374 and AbWSD1-V376, also AbWSD1-V372 is located on β 11, facing towards the cavity. Directly on top of AbWSD1-V372 a third valine is located (AbWSD1-V350), which is part of α -helix α 10 and it is also oriented towards the active site.

In order to analyze the sterical influence of the described valine residues on the positioning of acyl-CoA, these residues were mutated to the large but still hydrophobic tryptophan. The AbWSD1-V376W single mutant was generated to analyze the sterical importance of the C-terminal part of β 11. To get more information about the sterical function of the N-terminal part of β 11 and also about the region on top of this, the double mutant AbWSD1-V350W-V372W was generated. The influence of the mutations on substrate selectivity were analyzed by a nanoESI-MS/MS competition assay. For that, lysate of *E. coli* cells expressing the enzyme variants was incubated with six different acyl-CoA and eight different fatty alcohols. The generated WE species were analyzed by nanoESI-MS/MS. The method is optimized for the detection of WE species of 32 carbons and more (Iven *et al.*, 2013) and was used here for a direct comparison of produced WE species by AbWSD1 WT and mutants. The measured WE profiles of AbWSD1 WT, AbWSD1-V376W and AbWSD1-V350W-V372W are shown in the Figure S3.6. Figures 3.6c and d depict the relative amounts of the chain length specificities for the fatty acid and the alcohol moieties. Compared to AbWSD1 WT, AbWSD1-V376W and AbWSD1-V350W-V372W show a higher preference for the incorporation of 18:0 CoA into WE and a lower preference for the incorporation of 20:0 CoA. In terms of fatty alcohol selectivity the differences are not that pronounced between the AbWSD1 WT and the two mutants. AbWSD1-V350W-V372W seems to have a higher preference for 14:0 OH and a lower preference for 16:0 OH when compared to the AbWSD1 WT. In addition to AbWSD1-V376W, also AbWSD1-V376A and AbWSD1-V376F were analyzed by the nanoESI-MS/MS assay. Both mutants showed a similar substrate preference as AbWSD1 WT (data not shown).

Compared to WT, AbWSD1-V376W and AbWSD1-V350W-V372W showed less WE forming activity and at least no detectable DGAT activity (Figure 3.5a, Figure S3.7). Due to that, it is not possible to conclude, that the preference for the incorporation of shorter acyl-CoA into WE is caused by sterical hindrance or, whether it is an artefact caused by the lower enzymatic activity. Interestingly, for AbWSD1-V376A and AbWSD1-V376F a reduced DGAT activity was observed as well, whereas the WS activity was comparable to WS activity of AbWSD1 WT (Figure S3.7).

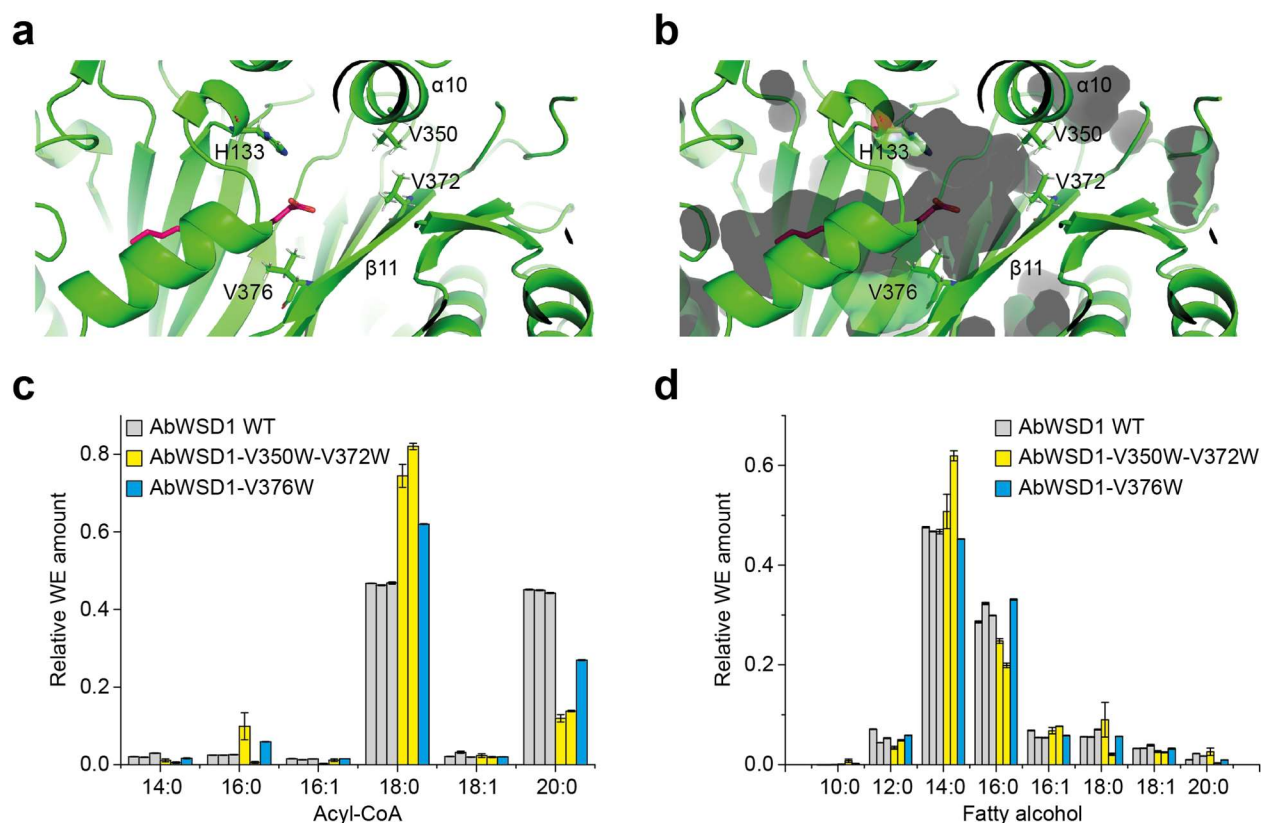


Figure 3.6. Amino acids forming the active site opposite to the catalytic histidine.

(a) (b) Close up of the active site of AbWSD1 without (a) and with (b) inner curvatures displayed. The catalytic histidine is depicted as well as the amino acid residues that were mutated in this study. Oxygen atoms are depicted in red, nitrogen atoms in blue (c) (d) WE competition assay. *E. coli* lysate expressing the enzyme variants was incubated with six different acyl-CoA and eight different fatty alcohols. The produced WE species were analyzed by nanoESI-MS/MS. The method is optimized for the detection of WE species with 32 carbons or more (Iven *et al.*, 2013). To determine enzyme specificities, detected WE species were grouped by the incorporated acyl-CoA (c) and fatty alcohol species (d). Each bar represents the mean of three measurements of one biological replicate \pm standard deviation. Bars of the same color depict different biological replicates. For a better comparison of AbWSD1 WT and the mutants, the data for AbWSD1 WT, which is the same presented in Figure 3.5, is displayed again.

A conformational change of helix α 10 may facilitate the binding of the CoA unit

Petronikolou and Nair (2018) identified two substrate pockets within the structure of MaWSD1. They allocated the potential acyl-CoA binding site in pocket 1 and assigned pocket 2 as the fatty alcohol binding site (Petronikolou & Nair, 2018). In order to study cavities within AbWSD1 and to compare them with MaWSD1, cavities within both proteins were analyzed using CAVER 3.0.1 PyMol plugin (Chovancova *et al.*, 2012; Pavelka *et al.*, 2016). The CAVER analysis revealed three potential cavities in AbWSD1 and four cavities around the active site of MaWSD1 (Figure S3.8). Based on Petronikolou and Nair (2018) and results described here, two out of these four cavities are involved in substrate binding: Cavity 1 resembles pocket 1

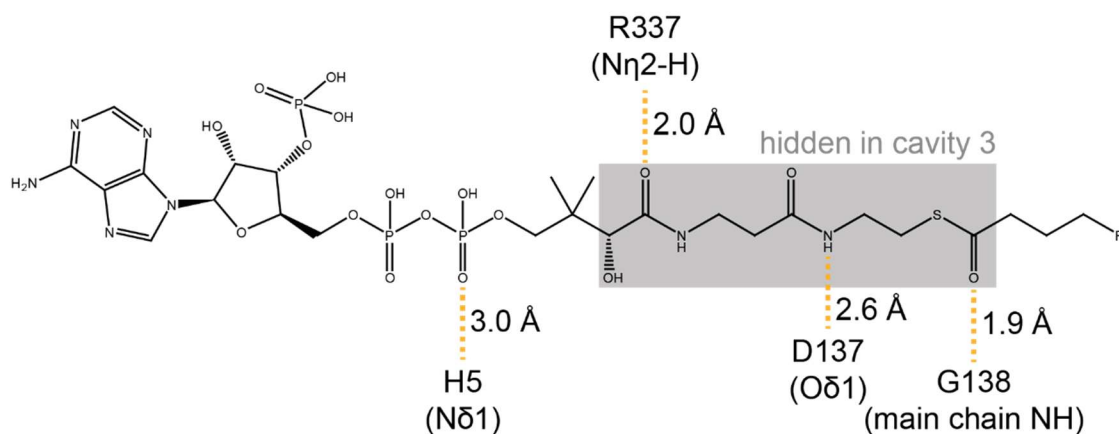
and binds the acyl chain and cavity 2 in MaWSD1 is assigned to the narrowed pocket 2 of AbWSD1 and harbors the fatty alcohol.

Petronikolou and Nair (2018) proposed binding of acyl-CoA with the acyl chain hidden in pocket 1, the phosphoadenosine moiety exposed to the solvent and the pantetheine part linking both. As a consequence of the inward position of AbWSD1- α 10, the large aperture in front of the active site as present in MaWSD1 (Petronikolou & Nair, 2018) is closed in AbWSD1 and cavity C3 is generated instead (Figure S3.8). To investigate whether a binding of acyl-CoA, especially of the pantetheine linker and the phosphoadenosine moiety might also be possible in cavity C3, palmitoyl-CoA was modelled into the structure of AbWSD1 (Figure S3.9a). Upon positioning of palmitoyl-CoA the following prerequisites were considered: 1. the acyl chains of the co-crystallized myristic acid and the modelled palmitoyl-CoA are at similar positions; 2. the hydrogen bonding distance between AbWSD1-G138 main chain NH and the carboxyl group of the co-crystallized myristic acid is retained in the model by the AbWSD1-G138 main chain NH and the thioester CO (Figure 3.2b); 3. the sulfur atom of the thioester is in close proximity to the proposed catalytic AbWSD1-H133 to allow a protonation of the CoA-S⁻ after the thioester bond cleavage as proposed by Stöveken *et al.* (2009); 4. the carbonyl carbon of the thioester is facing towards the alcohol cavity to be accessible for the nucleophilic attack of the oxyanion; 5. the pantetheine part is modelled in the upper part of the cavity to leave some space in the catalytic pocket for the fatty alcohol and DAG. When sticking to these prerequisites palmitoyl-CoA is positioned in AbWSD1 as shown in Figure S3.9a. Due to the short length of cavity C3 only the pantetheine linker of palmitoyl-CoA is buried in the cavity and the phosphoadenosine part is exposed to the solvent (Figure 3.7a, Figure S3.9b). This would also allow a binding of acyl-ACP, which harbors the larger ACP instead of the phosphoadenosine part. By sticking to prerequisites 3 and 5, the thioester bond of the modelled palmitoyl-CoA may be slightly twisted compared to the position of the carboxyl group of the co-crystallized myristic acid (Figure S3.9a, c). In the model, palmitoyl-CoA is able to form four hydrogen bonds with amino acids from AbWSD1 (Figure 3.7): thioester CO – AbWSD1-G138 (main chain NH); first peptide bond NH – AbWSD1-D137 (O δ 1); second peptide CO – AbWSD1-R337 (N η 2-H); first phosphate PO – AbWSD1-H5 (N δ 1). Interestingly, AbWSD1-D137 and AbWSD1-G138 are part of the conserved catalytic motif. The corresponding amino acids in MaWSD1 are MaWSD1-N5, MaWSD1-D140, MaWSD1-G141 and MaWSD1-H342. The positions of the first three amino acids are similar in the structures of AbWSD1 and MaWSD1. However, MaWSD1-H342 is differently located on top of MaWSD1- α 8 facing towards the outside of the protein (Figure S3.9d). The C-terminal part of MaWSD1- α 8 is the region that is present as a loop region in AbWSD1 on the N-terminal site of AbWSD1- α 10 which is positioned inward compared to the corresponding MaWSD1- α 9.

The position of MaWSD1-H342 seems too far away from the active site in order to interact with CoA. However, a conformational change within MaWSD1, which moves $\alpha 9$ closer to $\alpha 1$ might lead to a shortening of $\alpha 8$ at the C-terminal part and together with this, a positional change of MaWSD1-H342 towards a similar position as AbWSD1-R337 might be possible. Since AbWSD1 crystallized with a bound myristic acid and MaWSD1 not, it might be possible, that this described conformational change occurs upon acyl-CoA binding.

To analyze, whether the incubation with substrates leads to a conformational change in AbWSD1, dynamic light scattering (DLS) was performed. But, as the particle sizes in tested solutions with AbWSD1 were not homogenous, it was not possible to detect small differences in protein size after substrate addition (data not shown).

a



b

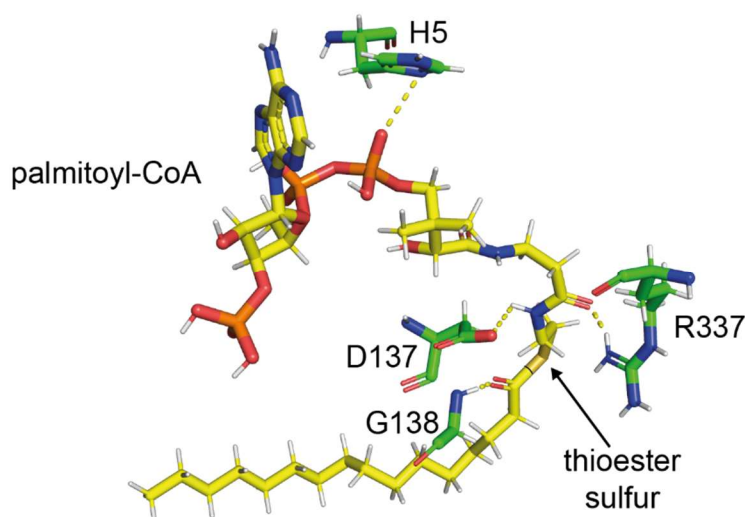


Figure 3.7. Modelling of palmitoyl-CoA into the structure of AbWSD1.

(a) Chemical structure of palmitoyl-CoA. The grey box highlights the area that is buried in cavity C3. The yellow dashed lines mark potential hydrogen bonds between the molecule and amino acids of AbWSD1. **(b)** 3D orientation of the modelled palmitoyl-CoA and the amino acids forming potential hydrogen bonds (yellow dashed lines) in AbWSD1. Oxygen atoms are depicted in red, nitrogen atoms in blue, phosphorus atoms in orange and the sulfur atom is depicted in dark yellow.

The loop region from area 2 is important for DAG binding

AbWSD1 is a bifunctional enzyme, that is not only capable to produce WE from acyl-CoA and fatty alcohols, but also TAG from acyl-CoA and DAG (Stöveken *et al.*, 2005). However, DAG and fatty alcohol clearly differ on the structural level. Whereas the fatty alcohol only consists of an alkyl chain with the hydroxyl group at one end, DAG consists of two acyl chains esterified to a glycerol backbone. The second carbon chain does not only lead to a larger molecule, but also the presence of the esterified glycerol backbone might result in the need of a more hydrophilic binding environment.

To analyze, whether cavity 4 might be involved in DAG binding, amino acid exchange mutants of residues surrounding this cavity were generated. The cavity is formed by the loop region from area 2, the α -helix $\alpha 6$ and the C-terminal part of $\beta 11$ together with the subsequent loop region (Figure S3.8b). For this purpose, a valine residue from $\alpha 6$ (AbWSD1-V139) and an isoleucine residue from the loop region of area 2 (AbWSD1-I303) facing each other were chosen (Figure 3.5b).

Mutations of AbWSD1-V139 towards alanine, phenylalanine, tryptophan and isoleucine resulted in changes in TAG production, but did not affect WE production when the mutants were compared to WT (Figure S3.7). The generated AbWSD1-V139W-I303W double mutant did not produce TAG in detectable amounts anymore (Figure 3.5a, Figure S3.2). The WE production as well as the acyl-CoA and fatty alcohol specificities were not altered in the double mutant (Figures 3.5a,c,d, Figures S3.2, S3.6). After one hour incubation of *E. coli* lysate expressing the WT or the mutant enzyme with 18:1 OH and 18:1 CoA, the produced WE amounts of the mutant were comparable with that of the WT enzyme (Figure 3.5a, Figure S3.2). An analysis of AbWSD1-V139W-I303W with the nanoESI-MS/MS competition assay also showed that the substrate selectivity towards acyl-CoA and fatty alcohol is not changed compared to the WT enzyme (Figures 3.5c,d, Figure S3.6).

Within the class of WSD, enzymes are described that are not capable to produce TAG (Kalscheuer *et al.*, 2007; King *et al.*, 2007; Vollheyde *et al.*, 2020). Having amino acids identified that form the potential DAG binding site, it may now be possible to examine, whether the ability to produce TAG can be predicted from the amino acid sequence. To investigate this, a multiple sequence alignment of 25 WSD from bacteria and plants was generated. Out of these 25 WSD, 17 enzymes were described to harbor WS and DGAT activity, three only have WS activity, three others were only tested on WE production and exhibited WS activity and the last two enzymes are only able to form TAG (Table S3.4). Figure 3.8 depicts the parts of the multiple sequence alignment that contain the DAG cavity forming residues of AbWSD1. It can be seen, that mono- and bifunctional WSD do not form groups in the alignment. Differences caused by different phylogenetic origins seem to be more pronounced than differences that

cause differences in substrate specificities. An evaluation of parts of the potential DAG cavity revealed no correlation between DAG cavity forming amino acid residues and the ability to produce WE or TAG.

Amino acids from tDGAT of *Thermonospora curvata* that were identified to have an influence on the DGAT activity upon mutation (Röttig *et al.*, 2015; Santín *et al.*, 2019a) as well as AbWSD1-G355, that was shown by Röttig *et al.* (2015) to lead to a lack of DGAT activity of AbWSD1 when exchanged to isoleucine, are marked in the sequence alignment (Figure S3.5). None of these residues align with amino acid residues that form the proposed DAG binding site in AbWSD1.

	I	II	III	IV	V	VI	VII
PhWS1	VHHSIGDGTSLISLLAC	LRPSA	GWGNWFGY	FEALY	FSNVVGPQE		
AtWSD1	IHHSIGDGMISLMLLAC	LRPAT	RWGNFIGT	LEAFF	FSNVKGPDE		
TrWSD4	ISHIVGDGIAQVEVLMRL	IRSKS	NPRNKFTY	PSPVY	VSNVPGPQD		
TrWSD5	ADHTHADGASAVSALLSM	VRPSG	WFGNHIVV	PDMIV	ISNVLFSLT		
MaWSD5	LHHCYADGLSLIGIFDRI	IRARL	EPGNCFGT	WCPGL	VSNVPGTPE		
ScSco1280	TDHTFQDGMGAYTARAL	VRAPG	APGNRMVT	RFRDA	GAFVAGPVS		
RoAtf1	VHHSITDGVSGMQIAREI	LRAET	VGGNRITL	PAIPL	ASNVVGPSV		
MtTgs1	LHHCMDGIAATHLLAGL	TRSNS	KTDNRVSL	GQRQF	ATNVPGPRR		
ScSco0958	FHHALADGLRALTLAAGV	RFRPR	PQGNRLSG	GPGRG	VTSVPLPSL		
SaSAV7256	FHHALADGLRALMLAAL	RFRPR	PQGNRLSG	GFNRG	VTSVPLPSL		
MtTgs4	VHHALIDGEGGLRAMRNF	LREKS	GGGNRVSA	GRGMQ	ISNMKGPTTE		
MtTgs3	SHQALINGVTALAIGHVI	---	---	---	---		
TctDGAT	VHHAAVDGVLTATELLAAL	LRRGR	AGGNRMSA	FARSS	VSNVPGPDF		
AlbAtfA1	IHHSVMDGISAMRIASKT	LRQDD	TGGNQIGM	FSQMS	ISNIPGPKE		
MhWS1	VHHSILDGVSAMRMATRM	LRRDD	SGGNQVGV	YRHMS	ISNVPGPSR		
MaWSD1	VHHSILDGVSAMRMATRM	LRRDD	SGGNQVGV	YRHMS	ISNVPGPSR		
AbWSD1	IHHAMVDGVAGMRLIEKS	IRNDD	DVSNRITM	FKRMT	ISNVPGPKE		
PaWS	IHHSILDGIAAMRLVKKKS	LRITD	IAGNQLSF	FRRMN	ISNVPGSEK		
PcPs1	IHHSILDGIAAMRLVKKKS	LRITD	VAGNQLSF	FRRMN	ISNVPGSEK		
RoAtf2	LHHSIMDGVSGLRLLMRT	LRDEQ	AGGNAVGV	FGSLT	ISNVPGPRK		
RjRh1	LHHSIMDGVSGLRLLMRT	LRDEQ	AGGNAVGV	FGSLT	ISNVPGPRK		
MtTgs2	MHHALIDGVSAMKLAQRT	IRSKE	AGGNLVGS	LSLEP	ISNVPGPVD		
MhWS2	MHHSIMIDGISGVRLMQRV	IRPAD	TGT-QISF	LOKLP	ISNVPGPEG		
MaWSD2	MHHSIMIDGISGVRLMQRV	IRPAD	TGT-QISF	LOKLP	ISNVPGPED		
AlbAtfA2	MHHSIMVDGVAGMRLMCSR	LRISAD	ECGNAITT	LCIMQ	ISNVPGPKE		

; *

WS and DGAT activity tested, enzyme has WS and DGAT activity
WS and DGAT activity tested, enzyme only has WS activity
Only WS activity tested, enzyme has WS activity
WS and DGAT activity tested, enzyme only has DGAT activity

I	II	III	IV	V	VI	VII
D137	M142	E146	N(A)294	S300	R337	N375
G138	R(A)143			N301		V376
V139				R302		P377
				I303		G378
						P379

Figure 3.8. Sequence alignment of mono- and bifunctional WSD.

The displayed part of the sequence alignment depicts the amino acids that align to the proposed DAG cavity in AbWSD1. The color code provides information whether the enzyme was tested for WS or DGAT activity and whether the enzyme exhibits the tested activity. A detailed list of all enzymes used for the sequence alignment can be found in Table S3.4. The whole sequence alignment can be found in Figure S3.5.

Discussion

The role of conserved active site residues

The class of bacterial bifunctional WSD was discovered 17 years ago (Kalscheuer & Steinbüchel, 2003). Since then a number of enzymes were characterized (Kalscheuer & Steinbüchel, 2003; Daniel *et al.*, 2004; Kalscheuer *et al.*, 2004; Stöveken *et al.*, 2005; Holtzapfle & Schmidt-Dannert, 2007; Kalscheuer *et al.*, 2007; King *et al.*, 2007; Alvarez *et al.*, 2008; Arabolaza *et al.*, 2008; Li *et al.*, 2008; Kaddor *et al.*, 2009; Barney *et al.*, 2012; Shi *et al.*, 2012; Villa *et al.*, 2014; Röttig *et al.*, 2015; Lázaro *et al.*, 2017; Zhang *et al.*, 2017; Miklaszewska *et al.*, 2018; Petronikolou & Nair, 2018; Santín *et al.*, 2019a; Vollheyde *et al.*, 2020). The WSD from *Acinetobacter* and *Marinobacter* however are the best-characterized WSD so far. With the aim to gain a more detailed information on the enzymes' catalytic mechanism, several amino acid exchange mutants of AbWSD1, MaWSD1 and MaWSD2 were analyzed (Stöveken *et al.*, 2009; Barney *et al.*, 2013; Röttig & Steinbüchel, 2013b; Villa *et al.*, 2014; Barney *et al.*, 2015; Petronikolou & Nair, 2018). However, without any available crystal structure of WSD, it was only possible to draw limited conclusions about the role of the mutated residues. This situation changed when the first crystal structure of a WSD (MaWSD1) was published recently (Petronikolou & Nair, 2018). The AbWSD1 structure presented here further contributes to our understanding, since it also contains a bound fatty acid, which clarifies the location of the active site. A comparison of both WSD structures revealed that the two proteins share a nearly identical tertiary structure and that acyl-CoA binding causes a conformational change of the active site.

The availability of two structures allows a detailed structure-function analysis of WSD, which also takes published analyses of general enzymatic characteristics and amino acid exchange mutants of several WSD into account. In 2009, a catalytic mechanism for AbWSD1 was proposed that is based on a histidine residue (Stöveken *et al.*, 2009). Mutagenesis of the two histidines from the conserved HHxxxDG motif significantly reduced the enzymatic activity of AbWSD1 (Stöveken *et al.*, 2009). However, although the substitution of the second histidine had a larger impact on the enzymatic activity than the exchange of the first one, it remained unclear, which one of the two histidines abstracts the hydrogen from the fatty alcohol's hydroxyl group (Scheme 3.1b). Similar results were also obtained upon the substitution of the two histidines in MaWSD2 (Villa *et al.*, 2014). The crystal structures of AbWSD1 and MaWSD1 show that the second histidine may be the one that is involved in catalysis because only the second histidine of MaWSD1 (MaWSD1-H136) faces towards pocket 2, whereas MaWSD1-H135 is twisted away from it (Petronikolou & Nair, 2018). A similar observation was made in this study. The orientation of AbWSD1-H133 towards the carboxylate group of the co-crystallized myristic acid provides even stronger evidence that the second histidine is involved

in catalysis (Figure 3.2a). The structural importance of the first histidine of the catalytic motif is supported by mutational studies for both AbWSD1 and MaWSD2 and can be explained by the fact that AbWSD1-H132 is located in hydrogen bonding distance to AbWSD1-E15 as MaWSD1-H135 is it to MaWSD1-E15 (Figure S3.10) (Röttig & Steinbüchel, 2013b; Villa *et al.*, 2014; Petronikolou & Nair, 2018). The existence of this hydrogen bond was also supported by the mutation of AbWSD1-E15 towards lysine. It resulted in a severe reduction in enzymatic activity and this residue was found to be conserved among different WSD (Röttig & Steinbüchel, 2013b). A second hydrogen bond of AbWSD1-H132 with AbWSD1-W112 is part of a conserved motif as well. This so-called PLW motif was studied in MaWSD2 (Villa *et al.*, 2014). It consists of a proline, a leucine and the tryptophan residue (Figure S3.10). Mutations of the proline and the leucine residues towards alanine led to a reduced enzymatic activity of MaWSD2. The tryptophan-alanine-mutant however may result in major structural changes, since it was found to be insoluble. Together the position of the PLW motif and the hydrogen bond towards AbWSD1-H132 strongly suggest that it is needed to facilitate the structural integrity of the catalytic motif as already suggested by Villa *et al.* (2014).

Apart from the two histidine residues an aspartate and a glycine residue are also part of the conserved catalytic motif. Whereas an AbWSD1-D137A substitution did not result in significant decrease of WS activity, the MaWSD1-D140A variant had only around 50 % WS activity (Stöveken *et al.*, 2009; Petronikolou & Nair, 2018). Therefore, the authors speculated that MaWSD1-D140 might be important for structural integrity of the catalytic site loop because it forms hydrogen bonds with residues in MaWSD1- α 4. This is possible in AbWSD1 as well, where AbWSD1-D137 forms hydrogen bonds with residues of AbWSD1- α 6 (corresponding to MaWSD1- α 4). However, additional hydrogen bonds between AbWSD1-D137 and AbWSD1-R302 are found in AbWSD1. AbWSD1-R302 is one of the residues that forms the proposed DAG cavity and AbWSD1-R302 is part of the loop region of area 2, which is missing in the MaWSD1 crystal structure. The modelling of palmitoyl-CoA into the AbWSD1 structure indicates that AbWSD1-D137 could form a hydrogen bond to the pantetheine part, suggesting that the conserved aspartate might also be needed for the right positioning of acyl-CoA.

Following this line, AbWSD1-G138 is in hydrogen bonding distance to the carboxyl group of the co-crystallized myristic acid. This rises the hypothesis that the main chain NH of AbWSD1-G138 might also interact with the carbonyl group of the acyl-CoA's thioester as shown for the modelled palmitoyl-CoA (Figure 3.7). The main chain NH of the glycine residue might function in a similar manner as an oxyanion hole in serine proteases (Hedstrom, 2002). It could stabilize the negatively charged oxyanion that is formed upon a possible intermediate state during the nucleophilic attack of the oxyanion of the fatty alcohol on the carbonyl C of the thioester. In line with this, a substitution of the glycine residue towards alanine in AbWSD1 did not significantly affect the WS activity of the enzyme (Stöveken *et al.*, 2009), because alanine is not much

larger than glycine and the important interaction with the carbonyl oxygen is taking place via the main chain.

The combination of both available WSD structures lead to unravelling their substrate binding sites

The two bacterial WSD structures do not only allow the correct assignment of the active site, but also the identification of substrate binding sites. Based on their own mutational studies and supported by the publications of Barney and colleagues (Barney *et al.*, 2013; Barney *et al.*, 2015; Petronikolou & Nair, 2018), Petronikolou and Nair (2018) assigned the binding sites for acyl-CoA and fatty alcohol. The position of the co-crystallized myristic acid within the structure of AbWSD1 described in this study provides additional evidence for the acyl-CoA binding site located in pocket 1 (Figure 3.3b). Especially, one α -helix (AbWSD1- α 6/MaWSD1- α 4) and one β -strand (AbWSD1- β 1/MaWSD1- β 1) aligning pocket 1 are involved in acyl-CoA selectivity. Amino acid substitutions on those two secondary structure elements lead to a changed acyl-CoA selectivity and are therefore potential mutation sites in order to produce tailor-made WE (Petronikolou & Nair, 2018). Even a more pronounced decrease in enzymatic activity for an amino acid substitution on the β -strand (MaWSD1-G25) than on the α -helix was observed. Corresponding to that, it was observed in this study, that mutations at a similar position on the β -strand of AbWSD1 (AbWSD1-V23-G24) resulted in no detectable WE and TAG formation for the enzyme variant in the TLC-based enzymatic activity test (Figure 3.4, Figure 3.5a). The N-terminal part of β 1 is in close spatial distance to the active site. Mutations here might not only influence the width of pocket 1, but also the orientation of the catalytic site. In contrast to that, mutations on the α -helix (AbWSD1- α 6/MaWSD1- α 4) might be balanced out by the enzyme, since the helix is located at the border of the enzyme, which might allow an outward movement of the helix in case of sterical hindrance.

In addition to the amino acids around the substrate cavities, residues around the active site also have an influence on the acyl-CoA selectivity of the enzyme. Indeed the amino acid exchange mutants AbWSD1-V376W and AbWSD1-V350W-V372W showed a higher preference for shorter acyl-CoA compared to the WT enzyme in the competition assays (Figure 3.6). This preference for shorter acyl-CoA may be explained by sterical hindrance. AbWSD1-V372 and AbWSD1-V376 are both located on β 11, which confines the active site pocket opposite to the catalytic histidine. Mutations along this β -strand may have an influence on the positioning of the substrate within the active site. The substitution of the two valines by tryptophan may prevent the bound acyl-CoA from entering deeper into pocket 1, prohibiting the binding of long acyl-CoA. Interestingly, there is also a serine (AbWSD1-S374) located on AbWSD1- β 11 (Figure S3.4). This residue is conserved among different WSD and the

AbWSD1-S374P mutation resulted in a reduction in enzymatic activity (Röttig & Steinbüchel, 2013a; Röttig & Steinbüchel, 2013b; Villa *et al.*, 2014). This might be due to the fact, that proline which is known to be a “structural disruptor” might disrupt β 11. However, a structural alignment of the modeled structure of MaWSD2 with the crystal structure of sorghum hydroxycinnamoyltransferase (HCT), which was crystallized with a bound *p*-coumaroyl-CoA, revealed, that the corresponding serine of MaWSD2 (MaWSD2-S388) may be involved in interacting with the oxyanion of acyl-CoA and therefore may be important for right positing of the substrate (Villa *et al.*, 2014). However, due to the position of the carboxyl group of the co-crystallized myristic acid and the hydrogen bonding distance to the main chain NH of AbWSD1-G138 it is more likely, that AbWSD1-G138 forms the oxyanion hole to stabilize bound acyl-CoA. But, it can be speculated, that AbWSD1-S374 (corresponding to MaWSD2-S388) may be needed to stabilize the oxyanion that is formed at the acyl acceptor after hydrogen abstraction.

In addition to acyl-CoA and fatty alcohol, AbWSD1 also uses DAG as a substrate. Although the reaction mechanism of WE and TAG formation is similar, the DAG binding site has to fulfill different requirements than the fatty alcohol binding site. Here we propose a potential DAG cavity within AbWSD1. Amino acid substitutions of residues aligning this cavity with more space-filling ones resulted in the loss of TAG production while WE production was not changed (Figure 3.5). This strongly suggests that AbWSD1-V139 and AbWSD1-I303 are involved in DAG binding. However, the adjacent cavity might be too small to accommodate both acyl chains and DAG binds with one acyl chain in pocket 2 like the fatty alcohol and only the second acyl chain will then bind to the here identified cavity. This model is supported by the AbWSD1-G355I mutant which lost TAG formation as well (Röttig *et al.*, 2015). Interestingly, AbWSD1-G355I is located at the fatty alcohol binding site and has an additional influence on the fatty alcohol selectivity (Barney *et al.*, 2013). Hence, the fatty alcohol binding site might also be important for the DAG binding of AbWSD1. Recently, ten different enzyme variants of tDGAT from *T. curvata* were identified that show an altered DGAT activity compared to the WT enzyme (Santín *et al.*, 2019a). Three enzyme variants showed reduced TAG production and two of them (tDGAT-T5I, tDGAT-D71Y) still produced WE in comparable amounts to the WT enzyme. These two residues are located in proximity to the fatty alcohol binding site in the modeled tDGAT structure (Santín *et al.*, 2019a). In a sequence alignment of AbWSD1 and tDGAT, the corresponding amino acid to tDGAT-D71 is AbWSD1-N63. This residue is located on AbWSD1- β 2 which might only have an indirect effect on the shape of pocket 2. The corresponding residue to tDGAT-T5 is AbWSD1-H5. We propose that this residue forms a hydrogen bond to the acyl-CoA substrate (Figure 3.7). It might be possible that mutations in this residue cause a slightly tilted position of the acyl-CoA substrate in the catalytic site. Hence,

the binding or right positioning of large DAG molecules is abolished compared to positioning or binding of a fatty alcohol.

By modelling palmitoyl-CoA into the crystal structure of MaWSD1, Petronikolou and Nair (2018) assigned the position of the phosphoadenosine part on the outside of the protein and the pantetheine linker connecting the phosphoadenosine part with the acyl chain in the inside of the protein. Due to the outward position of MaWSD1- α 9, the entrance towards the active site of the protein is much larger in MaWSD1 compared to AbWSD1, where the entrance is narrowed to cavity C3 by the inward position of AbWSD1- α 10. By modelling palmitoyl-CoA into the AbWSD1 structure we show that binding of the CoA's pantetheine part is still possible in cavity C3 and that the molecule is able to form hydrogen bonds to AbWSD1-H5, AbWSD1-D137, AbWSD1-G138 and AbWSD1-R337 (Figure 3.7). However, the phosphoadenosine part of CoA is still located on the outside of the protein. Thus, an alternative binding of acyl-ACP in a similar position as acyl-CoA could also be possible, since the larger ACP moiety would be located on the outside of the enzyme without any sterical hindrance by the protein. The here described potential binding of acyl-CoA to AbWSD1 with the phosphoadenosin part outside of the protein, the pantetheine linker reaching into the enzyme to the catalytic histidine and the acyl chain buried in the protein, is similar to the position of oleoyl-CoA in the structures of human DGAT1 (hDGAT1) (Qian *et al.*, 2020; Sui *et al.*, 2020; Wang *et al.*, 2020) and human acyl-CoA:cholesterol acyltransferase 1 (ACAT1) (Qian *et al.*, 2020). The structures were solved with bound acyl-CoA in a similar orientation as described here: the phosphoadenosin part is located outside of the proteins, the pantetheine linker is placed in the cavity towards the active site and the acyl chain is located in the inside of the protein. As hDGAT1 and ACAT1 belong to the class of membrane-bound *O*-acyltransferases and not to the class of WSD, a general binding concept for acyl-CoA caused by the molecule's amphipathic nature seems to be conserved.

The structure comparison revealed a conformational change upon substrate binding and WSD bind their substrates with an induced fit model

The comparative analysis of the here published crystal structure of AbWSD1 with the published structure of MaWSD1 revealed that both proteins share an almost identical tertiary structure. The structure of AbWSD1 mostly differs in area 1 from MaWSD1 as well as in the co-crystallized myristic acid positioned in pocket 1. We assume, that the differences in area 1 result from a conformational change induced by the binding of myristic acid to AbWSD1. In that case, MaWSD1 would resemble the open (non-substrate bound) conformation and AbWSD1 the closed (substrate bound) one. In the open conformation AbWSD1- α 10/MaWSD1- α 9 is in an outward position and pocket 2 is large and can bind the fatty alcohol.

In addition, pocket 1, which harbors the acyl-CoA, is easily accessible. In the closed conformation, AbWSD1- α 10/MaWSD1- α 9 is shifted towards α 1. This conformational change leads to a closure of pocket 2 and of pocket 1's entrance (Figure 3.3, Figure S3.9). Upon this structural rearrangement, the potential CoA-binding residues AbWSD1-R337/MaWSD1-H342 are shifted into a position allowing the interaction with the CoA moiety at the in this study proposed position. Due to the fact, that AbWSD1 crystallized in the closed conformation with only a bound fatty acid (without CoA), it is also possible that the binding of the acyl chain might induce this structural rearrangement.

Barney *et al.* (2012) observed that the order of substrate addition has an influence on the enzymatic activity of bacterial WSD. Based on this observation it was hypothesized that this serves as an allosteric regulation of enzymatic activity based on acyl-CoA and fatty alcohol concentrations in the cell. In addition, product inhibition of AbWSD1 was proposed due to a decreased WS activity upon increasing free amounts of CoA (Stöveken *et al.*, 2005). However, whether this effect was due to competitive or noncompetitive inhibition was not further examined. Based on these observations and the two published crystal structures showing different conformations, we hypothesize an induced fit model (Koshland, 1958) as an enzyme substrate interaction model (Figure 3.9). The binding of acyl-CoA induces a conformational change, that closes pocket 2 and forms the CoA binding site and this closed conformation is resembled by the structure of AbWSD1. This occurs independent from the binding of the fatty alcohol. It is also conceivable that already the binding of free CoA might induce the conformational change. Due to the observations from Barney *et al.* (2012) it can be hypothesized, that the fatty alcohol is only able to bind to the open conformation (represented by the structure of MaWSD1). Consequently, the fatty alcohol has to bind first to the open conformation of the enzyme and the acyl-CoA binds next, inducing a conformational change. The structural rearrangement finally leads to correct binding of the CoA-moiety by forming several hydrogen bonds. This facilitates the positioning of the acyl chain and the thioester bond. The conformational change might also lead to a right positioning of the hydroxyl group of the fatty alcohol to allow the abstraction of the hydrogen by the catalytic histidine (AbWSD-H133/MaWSD1-H136). Therefore, the highest enzymatic activity is only achieved, when the enzyme is pre-incubated with the fatty alcohol or when the fatty alcohol concentration is much higher than that of acyl-CoA. By the time when the acyl-CoA is added to start the reaction, all enzymes are present in solution as [enzyme-fatty alcohol-complex] in the open conformation. Binding of the acyl-CoA to this complex directly leads to a conformational change and to the formation of WE. In case of the pre-incubation with acyl-CoA or at high free CoA concentrations, all enzymes are present in solution as [enzyme-acyl-CoA-complex] or [enzyme-CoA-complex] in the closed conformation. In order to facilitate WE production, the

[enzyme-acyl-CoA-complex] and [enzyme-CoA-complex] have to dissociate first to allow the fatty alcohol to bind to the open conformation.

To gain more evidence for the binding and reaction mechanism of WSD, it is necessary to determine the exact kinetic parameters as well as different rate and binding constants of acyl-CoA and fatty alcohol with and without the other substrates bound to the enzyme. However, due to the hydrophobic character of the substrates and the protein it is very challenging to determine accurate kinetic values.

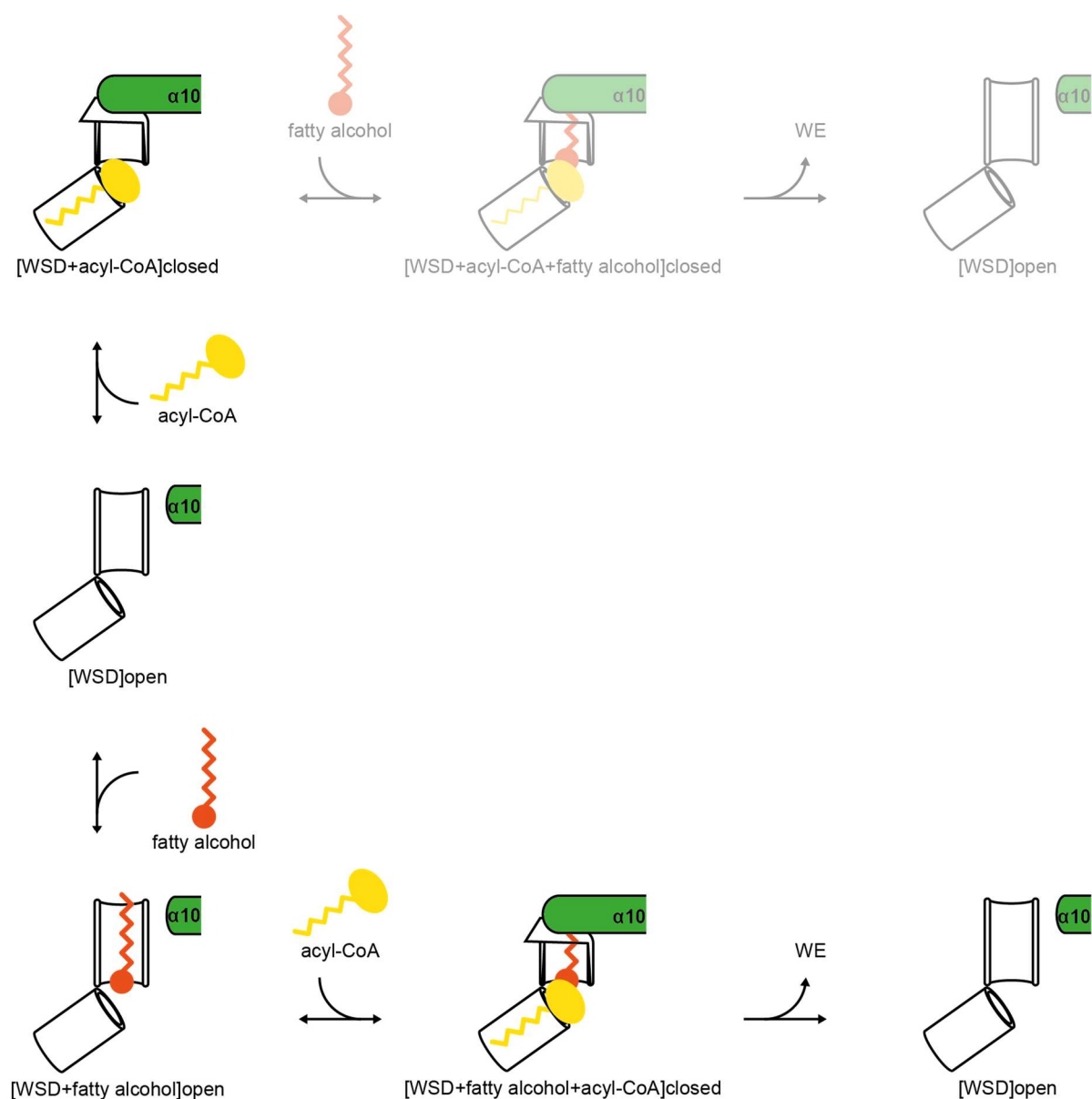


Figure 3.9. Proposed catalytic cycle of WSD.

Depicted are the acyl-CoA (cylinder) and fatty alcohol (half-open cylinder) binding sites as well as acyl-CoA (yellow), fatty alcohol (orange) and α -helix 10 (green tube) that is proposed to move inward upon acyl-CoA binding. For WE formation, the fatty alcohol has to bind the protein prior to acyl-CoA, since acyl-CoA binding closes the binding site.

Conclusions

Tailor-made WE production facilitated by bacteria from low cost substrates is of high interest for industrial application. In order to generate WSD variants that specifically produce the desired WE type, it is important to know the structural determinants for acyl-CoA and fatty alcohol specificities. The fatty acid bound crystal structure of AbWSD1 presented here, together with a detailed structural comparison with MaWSD1 and a detailed reevaluation of enzymatic characterization studies published within the last years, revealed more detailed insights into structure-function-relations of bacterial bifunctional WSD. The knowledge about potential substrate binding sites as well as the proposed substrate binding mechanism will help to generate WSD variants for the needed purposes.

Author information

Corresponding Author

* Ivo Feussner, ifeussn@uni-goettingen.de, Tel.: +49 (0)551 / 39-25743, Fax: +49 (0)551 / 39-25749

Author Contributions

KV generated the amino acid exchange variants, performed the TLC-based enzymatic activity assays, prepared the samples for the nanoESI-MS/MS competition assay, analyzed and evaluated the obtained data, generated the multiple sequence alignment for the prediction of DGAT activity, modelled acyl-CoA into the structure of AbWSD1 and drafted the manuscript except for the crystallization part. KK solved the crystal structure, wrote the corresponding part of the manuscript and edited the drafted manuscript. SK cloned AbWSD1 into the expression vectors. FL and SK established the protein purification protocol for crystallization and crystallized the protein. CH measured the samples for the nanoESI-MS/MS assay. IF designed and supervised the study and edited the drafted manuscript. All authors read and approved the final manuscript.

Funding Sources

KV was supported by the GGNB Program Microbiology and Biochemistry. SK was supported by the GGNB Program Biomolecules: Structure – Function – Dynamics and acknowledges

funding through the Fond of the Chemical Industry. IF acknowledges funding through the German Research Foundation (DFG, INST 186/822-1).

Acknowledgements

The authors are thankful to Dr. Achim Dickmanns and Dr. Alaa Shaikhqasem for DLS measurements and helpful discussions. Furthermore, the authors are grateful to Dr. Piotr Neumann and Dr. Viktor Sautner for helpful discussions.

SUPPORTING INFORMATION

The crystal structure of the bifunctional wax synthase 1 from *Acinetobacter baylyi* (AbWSD1) reveals a conformational change upon substrate binding

Katharina Vollheyde^{1‡}, Karin Kühnel^{2‡}, Felix Lambrecht¹, Steffen Kawelke¹, Cornelia Herrfurth^{1,3}, Ivo Feussner^{1,3,4*}

¹University of Goettingen, Albrecht-von-Haller-Institute for Plant Sciences, Department for Plant Biochemistry, D-37077 Goettingen, Germany

²Max Planck Institute for Biophysical Chemistry, Department of Neurobiology, D-37077 Goettingen, Germany

³University of Goettingen, Goettingen Center for Molecular Biosciences (GZMB), Service Unit for Metabolomics and Lipidomics, D-37077 Goettingen, Germany

⁴University of Goettingen, International Center for Advanced Studies of Energy Conversion (ICASEC) and Goettingen Center for Molecular Biosciences (GZMB), D-37077 Goettingen, Germany

‡These authors contributed equally.

Supporting Figures

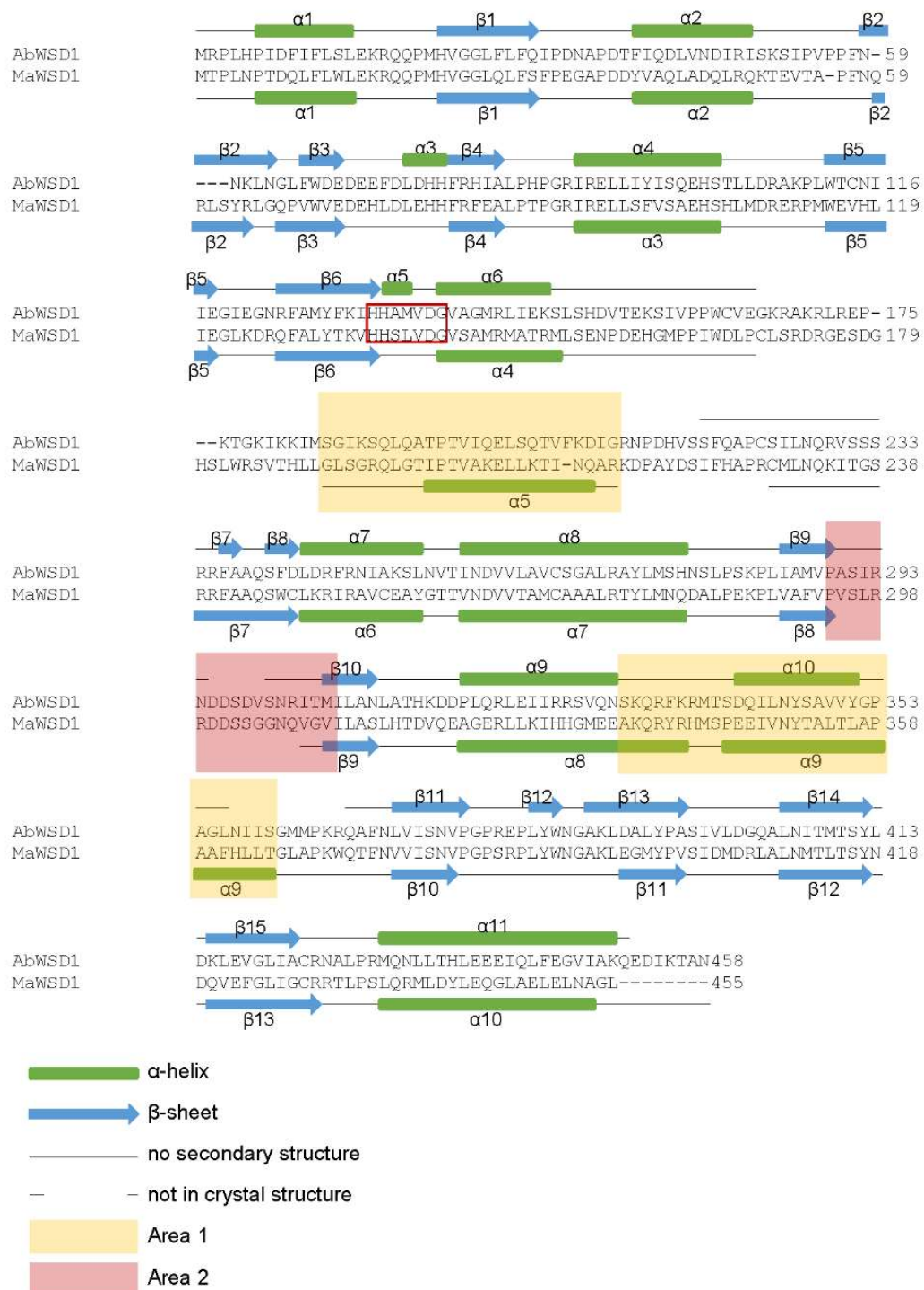


Figure S3.1. Sequence alignment of AbWSD1 and MaWSD1.

The sequence alignment was generated with Clustal Omega (Madeira *et al.*, 2019) using default settings. Secondary structure elements of AbWSD1 and MaWSD1 chain B are depicted by a green box (α -helix), a blue arrow (β -sheet), a black line (no secondary structure) or no line (not present in crystal structure). The yellow (Area 1) and red (Area 2) boxes highlight regions, that structurally differ in AbWSD1 and MaWSD1.

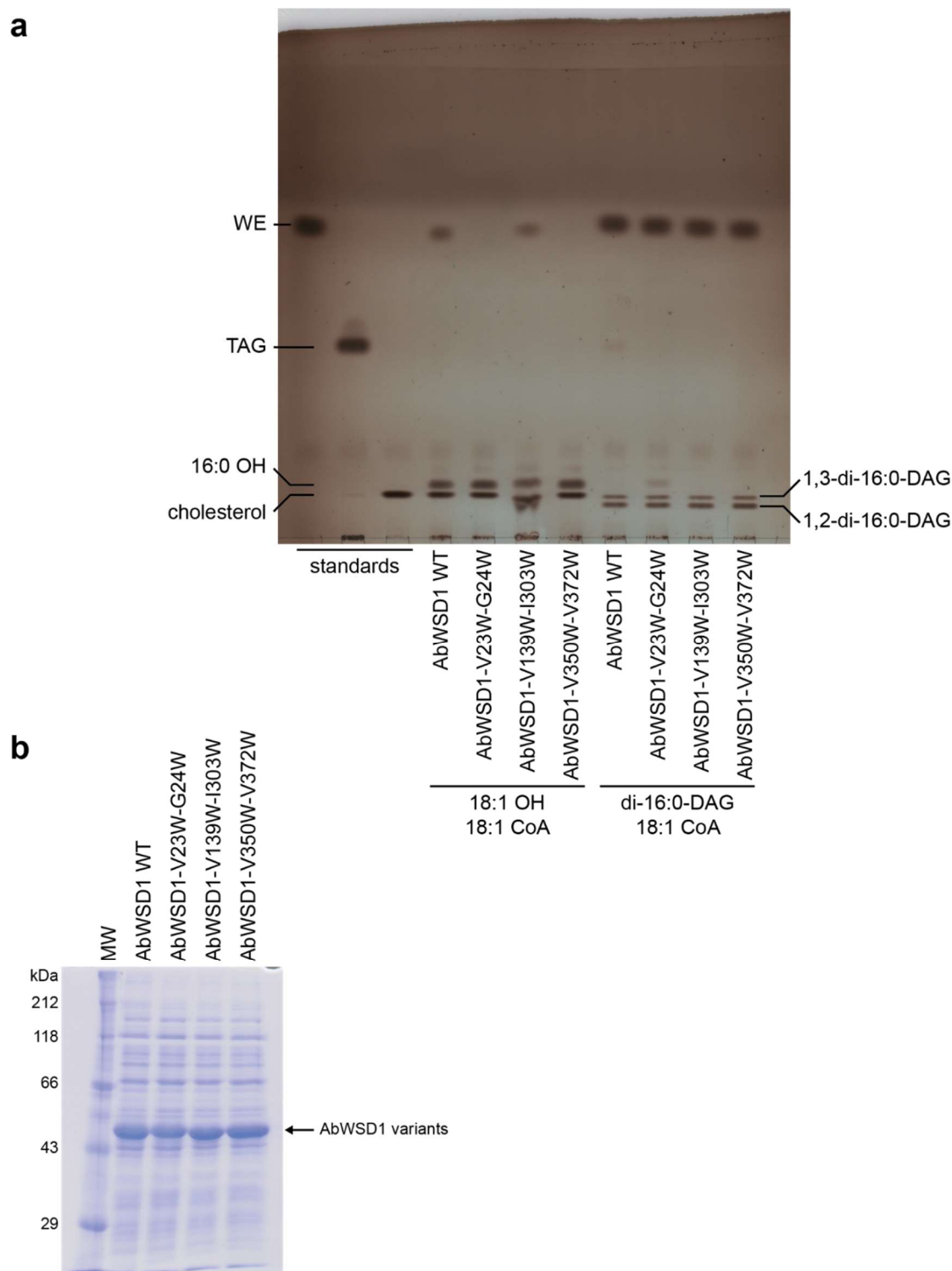


Figure S3.2. Analysis of WS and DGAT activity of AbWSD1 WT, AbWSD1-V23W-G24W, AbWSD1-V139W-I303W and AbWSD1-V350W-V372W.

(a) Analysis of WS and DGAT activity of different AbWSD1 variants. *E. coli* lysate of cells expressing AbWSD1 WT or the generated amino acid exchange mutants was incubated for one hour at room temperature either with 18:1 CoA and 18:1 OH to test for WS activity or with 18:1 CoA and di-16:0-DAG to test for DGAT activity. Neutral lipids were extracted from the reaction mix and separated by TLC. 5 μ g of cholesterol and 5 μ g of di-17:0-WE were used as internal extraction standards for WS and DGAT activity samples, respectively. Spots of the internal extraction standards can be seen on the TLC plate in the corresponding samples. **(b)** SDS-PAGE of *E. coli* lysate expressing the AbWSD1 variants. 7.5 μ g total protein was loaded on the gel for each sample.

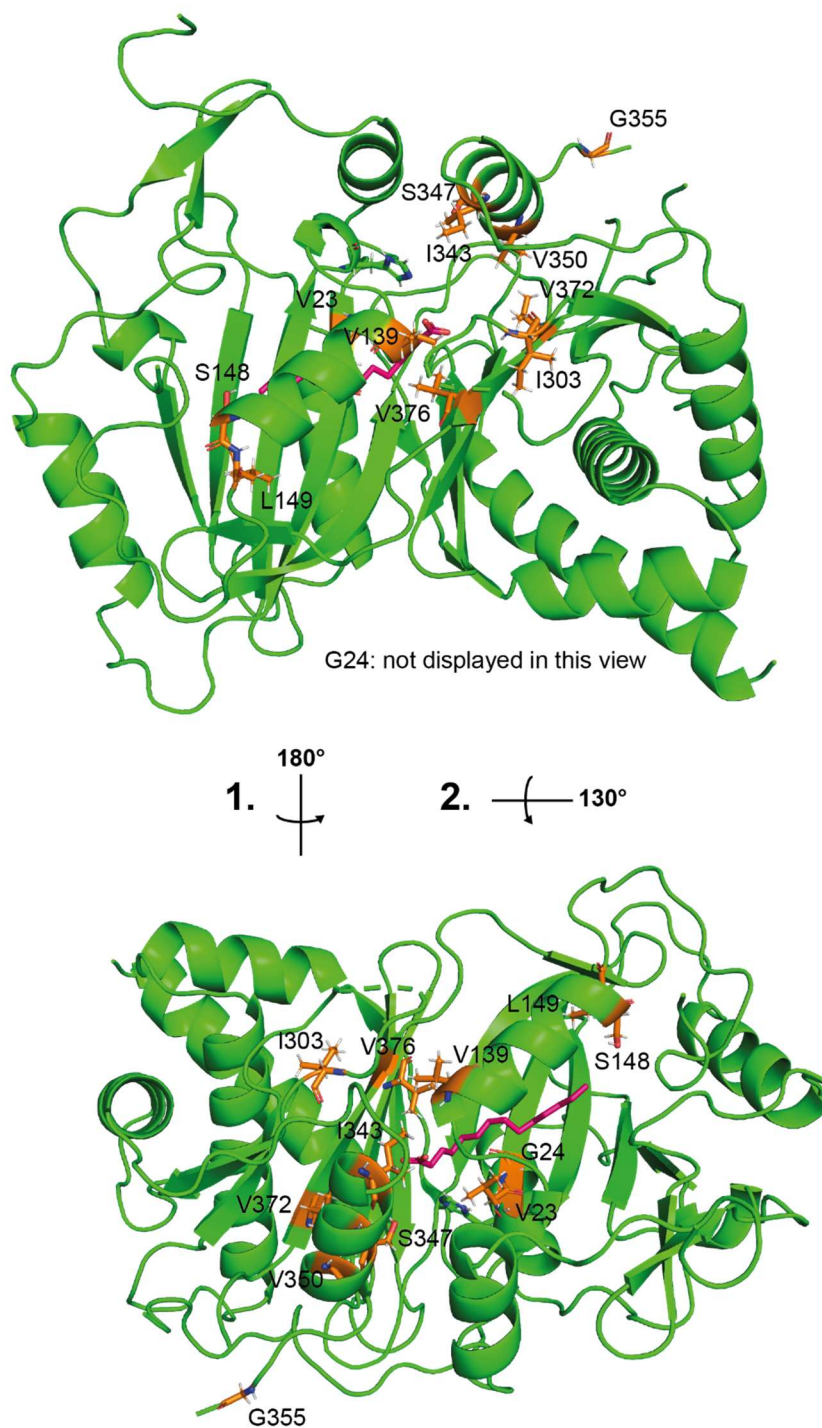
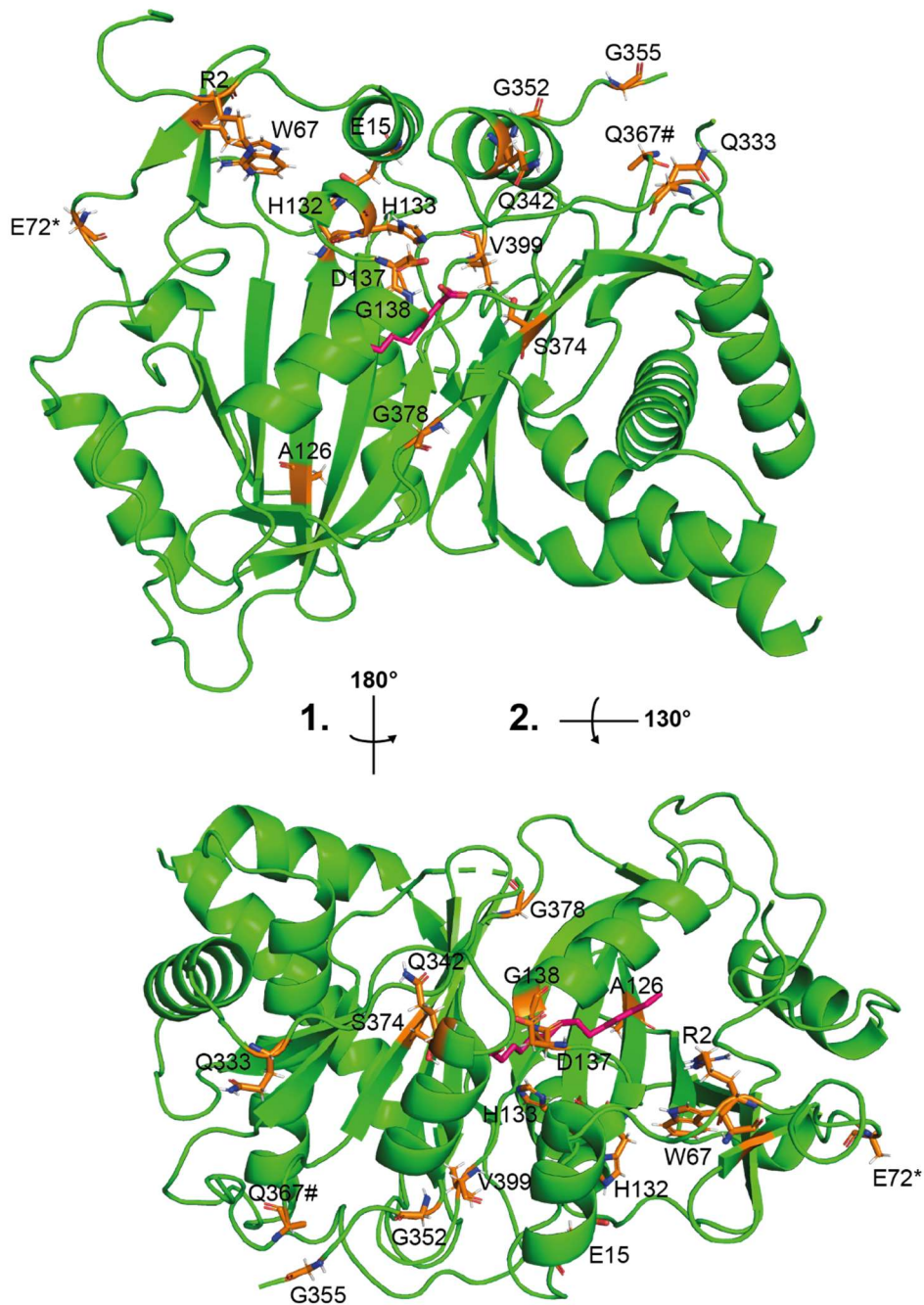


Figure S3.3. Generated and analyzed AbWSD1 amino acid exchange mutants (this study). Marked in orange are residues that were mutated in this study. Residue G355 has been mutated before by Barney *et al.* (2013). Oxygen atoms are depicted in red, nitrogen atoms in blue.



*E72: A in structure

#Q367: A in structure

L172: not displayed in structure

L201: not displayed in structure

S217: not displayed in structure

Figure S3.4. Published and analyzed AbWSD1 amino acid exchange mutants.

Marked in orange are amino acids that were mutated in AbWSD1 and analyzed by others (Stöveken *et al.*, 2009; Barney *et al.*, 2013; Röttig & Steinbüchel, 2013b; Röttig *et al.*, 2015; Röttig *et al.*, 2016). Oxygen atoms are depicted in red, nitrogen atoms in blue. A list of the publications corresponding to the generated amino acid exchange mutants can be found in Table S3.5.

PhWS1	PI-----KDKLVHT-LLKHPFTSLM--V-----VDEENLADMKWVQ-TKIDLDQHI	112
AtWSD1	AF-----VDGINNT-LINAPRFSSKM--E-----INYKKKGEPVWIP-VKLRVDDHI	89
TrWSD4	GF--EAVRETVGKR-LLQIPRFRSKLTAR-----RFPKAM-EFVELDDDEIDMDYHF	157
TrWSD5	EV----LRNEVHEK--LVDKVFRYRA-----VPRERKGWYWEAGPIDDAYHF	93
MaWSD5	RF--REFLEVY----WLAWERFRCRP--VWRA-----PAWYWEKDLTFSAPQHL	73
ScSco1280	SV-----RARVAER-VHHVPALRYRIARD-----RRKFRRVDRIAADRHV	88
RoAtf1	RF-----VDMMRRA-VDLVPLFRRTA--I-----EAPMGFAPPRWADDHDFDLSWHL	78
MtTgs1	AF-LSSLAQR-----LRPCTRFQRL--R-----LRPFDLGAPKWVDDPDFDLGRHV	83
ScSco0958	AL-AADLLA----ARAPAVPGLMRIRDWTQPP-MALRRPFAFGGATREPDPRDFPLDHV	93
SaSAV7256	AH-AADLLA----SRAAAVPGLMRIRDVWQPLAFPLTFPLPFGGATREPAPDFDPLDHV	94
MtTgs4	SF-GPRLFDAYRH--SQAAPFNHKL--KWL-----GT----DVAAWET-VEPDMGYHI	81
MtTgs3	SY--EALLETVEQR-LPQIPRYRQKV--Q-----EVKLGARPVWIDDRDFDITYHV	84
TctDGAT	RLTAEDLIEVIRERAHLAPRPLRMRL--A-----AVPLGITRPFYWEDDPFDPARH	87
AlbAtfa1	KY-VSELAQQRDY-CHPVAPFNQRL--T-----RRLGQYYWTRDKQFDIDHFF	82
MhWS1	DY-VAQLADQLRQK-TEVTAPFNQRL--S-----YRLGQPVWVEDEHLDLEHHF	82
MaWSD1	DY-VAQLADQLRQK-TEVTAPFNQRL--S-----YRLGQPVWVEDEHLDLEHHF	82
AbWSD1	TF-IQDLVNDIRISKSIPTVPPFNKL--N-----GLFWDEDEEFDLDHFF	79
PaWS	SF-VHQLVKQMQSDVPPPTFFPNQVL--E-----H---MMFWKEDKNFDVEHHL	80
PcPs1	SF-VHQLVKQMQDSHVPPTFFPNQVL--E-----H---MVFWKKDKNFDVEHHL	80
RoAtf2	DY-VKSMHETLLKH-TDVPDTPFRKKP--A-----GPVGSGLNLWVADESVDLEYHV	82
RjRh1	DY-VKSMHETLLEH-TDVPDPAFRKKP--A-----GPVGSGLNLWVADESVDLEYHV	82
MtTgs2	EF-VREFTERLVAN-DEFQPMFRKHP--A-----TIGGGIARVAVAYDDDDIDIDYHV	85
MhWS2	TF-LRDMVTRMKEA-GDVAPPWGYKL--AWS-----GFLGRVIAPAWKVKDIDLDYHV	87
MaWSD2	TF-LRDMVTRMKEA-GDVAPPWGYKL--AWS-----GFLGRVIAPAWKVKDIDLDYHV	87
AlbAtfa2	DY-VESIYRYLVDV-DSICRPFNQKI--Q-----SHLPLYLDATWVEDKNFDIDYHV	86

* .

PhWS1	IVPEVDETQLESFDPKFVEDYIYNLTKT-SLDRTKPLWDLHLVNVKTR-----DAEAVALL	166
AtWSD1	IVPDLEYSNIQNPQDFVEDYTSNIANI-PMDSKPLWEFHLNLMKTS-----KAESLAIV	143
TrWSD4	RQAFQDRTA---TLDEVDFVGSMSDFGNHMDKPLWQITYIIPKLED-----GRAVLIT	208
TrWSD5	QHHAGFE-----DEQHWQEYLQQLVDD-GLDYSKPWWRYVVVDKLPC-----GRAAVIG	141
MaWSD5	DVA-L-DRF---EPEQLQDWSERLNE-PLPLYRPRWKFWLAPNAQG-----GAALVL	120
ScSco1280	HEAWLPEDT---DGSATSR--LMSRP-MSTDRPPWDVWLHVGPAE-----RHTLVY	135
RoAtf1	RRYTLPEPR---TWDGVLDFARTAEMT-AFDKRRPLWEFTVLDGLHD-----GRSALVM	128
MtTgs1	WRIALPRPG---NEDQLFELIADLMAR-RLDRGRPLWEVWVIEGLAD-----SKWAILT	133
ScSco0958	RLHAP-----ATDFHARAGRLMER-PLERGRPPWEAHVLPGADG-----GSFAVLF	138
SaSAV7256	RLHAP-----AADFHAVAGRLMQR-PLERGRPPWEAHVLPGEDG-----TSFAVLF	139
MtTgs4	RHLALPAPG---SMQQFHETVSFLNTG-LLDRGHMWEVYIIDGIER-----GRIAILL	131
MtTgs3	RRSALPSPG---SDEQLHELIARLAAR-PLDKSRPLWEMYLVEGLEK-----NRIALYT	134
TctDGAT	FEVGLPDPG---NAAQLADVAMLHER-PLRARPLWEAVIQGLEG-----GRTAVYI	137
AlbAtfa1	RHEALPKPG---RIRELLSLVSAEHSN-LLDRERPMWEAHLIEGIRG-----RQFALYI	132
MhWS1	RFEALPTPG---RIRELLSFVSAEHSN-LMDRERPMWEVHLIEGLKD-----RQFALYT	132
MaWSD1	RFEALPTPG---RIRELLSFVSAEHSN-LMDRERPMWEVHLIEGLKD-----RQFALYT	132
AbWSD1	RHIALPHG---RIRELLIYSQEHST-LLDRAKPLWTCNIEGIEG-----NRFAMYF	129
PaWS	HHVALPKPA---RVRELLMYVSREHGR-LLDRAMPLWECHVIEGIQPETEGSPERFALYF	136
PcPs1	HHVALPKPA---RVRELLMYVSREHGR-LLDRAMPLWECHVIEGIQPESEGSPPERFALYF	136
RoAtf2	RHSALPAPY---RVRELLTTLTSLRHGT-LLDRHRPLWEMYLIEGLSD-----GRFAIYT	132
RjRh1	RHSALPAPY---RVRELLTTLTSLRHGT-LLDRHRPLWEMYLIEGLSD-----GRFAIYT	132
MtTgs2	RRSALPSPG---RVRDLLELTSRLHTS-LLDRHRPLWELHVVEGLND-----GRFAMYT	135
MhWS2	RHSALPRPG---GERELGILVSRHLSN-PLDFSRPLWECHVIEGLEN-----NRFALYT	137
MaWSD2	RHSALPRPG---GERELGILVSRHLSN-PLDFSRPLWECHVIEGLEN-----NRFALYT	137
AlbAtfa2	RHSALPRPG---RVRELLALVSRLHAQ-RLDPSRPLWESYLIEGLEG-----NRFALYT	136

* *

PhWS1	RVHHSGLDGTSLISLLACTRQTADDELKLPITPKRR-----PTPSGY-----	210
AtWSD1	KIHHSIGDGMSLMSLLACSRKISDPDALVSNNTATKK-----P-----	182
TrWSD4	NISHIVGDGIAQVEVLMRLLDPVKESKGEKVQKPRTGAN-K-KRKPPALG-----	256
TrWSD5	IADHTHADGASAVSALLSMCEGQGDNPVFSKKTSSGAGSKKGRAGRGR-----	191
MaWSD5	RLHHCYADGLSLLGIFDRLLCPASPRQYPA--VYGSTE-----EPRAG-AWMAAAQSW	169
ScSco1280	RTDHTFQDGMGAAYTARALLGDHPEGGPAPQRPAPRPTAH-----G-----	175
RoAtf1	KVHHSITDGVSGMQIAREIVDFTRDGGPRPDRTDHRTAAPNGKSPTPRGRLSWYRNSATD	188
MtTgs1	KLHHCMDAGIAATHLLAGLSDESMSDSFASNIHTTMQSQSA-SVRR--GG-FR---VNP-	185
ScSco0958	KFHHALADGLRALTLAAGVLDPM----DLPAPRPRPEQ-----PPRGL-L-----PD	180
SaSAV7256	KFHHALADGLRALMLAAALMDPM----DMPTPRPRPAE-----PARGL-L-----PD	181
MtTgs4	KVHHALIDGEGGLRAMRNFLSDSPDDTTLAGPWSAQGADR-PRRTPATV-----	180
MtTgs3	KSHQALINGVTALAIGHVIADTRRRPPAFPEDIWWPERDPG-TTRL----LLRAVGDWL	189
TctDGAT	KVHHAAVDGVLATETLAALLDLSQPPEPPDDTVPQQAPA-LAERVRTGLLRALAHVPR	196
AlbAtfA1	KIHHSVMDGISAMRIASKTLSTDPSEMAPAWAFNTKKRS-RSLPSNPV-----DMASS	186
MhWS1	KVHHSILDVGSAMRMTATRLSENPFDEHGMPPIDWLPCLSRD-RGESDG-H-----SLWRS	185
MaWSD1	KVHHSILDVGSAMRMTATRLSENPFDEHGMPPIDWLPCLSRD-RGESDG-H-----SLWRS	185
AbWSD1	KIHHAMVDGVAGMRLIEKSLSHDVTEKSIVPPWCVEGKRAK-RLREPKTG-----KI---	180
PaWS	KIHHSILDVGIAMRLVKKSLSQSPNEPVTLPVWISLMAHHRN-QIDAIQPK-----E---	186
PcPs1	KIHHSILDVGIAMRLVKKSLSQSPNEPVTLPVWISLMAHHRN-QIDAILPK-----E---	186
RoAtf2	KLHHSIMDGVSGRLRLMRTLSLTDPDVDRAPPWNLPARRASA-NGAAP-----APD	181
RjRh1	KLHHSIMDGVSGRLRLMRTLSLTDPDVDRAPPWNLPARRASA-NGAAP-----APD	181
MtTgs2	KMHHALIDGVSAMKLAQRTLSADPDAAEVRAIWNLPARRPT-RP-----PSD	181
MhWS2	KMHHSIMDGISGVRLMQRVLTDPERCNMPPWTVRPHQRR-GAKTDKEA-----SVPAA	191
MaWSD2	KMHHSIMDGISGVRLMQRVLTDPERCNMPPWTVRPHQRR-GAKTDKEA-----SVPAA	191
AlbAtfA2	KMHHSIMDGVAGMHLMQSRLATCAE-DRLPAPWSGEWDAEK-KPRKSRGAA----AANAG	190
	: :*	
PhWS1	-ST-KE-ESFK----LWHYLAVIWLFIWMIGNT---LVD-----VLMFII-----TVIFL	250
AtWSD1	-----ADSM----AWWLFVGFWMFIRVTFIT---IVE-----FSKLML-----TVCFL	218
TrWSD4	-----PFTKAKVFMGGVWEGFFSVISSP-----D-----KKNLTL---R---	286
TrWSD5	----KLSGYER----LVALWEGVWGPISQ-----IL-----AND----VQSRL	223
MaWSD5	LEARMAEALPA-----VSGSVDAPST-PGTGKSMAGRALENSLRLVHEFSEFLVTPE	220
ScSco1280	----LADALGE-----VVAA-----FRA	189
RoAtf1	VARRASNTLGRNSVRLVTRPRATWRDAAALAGS-----TLRL---T-RPV	229
MtTgs1	-SE----ALTA----STAVMAGIVRAAKG-----ASEI---AAGVL	214
ScSco0958	VRA-LP-----DRLRGALSDAGRA-----LD-----IGAAA---ALSTL	210
SaSAV7256	VRK-LP-----ELLRGTLSDVGRA-----LD-----IGASV---ARATL	211
MtTgs4	-SR-RAQLQGQ---LQGMKGLTKLPSGLFGVSADAAD-LGAQALSILKARK---ASLPF	230
MtTgs3	--R-PGAQLQA---VGSAVAGLVTVNSGQ-----LVE-T--GRKVLDIAR---TVARG	229
TctDGAT	GAR-MLARTAP----YLDEIPGLAQLPGVQP-----LAR-AIQGALGRDGVV---PLPRT	242
AlbAtfA1	MAR-LTASISK----QAATVPLGLAREVYK-----VT-----QKAKKDENV---V-SIF	225
MhWS1	VTH-LLGLSDR----QLGTIPTVAKELLK-----TI-----NQARKDPAY---D-SIF	224
MaWSD1	VTH-LLGLSGR----QLGTIPTVAKELLK-----TI-----NQARKDPAY---D-SIF	224
AbWSD1	-KK-IMSGIKS---QLQATPTVIQELSQ-----TVF---KDIGNPDH---V-SSF	219
PaWS	-RS-ALRILKE----QVSTIKPVFTELLN-----NF----KNY-NDDSY---V-STF	223
PcPs1	-RS-ALRILKE----QVSTIKPVFTELLD-----NF----KNY-NDDSY---V-STF	223
RoAtf2	LWS-VVNGVRR----TVGEVAGLAPASLR-----IAR-----TAMQHDH---R-FPY	220
RjRh1	LWS-VMNGVRR----TVGEVAGLAPASLR-----IAR-----TAMQHDH---R-FPY	220
MtTgs2	GSS-LLDALFK---MAGSVVGLAPSTLK-----LAR-----AALLEQQL---T-LPF	220
MhWS2	VSQ-AMDALKL---QADMAPRLWQAGNR-----LVH-S--VRHPEDGL---T-APF	231
MaWSD2	VSQ-AMDALKL---QADMAPRLWQAGNR-----LVH-S--VRHPEDGL---T-APF	231
AlbAtfA2	MK-----GTMNNLRRGGGQ-----LVD-L--LRQPKDGNV---K-TIY	221

PhWS1	KDTKTPINTVPDSESRVRRIV----	HRIIDLDDKLKLV-KNAMNMTINDVALGITQAGLSK	305
AtWSD1	EDTKNPLMGNPSDGFQSWKVV----	HRIISFEDVKLI-KDTMNMKVNDVLLGMTQAGLSR	273
TrWSD4	---LKDVNKP-----SPTKRCTF---	SETIPLDKVKELKNMYEGATLNDVVLVTLTLRA	336
TrWSD5	KQPSGKFPKHW-----RFATPPGEHL	DKMLKEIKDRVPGATVNDVMLALTALGIKE	276
MaWSD5	DS-PSELKRSL---LGRRSCRW---	SSPIPLSRFRTI-ARATSTTINDVLLACVAAAVKP	272
ScSco1280	PTPKPAFDGDF---TGRVDVC----	HADTPLARLRAI-ARAHGGTVTDVYLAALSHAVRT	241
RoAtf1	VSTLSPVMKKR---STRRHCA----	VLDVPVEALAQA-AAAGAGSINDAFLAAVLLGMAK	281
MtTgs1	SPAASSLNGPI---SDLRRYS----	AAKVPLADVEQV-CRKFVDVTINDVALAAIT	TESYRN 266
ScSco0958	DVRSSPALTAAS--SGTRRTA----	GVSVDLDDVHHV-RKTTGGTVNDVLI	IAVVAGALRR 263
SaSAV7256	GARSSSALTSEP--SGTRRTA----	GVLIDLDAVHRV-RKTVGGTVNDVLI	IAIVAGALRT 264
MtTgs4	TARRTLFNNTAK--SAARAYG----	NVELPLADV KAL-AKATGTSVNDV	VMTVIDDALHH 283
MtTgs3	TAPSSPLNATV---SRNRRFT----	VARASLDDYRTV-RARYDCDSTTWC-----	271
TctDGAT	VAPPTPFNGTI---SARRAVA----	FGELPLAEIRRI-RRELGGSVNDV	VMLVATALHR 294
AlbAtfa1	QAPDTILNNTI---TGSRRFA----	AQSFPLPRLKVI-AKAYNCTINTV	VLSMCGHALRE 277
MhWS1	HAPRCMLNQKI---TGSRRFA----	AQSWCLKRIRAV-CEAYGTTVNDV	VVTAMCAAALRT 276
MaWSD1	HAPRCMLNQKI---TGSRRFA----	AQSWCLKRIRAV-CEAYGTTVNDV	VVTAMCAAALRT 276
AbWSD1	QAPCSILNQRV---SSRRFA----	AQSFDLDRFNI-AKSLNVTINDV	VLAUCSALRA 271
PaWS	DAPRSILNRRI---SASRRIA----	AQSYDIKRFNDI-AERINISKNDV	VLAUCSAGAIRR 275
PcPs1	DAPRSILNRRI---SASRRIA----	AQSYDIKRFNDI-AERINISKNDV	VLAUCAGAIRR 275
RoAtf2	EAPRTMLNVPI---GGARRFA----	AQSWPLERVHAV-RKAAGVSVNDV	VMMAMCAGALRG 272
RjRh1	EAPRTMLNVPI---GGARRFA----	AQSWPLERVHAV-RKVAGVSVNDV	VMMAMCAGALRG 272
MtTgs2	AAPHSMFNKV---GGARRCA----	AQSWSLDRIKSV-KQAAGVTVND	AVLAMCAGALRY 272
MhWS2	TGPVSVLNHRV---TAQRRFA----	TQHYQLDRLKNL-AHASGGSLNDI	VLYLCGTALRR 283
MaWSD2	TGPVSVLNHRV---TAQRRFA----	TQHYQLDRLKNL-AHASGGSLNDI	VLYLCGTALRR 283
AlbAtfa2	RAPKTQLNRRV---TGARRFA----	AQSWLSRIKAA-GKQHGGTVNDI	FLAMCGGALRR 273

PhWS1	YLNRRYAVDEEDKGDTERNNL	PKNIRLRSCLVINLRPSAGIEDLAD	MMKGPKEKRGWG 365
AtWSD1	YLSSKYDGS-----TAEKKKILE	KLRVRGAVAINLRPATKIEDLAD	MMAKGSK--CRWG 325
TrWSD4	YFREVGDKGAL-----RNKVRAQ	FPINIRSKSEG-----PFR--N--	DNPR 373
TrWSD5	YYKSINDPIMQ--G-----TADLR	GTAAANVRPSGVD-----YL---	SDKWFG 314
MaWSD5	RLGMTPEQLD-----ETVMHAA	VPVDIRARLPD-----GVR---	PEEGEPG 310
ScSco1280	WYLKDTGSAH-----PPLPVS	I PMSVRAPGE-----EYAPG	272
RoAtf1	YHRLHGAEI-----SELRMTLP	ISLRAETD-----PVGG	310
MtTgs1	VLIQRGERPR-----FDSLRTL	VPVSTRSNSA-----LSKTD	298
ScSco0958	WLDERGDGSE-----GVAPRALI	PVSRRRPRS-----AHPQG	295
SaSAV7256	WLDERGDGSA-----GVAPRALI	PVSRRRPRT-----AHPQG	296
MtTgs4	YLAHQASTD-----RPLVAFMP	MSLREKSG-----EGGG	313
MtTgs3	-----	-----	271
TctDGAT	WLDKRGELPD-----RPLVAA	VPVSLRRGRD-----GDAAGG	326
AlbAtfa1	YLISQHALPD-----EPLIAM	VPM SLRQDD-----STGG	306
MhWS1	YLMNQDALPE-----KPLVAF	VPVSLRRDD-----SSGG	305
MaWSD1	YLMNQDALPE-----KPLVAF	VPVSLRRDD-----SSGG	305
AbWSD1	YLMSHNSLPS-----KPLIAM	VPASIRNDD-----SDVS	300
PaWS	YLISMDALPS-----KPLIAF	VPMSLRTDD-----SIAG	304
PcPs1	YLISMDALPS-----KPLIAF	VPMSLRTDD-----SVAG	304
RoAtf2	YLEEQKALPD-----EPLIAM	VPVSLRDEQK-----ADAGG	303
RjRh1	YLEEQNALPD-----EPLIAM	VPVSLRDEQQ-----ADAGG	303
MtTgs2	YLIERNALPD-----RPLIAM	VPVSLRSKED-----ADAGG	303
MhWS2	FLAEQNNLPD-----TPLTAGI	PVNIRPADD-----EGTGT	314
MaWSD2	FLAEQNNLPD-----TPLTAGI	PVNIRPADD-----EGTGT	314
AlbAtfa2	YLLSQDALSD-----QPLVAQ	VPVALRSADQ-----AGEGG	304

PhWS1	NWFGYVLLPFKIALRDDPLDYVKEAKATVDRKKRSFEALYTLMAEVLKIFGKIVAT--	423
AtWSD1	NFIGTVIFPLWVKSEKDPLEYIRRAKATMDRKKISLEAFFFYGIKFTLKFVGGKAVE--	383
TrWSD4	NKFTYGFMPFHVSGNRDASATFWRTKRTLDKIKSSPSPVVQHVGKVISNIMPLKALNA-	432
TrWSD5	NHIVVQTARYPLHEG-RV-ETLLSFRDQSRMRKASPDMIVRRYLMEAMSYPDRKVV---	369
MaWSD5	NCFGTVFVPLVDGE-SALERLFRIKHETRKLKKSWSQPGLAWGLTACASLLPDVGRK---	366
ScSco1280	NRMVTARLLLPCDEE-SPQRALARVAVAGTGRLLRESRRRDAMRLLLS---ASPRALGATVG	328
RoAtf1	NRITLARFALPADID-DPAELMHRVHATVDAWRHEPAIPLSPTIAGALNLLP-----	361
MtTgs1	NRVSLMLPNLPVDQE-NPLQRLRIVHSRLTRAKAGGQRQFGNTLMAIANRPFPMATAVAV	357
ScSco0958	NRLSGYLMRLPVGDP-DPLARLGTVRAAMDRNKDAGPGRGAGAVALLADH-VPALGHRLG	353
SaSAV7256	NRLSGYLIRLPVDDP-DPLGLRLTVRMAMDRNKDAGPNRGAGAVALLADH-VPPLGHRLG	354
MtTgs4	NRVSAELVPMGAPKA-SPVERLKEINAATTRAKDKGRGMQTTSRQAYALLLGLSLTVADA	372
MtTgs3	-----	271
TctDGAT	NRMSAMVTPLATHLA-DPAERFAAIRGDLAAAKRRFARSSGAWLEGLSELVPAPLAGPLL	385
AlbAtfa1	NQIGMILANLGHTHIC-DPANRLRVIHDSVEEAKSRFSQMSPEEILNFTALTMAPTGLNLL	365
MhWS1	NQVGVILASLHTDVQ-DAGERLLKIHGMEEAKQRYRHMSPEEIVNYTALTLPAAFHLL	364
MaWSD1	NQVGVILASLHTDVQ-EAGERLLKIHGMEEAKQRYRHMSPEEIVNYTALTLPAAFHLL	364
AbWSD1	NRI TMILANLATHKD-DPLQRLLEIIRRSVQNSKQRFK EMTSDQILNYS AVVYGPAGLNII	359
PaWS	NQLSFVLANLGHTHLD-DPLSRIKLIHRSMNNSKRRFRRMNQAQVINYSIVSYAWEGINLA	363
PcPs1	NQLSFVLANLGHTHLD-DPLSRIKLIHRSMNNGKRRFRRMNQAQVINYSVVSYAWEGINLA	363
RoAtf2	NAVGVTLNCLATDVD-DPAERLTAISASMSQKELFGSLTSMQALAWSAFNMSPIALTPV	362
RjRh1	NAVGVTLNCLATDVD-DPAERLTAISASMSQKELFGSLTSMQALAWSAVNMSPIALTPV	362
MtTgs2	NLVGSVLCNLATHVD-DPAQRIQITISASMDGNKKVLSLSELQQLVLAALSALNMAPLTLAGV	362
MhWS2	-QISFMIASLATDEA-DPLNRLQQIKTSTRRAKEHLQKLPKSALTQYTMLLMSPIILQLM	372
MaWSD2	-QISFMIASLATDEA-DPLNRLQQIKTSTRRAKEHLQKLPKSALTQYTMLLMSPIILQLM	372
AlbAtfa2	NAITTVQVSLGTHIA-QPLNRLAAIQDSMKAVKSRLGDMQKSEIDVYTVLTMPLSLGQV	363
PhWS1	-----AVTVRVFSNATVCFSNVVGPEEIGFCGHPISE-----YLAP-SIYGQ-PSALMI	470
AtWSD1	-----AFGKRIFGHTSLAFSNVKGPDDEEISFFHHPISE-----YIAG-SALVG-AQALNI	430
TrWSD4	-----QLLNLAAKATAQVSNVPGPQDAVTVAGTEVD-----DMRFLLYS---PLSFYV	477
TrWSD5	-----EIVVEANAKFSIMISNVFLSLTKLSLFGQEIIE-----DVRFVACS---PLGFYA	415
MaWSD5	-----PLADLFFRKASAVVSNVPGTPETRYLAGCPIT-----EQMFVWPQAG-DIGLGV	414
ScSco1280	T-----RLVRGAFVAGPVSSVNFGTALVHQVAARRSAVFAGVAS-GIRCVT	374
RoAtf1	----ASTLGNMLKQRAFVASNVVGPVPLFIAGSEVL-----HYYAFSPTL--GSAFNV	409
MtTgs1	G----LLMRLPQRGVVTVATNVPGPRRPLQIMGRRVL-----DLYPVSPIAM-QLRTSV	406
ScSco0958	G---PLVSGAARLWFDLLVTSVPLPSLGLRLGGHPLT-----EVYPLAPLAR-GHSLAV	403
SaSAV7256	G---PVVQAARLLFDILVTSVPLPSLGLKLGGSPLT-----EVYFPAPLAR-GQSLAV	404
MtTgs4	L----PLL GK-LPSANVVISNMKGPTQLYLAGAPLV-----AFSGLPIVPP-GAGLNV	420
MtTgs3	-----	271
TctDGAT	RLALQARPGEYLRPVNLLVSNVPGPDFPLYLRGARVL-----GYFPI SVVSDLTGGLNI	439
AlbAtfa1	T----GLAPK-WRAFNVISNIPGPKPLYWNGAQLQ-----GVYPVSIALD-RIALNI	413
MhWS1	T----GLAPK-WQTFNVVISNVPGSRPLYWNGAKLE-----GMYPVSIDMD-RLALNM	412
MaWSD1	T----GLAPK-WQTFNVVISNVPGSRPLYWNGAKLE-----GMYPVSIDMD-RLALNM	412
AbWSD1	S ---- GMPK-RQAFNLVISNVPGPREPLYWNGAKLD ----- ALYPASIVLD-GQALNI	407
PaWS	T----DLFPK-KQAFNLII SNVPGSEKPLYWNGARLE-----SLYPASIVFN-GQAMNI	411
PcPs1	T----GLFPK-KQAFNLII SNVPGSEKSLYWNGARLQ-----SLYPASIVFN-GQAMNI	411
RoAtf2	P----GFVRFTPPPFNVIISNVPGPRKTMWNGSRLD-----GIYPTSVVLD-GQALNI	411
RjRh1	P----GFVRFTPPPFNVIISNVPGPRKTMWNGSRLD-----GIYPTSVVLD-GQALNI	411
MtTgs2	P----GFLSAPPPFNIVISNVPGPVDPLYGTARLD-----GSYPLSNIPD-GQALNI	411
MhWS2	S----GLGGRMPVFNVTISNVPGPEGTLYYEGARLE-----AMYPVSLIAH-GGALNI	421
MaWSD2	S----GLGGRMPVFNVTISNVPGPEDTLYYEGARLE-----AMYPVSLIAH-GGALNI	421
AlbAtfa2	T----GLSGRVSPMFLNVIISNVPGKETLHLNGAEMLE-----ATYPVSLVLH-GYALNI	412

PhWS1	NFQSYIDKMIIVVA-----VDEGAIPDPQQLLDDFENSLHLIKEAVLERGLVKNLK----	521
AtWSD1	HFISYVDKIVINLA-----VDTTIIQDPNRLCDDMVEALEIIKSATQGEIFHKTEV----	481
TrWSD4	GLLTYNGNLSASF CIDSALADPRLISKHWLP-----EFEKFYAHAKEAAGESGLIR---	528
TrWSD5	GAATYVDKVSFGLV-----ATEDVKTDPSVMLPLFRSECEKLVHKEVMALDPD-----	462
MaWSD5	SIVSYAGVQVQFGVV-----ADEAVMADPAAF---LEDCLAELDQLD-----	452
ScSco1280	TLTSQHDTAACLTVVHDEALATADELPLDLWLA-----ALLELERP-----	413
RoAtf1	TLMSYTRCCVGIN-----ADTDAIPDLATLLTDSIADGFRAVLGLCTKTTDTRVVAS--	462
MtTgs1	AMLSYADDLYFGIL-----ADYDVVADAGQLARGIEDAVARLVVAISKRRKVTRRRGALS-	460
ScSco0958	AVSTYRGRVHYGLL-----ADAKAVPDLDR LAVAVAEVETLLTACRP-----	446
SaSAV7256	AVSTYRGRVHYGLV-----ADAKAVPDLGRLARAVTEEMETLLTVCGP-----	447
MtTgs4	TFASINTALCIAIG-----AAPEAVHEPSRLAELMQRAFTLQTEAGTTSPTTSKSRTP-	474
MtTgs3	-----	271
TctDGAT	TVLSYDGLKLDVGIV-----TCRQMIPDPWEIMDHLDDALGELRGLIDG-----	482
AlbAtfA1	TLTSYVDQMEFGLI-----ACRRTLPSMQRLLDYLEQSIRELEIGAGIK-----	457
MhWS1	TLTSYNDQVEFGLI-----GCRRTLPSLQRM LDYLEQGLAELELNAGL-----	455
MaWSD1	TLTSYNDQVEFGLI-----GCRRTLPSLQRM LDYLEQGLAELELNAGL-----	455
AbWSD1	TMTSYLDKLEVGLI-----ACRNALPRMQLLTHLEEEIQLFEGVI AKQEDIKTA-----	457
PaWS	TLASYLDKMEFGIT-----ACSKALPHVQDMLMLIEEELQLLESVSKLEFNGITVKDKS	466
PcPs1	TLASYLDKIEFGIT-----ACSKALPHVQDMLMLIEEELQLLEKVSKELEFNGITVEDKS	466
RoAtf2	TLTTNGGNLDFGVI-----GCRRSVPSLQRI LFYLETALGELEAALL-----	453
RjRh1	TLTTNGGNLDFGVI-----GCRRSVPSLQRI LFYLETALGELEAALL-----	453
MtTgs2	TLVNNAGNLDFGLV-----GCRRSVPHLQRL LAHLESSLKDLEQAVGI-----	454
MhWS2	TCLSYAGSLNFGFT-----GCRDTLPSMQKLAVYTGEALDELESLILPPKKRARTRK---	473
MaWSD2	TCLSYAGSLNFGFT-----GCRDTLPSMQKLAVYTGEALDELESLILPPKKRARTRK---	473
AlbAtfA2	TVVSYKNSLEFGVI-----GCRDTLPHIQRFVLVYLEESLVELEP-----	451

PhWS1	-----	521
AtWSD1	-----	481
TrWSD4	-----KPRSCLDCL-----	537
TrWSD5	YFEKQDKPLAVSPALVSALAALLVAILLSVLLL	495
MaWSD5	-----	452
ScSco1280	-----	413
RoAtf1	-----	462
MtTgs1	-----LVV-----	463
ScSco0958	-----	446
SaSAV7256	-----	447
MtTgs4	-----	474
MtTgs3	-----	271
TctDGAT	-----	482
AlbAtfA1	-----	457
MhWS1	-----	455
MaWSD1	-----	455
AbWSD1	---N-----	458
PaWS	EKK----LKKLAP-----	475
PcPs1	GYKGNKTKKLAP-----	479
RoAtf2	-----	453
RjRh1	-----	453
MtTgs2	-----	454
MhWS2	-----	473
MaWSD2	-----	473
AlbAtfA2	-----	451

WS and DGAT activity tested, enzyme has WS and DGAT activity
WS and DGAT activity tested, enzyme has only WS activity
Only WS activity tested, enzyme has WS activity
WS and DGAT activity tested, enzyme has only DGAT activity

Figure S3.5. Multiple sequence alignment of WSD with published enzymatic activity. (Figure legend: see next page)

Figure S3.5. Multiple sequence alignment of WSD with published enzymatic activity.

The color code displays whether the enzyme was tested for WS or DGAT activity and whether the enzyme exhibits the tested activity. A list of all WSD and their published activities can be found in Table S3.4. Underlined residues mark amino acids of the catalytic motif of AbWSD1. Light green highlighted residues are amino acids that form the proposed DAG cavity in AbWSD1. Highlighted residues in TctDGAT mark amino acids, whose mutations lead to increased (dark blue) or reduced (dark green) TAG production of the enzyme (Santín *et al.*, 2019b).

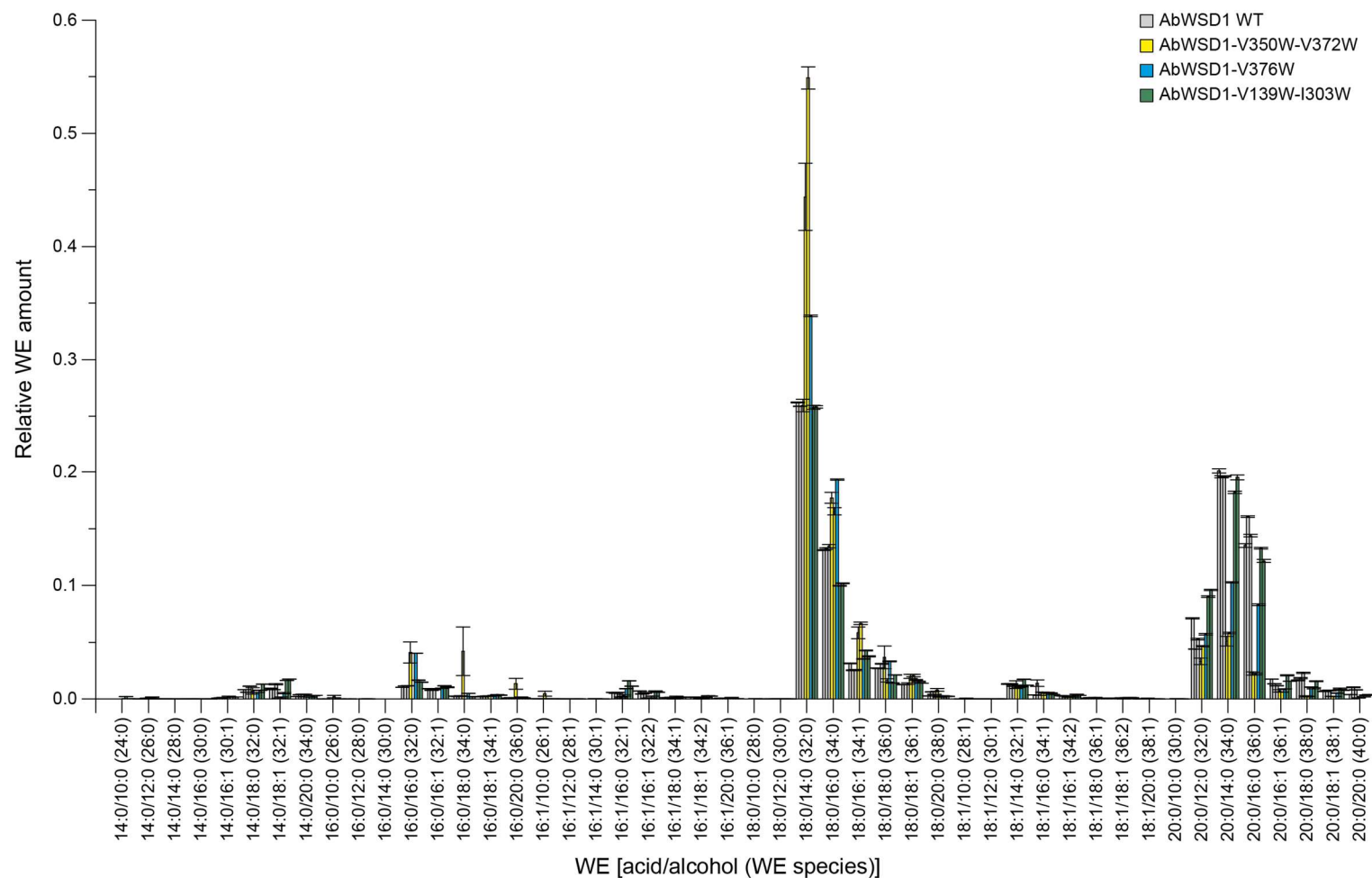


Figure S3.6. WE profile of AbWSD1 WT and different mutant variants.

E. coli lysate expressing the enzyme variants was incubated with six different acyl-CoA and eight different fatty alcohols. The produced WE species were analyzed by nanoESI-MS/MS. The method is optimized for the detection of WE species with 32 carbons or more (Iven *et al.*, 2013). Each bar represents the mean of three measurements of one biological replicate \pm standard deviation. Bars of the same color depict different biological replicates.

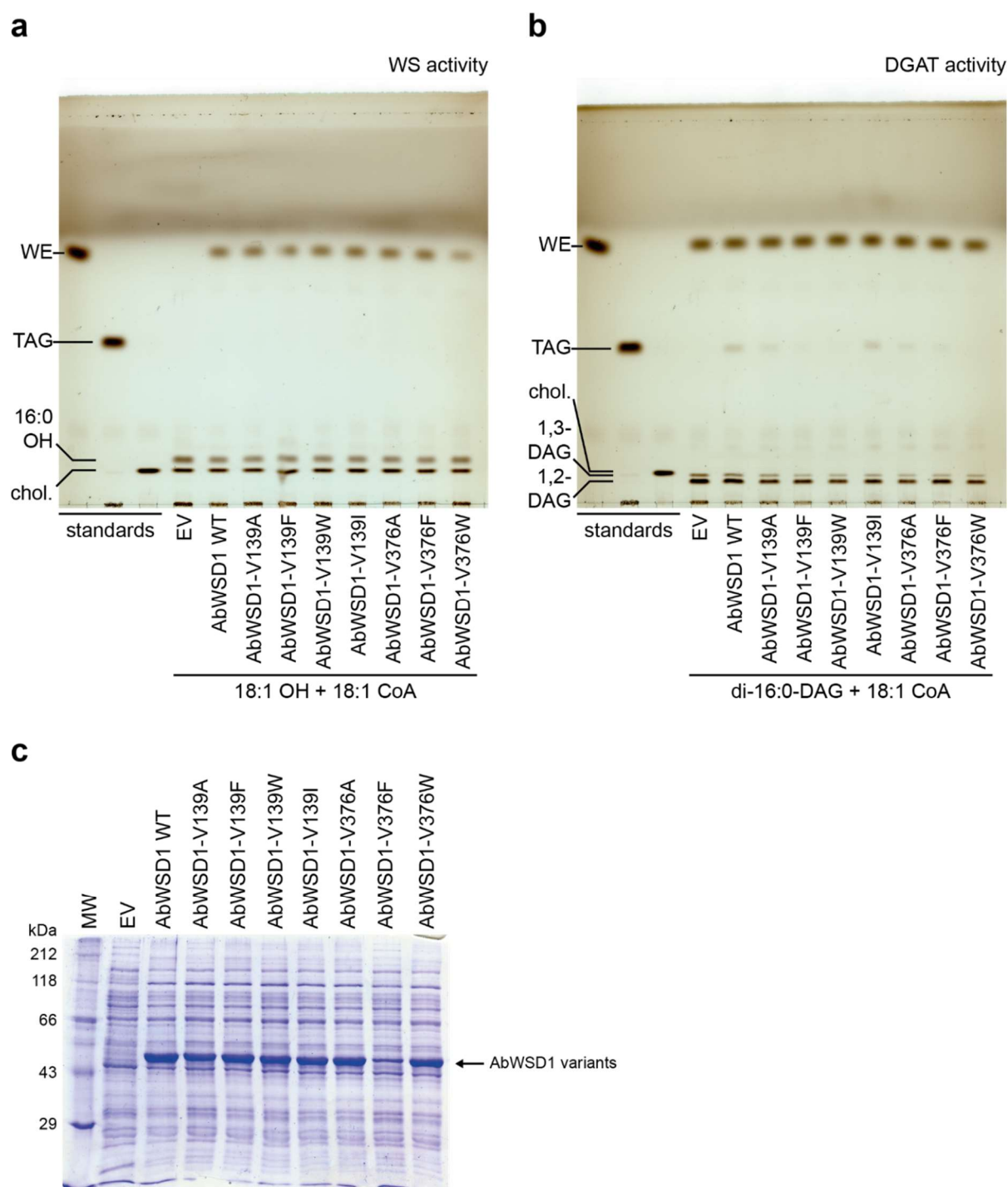


Figure S3.7. Analysis of WS and DGAT activity of AbWSD1 WT and AbWSD1-V139 and AbWSD1-V376 mutants.

(a) (b) Analysis of WS **(a)** and DGAT **(b)** activity of different AbWSD1 variants. *E. coli* lysate of cells expressing AbWSD1 WT or the generated amino acid exchange mutants was incubated for one hour at room temperature either with 18:1 CoA and 18:1 OH to test for WS activity **(a)** or with 18:1 CoA and di-16:0-DAG to test for DGAT activity **(b)**. Neutral lipids were extracted from the reaction mix and separated by TLC. 5 μ g of cholesterol (chol.) and 5 μ g of di-17:0-WE were used as internal extraction standards for WS **(a)** and DGAT **(b)** activity samples, respectively. Spots of the internal extraction standards can be seen on the TLC plates in the corresponding samples. **(c)** SDS-PAGE of *E. coli* lysate expressing the AbWSD1 variants. 7.5 μ g total protein was loaded on the gel for each sample.

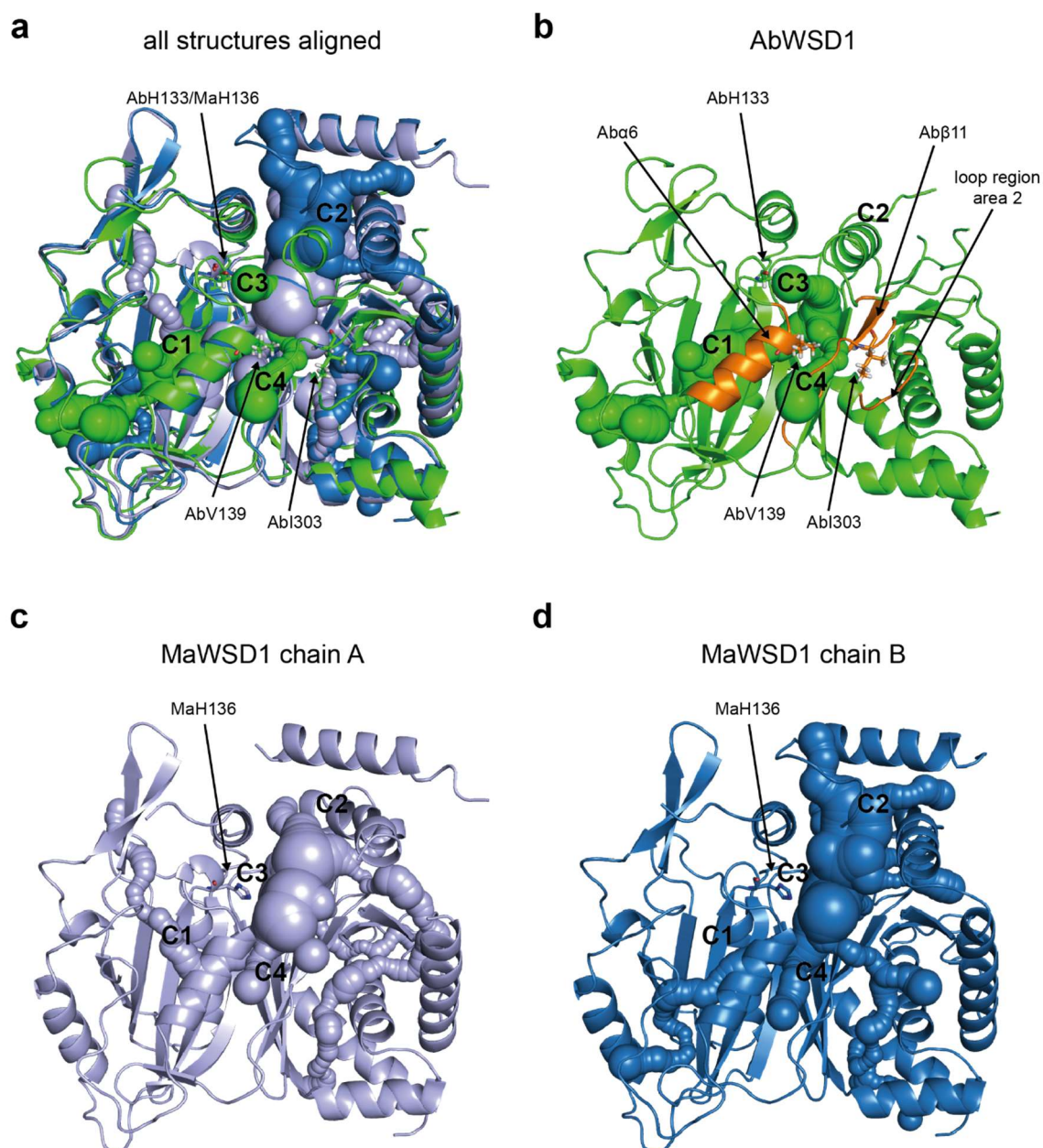


Figure S3.8. Cavities calculated by Pymol plugin Caver 3.0.1.

Depicted are the crystal structures of all aligned (**a**), only AbWSD1 with in orange highlighted amino acids and their corresponding secondary structure elements that form C4 (**b**), MaWSD1 chain A (**c**) and MaWSD1 chain B (**d**) together with the calculated cavities using the Pymol plugin CAVER 3.0.1 (Chovancova *et al.*, 2012; Pavelka *et al.*, 2016). The following settings were applied to CAVER: Input: only 20_AA; starting point: AbH133-AbS374/MaH136-MaS379; shell radius: 5; rest: default settings. Oxygen atoms are depicted in red, nitrogen atoms in blue.

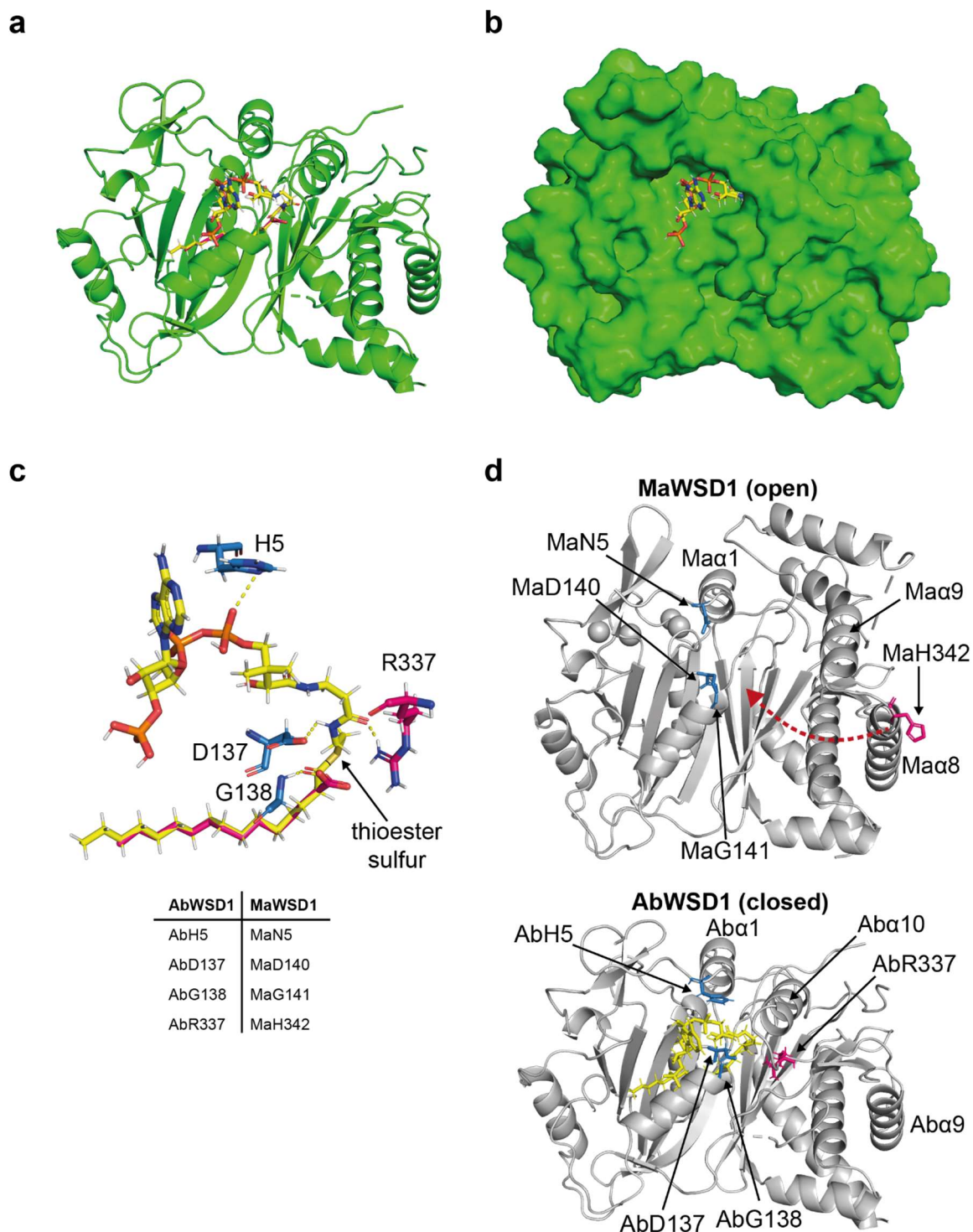
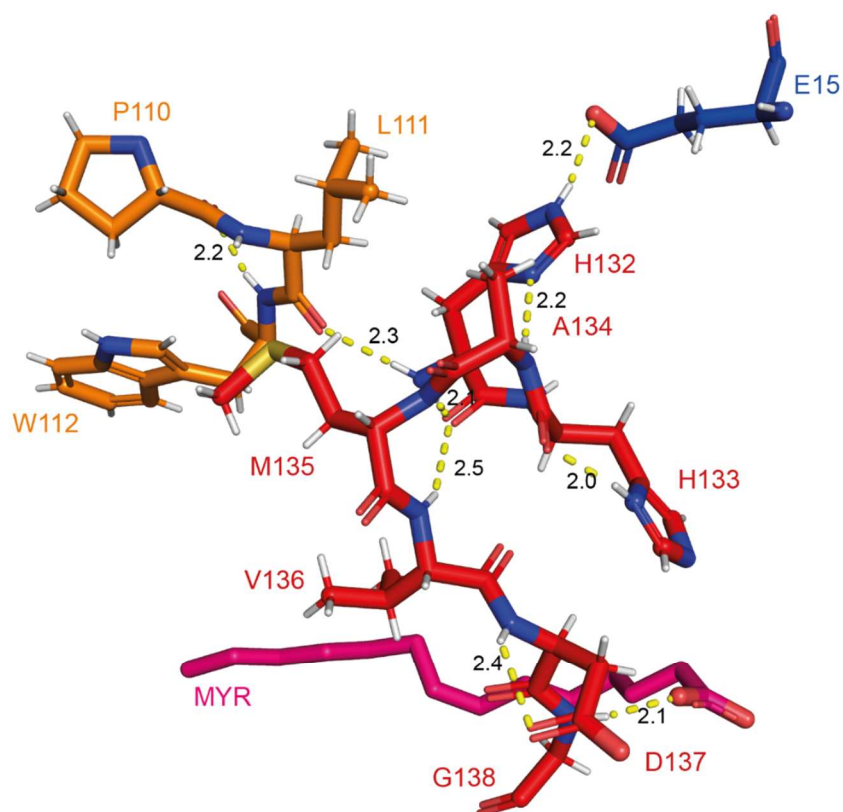


Figure S3.9. Binding site with modelled palmitoyl-CoA.

(a) Cartoon representation of AbWSD1 with co-crystallized myristic acid (pink) and modelled palmitoyl-CoA (yellow). (b) Surface of AbWSD1 with modelled palmitoyl-CoA (yellow), having the acyl chain and the pantetheine linker buried in the protein and the phosphoadenosine part exposed to the outside of the protein. (c) 3D orientation of the co-crystallized myristic acid (pink), the modelled palmitoyl-CoA (yellow) with the hydrogen bonds forming amino acids of AbWSD1 (blue and pink) as well as a table depicting the corresponding amino acids in MaWSD1. (d) Comparison of the positions of the with palmitoyl-CoA hydrogen bonds forming amino acids in AbWSD1 and MaWSD1. Oxygen atoms are depicted in red, nitrogen atoms in blue, phosphorus atoms in orange and sulfur atoms in dark yellow.



H132 (Nε2-H)	E15 (Oε2)	2.2 Å
H132 (Nδ1)	A134 (main chain NH)	2.2 Å
H132 (main chain NH)	L111 (main chain CO)	2.3 Å
H132 (main chain CO)	M135 (main chain NH)	2.1 Å
H132 (main chain CO)	V136 (main chain NH)	2.5 Å
H133 (main chain CO)	H133 (Nδ1-H)	2.0 Å
D137 (main chain NH)	D137 (Oδ1)	2.4 Å
G138 (main chain NH)	MYR (carbonyl group)	2.1 Å
W112 (main chain NH)	P110 (main chain CO)	2.2 Å

Figure S3.10. Hydrogen bonds formed by residues from the catalytic motif.

The residues of the catalytic motif are displayed in red. The amino acids of the conserved PLW motif (Villa *et al.*, 2014) are highlighted in orange. The conserved and mutated amino acid E15 (Röttig & Steinbüchel, 2013b) is displayed in blue. The co-crystallized myristic acid (MYR) is depicted in pink. Yellow dashed lines represent hydrogen bonds labeled with their corresponding length. Oxygen atoms are depicted in red, nitrogen atoms in blue and the sulfur atom is depicted in yellow.

Supporting Tables

Table S3.1. Primer sequences.

Primer name	Primer sequence (5'→3')
pCOLD-His ₆ -TF-AbWSD1 For	ACGGAATTCATGCGTCCGCTGCACCCGAT
pCOLD-His ₆ -TF-AbWSD1 Rev	ACGGGATCCTTAGTTGGCTGTCTTAATGT
pET28a-His ₆ -AbWSD1 For	ACGGGATCCATGCGTCCGCTGCACCCGAT
pET28a-His ₆ -AbWSD1 Rev	ACGAAGCTTTTAGTTGGCTGTCTTAATGT
AbWSD1-V23W-G24W For	GCCAGCAGCCTATGCACTGGTGGGGCCTGTTCTGTTCCAGATCCC
AbWSD1-V23W-G24W Rev	GGAACAGGAACAGGCCCCACCAGTGCATAGGCTGCTGGCGCTTTTC C
AbWSD1-V139A For	CGCCATGGTGGACGGCGCAGCAGGCATGCGTCTGATCG
AbWSD1-V139A Rev	CAGACGCATGCCTGCTGCGCCGTCCACCATGGCGTGATGG
AbWSD1-V139F For	CGCCATGGTGGACGGCTTTGCAGGCATGCGTCTGATCG
AbWSD1-V139F Rev	CAGACGCATGCCTGCAAAGCCGTCCACCATGGCGTGATGG
AbWSD1-V139I For	CGCCATGGTGGACGGCATTGCAGGCATGCGTCTGATCG
AbWSD1-V139I Rev	CAGACGCATGCCTGCAATGCCGTCCACCATGGCGTGATGG
AbWSD1-V139W For	CGCCATGGTGGACGGCTGGGCAGGCATGCGTCTGATCG
AbWSD1-V139W Rev	CAGACGCATGCCTGCCAGCCGTCCACCATGGCGTGATGG
AbWSD1-I303W For	CGATGTGAGCAACCGCTGGACAATGATCCTGGCCAACCTGG
AbWSD1-I303W Rev	GGCCAGGATCATTGTCCAGCGGTTGCTCACATCGCTGTC
AbWSD1-S148A For	TCTGATCGAGAAGGCACTGAGTCACGACGTTACCG
AbWSD1-S148A Rev	CGTCGTGACTCAGTGCCTTCTCGATCAGACGCATGC
AbWSD1-S148A-L149A For	GTCTGATCGAGAAGGCAGCAAGTCACGACGTTACCGAGAAGAGCAT CGTGC
AbWSD1-S148A-L149A Rev	GGTAACGTCGTGACTTGCTGCCTTCTCGATCAGACGCATGCCTGCA ACGCC

AbWSD1-L149A For	CTGATCGAGAAGAGCGCAAGTCACGACGTTACCGAGAAGAGCATCG TGC
AbWSD1-L149A Rev	GGTAACGTCGTGACTTGCCTCTTCTCGATCAGACGCATGCCTGCA AC
AbWSD1-V350W For	GAACTACAGCGCAGTGTGGTACGGCCCTGCCGGCTTAAATATC
AbWSD1-V350W Rev	GCCGGCAGGGCCGTACCACACTGCGCTGTAGTTCAGAATTTG
AbWSD1-V372W For	CGTCAGGCCTTTAATCTGTGGATCAGCAACGTTCCGGGTCC
AbWSD1-V372W Rev	CGGAACGTTGCTGATCCACAGATTAAGGCCTGACGCTTCG
AbWSD1-V376A For	CTGGTGATCAGCAACGCACCGGGTCCGCGTGAACCG
AbWSD1-V376A Rev	CACGCGGACCCGGTGCGTTGCTGATCACCAGATTAAGG
AbWSD1-V376F For	CTGGTGATCAGCAACTTCCGGGTCCGCGTGAACCG
AbWSD1-V376F Rev	CACGCGGACCCGAAAGTTGCTGATCACCAGATTAAGG
AbWSD1-V376W For	CTGGTGATCAGCAACTGGCCGGTCCGCGTGAACCG
AbWSD1-V376W Rev	CACGCGGACCCGGCCAGTTGCTGATCACCAGATTAAGG

Table S3.2. Data collection and refinement statistics.

	Native AbWSD1	SeMet AbWSD1
Beamline SLS	X10SA	X6SA
Wavelength (Å)	0.9788	0.9764
Space group	I 4 2 2	I 4 2 2
Cell dimensions		
a, b, c (Å)	117.1, 117.1, 141.2	117.8, 117.8, 139.7
α , β , γ (°)	90, 90, 90	90, 90, 90
Resolution (highest res. shell) (Å)	45-2.10 (2.17-2.10)	50-2.5 (2.6- 2.5)
R-factor (%)	7.7 (60.2)	9.6 (59.9)
No. of observed reflections /unique reflections	381836 (29155)	297939 / 32789
I/ σ (I)	26.6 (4.3)	18.9 (3.5)
Completeness (%)	99.6 (98.6)	98.6 (91.5)
Wilson B factor (Å ²)	38.4	54.2
Refinement		
Molecules per unit cell	1	
R _{work} /R _{free} (%)	18.1/20.9	
Residues included in model	1-165, 218-294, 300-356, 367-451	
Number of protein atoms	3217	
Number of ligand atoms	16	
Number of water molecules	139	
B-factors (Å ²) overall	36.6	
Protein	36.5	
Ligand	42.2	
Water	38.7	

r.m.s.d.		
Bond lengths (Å)	0.003	
Bond angles (°)	0.59	
Ramachandran favored/allowed/outliers (%)	98.2/1.8/0	

Table S3.3. Generated and analyzed AbWSD1 amino acid exchange mutants (this study).

The column "Experiments" depicts, which analysis method was performed (TLC, photometer, nanoESI-MS/MS, CD spectroscopy), which activity was tested (WS, DGAT) and what kind of protein was used for the analysis (*E.coli* lysate, purified protein). Residue G355 has been mutated before by Barney *et al.* (2013).

Amino acid exchange	Location of the amino acid residue within the AbWSD1 structure	Experiments	Location of the amino acid residue around a cavity
V23W G24W	$\beta 1, \beta 1$	TLC, WS/DGAT, lysate/purified protein nanoESI-MS/MS, WS, lysate CD spectroscopy	Formation of acyl-CoA cavity close to the active site
V139A	$\alpha 6$	TLC, WS/DGAT, lysate nanoESI-MS/MS, WS, lysate	Formation of DAG cavity
V139F	$\alpha 6$	TLC, WS/DGAT, lysate nanoESI-MS/MS, WS, lysate	Formation of DAG cavity
V139W	$\alpha 6$	TLC, WS/DGAT, lysate nanoESI-MS/MS, WS, lysate	Formation of DAG cavity
V139I	$\alpha 6$	TLC, WS/DGAT, lysate nanoESI-MS/MS, WS, lysate	Formation of DAG cavity
V139W I303W	$\alpha 6$, loop between $\beta 9$ and $\beta 10$	TLC, WS/DGAT, lysate/purified protein nanoESI-MS/MS, WS, lysate CD spectroscopy	Formation of DAG cavity
S148A	First C-terminal residue after $\alpha 6$	TLC, WS/DGAT, lysate Photometer, WS, purified protein nanoESI-MS/MS, WS, lysate	Formation of acyl-CoA cavity at the end of the cavity

S148A L149A	First C-terminal residue after $\alpha 6$, second C-terminal residue after $\alpha 6$	TLC, WS/DGAT, lysate Photometer, WS, purified protein nanoESI-MS/MS, WS, lysate	Formation of acyl-CoA cavity at the end of the cavity
S148A I343F	First C-terminal residue after $\alpha 6$, $\alpha 10$	TLC, WS, lysate TLC, DGAT, lysate/purified protein nanoESI-MS/MS, WS, lysate	Formation of acyl-CoA cavity at the end of the cavity, formation of CoA cavity
L149A	Second C-terminal residue after $\alpha 6$	TLC, WS/DGAT, lysate Photometer, WS, purified protein nanoESI-MS/MS, WS, lysate	Formation of acyl-CoA cavity at the end of the cavity
I343F	$\alpha 10$	TLC, WS, lysate TLC, DGAT, lysate/purified protein nanoESI-MS/MS, WS, lysate	Formation of CoA cavity
I343Y	$\alpha 10$	TLC, WS/DGAT, lysate/purified protein nanoESI-MS/MS, WS, lysate	Formation of CoA cavity
I343W	$\alpha 10$	TLC, WS, lysate TLC, DGAT, lysate/purified protein nanoESI-MS/MS, WS, lysate	Formation of CoA cavity
S347F	$\alpha 10$	TLC, WS, lysate TLC, DGAT, lysate/purified protein nanoESI-MS/MS, WS, lysate	Formation of CoA cavity
S347Y	$\alpha 10$	TLC, WS/DGAT, lysate/purified protein Photometer, WS, purified protein	Formation of CoA cavity

		nanoESI-MS/MS, WS, lysate	
S347W	α 10	TLC, WS, lysate TLC, DGAT, lysate/purified protein nanoESI-MS/MS, WS, lysate	Formation of CoA cavity
V350W V372W	α 10, β 11	TLC, WS/DGAT, lysate/purified protein nanoESI-MS/MS, WS, lysate CD spectroscopy	Formation of curvature opposite to the active site
G355I	Loop region between α 10 and β 11	nanoESI-MS/MS, WS, lysate	Formation of fatty alcohol cavity
V376A	β 11	TLC, WS/DGAT, lysate nanoESI-MS/MS, WS, lysate	Formation of curvature opposite to the active site
V376F	β 11	TLC, WS/DGAT, lysate nanoESI-MS/MS, WS, lysate	Formation of curvature opposite to the active site
V376W	β 11	TLC, WS/DGAT, lysate nanoESI-MS/MS, WS, lysate	Formation of curvature opposite to the active site

Table S3.4. List of WSD with published enzymatic activity.

The color code displays whether the enzyme was tested for WS or DGAT activity and whether the enzyme exhibits the tested activity. If one row is colored with two colors, both conditions apply to the enzyme. For the evaluation of the sequence alignment yellow was chosen for the coloring of those proteins. FAEE: fatty acid ethyl ester.

Organism (Phylogenetic clade)	Protein	NCBI Accession Number	Protein name in sequence alignment	WS activity	DGAT activity	Reference
<i>Acinetobacter baylyi</i> ADP1 (bacterium)	AtfA, Ac1, WS/DGAT	WP_004922247.1	AbWSD1	<i>In vitro</i> WS activity <i>In vivo</i> WS activity <i>In vitro</i> WS activity <i>In vitro</i> WS activity, <i>in vivo</i> FAEE production <i>In vitro</i> WS activity <i>In vivo</i> FAEE production <i>In vitro</i> WS activity	<i>In vitro</i> DGAT activity <i>In vivo</i> DGAT activity <i>In vitro</i> DGAT activity DGAT activity not tested DGAT activity not tested <i>In vivo</i> DGAT activity DGAT activity not tested	(Kalscheuer & Steinbüchel, 2003) (Kalscheuer <i>et al.</i> , 2004) (Stöveken <i>et al.</i> , 2005) (Shi <i>et al.</i> , 2012) (Barney <i>et al.</i> , 2012) (Röttig <i>et al.</i> , 2015) (Röttig <i>et al.</i> , 2016)
<i>Marinobacter hydrocarbonoclasticus</i> (bacterium)	WS1	ABO21020.1	MhWS1	<i>In vitro</i> WS activity <i>In vivo</i> FAEE production	<i>In vitro</i> DGAT activity <i>In vivo</i> DGAT activity	(Holtzapfle & Schmidt-Dannert, 2007) (Röttig <i>et al.</i> , 2015)
	WS2	ABO21021.1	MhWS2	<i>In vitro</i> WS activity <i>In vitro</i> WS activity, <i>in vivo</i> FAEE production <i>In vivo</i> FAEE production <i>In vitro</i> WS activity <i>In vivo</i> WS activity, <i>in vitro</i> WS activity	No <i>in vitro</i> DGAT activity detectable DGAT activity not tested <i>In vivo</i> low DGAT activity DGAT activity not tested No DGAT activity	(Holtzapfle & Schmidt-Dannert, 2007) (Shi <i>et al.</i> , 2012) (Röttig <i>et al.</i> , 2015) (Röttig <i>et al.</i> , 2016) (Miklaszewska <i>et al.</i> , 2018)
<i>Marinobacter aquaeolei</i> VT8 (bacterium)	Ma1, WS/DGAT	WP_011783747.1	MaWSD1	<i>In vitro</i> WS activity <i>In vitro</i> WS activity <i>In vivo</i> WS activity	DGAT activity not tested <i>In vitro</i> DGAT activity <i>In vivo</i> DGAT activity	(Barney <i>et al.</i> , 2012) (Petronikolou & Nair, 2018) (Vollheyde <i>et al.</i> , 2020)
	Ma2	WP_011786509.1	MaWSD2	<i>In vitro</i> WS activity <i>In vitro</i> WS activity <i>In vivo</i> WS activity	DGAT activity not tested <i>In vitro</i> DGAT activity No <i>in vivo</i> DGAT activity	(Barney <i>et al.</i> , 2012) (Villa <i>et al.</i> , 2014) (Vollheyde <i>et al.</i> , 2020)
	MaWSD5	GenBank: ABM20482.1	MaWSD5	<i>In vivo</i> and <i>in vitro</i> WS activity	No <i>in vivo</i> and no <i>in vitro</i> DGAT activity	(Vollheyde <i>et al.</i> , 2020)

<i>Alcanivorax borkumensis</i> SK2 (bacterium)	AtfA1	WP_011590012.1	AlbAtfA1	High levels of <i>in vitro</i> WS activity, <i>in vivo</i> WS activity <i>In vivo</i> FAEE production <i>In vitro</i> WS activity	Lower <i>in vitro</i> DGAT activity, <i>in vivo</i> DGAT activity <i>In vivo</i> DGAT activity DGAT activity not tested	(Kalscheuer <i>et al.</i> , 2007) (Röttig <i>et al.</i> , 2015) (Röttig <i>et al.</i> , 2016)
	AtfA2	WP_011589085.1	AlbAtfA2	Substantial <i>in vitro</i> WS activity, no WS activity <i>in vivo</i> <i>In vivo</i> FAEE production	Negligible <i>in vitro</i> DGAT activity, no DGAT activity <i>in vivo</i> No <i>in vivo</i> DGAT activity	(Kalscheuer <i>et al.</i> , 2007) (Röttig <i>et al.</i> , 2015)
<i>Rhodococcus opacus</i> PD630 (bacterium)	Atf1	ACX81314.1	RoAtf1	<i>In vitro</i> WS activity <i>In vitro</i> WS activity, <i>in vivo</i> FAEE production <i>In vivo</i> FAEE production	Almost no DGAT activity <i>in vitro</i> , <i>in vivo</i> DGAT activity (reduced TAG after knockout) DGAT activity not tested No <i>in vivo</i> DGAT activity	(Alvarez <i>et al.</i> , 2008) (Shi <i>et al.</i> , 2012) (Röttig <i>et al.</i> , 2015)
	Atf2	EHI41112.1	RoAtf2	<i>In vitro</i> WS activity (lower than DGAT activity) <i>In vivo</i> FAEE production	<i>In vitro</i> DGAT activity No <i>in vivo</i> DGAT activity	(Alvarez <i>et al.</i> , 2008) (Röttig <i>et al.</i> , 2015)
<i>Rhodococcus jostii</i> RHA1 (bacterium)	Rh1	WP_011594556.1	RjRh1	<i>In vitro</i> WS activity	DGAT activity not tested	(Barney <i>et al.</i> , 2012)
<i>Mycobacterium tuberculosis</i> H37Rv (bacterium)	Tgs1	NP_217646.1	MtTgs1	Really low / almost no <i>in vitro</i> WS activity	<i>In vitro</i> DGAT activity	(Daniel <i>et al.</i> , 2004)
	Tgs2	NP_218251.1	MtTgs2	Lower <i>in vitro</i> WS activity	<i>In vitro</i> DGAT activity	(Daniel <i>et al.</i> , 2004)
	Tgs3	NP_217751.1	MtTgs3	No <i>in vitro</i> WS activity	<i>In vitro</i> DGAT activity	(Daniel <i>et al.</i> , 2004)
	Tgs4	NP_217604.1	MtTgs4	Really low <i>in vitro</i> WS activity	<i>In vitro</i> DGAT activity	(Daniel <i>et al.</i> , 2004)
<i>Streptomyces coelicolor</i> A3(2) (bacterium)	Sco0958	NP_625255.1	ScSco0958	No WS activity <i>in vitro</i> <i>In vivo</i> FAEE production	<i>In vitro</i> DGAT activity, <i>in vivo</i> DGAT activity No <i>in vivo</i> DGAT activity	(Arabolaza <i>et al.</i> , 2008) (Röttig <i>et al.</i> , 2015)
	Sco1280	NP_625567.1	ScSco1280	No WS activity <i>in vitro</i>	No <i>in vitro</i> DGAT activity, no <i>in vivo</i> DGAT activity, however DGAT activity is discussed	(Arabolaza <i>et al.</i> , 2008)

<i>Streptomyces avermitilis</i> MA-4680 (bacterium)	SAV7256	WP_010988651.1	SaSAV7256	<i>In vitro</i> WS activity <i>In vivo</i> FAEE production	<i>In vitro</i> DGAT activity (lower than WS activity) No <i>in vivo</i> DGAT activity	(Kaddor <i>et al.</i> , 2009) (Röttig <i>et al.</i> , 2015)
<i>Psychobacter arcticus</i> 273-4 (bacterium)	PaWS, DGAT	WP_011279534.1	PaWS	<i>In vitro</i> WS activity, <i>in vivo</i> FAEE production	DGAT activity not tested	(Shi <i>et al.</i> , 2012)
<i>Thraustochytrium roseum</i> (bacterium)	TrWSD4	ASA49417.1	TrWSD4	<i>In vitro</i> WS activity, <i>in vivo</i> WS activity	<i>In vitro</i> DGAT activity (lower than WS activity), no <i>in vivo</i> DGAT activity	(Zhang <i>et al.</i> , 2017)
	TrWSD5	ASA49418.1	TrWSD5	<i>In vitro</i> WS activity, <i>in vivo</i> WS activity	<i>In vitro</i> DGAT activity (lower than WS activity), no <i>in vivo</i> DGAT activity	(Zhang <i>et al.</i> , 2017)
<i>Psychobacter cryohalolentis</i> K5 (bacterium)	Ps1	WP_011512619.1	PcPs1	<i>In vitro</i> WS activity	DGAT activity not tested	(Barney <i>et al.</i> , 2012)
<i>Thermomonospora curvata</i> (bacterium)	tDGAT	UniProt: ACY99349	TctDGAT	<i>In vivo</i> WS activity <i>In vivo</i> WS activity	<i>In vivo</i> DGAT activity <i>In vivo</i> DGAT activity	(Lázaro <i>et al.</i> , 2017) (Santín <i>et al.</i> , 2019a)
<i>Petunia hybrida</i> (plant)	PhWS1	AAZ08051.1	PhWS1	<i>In vivo</i> WS activity, <i>in vitro</i> WS activity	No <i>in vivo</i> DGAT activity, no <i>in vitro</i> DGAT activity	(King <i>et al.</i> , 2007)
<i>Arabidopsis thaliana</i> (plant)	AtWSD1	AED94163.1	AtWSD1	<i>In vitro</i> WS activity, <i>in vivo</i> WS activity	<i>In vitro</i> DGAT activity, no <i>in vivo</i> DGAT activity	(Li <i>et al.</i> , 2008)
WS and DGAT activity tested, enzyme has WS and DGAT activity						
WS and DGAT activity tested, enzyme has only WS activity						
Only WS activity tested, enzyme has WS activity						
WS and DGAT activity tested, enzyme has only DGAT activity						

Table S3.5. List of published amino acid exchange mutants in different WSD.

Stop codon insertions at the corresponding positions are indicated by *.

Protein	Mutation	Experiments	If applicable, assigned role of the residue based on its publication and on this study	Reference
<i>Acinetobacter baylyi</i> WSD1 (AtfA1, Ac1, WS/DGAT)	H132L	Highly reduced WS activity	Important for the structural integrity of the catalytic motif	(Stöveken <i>et al.</i> , 2009)
	H133L	Almost inactive protein (WS activity)	Catalytic histidine	(Stöveken <i>et al.</i> , 2009)
	H132L H133L	Inactive protein (WS activity)	Both histidines are needed for unrestricted activity	(Stöveken <i>et al.</i> , 2009)
	D137A	No significant decrease in WS activity	Positioning of acyl-CoA	(Stöveken <i>et al.</i> , 2009)
	G138A	No significant decrease in WS activity	Positioning of acyl-CoA	(Stöveken <i>et al.</i> , 2009)
	R2C	No significant decrease in WS activity		(Röttig & Steinbüchel, 2013b)
	E15K	Highly reduced WS activity	Hydrogen bond towards H132, structural integrity of the catalytic motif	(Röttig & Steinbüchel, 2013b)
	W67G	Reduced WS activity	Possible hydrogen bond to D8, structural integrity of the protein	(Röttig & Steinbüchel, 2013b)
	W67*	Highly reduced WS activity	Possible hydrogen bond to D8, structural integrity of the protein, mutation leads to truncated protein without active site residues	(Röttig & Steinbüchel, 2013b)
	E72*	Highly reduced WS activity	Mutation leads to truncated protein without active site residues	(Röttig & Steinbüchel, 2013b)
	A126D	Highly reduced WS activity	Structural integrity of the protein	(Röttig & Steinbüchel, 2013b)
	L172*	Reduced WS activity	Not present in crystal structure, mutation leads to truncated protein	(Röttig & Steinbüchel, 2013b)
	L201F	No significant decrease in WS activity	Not present in crystal structure, linker between N- and C-terminus	(Röttig & Steinbüchel, 2013b)

	S217L	No significant decrease in WS activity	Not present in crystal structure, linker between N- and C-terminus	(Röttig & Steinbüchel, 2013b)
	Q333*	Highly reduced WS activity	Mutation leads to truncated protein, lacking the inward moving α -helix (α 10) and parts of the fatty alcohol binding site	(Röttig & Steinbüchel, 2013b)
	Q342R	Reduced WS activity	Structural integrity of the protein, part of the inward moving helix (α 10)	(Röttig & Steinbüchel, 2013b)
	G352D	Reduced WS activity		(Röttig & Steinbüchel, 2013b)
	Q367*	Highly reduced WS activity	Mutation leads to truncated protein lacking part of the fatty alcohol binding site	(Röttig & Steinbüchel, 2013b)
	S374P	Reduced WS activity	Part of the active site curvature (located on β 11), speculated role during catalysis	(Röttig & Steinbüchel, 2013b)
	G378S	Reduced WS activity	Part of the DAG binding site and located C-terminally of β 11, mutation to larger residue might change position of β 11	(Röttig & Steinbüchel, 2013b)
	G378D	Reduced WS activity	Part of the DAG binding site and located C-terminally of β 11, mutation to larger residue might change position of β 11	(Röttig & Steinbüchel, 2013b)
	V399G	Reduced WS activity		(Röttig & Steinbüchel, 2013b)
	G355I	Changed alcohol selectivity towards shorter fatty alcohols	Located at the fatty alcohol binding pocket	(Barney <i>et al.</i> , 2013)
	G355I	Higher affinity towards shorter fatty alcohols	Located at the fatty alcohol binding pocket	(Röttig <i>et al.</i> , 2015; Röttig <i>et al.</i> , 2016)
<i>Marinobacter aquaeolei</i> WSD1 (Ma1, WS/DGAT)	A360V	Changed alcohol selectivity towards shorter fatty alcohols	Located at the fatty alcohol binding pocket	(Barney <i>et al.</i> , 2013)
	A360I	Changed alcohol selectivity towards shorter fatty alcohols	Located at the fatty alcohol binding pocket	(Barney <i>et al.</i> , 2013)
	A360I	Positive effect on WE production with short chain alcohols	Located at the fatty alcohol binding pocket	(Röttig <i>et al.</i> , 2016)
	A360F	Changed alcohol selectivity towards shorter fatty alcohols	Located at the fatty alcohol binding pocket	(Barney <i>et al.</i> , 2013)
	T355I	No alteration in alcohol selectivity		(Barney <i>et al.</i> , 2015)

	L356W	Different selectivity for fatty alcohols	Located at the fatty alcohol binding pocket	(Barney <i>et al.</i> , 2015)
	L356Y	No alteration in alcohol selectivity for one assay	Located at the fatty alcohol binding pocket	(Barney <i>et al.</i> , 2015)
	L356F	Differences for small and medium alcohol selectivity	Located at the fatty alcohol binding pocket	(Barney <i>et al.</i> , 2015)
	L356V	Differences for small and medium alcohol selectivity	Located at the fatty alcohol binding pocket	(Barney <i>et al.</i> , 2015)
	L356A	Differences for small and medium alcohol selectivity	Located at the fatty alcohol binding pocket	(Barney <i>et al.</i> , 2015)
	A357V	No alteration in alcohol selectivity		(Barney <i>et al.</i> , 2015)
	A359I	No alteration in alcohol selectivity for one assay		(Barney <i>et al.</i> , 2015)
	A360W	Significant loss in activity affecting both assays	Located at the fatty alcohol binding pocket	(Barney <i>et al.</i> , 2015)
	A360F	Significant loss in activity affecting both assays	Located at the fatty alcohol binding pocket	(Barney <i>et al.</i> , 2015)
	A360I	Different selectivity for fatty alcohols	Located at the fatty alcohol binding pocket	(Barney <i>et al.</i> , 2015)
	A360V	Different selectivity for fatty alcohols	Located at the fatty alcohol binding pocket	(Barney <i>et al.</i> , 2015)
	F361L	No alteration in alcohol selectivity		(Barney <i>et al.</i> , 2015)
	T365F	No alteration in alcohol selectivity		(Barney <i>et al.</i> , 2015)
	Q372F	Differences for small and medium alcohol selectivity		(Barney <i>et al.</i> , 2015)
	V376F	No alteration in alcohol selectivity for one assay		(Barney <i>et al.</i> , 2015)
	V376L	No alteration in alcohol selectivity for one assay		(Barney <i>et al.</i> , 2015)
	V376A	No alteration in alcohol selectivity		(Barney <i>et al.</i> , 2015)
	L395A	No alteration in alcohol selectivity		(Barney <i>et al.</i> , 2015)
	G397I	No alteration in alcohol selectivity		(Barney <i>et al.</i> , 2015)
	G397A	No alteration in alcohol selectivity		(Barney <i>et al.</i> , 2015)
	M405W	Differences for small and medium alcohol selectivity	Located at the fatty alcohol binding pocket	(Barney <i>et al.</i> , 2015)

	M405F	Differences for small and medium alcohol selectivity	Located at the fatty alcohol binding pocket	(Barney <i>et al.</i> , 2015)
	M405L	Differences for small and medium alcohol selectivity	Located at the fatty alcohol binding pocket	(Barney <i>et al.</i> , 2015)
	M405A	Differences for small and medium alcohol selectivity	Located at the fatty alcohol binding pocket	(Barney <i>et al.</i> , 2015)
	A409L	No alteration in alcohol selectivity for one assay		(Barney <i>et al.</i> , 2015)
	N411V	No alteration in alcohol selectivity for one assay		(Barney <i>et al.</i> , 2015)
	D8A	Only 24.1 % of WS activity with palmitoyl-CoA (compared to WT enzyme)		(Petronikolou & Nair, 2018)
	G25V	Only 1.0 % of WS activity with palmitoyl-CoA (compared to WT enzyme), only 46.9 % of WS activity with hexanoyl-CoA (compared to WT enzyme), competition assays: no changes in alcohol specificity, but higher preference for shorter acyl-CoA (compared to WT enzyme)	Located at the acyl-CoA binding pocket	(Petronikolou & Nair, 2018)
	H136N	Only 1.5 % of WS activity with palmitoyl-CoA (compared to WT enzyme)	Catalytic histidine	(Petronikolou & Nair, 2018)
	D140A	Only 49.6 % of WS activity with palmitoyl-CoA (compared to WT enzyme)	Positioning of acyl-CoA	(Petronikolou & Nair, 2018)
	A144V	Only 43.3 % of WS activity with palmitoyl-CoA (compared to WT enzyme)	Located at the acyl-CoA binding pocket	(Petronikolou & Nair, 2018)
	A144F	Only 53 % of WS activity with palmitoyl-CoA (compared to WT enzyme), 654.6 % of WS activity with hexanoyl-CoA (compared to WT enzyme), competition assays: no changes in alcohol specificity, but higher preference for shorter acyl-CoA (compared to WT enzyme)	Located at the acyl-CoA binding pocket	(Petronikolou & Nair, 2018)
<i>Marinobacter aquaeolei</i> WSD2 (Ma2)	H140A	Reduced WS activity, reduced DGAT activity	Important for structural integrity of the catalytic motif	(Villa <i>et al.</i> , 2014)
	H141A	Reduced WS activity, reduced DGAT activity (higher reduction in both activities than H140A)	Catalytic histidine	(Villa <i>et al.</i> , 2014)
	D145A	Reduced WS activity, reduced DGAT activity	Positioning of acyl-CoA	(Villa <i>et al.</i> , 2014)
	P118A	Reduced WS activity, reduced DGAT activity	Important for structural integrity of the catalytic motif	(Villa <i>et al.</i> , 2014)
	L119A	Reduced WS activity, reduced DGAT activity	Important for structural integrity of the catalytic motif	(Villa <i>et al.</i> , 2014)

	W120A	Insoluble protein	Important for structural integrity of the catalytic motif	(Villa <i>et al.</i> , 2014)
	N270A	Reduced WS activity, reduced DGAT activity		(Villa <i>et al.</i> , 2014)
	D271A	Reduced WS activity, reduced DGAT activity		(Villa <i>et al.</i> , 2014)
	R305A	Reduced WS activity, reduced DGAT activity		(Villa <i>et al.</i> , 2014)
	N- and C-terminal domain	Co-expression and co-purification of the N-terminal domain (1-176) and the C-terminal domain (178-473) resulted in the purification of a complex formed by both domains; the reconstituted enzyme displays WS and DGAT activity in a comparable range to the WT		(Villa <i>et al.</i> , 2014)
<i>Thermomonospora curvata</i> tDGAT	P35L	More TAG production, a little bit more WE production		(Santín <i>et al.</i> , 2019a)
	D80E	A bit more TAG production, a bit more WE production		(Santín <i>et al.</i> , 2019a)
	V87I	More TAG production, WE production similar to WT		(Santín <i>et al.</i> , 2019a)
	D114G	More TAG production, more WE production		(Santín <i>et al.</i> , 2019a)
	G17C/V32L/A94G	More TAG production, a little bit more WE production		(Santín <i>et al.</i> , 2019a)
	L166P	A bit more TAG production, a bit more WE production		(Santín <i>et al.</i> , 2019a)
	T5I	Reduced TAG production, more WE production	Corresponding residue of AbWSD1 is proposed to hydrogen bond with acyl-CoA	(Santín <i>et al.</i> , 2019a)
	L29P	Reduced TAG production, reduced WE production		(Santín <i>et al.</i> , 2019a)
	D71Y	Reduced TAG production, more WE production		(Santín <i>et al.</i> , 2019a)

3.2 Additional work to manuscript Article II

Katharina Vollheyde generated the AbWSD1 mutant variants. She performed the DTNB-based and TLC-based activity assays and the SDS-PAGE. Katharina Vollheyde purified and prepared the proteins for circular dichroism (CD) measurements. With the help of Dr. Viktor Sautner from the Department of Molecular Enzymology (Georg-August-University, Göttingen), she processed, recalculated and evaluated the obtained CD spectra. Dr. Viktor Sautner recorded the CD spectra.

No major structural differences were observed between AbWSD1 WT and AbWSD1-V139W-I303W

To analyze whether mutations in AbWSD1 alter the structure of the protein variants compared to AbWSD1 WT, CD spectra from AbWSD1 WT, AbWSD1-V139W-I303W, AbWSD1-V350W-V372W and AbWSD1-V23W-G24W were recorded. For AbWSD1 WT and AbWSD1-V139W-I303W, the curves showed a similar shape, however, the curve of AbWSD1-V139W-I303W had a smaller amplitude (Figure 3.10a). When analyzing the SDS-PAGE gels with samples of the purification and sample preparation process, it appeared, that the amount of AbWSD1-V139W-I303W used for the measurements did not differ much from the AbWSD1 WT amount, but the measured protein concentration of AbWSD1-V139W-I303W, which was used to calculate the CD spectrum was almost twice as high as the concentration of the AbWSD1 WT protein (Figure 3.10e,f). Due to this, the concentration of the mutant was recalculated based on the SDS-PAGE (detailed calculation see materials and methods part below) and the new concentration was used to recalculate the CD spectrum of the AbWSD1-V139W-I303W. The recalculated spectrum looks similar to the AbWSD1 WT spectrum, suggesting a similar fold of the mutant compared to AbWSD1 WT (Figure 3.10b). As AbWSD1-V139W-I303W showed a WS activity similar to AbWSD1 WT (manuscript Article II), but no TAG formation was detected for the mutant, it can be assumed, that the introduced amino acid substitutions, do not lead to general structural rearrangements within the protein, causing the change in activity, but to a closure or narrowing of the proposed DAG cavity, preventing TAG production.

For AbWSD1-V23W-G24W and AbWSD1-V350W-V372W, CD spectra with smaller amplitudes compared to AbWSD1 WT were obtained as well. However, as only small protein amounts were obtained after purification and buffer exchange and low or even no enzymatic

activity was detected for the purified proteins, an evaluation and discussion of the CD spectra of both AbWSD1 variants was not possible.

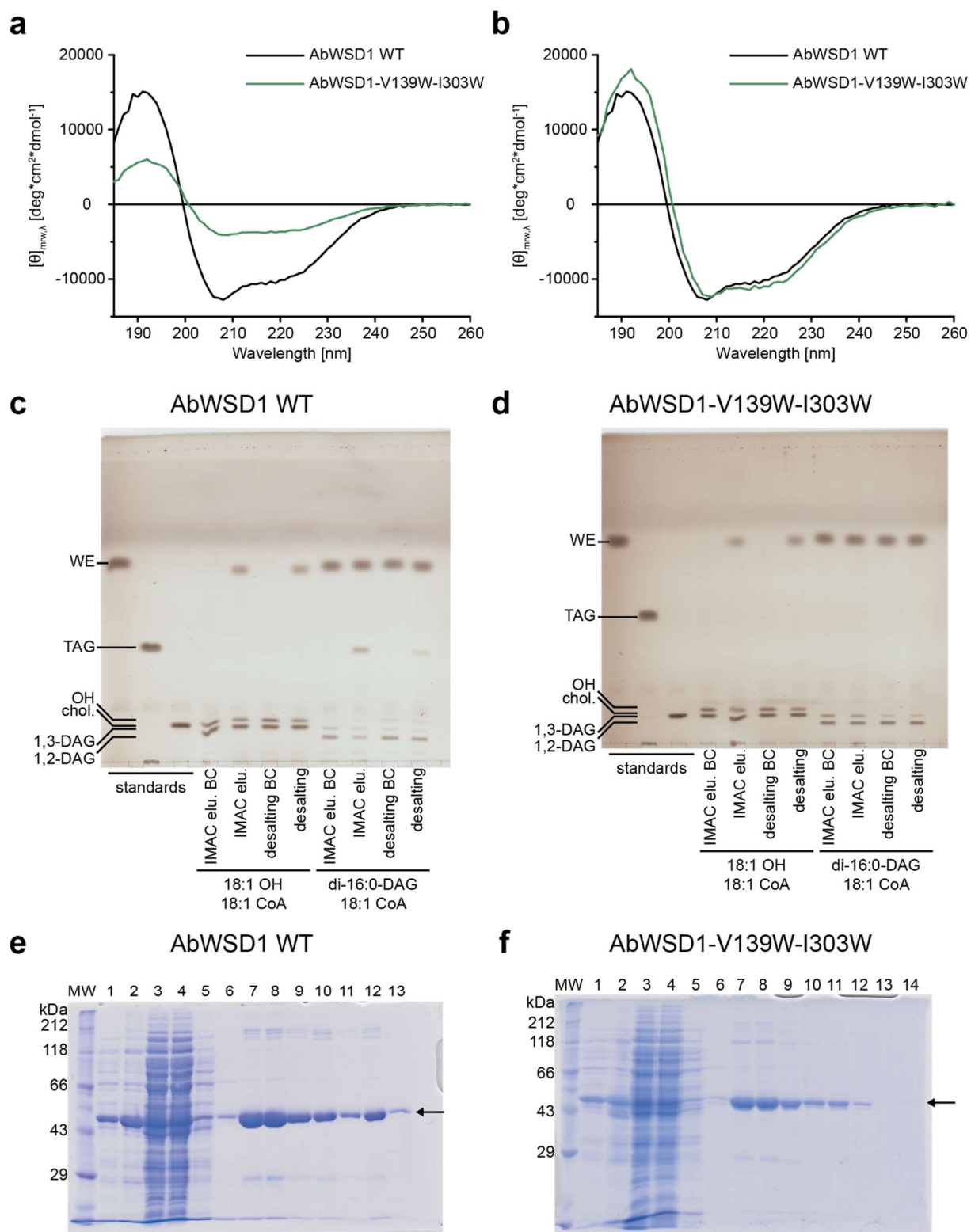


Figure 3.10. CD spectroscopy. (Figure legend: see next page)

Figure 3.10. CD spectroscopy.

AbWSD1 WT and AbWSD1-V139W-I303W were purified from *E. coli* lysate by IMAC and subsequent desalting (buffer exchange to CD buffer using a PD10 column). **(a) (b)** CD spectra of AbWSD1 WT (black) and AbWSD1-V139W-I303W (green) calculated with the measured protein concentration **(a)** and the recalculated protein concentration **(b)**. **(c) (d)** WS and DGAT activity analysis of IMAC purified (IMAC elu.: IMAC elution) and desalted enzyme (desalting). As negative control, the respective buffer was used in the activity assay (BC: buffer control). 20 μ L protein (AbWSD1 WT IMAC elu.: ~20 μ g protein; AbWSD1 WT desalting: ~5 μ g protein; AbWSD1-V139W-I303W IMAC elu.: ~15 μ g protein; AbWSD1-V139W-I303W desalting: ~5 μ g protein) or 20 μ L buffer were incubated with 18:1 CoA and 18:1 OH to test for WS activity or 18:1 CoA and di-16:0-DAG to test for DGAT activity. Neutral lipids were extracted from the reaction mix and separated by TLC. 5 μ g of cholesterol (chol.) and 5 μ g of di-17:0-WE were used as internal extraction standard for WS and DGAT activity samples, respectively. **(e) (f)** SDS-PAGE of AbWSD1 WT and AbWSD1-V139W-I303W purification. **(e)** Loading order (7.5 μ L protein solution mixed with 2.5 μ L 4x Laemmli buffer were loaded on the gel): 1 lysate (1:50 diluted), 2 pellet (1:100 diluted), 3 supernatant (1:2 diluted), 4 IMAC flowthrough (1:2 diluted), 5 IMAC buffer A wash 1 (1:2 diluted), 6 IMAC ATP wash, 7 IMAC Elution 2/3 non centrifuged, 8 IMAC Elution 2/3 centrifuged, 9 PD10 1. Elution non centrifuged, 10 PD10 1. Elution centrifuged, 11 PD10 1. Elution centrifuged diluted for CD (this sample was used for the CD measurement), 12 PD10 1. Elution centrifuged undiluted for CD, 13 PD10 2. Elution non centrifuged. **(f)** Loading order (7.5 μ L protein solution mixed with 2.5 μ L 4x Laemmli buffer were loaded on the gel): 1 lysate (1:50 diluted), 2 pellet (1:100 diluted), 3 supernatant (1:2 diluted), 4 IMAC flowthrough (1:2 diluted), 5 IMAC buffer A wash 1 (1:2 diluted), 6 IMAC ATP wash, 7 IMAC Elution 2/3 non centrifuged, 8 IMAC Elution 2/3 centrifuged, 9 PD10 1. Elution non centrifuged, 10 PD10 1. Elution centrifuged, 11 PD10 1. Elution centrifuged for CD (undiluted), 12 PD10 1. Elution centrifuged for CD (0.1mg/mL) (this sample was used for the CD measurement), 13 PD10 buffer for dilution of CD sample (this sample was used for the CD measurement), 14 PD10 2. Elution non centrifuged.

The order of substrate addition influences the reaction velocity

In 2012, Barney *et al.* (2012) published substrate specificity analyses of five bacterial WSD and reported an influence of the order of substrate addition on the reaction rate. The authors showed, that the reaction rate was reduced up to 95 % for all five analyzed proteins when the enzymes were pre-incubated with the acyl-CoA (fatty alcohol added to start the reaction), compared to when the enzyme was pre-incubated with the fatty alcohol (acyl-CoA added to start the reaction). AbWSD1 and MaWSD1, which were both included into this study, showed the largest differences in reaction rates between pre-incubation with acyl-CoA and pre-incubation with fatty alcohol (AbWSD1: reduction of the reaction to 5 % for pre-incubation with acyl-CoA; MaWSD1: reduction to 12 %).

Using 16:1 CoA and 18:1 OH as substrates for AbWSD1, similar results were obtained here (Figure 3.11). The highest activity was observed when AbWSD1 was pre-incubated with fatty alcohol and acyl-CoA was added to start the reaction. When the fatty alcohol was added last, the reaction rate was reduced to 22 % (Table 3.1). Adding the enzyme last resulted in a reaction rate between the two others, with the rate being reduced to 36 % (Table 3.1).

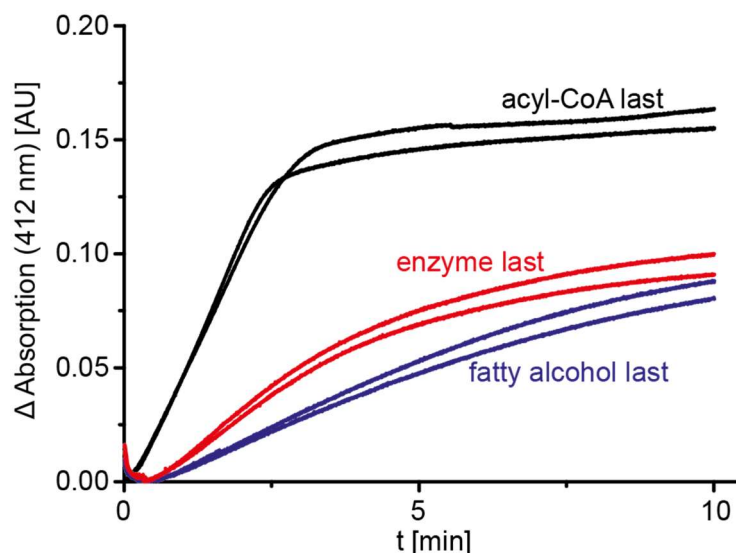


Figure 3.11. Test of enzymatic activity based on the order of substrate addition.

The WS activity of purified AbWSD1 WT was analyzed by a 5,5'-dithiobis-(2-nitrobenzoic acid) (DTNB)-based enzymatic activity assay as described by Barney *et al.* (2012). Each reaction mix consisted of reaction buffer supplemented with 16:1 CoA (10.6 μM), 18:1 OH (20 μM), 1 μg purified enzyme and DTNB (0.2 mg/mL). All reaction components except one were mixed and pre-incubated before the reaction was started by adding the missing component (acyl-CoA: black line, fatty alcohol: blue line, enzyme: red line). The reaction was monitored with a photometer by recording the change of absorption at 412 nm. The experiment was performed once by recording each reaction two times (two lines per condition).

Table 3.1. Dependency of specific WS activity on the order of substrate addition.

Specific activities were calculated from the WS activity measurements depicted in Figure 3.11, using a molar extinction coefficient of DTNB of $14150 \text{ M}^{-1}\text{cm}^{-1}$ (Barney *et al.*, 2012). The listed specific WS activities are mean values of two measurements performed with AbWSD1 obtained from one purification. Relative specific WS activities were calculated by setting the WS activity when acyl-CoA was added last to 1.

Substance added last	Specific WS activity [(nmol product) (mg protein) ⁻¹ min ⁻¹] (mean of two measurements)	Ratio of specific WS activity (Specific WS activity divided by the specific WS activity when acyl-CoA was added last)
Acyl-CoA (pre-incubation with fatty alcohol and enzyme)	3997	1.00
Fatty alcohol (pre-incubation with acyl-CoA and enzyme)	861	0.22
Enzyme (pre-incubation with acyl-CoA and fatty alcohol)	1429	0.36

Methods part for additional AbWSD1 part

CD spectroscopy

AbWSD1 and the variants were purified via gravity flow IMAC (see section 3.1 Article II). Combined elution fractions 2 and 3 were centrifuged (10000 *g*, 10 min, 4 °C) to remove precipitated protein. The supernatant was applied to a PD-10 Desalting Column (GE Healthcare) for buffer exchange. By sticking to the manufacture's manual using the gravity protocol, the sample buffer was exchanged to a CD compatible desalting buffer (10 mM sodium phosphate buffer pH 7.4, 150 mM NaF, 10 mM OGP). The eluted protein fraction was centrifuged (10000 *g*, 10 min, 4 °C) to remove precipitated protein. Protein concentration was determined in solution by recording the absorbance at 280 nm and the sample was diluted to a final protein concentration of 0.1 mg/mL. Shortly before the CD measurement, exact protein concentration of the diluted protein sample was determined again by recording absorbance at 280 nm. The CD spectra were recorded on a Chirascan CD spectrometer (Applied Photophysics, Surrey, United Kingdom) using a wavelength range from 185 nm to 260 nm, a step size of 1 nm, an accumulation time per step of 1 s and a 1 mm cuvette. For each protein variant 20-40 measurements were recorded (AbWSD1 WT: 20 measurements, AbWSD1-V139W-I303W: 30 measurements, AbWSD1-V23W-G24W: 30 measurements, AbWSD1-V350W-V372W: 40 measurements) as well as 10 measurements for the corresponding buffer samples. For background subtraction, averaged buffer measurements were subtracted from the corresponding averaged protein measurements. The concentration of AbWSD1-V139W-I303W used for the calculation of the CD spectrum was recalculated as described in the following whereas the measured concentration of AbWSD1 WT was considered as correct (measured concentrations: AbWSD1 WT: 0.0897 mg/mL, AbWSD1-V139W-I303W: 0.1325 mg/mL). Using ImageJ 1.50i (Schneider *et al.*, 2012), the spot intensities of the samples, that were used for the CD measurement (AbWSD1 WT lane 11 (Figure 3.10e), AbWSD1-V139W-I303W lane 12 (Figure 3.10f) were determined on each SDS-PAGE picture as well as the spot intensities of the 29 kDa band of the molecular weight marker on the same gel. Afterwards, the relative protein spot intensity of each enzyme variant was calculated (protein spot intensity / 29 kDa spot intensity; AbWSD1 WT: 1.1544; AbWSD1-V139W-I303W: 0.5682). The calculated value for AbWSD1 WT was correlated to its measured protein concentration and by this the concentration of AbWSD1-V139W-I303W was recalculated to 0.0441 mg/mL ([relative spot intensity AbWSD1-V139W-I303W] * [0.0897 mg/mL] / [relative spot intensity AbWSD1 WT]).

TLC-based enzymatic activity assay

The assay was performed with purified protein as described in the section 3.1 of Article II. As purified protein either combined elution fractions 2 and 3 of gravity flow purified enzymes were used or further PD-10 desalted protein samples. The assay was set up with 20 μ L protein solution (the used protein amounts of purified enzyme are stated in the figure caption of the corresponding experiment) or 20 μ L buffer for control samples in a total volume of 1 mL enzymatic activity reaction buffer.

DTNB-based enzymatic activity assay

The DTNB-based enzymatic activity assay was performed according to Barney *et al.* (2012) with modifications described by Vollheyde *et al.* (2020). If not stated differently, fatty alcohol and acyl-CoA were purchased from Sigma. The assay was performed with gravity flow IMAC purified protein (elution fraction 3), described in section 3.1 of Article II, stored overnight on ice at 4 °C.

The reactions were set up with 20 μ M 18:1 OH (20 μ L of 1 mM stock solution in DMSO) and 12.5 μ L 16:1 CoA (stock: 0.85 mM in 20 mM phosphate buffer pH 7.34) and 10 μ L of a 0.1 μ g/ μ L protein solution. Except for one component (either fatty alcohol, acyl-CoA or the enzyme), all other were added to the cuvette. The reaction was started by adding the missing component and mixing the reaction mix vigorously by vortexing. WS activities were calculated via Lambert-Beer-Law with a DTNB extinction coefficient of 14150 $M^{-1}cm^{-1}$.

4 ARTICLE III

4.1 Plastidial localized wax ester biosynthesis results in the formation of shorter and more saturated wax esters

The manuscript is ready for submission.

Katharina Vollheyde cloned the constructs, generated and screened the transgenic *A. thaliana* plants. She performed the western blot analysis of the transgenic seeds. She prepared the seedlings for confocal microscopy and displayed the images. Katharina Vollheyde furthermore performed the GC-FID analysis and processed, analyzed, displayed and discussed the obtained data. She prepared the samples for the nanoESI-MS/MS measurement and processed, analyzed, displayed and discussed the obtained data. Katharina Vollheyde wrote the first draft of the manuscript.

Plastidial localized wax ester biosynthesis results in the formation of shorter and more saturated wax esters

Katharina Vollheyde¹, Ellen Hornung¹, Cornelia Herrfurth^{1,2}, Till Ischebeck^{1,3}, Ivo Feussner^{1,2,3*}

¹University of Goettingen, Albrecht-von-Haller-Institute for Plant Sciences, Department for Plant Biochemistry, D-37077 Goettingen, Germany

²University of Goettingen, Goettingen Center for Molecular Biosciences (GZMB), Service Unit for Metabolomics and Lipidomics, D-37077 Goettingen, Germany

³University of Goettingen, Goettingen Center for Molecular Biosciences (GZMB), Department for Plant Biochemistry, D-37077 Goettingen, Germany

* Corresponding author

ifeussn@uni-goettingen.de

Tel.: +49 (0)551 / 39-25743

Fax: +49 (0)551 / 39-25749

Running head: Plastidial localized wax ester biosynthesis

Keyword

Arabidopsis thaliana, fatty acid reductase, *Marinobacter aquaeolei*, metabolic engineering, wax ester, wax synthase

Summary

Wax esters (WE) are neutral lipids. They consist of a fatty alcohol that is esterified to a fatty acid. Dependent on chain length and desaturation degree of the acyl and alcohol moieties, WE have diverse physicochemical properties. Due to these properties, WE are requested in industry for instance as lubricants, coatings, in cosmetics and for the production of candles. Industrial WE are produced chemically from fossil fuel or plant derived triacylglycerol (TAG). As fossil fuel resources are finite, efforts for the synthesis of tailor-made WE in transgenic plants were made over the last years. Here we report the analysis of ten WE producing constructs in *Arabidopsis thaliana*. The constructs expressed different combinations of a fatty acid reductase (FAR) and two wax synthases/acyl-coenzyme A (CoA):diacylglycerol O-acyltransferases (WSD) namely WSD2 and WSD5 from the bacterium *Marinobacter aquaeolei*. In order to get access to different substrate pools, constructs with and without plastidial localization signals were generated. Expression was controlled either by seed specific promoters or by the ubiquitous 35S promoter. WE formation was observed with plastid and cytosol localized FAR and WSD, whose expression was driven by seed specific promoters. Plastidial localization of proteins was confirmed by confocal microscopy. Detailed WE analysis by gas chromatography coupled to flame ionization detection (GC-FID) and nano electrospray ionization coupled to tandem mass spectrometry (nanoESI-MS/MS) revealed the production of shorter and more saturated WE by plastidial localized WE biosynthesis compared to cytosolic WE synthesis. Hence, a shift of WE formation into seed plastids is a suitable approach for tailor-made WE production.

Introduction

WE are neutral lipids that consist of a fatty alcohol moiety esterified to a fatty acid. WE can have diverse physical and chemical properties, which are influenced by chain length and desaturation degree of incorporated alcohol and acyl moieties (Patel *et al.*, 2001). Dependent on their physicochemical properties, WE fulfill diverse functions in nature: As part of the plant cuticle, WE protect plants against UV radiation and desiccation (Post-Beittenmiller, 1996; Samuels *et al.*, 2008). They are part of the human skin and lead to the evaporation retarding

effect of the eye's tear film (Jacobsen *et al.*, 1985; Craig & Tomlinson, 1997; Rantamäki *et al.*, 2013). Some bacteria, as *Acinetobacter baylyi*, as well as the slow growing desert plant jojoba (*Simmondsia chinensis*) produce WE as energy storage molecules (Fixter *et al.*, 1986; Sturtevant *et al.*, 2020). Due to their diverse properties, there is a high demand for WE for industrial applications: WE are used for example in inks, as coatings, for the production of candles, in cosmetics and as lubricants (Rontani, 2010; Wei, 2012). In former times mostly obtained from sperm whale, WE are synthesized chemically from fossil fuel or plant derived TAG nowadays (Vanhercke *et al.*, 2013; Karmakar *et al.*, 2017). In addition, WE are also expensively extracted from *S. chinensis* seeds (Sturtevant *et al.*, 2020).

Due to finite sources of fossil fuel, attempts are made to synthesize WE sustainably in transgenic plants (Lardizabal *et al.*, 2000; Heilmann *et al.*, 2012; Aslan *et al.*, 2014; Aslan *et al.*, 2015a; Aslan *et al.*, 2015b; Iven *et al.*, 2016; Zhu *et al.*, 2016; Ivarson *et al.*, 2017; Ruiz-Lopez *et al.*, 2017; Yu *et al.*, 2018; Vollheyde *et al.*, 2020). As a prerequisite for tailor-made WE production, WE biosynthesis and its regulation screws for the production of specific WE species have to be understood in detail. Acyl carrier protein (ACP) or CoA activated fatty acids and fatty alcohols are the building blocks of WE. As fatty alcohols derive from acyl-CoA/ACP by the reduction of the carboxyl group catalyzed by FAR (Reiser & Somerville, 1997; Wahlen *et al.*, 2009; Hofvander *et al.*, 2011; Willis *et al.*, 2011), acyl-CoA/ACP availability is the bottleneck for enzyme catalyzed WE formation. In successive rounds of condensation, reduction and dehydration reactions acyl-ACP are synthesized in plastids from acetyl-CoA (Hölzl & Dörmann, 2019). Plastidial *de novo* fatty acid synthesis yields saturated and monounsaturated activated fatty acids of 16 and 18 carbon chain length (Hölzl & Dörmann, 2019). Mostly 16:0 (number carbon atoms:number double bonds) and 18:1 fatty acids are exported from plastids and enter as CoA derivatives the cytosolic acyl-CoA pool (Ohlrogge & Jaworski, 1997; Hölzl & Dörmann, 2019). Here they are modified further by desaturases or endoplasmic reticulum bound elongases (Hölzl & Dörmann, 2019).

Two enzymes catalyze the formation of WE: FAR and WS. FAR derived fatty alcohols are esterified with another acyl-CoA/ACP molecule by wax synthases (WS) to yield WE (Lardizabal *et al.*, 2000; Samuels *et al.*, 2008). WS belong to the class of acyltransferases and are distributed over the whole tree of life (Röttig & Steinbüchel, 2013a). Dependent on the evolutionary origin, WS are classified into three major groups (Röttig & Steinbüchel, 2013a): WS similar to acyl-CoA:diacylglycerol O-acyltransferase (DGAT) 1 are enzymes with six to nine transmembrane domains. DGAT2-like WS have one to two transmembrane domains at their N-terminus. The third class of WS consists of bifunctional WS/DGAT (WSD) enzymes (Kalscheuer & Steinbüchel, 2003). The term bifunctional results from the ability of some WSD to not only catalyze the formation of WE, but also the synthesis of TAG from diacylglycerol and

acyl-CoA/ACP (Kalscheuer & Steinbüchel, 2003; Daniel *et al.*, 2004; Holtzapfle & Schmidt-Dannert, 2007; Kalscheuer *et al.*, 2007; Lázaro *et al.*, 2017; Zhang *et al.*, 2017). First identified in bacteria, WSD proteins have been also found in plants (King *et al.*, 2007; Li *et al.*, 2008; Shalini & Martin, 2020).

In order to produce WE in crop plants, WS and FAR enzymes need to be expressed in chosen organisms. Which and how much WE are synthesized by the expressed enzyme combination is dependent on the activities and substrate specificities of FAR and WS proteins as well as the availability of acyl-CoA/ACP. Until now, several combinations of FAR and WS enzymes have been expressed in *A. thaliana*, *Camelina sativa*, *Crambe abyssinica*, *Brassica carinata*, *Lepidium campestre* and *Nicotiana benthamiana* plants (Lardizabal *et al.*, 2000; Heilmann *et al.*, 2012; Aslan *et al.*, 2014; Aslan *et al.*, 2015a; Aslan *et al.*, 2015b; Iven *et al.*, 2016; Zhu *et al.*, 2016; Ivarson *et al.*, 2017; Ruiz-Lopez *et al.*, 2017; Yu *et al.*, 2018; Vollheyde *et al.*, 2020). When introducing WE production into plants, researchers aim for as high WE amounts as possible and production of mainly certain WE species that are requested for special applications. Especially monounsaturated long chain WE are desired in industry due to excellent lubrication properties (Heilmann *et al.*, 2012). High WE amounts of 89 to 108 mg/g seed were obtained by expressing a FAR from the bacterium *M. aquaeolei* (MaFAR) and a WS from *S. chinensis* (ScWS) in *A. thaliana* seeds (Iven *et al.*, 2016). Different enzyme combinations expressed resulted in diverse WE that were synthesized. Expression of mouse FAR and mouse WS for instance resulted in the formation of WE with mainly polyunsaturated 18 carbon acyl moieties (Heilmann *et al.*, 2012; Iven *et al.*, 2016). In contrast to that, enzyme combinations with MaFAR and ScWS, WSD1 from *A. baylyi* (AbWSD1) or WSD5 from *M. aquaeolei* (MaWSD5) produced WE mainly from monounsaturated 18 and 20 carbon acyl and alcohol moieties (Iven *et al.*, 2016; Yu *et al.*, 2018; Vollheyde *et al.*, 2020). A major influence on which WE species are produced however was found to have not the expressed enzymes, but which substrates are available for WE biosynthesis. An expression of different WE producing enzymes in a *fad2 fae1* mutant with highly decreased fatty acid biosynthesis beyond 18 carbons chain length and polyunsaturated fatty acids in seeds (Kunst *et al.*, 1992; Okuley *et al.*, 1994) resulted in more than 60 mol % 18:1/18:1 (alcohol moiety / acyl moiety) WE (Heilmann *et al.*, 2012; Iven *et al.*, 2016; Yu *et al.*, 2018). Expressing fatty acid elongases in combination with WE producing enzymes resulted in the synthesis of longer WE in *B. carinata*, *C. sativa* and *L. campestre* (Zhu *et al.*, 2016; Ivarson *et al.*, 2017). In contrast to that, shorter WE were generated in *C. sativa* upon co-expression of a 14:0 ACP thioesterase (Ruiz-Lopez *et al.*, 2017).

Substrate availability cannot only be changed by influencing, which substrates are synthesized, but also by changing the localization of WE biosynthesis to different cellular

compartments with diverse substrate pools. Here we analyzed, whether a change in WE biosynthesis to plastids has an influence on produced WE species. As plastids are the compartments of *de novo* fatty acid synthesis, mid and long chain saturated as well as monounsaturated acyl-ACP are present there. Similar to the recently published analysis of MaFAR/MaWSD5 plants (Vollheyde *et al.*, 2020), transgenic *A. thaliana* plants were generated expressing different combinations of MaFAR, MaWSD2 and MaWSD5 from the bacterium *M. aquaeolei*. Some constructs contained a plastidial target signal to direct WE biosynthesis to plastids. The analysis of generated transgenic plants allowed not only a direct comparison of substrate specificities of MaWSD2 and MaWSD5, but also a comparison of produced WE species and overall WE amount, when WE biosynthesis is directed either to plastids or to the cytosol.

Results

Generation of transgenic *A. thaliana* plants expressing combinations of MaFAR, MaWSD2 and MaWSD5

In order to analyze the influence of WE producing enzymes and their localization on WE species and overall WE amount, transgenic *A. thaliana* plants expressing WE producing enzymes were generated. Only recently, we published the generation and analysis of transgenic *A. thaliana* plants expressing *M. aquaeolei* MaFAR and MaWSD5 under seed specific promoters (Vollheyde *et al.*, 2020). In accordance to this, nine other constructs were generated consisting of combinations of MaFAR (Wahlen *et al.*, 2009; Hofvander *et al.*, 2011), MaWSD5 (Knutson *et al.*, 2017; Vollheyde *et al.*, 2020) and MaWSD2 (Barney *et al.*, 2012; Villa *et al.*, 2014; Vollheyde *et al.*, 2020), another WSD from *M. aquaeolei* that was used in another study of WE production in plants before (Yu *et al.*, 2018) (Figure 4.1).

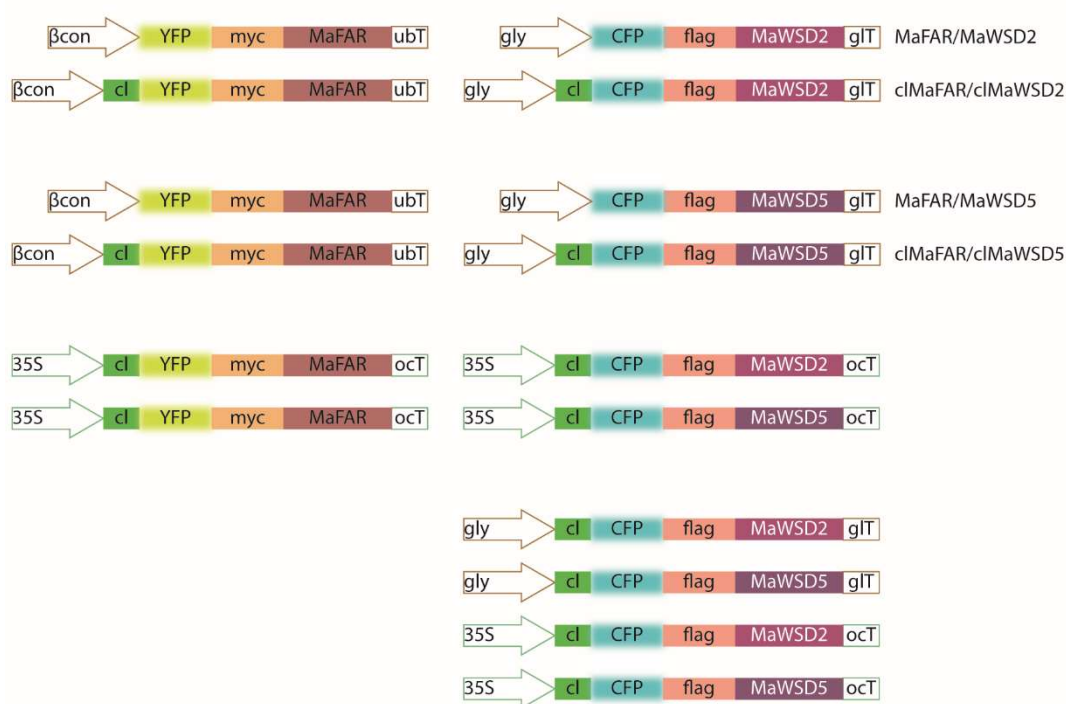


Figure 4.1. Constructs generated for *A. thaliana* transformation.

The MaFAR/MaWSD5 construct was published recently (Vollheyde *et al.*, 2020). βcon : β -conglycinin promoter (*Glycine max*), seed specific; gly: glycinin promoter (*G. max*), seed specific; 35S: 35S promoter, ubiquitous promoter; ubT: ubiquitin 3 terminator; glT: glycinin terminator; ocT: octopine synthase terminator.

Since it was shown before, that not only enzyme specificity but especially substrate availability influences which WE species are formed, several constructs were made harboring a plastidial tag to direct WE biosynthesis from the cytosol to plastids, the location of *de novo* fatty acid biosynthesis. For localization studies and western blot analyses, all constructs contain a fluorescent protein (either YFP or CFP) and an immunotag (either myc or flag tag). Similar to the published and analyzed MaFAR/MaWSD5 ($\beta\text{con}::\text{YFP-myc-MaFAR/gly}::\text{CFP-flag-MaWSD5}$) construct (Vollheyde *et al.*, 2020), a construct was created, expressing YFP- and myc-tagged MaFAR under the control of the seed specific β -conglycinin promoter and CFP- and flag-tagged MaWSD2 under the control of seed specific glycinin promoter ($\beta\text{con}::\text{YFP-myc-MaFAR/gly}::\text{CFP-flag-MaWSD2}$, from here on referred to as MaFAR/MaWSD2). Two additional constructs harbor the same enzyme combinations but with a 5' fusion of a plastidial localization sequence (Lee *et al.*, 2002) (cIMaFAR/cIMaWSD2, cIMaFAR/cIMaWSD5). Furthermore, two constructs were made aiming for an expression of plastidial constructs controlled by the 35S promoter (35S::cIMaFAR/35S::cIMaWSD2,

35S::cIMaFAR/35S::cIMaWSD5). To analyze the WE production when only a plastid-localized WSD is expressed, another four constructs were generated (gly::cIMaWSD2, gly::cIMaWSD5, 35S::cIMaWSD2, 35S::cIMaWSD5).

A. thaliana Col-0 plants were transformed with the generated constructs by floral dipping. A first and rapid screening for independent transgenic T1 plants was done by herbicide treatment with glufosinate. By this, 40 to 100 independent plants were obtained for each construct (Table 4.1). Despite of two transformation events and screening of a large number of seedlings, only 18 transgenic T1 plants were obtained for MaFAR/MaWSD2. For each construct, ca. 20 independent lines were screened for high WE content in T2 seeds by WE extraction and thin layer chromatography (TLC). For MaFAR/MaWSD5 ten new lines were screened in addition to the ones published by Vollheyde *et al.* (2020). In MaFAR/MaWSD2, cIMaFAR/cIMaWSD2, MaFAR/MaWSD5 and cIMaFAR/cIMaWSD5 plants, 50 % to 80 % of the screened lines showed WE formation in T2 seeds. No WE formation was detected in T2 seeds of lines expressing plastidial localized enzymes under the control of the 35S promoter or expressing the plastidial localized MaWSD2 or MaWSD5 alone. Since expression under the control of the 35S promoter should lead to expression of WE synthesizing enzymes in leaves, leaves of T1 plants, expressing the respective constructs were screened for WE formation as well. However, no WE were detected after WE extraction and subsequent TLC.

As significant WE amounts were obtained in T2 seeds of plants expressing the four constructs MaFAR/MaWSD2, cIMaFAR/cIMaWSD2, MaFAR/MaWSD5 and cIMaFAR/cIMaWSD5, three independent lines per construct with high WE levels were chosen for further analyses regarding protein expression, WE content and generated WE species (Table 4.1). For a comparison with results published for MaFAR/MaWSD5, three additional lines were analyzed in detail as the five already published ones were only analyzed by nanoESI-MS/MS (Vollheyde *et al.*, 2020).

MaFAR, MaWSD2 and MaWSD5 protein levels are different in seeds

Making use of their YFP-myc and CFP-flag tags, MaFAR, MaWSD2 and MaWSD5 protein levels were investigated by western blot analysis in protein extracts of MaFAR/MaWSD2, cIMaFAR/cIMaWSD2, MaFAR/MaWSD5 and cIMaFAR/cIMaWSD5 dry T2 seeds. A detection of MaFAR was achieved via an anti-myc IgG antibody and a detection of MaWSD2 as well as MaWSD5 was done via an anti-flag IgG antibody. In addition to that, anti-GFP IgG antibody was used for the detection of all three proteins via their YFP and CFP labels. MaFAR protein was detected in cIMaFAR/cIMaWSD2 and cIMaFAR/cIMaWSD5 constructs (Figure 4.2, Figure S4.1). Despite a weak signal in MaFAR/MaWSD5 line 17, no MaFAR protein was detected in MaFAR/MaWSD2 and MaFAR/MaWSD5 seeds. A signal corresponding to MaWSD5 protein

was obtained in all MaFAR/MaWSD5 and cMaFAR/cMaWSD5 lines. In contrast to that, MaWSD2 protein was only detected in the cMaFAR/cMaWSD2 lines and as a weak signal in MaFAR/MaWSD2 line 17.

Table 4.1. Overview of generated and analyzed transgenic *A. thaliana* plants.

Construct expressed (short name) (β con/gly: seed specific promoters, 35S: 35S promoter)	Number of independent lines after herbicide treatment	Number of screened heterozygous lines by TLC (number of lines with increased WE amounts)	Plant lines used for further analysis ([†] western blot [‡] confocal microscopy [§] analysis of WE species and WE amounts by GC-FID and nanoESI-MS/MS)
β con::YFP-myc-MaFAR gly::CFP-flag-MaWSD2 (MaFAR/MaWSD2)	18	T2 seeds: 17 (9)	^{†§} Lines 2, 6, 17
β con::cl-YFP-myc-MaFAR gly::cl-CFP-flag-MaWSD2 (cMaFAR/cMaWSD2)	85	T2 seeds: 36 (22)	^{†§} Lines 11, 28, 35
β con::YFP-myc-MaFAR gly::CFP-flag-MaWSD5 (MaFAR/MaWSD5)	52	T2 seeds: 19 (16) [9 (6) lines screened for Vollheyde <i>et al.</i> (2020), 10 (10) additional lines screened for this publication]	^{†§} Lines 11, 12, 17 (lines 2, 4, 5, 7, 10 (Vollheyde <i>et al.</i> , 2020))
β con::cl-YFP-myc-MaFAR gly::cl-CFP-flag-MaWSD5 (cMaFAR/cMaWSD5)	43	T2 seeds: 18 (12)	^{†§} Lines 4, 12, 18
35S::cl-YFP-myc-MaFAR 35S::cl-CFP-flag-MaWSD2 (35S::cMaFAR/35S::cMaWSD2)	72	T2 seeds: 22 (0) T1 leaves: 5 (0)	[‡] Line 21
35S::cl-YFP-myc-MaFAR 35S::cl-CFP-flag-MaWSD5 (35S::cMaFAR/35S::cMaWSD5)	56	T2 seeds: 23 (0) T1 leaves: 9 (0)	[‡] Lines 18, 19, 23
gly::cl-CFP-flag-MaWSD2	100	T2 seeds: 21 (0)	
gly::cl-CFP-flag-MaWSD5	95	T2 seeds: 21 (0)	
35S::cl-CFP-flag-MaWSD2	50	T2 seeds: 12 (0) T1 leaves: 5 (0)	
35S::cl-CFP-flag-MaWSD5	91	T2 seeds: 21 (0) T1 leaves: 38 (0)	

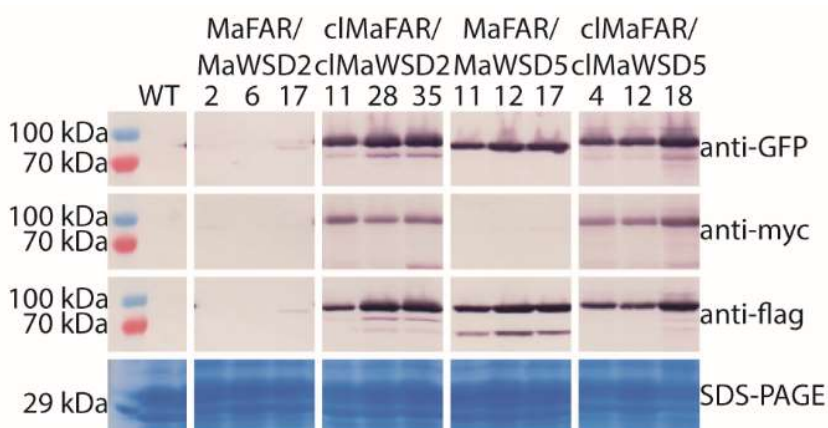


Figure 4.2. Western blot analysis of MaFAR/MaWSD2, cIMaFAR/cIMaWSD2, MaFAR/MaWSD5 and cIMaFAR/cIMaWSD5 seeds.

Equal amounts of total T2 seed protein extracts were loaded on SDS gels for western blot analyses and SDS-PAGE. Protein detection was achieved by anti-GFP, anti-myc and anti-flag IgG antibodies followed by the anti-Mouse IgG (whole molecule)—Alkaline Phosphatase. The SDS-PAGE gel, serving as loading control, was stained with coomassie. The experiment was performed once analyzing three independent plant lines per construct (MaFAR/MaWSD2: β con::YFP-myc-MaFAR/gly::CFP-flag-MaWSD2, cIMaFAR/cIMaWSD2: β con::cl-YFP-myc-MaFAR/gly::cl-CFP-flag-MaWSD2, MaFAR/MaWSD5: β con::YFP-myc-MaFAR/gly::CFP-flag-MaWSD5, cIMaFAR/cIMaWSD5: β con::cl-YFP-myc-MaFAR/gly::cl-CFP-flag-MaWSD5). For images of whole membranes and gel, see Figure S4.1.

WE producing enzymes can be targeted to plastids

In some constructs, MaFAR, MaWSD2 and MaWSD5 are expressed with a transit peptide with the aim to localize the WE producing enzymes to plastids. To examine, whether plastidial localization of the proteins is successful with the used transit peptide, 35S::cIMaFAR/35S::cIMaWSD2 and 35S::cIMaFAR/35S::cIMaWSD5 T2 seedlings were analyzed by confocal microscopy. In green tissue, plastidial localization can be confirmed by fluorescence overlay with chlorophyll autofluorescence. Besides a variety of WT seedlings obtained by segregation of heterozygous T1 mother plants showing no fluorescence, several seedlings were found with only YFP fluorescence. Whereas for 35S::cIMaFAR/35S::cIMaWSD5 seedlings with both fluorescence signals were found, no CFP fluorescence signal was detected in 35S::cIMaFAR/35S::cIMaWSD2 seedlings analyzed by confocal microscopy. Figure 4.3 depicts that CFP and YFP fluorescence overlay with chlorophyll autofluorescence, confirming plastidial localization of the expressed cIMaFAR and cIMaWSD5. Interestingly, CFP and YFP fluorescence sometimes overlays with chlorophyll autofluorescence of smaller plastids and not with the one of large chloroplasts. It is striking, that expressed cIMaFAR and cIMaWSD5 localize to subdomains within plastids. When CFP

and YFP fluorescence was detected, both signals hinted to a co-localization of the expressed enzymes at these subdomains.

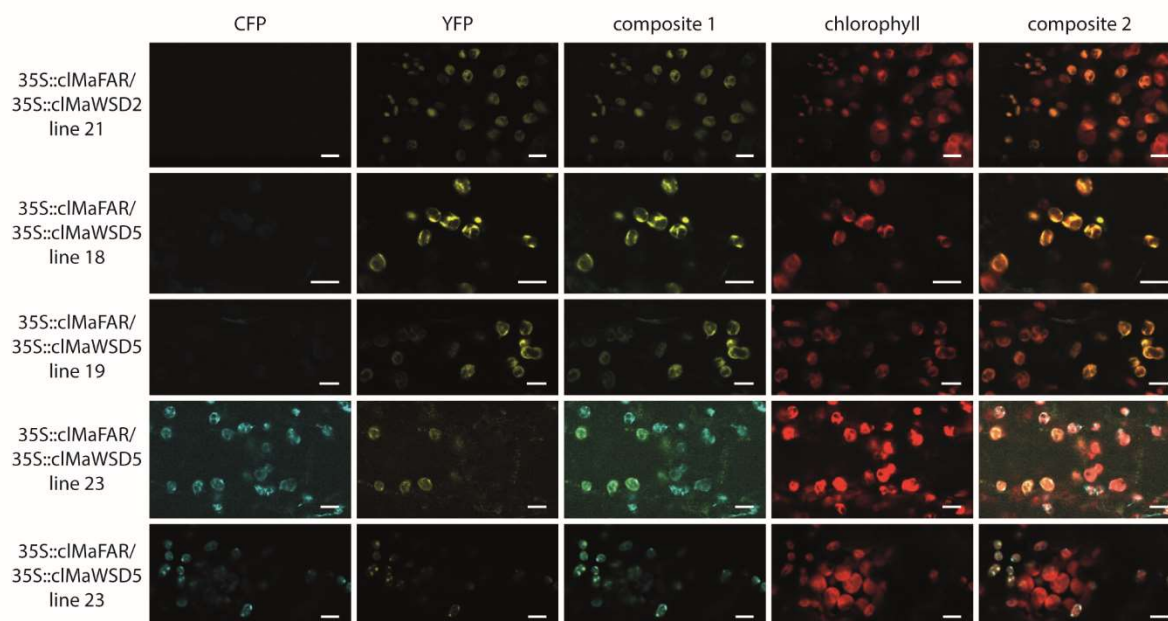


Figure 4.3. Localization studies of WE producing enzymes in seedlings using confocal microscopy.

Pictures were taken from transgenic 35S::cIMaFAR/35S::cIMaWSD2 (35S::cl-YFP-myc-MaFAR/35S::cl-CFP-flag-MaWSD2) and 35S::cIMaFAR/35S::cIMaWSD5 (35S::cl-YFP-myc-MaFAR/35S::cl-CFP-flag-MaWSD5) T2 seedlings. Pictures were processed with Image J 1.50i (Schneider *et al.*, 2012). The scale bar represents 6 μm .

Plastidial WE synthesis leads to a shift in WE length and degree of desaturation

In order to determine how much and which WE species are generated by the four constructs MaFAR/MaWSD2, cIMaFAR/cIMaWSD2, MaFAR/MaWSD5 and cIMaFAR/cIMaWSD5, T2 seeds were analyzed by GC-FID and nanoESI-MS/MS. Neutral lipid extraction from T2 seeds followed by separation of WE and TAG by TLC and subsequent analysis of both neutral lipids by GC-FID, revealed WE contents between 12 and 22 mg/g seed as well as TAG contents between 188 and 268 mg/g seed (Figure 4.4, Figure S4.2). For both analyzed enzyme combinations, the shift of WE biosynthesis to plastids did not result in significantly reduced WE amounts. However, a tendency towards lower levels upon plastidial WE biosynthesis was observed. Seeds expressing cIMaFAR/cIMaWSD2 contained ~50 % less WE than MaFAR/MaWSD2 seeds. In cIMaFAR/cIMaWSD5 seeds, the WE content was only ~60 % of the WE amount of MaFAR/MaWSD5 seeds (Figure 4.4a). No significant difference in TAG content was observed in seeds between the constructs (Figure 4.4b). However, MaFAR/MaWSD5 TAG content was slightly reduced compared to seeds expressing MaWSD2.

And in cIMaFAR/cIMaWSD5 seeds, the TAG content was reduced even more. Figure 4.4c shows, that MaFAR/MaWSD2 seeds contained on average 8 % WE, which was even higher in an individual line (Figure S4.2c). In cIMaFAR/cIMaWSD2 lines, the percentage of WE was 4 %. Due to accompanied changes in total TAG amount, WE content in MaFAR/MaWSD5 and cIMaFAR/cIMaWSD5 seeds accounted to 7 %.

In order to investigate whether plastidial localization of WE producing enzymes leads to changes in generated WE species, profiles of WE forming fatty acids and fatty alcohols were analyzed by GC-FID as well (Figure 4.5, Figure S4.3). The acyl moiety profile displays only small differences between MaFAR/MaWSD2 and MaFAR/MaWSD5. Both enzyme combinations led to WE formed mostly from 20:1 (n-9), 18:1 (n-9), 18:2 (n-6) and 16:0 fatty acids (Figure 4.5a). For MaFAR/MaWSD5 significantly higher content of 16:0 was detected.

Comparing MaFAR/MaWSD2 and cIMaFAR/cIMaWSD2, a plastidial WE biosynthesis led to a significantly reduced incorporation of 18:1 (n-9) accompanied with a higher content of 18:0 and 16:0 acyl moieties (Figure 4.5a). Although not significantly, a trend towards the reduction of WE with 20:1 (n-9) and 18:2 (n-6) acyl moieties was observed as well. Comparing MaFAR/MaWSD5 and cIMaFAR/cIMaWSD5, a reduced content of 20:1 (n-9) acyl moieties in the plastidial constructs was observed as well as a slight reduction in 16:0 even though these differences were not significant. This was accompanied with an increase in 18:0 and 18:1 (n-9) as well as a significant higher content of 18:1 (n-7) acyl moieties.

The summed up overall chain length and desaturation degree status of acyl moieties reflected the above mentioned trends: For both plastidial constructs a decrease in 20 carbon acyl moieties compared to the corresponding non-plastidial constructs was detected, although this decrease was not significant. Whereas the decrease in 20 carbon chain length species resulted mainly in a significant increase in 16 carbon acyl moieties for cIMaFAR/cIMaWSD2, acyl moieties with 18 carbon chain length increased in cIMaFAR/cIMaWSD5 seed WE (Figure 4.5c). The number of double bonds present in acyl moieties did not differ between MaFAR/MaWSD5 and cIMaFAR/cIMaWSD5. In contrast to that, a clear trend towards the incorporation of saturated acyl moieties was observed for cIMaFAR/cIMaWSD2 compared to the corresponding non-plastidial construct. While monounsaturated acyl species were favored by the non-plastidial construct, saturated and monounsaturated acyl moieties were equally distributed in cIMaFAR/cIMaWSD2.

Figure 4.5b displays the alcohol moiety profiles of extracted WE. No differences were observed between MaFAR/MaWSD2 and MaFAR/MaWSD5. In both enzyme combinations 20:1 (n-9) and 18:1 (n-9) were the preferred alcohol species incorporated into WE. Comparing the alcohol profiles of plastidial and corresponding non-plastidial constructs, a clear decrease in 20:1 (n-

9) alcohol species to almost half of the content was observed, as well as a decrease in 18:1 (n-9). This was accompanied with a large increase in 18:0 alcohol moiety as well as a slight, although not significant, increase in 16:0 in both plastidial constructs. Interestingly, in cIMaFAR/cIMaWSD2 the 18:0 alcohol moiety content was significantly more than in cIMaFAR/cIMaWSD5.

Figure 4.5d shows the summed up overall chain length and desaturation degree preference for alcohol moieties of WE in the analyzed constructs. Whereas alcohol moieties with 20 carbons chain length were preferred over 18 carbons chain length alcohols in non-plastidial constructs, the incorporation of fatty alcohols with 18 carbons chain length was preferred in plastidial constructs. A slight, although not significant, increase in 16 carbon alcohol species was observed in the same combinations as well in comparison to the corresponding non-plastidial constructs. A large shift occurred in the number of double bonds. MaFAR/MaWSD2 and MaFAR/MaWSD5 preferred monounsaturated alcohol moieties with ~70 mol %. In both plastidial enzyme combinations, the number of double bonds decreased significantly in alcohol moieties. In cIMaFAR/cIMaWSD5 saturated and monounsaturated species accounted to equal amounts of ~50 mol %. In cIMaFAR/cIMaWSD2, the content of saturated and monounsaturated alcohol moieties even inverted compared to MaFAR/MaWSD2 accounting for ~70 mol % saturated moieties in the plastidial construct.

Acyl and alcohol moiety profiles obtained by GC-FID analysis give a summarized overview about the composition of acyl and alcohol species forming the whole WE pool. Information about single WE species synthesized cannot be obtained by this analysis. In order to examine which WE species are produced in the four constructs MaFAR/MaWSD2, cIMaFAR/cIMaWSD2, MaFAR/MaWSD5 and cIMaFAR/cIMaWSD5, WE of the three independent plant lines per construct were analyzed by nanoESI-MS/MS. This method allows a detection of 784 even chain molecular WE species (Iven *et al.*, 2013). Figure 4.6 displays the top 20 molecular WE species synthesized by the four analyzed enzyme combinations. As already observed in the GC-FID profiles, MaFAR/MaWSD2 and MaFAR/MaWSD5 seed WE have a similar composition. The top 20 WE species in both constructs were mostly the same, despite smaller differences in the ranking position. In both constructs, 20:1/18:1 and 20:1/20:1 WE species were the two most abundant WE species, which accounted to ~20 mol %. In cIMaFAR/cIMaWSD2 seeds more than 50 mol % of all WE species contained 18:0 alcohol moieties, which formed the six most abundant WE species. 18:0/18:0 and 18:0/16:0 were the two main WE species in cIMaFAR/cIMaWSD2 seeds, accounting to 30 mol %. cIMaFAR/cIMaWSD5 plants showed a rather equally distributed WE profile lacking two main WE species standing out as observed in the other constructs. Similar to but not as consistent as in cIMaFAR/cIMaWSD2 seeds, 18:0 alcohol moieties were preferred by

cIMaFAR/cIMaWSD5 accounting for ~30 mol %. 18:1 and 18:2 acyl moieties formed the two most abundant WE species in cIMaFAR/cIMaWSD5.

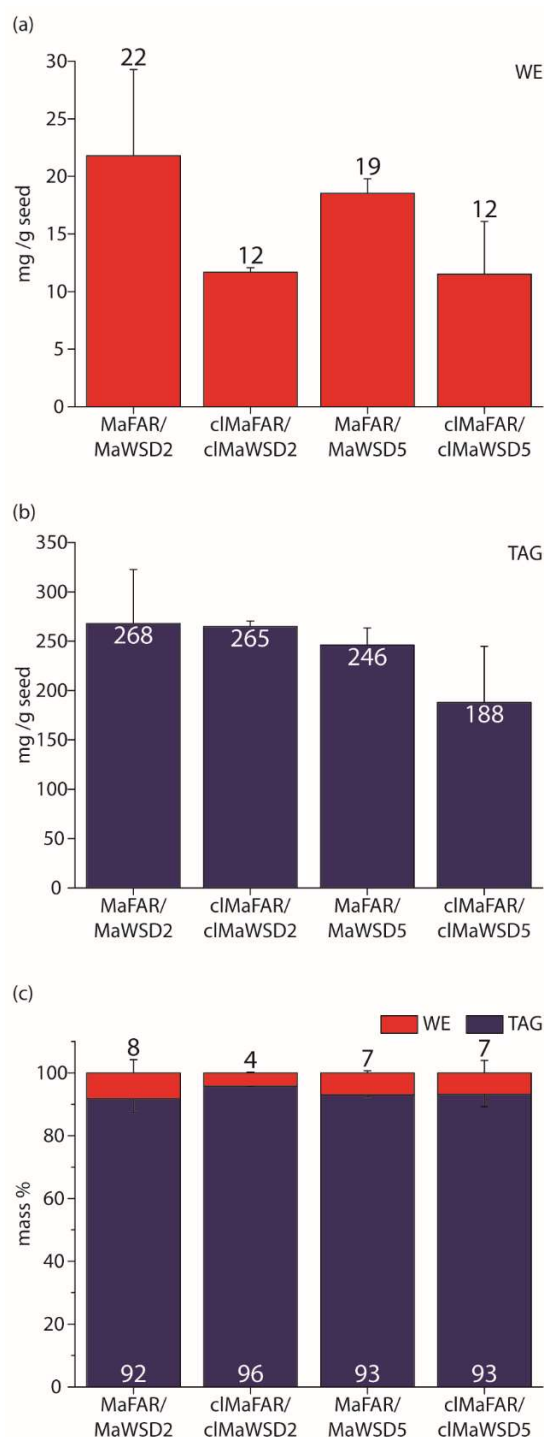


Figure 4.4. WE and TAG content of MaFAR/MaWSD2, cIMaFAR/cIMaWSD2, MaFAR/MaWSD5 and cIMaFAR/cIMaWSD5 seeds.

Absolute WE (a) and TAG (b) amounts in mg/g seed were obtained by GC-FID analysis. Both values were used to calculate their relative portion in mass % (c). Each bar represents the mean of three independent plant lines per construct determined in three extraction replicates (+SD). Analysis of variance (ANOVA) revealed no significant differences in absolute and relative WE and TAG contents between the constructs. For the data from each plant line, see Figure S4.2.

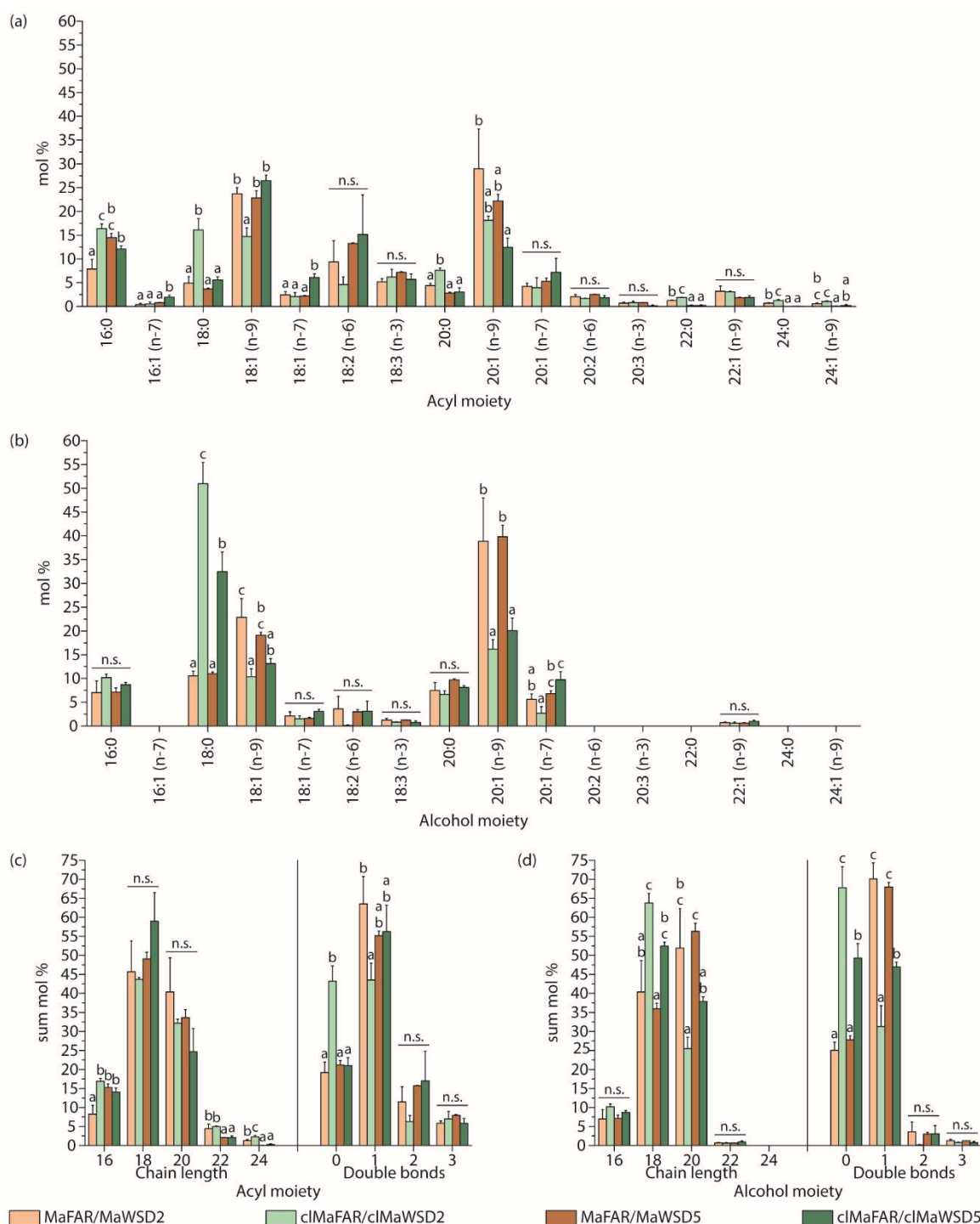


Figure 4.5. Acyl and alcohol moiety profiles of seed WE from MaFAR/MaWSD2, cIMaFAR/cIMaWSD2, MaFAR/MaWSD5 and cIMaFAR/cIMaWSD5.

Acyl (a) and alcohol (b) moiety profiles were obtained by GC-FID analysis. Displayed are relative abundances of WE moieties in mol %. Combined relative abundances of acyl (c) and alcohol (d) moieties with similar chain length or desaturation degree were attained by summing up relative abundances of respective moieties. Each bar represents the mean of three independent plant lines per construct determined in three extraction replicates (+SD). ANOVA analysis followed by *post-hoc* Tukey test was performed separately for each acyl and alcohol moiety as well as each chain length and double bond number (n.s.: not significant). For the data from each plant line, see Figure S4.3.

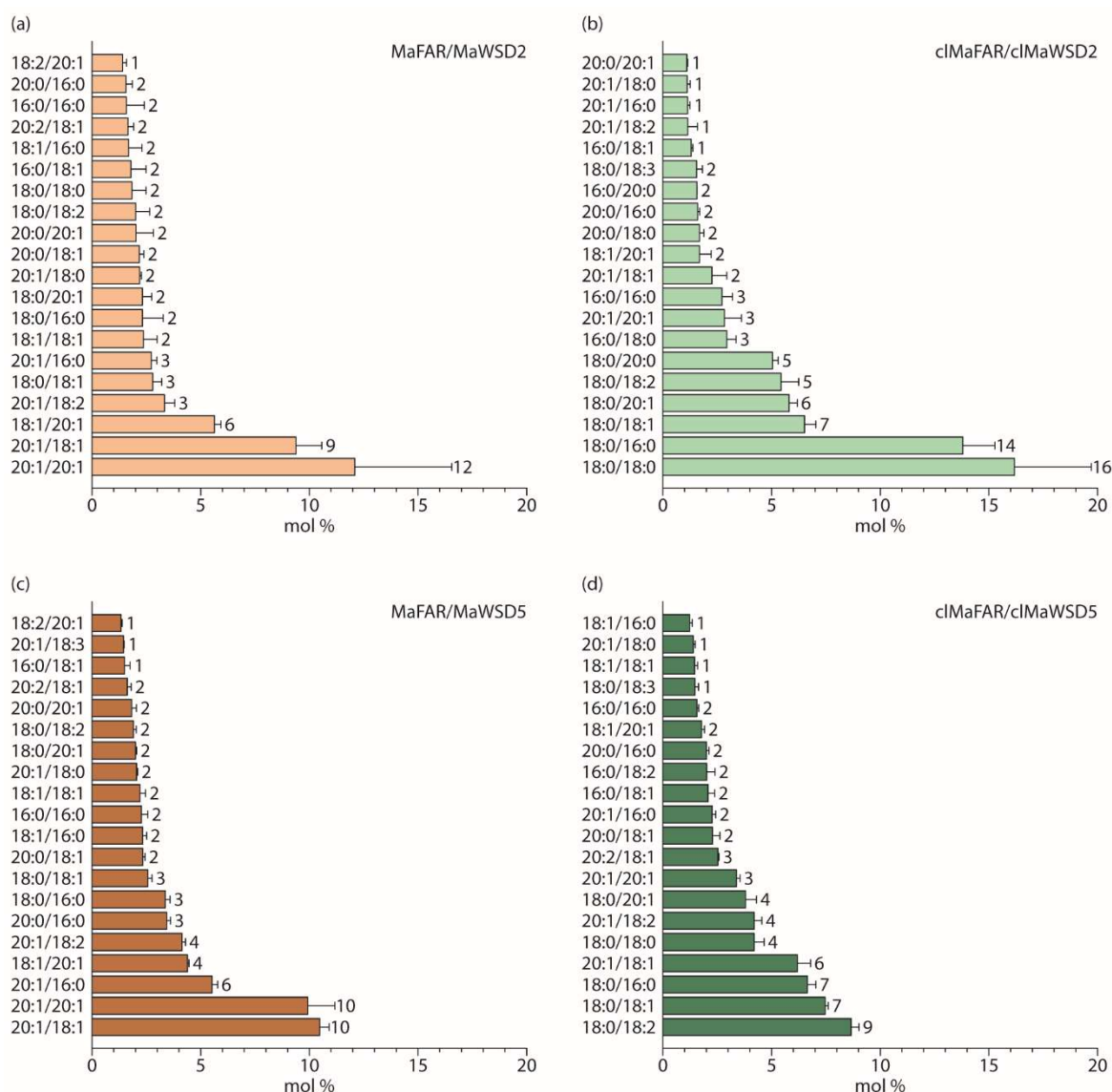


Figure 4.6. Analysis of seed WE species in MaFAR/MaWSD2, cIMaFAR/cIMaWSD2, MaFAR/MaWSD5 and cIMaFAR/cIMaWSD5.

Molecular WE species were analyzed by nanoESI-MS/MS in MaFAR/MaWSD2 (a), cIMaFAR/cIMaWSD2 (b), MaFAR/MaWSD5 (c) and cIMaFAR/cIMaWSD5 (d) T2 seeds. Displayed are relative abundances of the top 20 WE species (alcohol moiety/acid moiety) of each construct in mol %. Each bar represents the mean of three independent plant lines per construct determined in three measuring replicates (+SD).

Discussion

Here we report the analysis of transgenic WE producing *A. thaliana* plants. The ten studied constructs consisted of combinations of MaFAR, MaWSD2 and MaWSD5 from the bacterium *M. aquaeolei*. Besides different enzyme combinations, the influence of different promoters, as well as a shift of WE biosynthesis from the cytosol to the plastid was studied. We showed that the used plastidial signal peptide was sufficient to localize the expressed enzymes to plastids

(Figure 4.3). WE production was detected in plants expressing MaFAR and MaWSD combinations under the control of seed specific promoters with cytosolic and plastidial localized WE biosynthesis (Figure 4.4). Expression of plastidial localized enzymes under the control of the 35S promoter led neither to the detection of WE in seeds nor leaves. Similar results were observed for the expression of plastidial localized WSD alone. GC-FID and nanoESI-MS/MS analyses of MaFAR/MaWSD2, cMaFAR/cMaWSD2, MaFAR/MaWSD5 and cMaFAR/cMaWSD5 seeds revealed a shift towards shorter and more saturated WE species synthesized by plastidial localized enzymes (Figure 4.5 and 4.6).

Expressing MaFAR/MaWSD2, cMaFAR/cMaWSD2, MaFAR/MaWSD5 and cMaFAR/cMaWSD5 constructs under the control of seed specific promoters, seed WE amounts of 12 to 22 mg/g seed were obtained (Figure 4.4). This is consistent with WE amounts obtained with combinations of MaFAR and other bacterial WSD (Yu *et al.*, 2018). Yu *et al.* (2018) reached between 12 and 17 mg/g seed with constructs expressing MaFAR together with either PCOAbWSD1 (DNA sequence for first 20 amino acids plant codon optimized), TMMmAWAT2-AbWSD1 (60 amino acids N-terminal fusion of two transmembrane domains from mouse AWAT2 to AbWSD1) or MaWSD2 and 4 mg/g seed with a MaFAR/AbWSD1 construct.

Here it is shown, that seeds of transgenic MaFAR/MaWSD2 and MaFAR/MaWSD5 contained WE with equal amounts of 20:1 (n-9) and 18:1 (n-9) acyl moieties accounting for 20-25 mol % each, and to a bit lesser extent WE with 18:2 (n-6) and 16:0 acyl moieties, accounting for 10-15 mol % each (Figure 4.5). As fatty alcohol moiety, 20:1 (n-9) was favored by both enzyme combinations followed by 18:1 (n-9) (Figure 4.5). Yu *et al.* (2018) published acyl and alcohol profiles of seed WE produced by a MaFAR/MaWSD2 enzyme combination as well. In that study, MaFAR/MaWSD2 synthesized WE mainly from 18:0 fatty acids, followed by 18:1 fatty acids and from 18:1 fatty alcohols followed by 18:2 fatty alcohols. Whereas the here obtained results revealed WE are formed by MaFAR/MaWSD2 with almost equal contents of 18 and 20 carbon acyl moieties and a clear preference for monounsaturated acyl species, MaFAR/MaWSD2 from the study of Yu *et al.* (2018) favored saturated acyl moieties and almost exclusively produced WE with 18 carbon chain length. Differences can also be observed in the alcohol moieties. Here alcohol moieties of 18 and 20 carbon chain length were incorporated into WE by MaFAR/MaWSD2 to a nearly similar extent. Yu *et al.* (2018) observed a clear preference for 18 carbon fatty alcohols by the same enzyme combination. The preference for shorter substrates preferred by the MaFAR/MaWSD2 combination from Yu *et al.* (2018) compared to the here published MaFAR/MaWSD2 combination might be explained by different promoters that were chosen to regulate expression of the enzymes. Expression of MaFAR and MaWSD2 was controlled by the seed specific napin promoter in the publication of Yu *et al.*

(2018). Here, MaFAR expression was driven by the β -conglycinin promoter and MaWSD2 expression was regulated by the glycinin promoter. Although the β -conglycinin and the glycinin promoters are also seed specific promoters similar to the napin promoter, promoter activity during seed development might be different. Baud *et al.* (2002) showed that the fatty acid profile changes in developing *A. thaliana* seeds over time. Until torpedo stage, around 50 % of all seed fatty acids are 16:0 and 18:0 fatty acids. During proceeding seed development, the content of both fatty acids decreases and the amount of 18:3 and 20:1 fatty acids increases. This observation suggests that the napin promoter might be active during earlier time points in seed development when a higher content of saturated and shorter acyl substrates is present. The β -conglycinin and the glycinin promoter might promote protein expression during later time points in seed development when longer substrates, mainly 20:1 fatty acids are available. Another explanation for differences in WE acyl and alcohol moiety profiles of MaFAR/MaWSD2 constructs between this study and the work of Yu *et al.* (2018) might be the presence of N-terminal YFP-myc and CFP-flag fusions in the here analyzed constructs. They might have an influence on substrate specificities of the proteins. Yu *et al.* (2018) also observed differences in formed WE species by MaFAR/AbWSD1 and MaFAR/TMMmAWAT2-AbWSD1. In addition to that, differences in expression levels might be a third explanation, as Yu *et al.* (2018) obtained differences in WE acyl and alcohol profiles for MaFAR/AbWSD1 and MaFAR/PCOAbWSD1 as well, which only differ in the codon usage of the first 20 amino acids of AbWSD1.

WE species produced by MaFAR/MaWSD5 were analyzed recently (Vollheyde *et al.*, 2020). NanoESI-MS/MS results show, that cytosolic MaFAR/MaWSD2 and MaFAR/MaWSD5 formed similar WE species as published before (Figure 4.6). Upon localization of both enzyme combinations to plastids, altered WE profiles were obtained for both constructs compared to the corresponding non-plastidial constructs. Interestingly, differences in WE profiles were observed between cIMaFAR/cIMaWSD2 and cIMaFAR/cIMaWSD5. Whereas the cytosolic substrate pool provides acyl-CoA, which do not reveal differences in substrate specificities between MaWSD2 and MaWSD5, plastidial available substrates do so. As both constructs express the same FAR, substrate specificities of MaWSD2 and MaWSD5 can be compared directly. Plastidial expression revealed that MaWSD2 favors saturated substrates and 18 carbon chain length fatty alcohols, whereas MaWSD5 favors desaturated substrates under the tested conditions.

The here published study is not the first one analyzing plastidial WE biosynthesis, but the first one comparing WE biosynthesis in plastids directly with cytosolic biosynthesis catalyzed by the same enzyme combinations. In 2014, Aslan *et al.* (2014) published the investigation of WE biosynthesis by several WE-producing enzymes localized to chloroplasts in transiently

transformed *N. benthamiana* leaves. A fusion construct made out of a transit peptide, MaFAR and *Marinobacter hydrocarbonoclasticus* WS2 under the control of the 35S promoter showed reasonable WE formation in leaf chloroplasts. In 2015, the generation and analysis of stable transformed transgenic *N. benthamiana* plants expressing the same construct were published (Aslan *et al.*, 2015b). Transient and stable transformed leaves produced WE with similar acyl and alcohol moiety profiles, but WE amounts were markedly lower in stable transformed plants. The authors assumed a counter-selection for high expression of the construct during the regeneration process as surviving plants showed stunted growth and chlorotic leaves and stems. Here we observed no detectable WE formation in leaves and seeds, when expressing plastidial localized enzymes under the control of the 35S promoter. This observation might be explained by a counter-selection for high plastidial WE contents as well. As reasonable WE amounts were obtained in cIMaFAR/cIMaWSD2 and cIMaFAR/cIMaWSD5 seeds, high plastidial WE amounts might be more harmful in certain developmental stages than in others. Whereas plastidial WE might be tolerated during seed development, ubiquitous plastidial WE biosynthesis during seedling development might be detrimental. Seedling lethality of plants expressing enzymes under the control of the 35S promoter compared to plants expressing proteins under the control of seed specific promoters was not analyzed here. As screening for transgenic plants was performed through herbicide resistance, a detailed seedling lethality rate is hard to determine. A selection of plants expressing 35S constructs towards lower plastidial WE levels, would explain the difficulties to find seedlings for confocal microscopy expressing CFP and YFP tagged proteins in sufficient amounts for localization studies. Here a lot of seedlings expressed only one enzyme above the detection limit.

Although no significant differences in WE contents were obtained between the four constructs in this study, a trend towards lower WE amounts was observed when WE were synthesized in plastids compared to cytosolic WE formation (Figure 4.4). This might be either explained by the above-mentioned counter-selection towards plants with low plastidial WE levels or by insufficient storage capacities. The stroma volume can be calculated to account only to about 25 % of the cytosolic volume in an average C3 plant leaf for instance (Lawlor, 2001). The availability of acyl-ACP for WE synthesis might be another reason for lower WE amounts of seeds expressing plastidial constructs. Aslan *et al.* (2014) expressed the transcription factor AtWR11 in combination with FAR/WS constructs. This transcription factor is known to induce *de novo* fatty acid synthesis (Focks & Benning, 1998; Ma *et al.*, 2013). Although higher TAG levels were observed by Aslan *et al.* (2014), suggesting an increased fatty acid biosynthesis, increase in WE formation was only detected for one enzyme combination. It is conceivable that increased fatty acid biosynthesis levels lead to an increase in acyl-ACP export as well. If plastidial acyl-ACP levels actually remain stable, plastidial WE biosynthesis rates might be

difficult to increase without downregulating acyl-ACP export. Since plastidial synthesized fatty acids are building blocks for lipids outside of plastids, a total block of acyl-ACP export cannot be achieved.

WE were detected in all analyzed MaFAR/MaWSD2, cMaFAR/cMaWSD2, MaFAR/MaWSD5 and cMaFAR/cMaWSD5 seeds (Figure 4.4) although western blot analysis did not show in all plant lines detectable protein levels for MaFAR, MaWSD2 or MaWSD5 under our conditions (Figure 4.2). As western blot analysis was performed in dry seeds and WE formation takes place during seed development, differences in protein stability of the expressed enzymes have to be assumed. The detection of WE in all transgenic seeds strongly suggests the presence of all enzymes during seed development.

A demand for sustainable tailor-made WE production is increasing, as fossil fuel resource are finite. Here we report the analysis of transgenic *A. thaliana* plants expressing ten different enzyme combinations of the bacterial MaFAR, MaWSD2 and MaWSD5. A detailed lipid analysis revealed that a direction of WE formation towards plastids in seeds is possible. The availability of acyl-ACP with altered chain length and desaturation degree compared to acyl-CoA present in the cytosolic substrate pool, resulted in the production of shorter and more saturated WE in plastids compared to the cytosol. The here presented study shows, that a change in cellular localization of WE biosynthesis is a powerful tool to alter substrate availability for tailor-made WE production in plants.

Experimental procedures

Generation of transgenic *A. thaliana* plants

Transgenic *A. thaliana* plants were generated according to Vollheyde *et al.* (2020). Using Gateway technology (Thermo Fisher Scientific) binary transformation vectors were generated for simultaneous transformation of two enzymes as described before (Heilmann *et al.*, 2012).

Using fusion polymerase chain reaction, several constructs were generated from sequence combinations of *Escherichia coli* codon optimized MaFAR (Accession Number: WP_011785687.1), MaWSD2 (Accession Number: ABM20141.1), MaWSD5 (Accession Number: ABM20482.1), YFP, CFP, myc-tag, flag-tag and a plastidial localization sequence corresponding to an 80 amino acids signal peptide (Lee *et al.*, 2002). As fusion polymerase chain reaction was not successful for generating constructs containing MaWSD2, these constructs were made by classical cloning via an *ApaI* restriction site on the 5' end of the MaWSD2 sequence. Generated constructs were cloned into desired pENTRY vectors (pENTRYA carrying a 35S promoter, pENTRYB carrying a β -conglycinin promoter, pENTRYC

carrying a glycinin promoter, pENTRYD carrying a 35S promoter) via *Sall/Bam*HI restriction sites or *Xho*I/*Bgl*II restriction sites for MaWSD5 containing constructs. In total, nine pENTRY vectors were produced. By performing clonase reactions with the destination vector (pCAMBIA33) together with either a combination of pENTRYB, pENTRYC and an empty pENTRYA vector or with a combination of pENTRYA (empty one in case only a WSD was expressed) and pENTRYD vector, ten binary vectors were obtained. Primer sequences can be found in Table S4.1.

Screening of transgenic *A. thaliana* plants

Screening of transgenic *A. thaliana* plants by analysis of seed WE was performed as described previously (Vollheyde *et al.*, 2020).

For the screening of transgenic *A. thaliana* plants by leaf WE, three leaves were harvested per plant, pooled and lyophilized. For rapid screening, WE extraction was performed in 2 mL micro tubes. 500 μ L methanol were added to lyophilized leaf material and the samples were shaken for 20 min at 4 °C. Afterwards, 1 mL hexane was added to each sample and samples were shaken for 15 min at 4 °C. After centrifugation (5 min 11360 *g*), the upper hexane phase was transferred to a 1.5 mL micro tube. Subsequent to hexane evaporation in a Savant SPD131DDA SpeedVac Concentrator (Thermo Fisher Scientific) with a Savant RVT5105 Refrigerated Vapor Trap (Thermo Fisher Scientific), extracted lipids were dissolved in 50 μ L chloroform and spotted on a TLC silica plate (TLC Silica gel 60, 20 \times 20 cm, Merck Millipore). The TLC plate was developed with hexane/diethyl ether/acetic acid (90:10:1, *v/v/v*) as running solvent, which yielded best results in separating WE and carotenoids. Bands of neutral lipids were visualized by dipping the plate into a CuSO₄ solution (10 % (*w/v*) CuSO₄, 6.8 % (*v/v*) phosphoric acid) and subsequent heating of the plate to up to 190 °C.

Analysis of WE and TAG by GC-FID

Lipid extraction, sample preparation and GC-FID analysis of WE and TAG was performed as described previously (Iven *et al.*, 2016).

Analysis of WE species by nanoESI-MS/MS

The analysis of WE was performed by nanoESI-MS/MS with a 6500 QTRAP® tandem mass spectrometer (AB Sciex) as previously described (Iven *et al.*, 2013).

Western Blot

Proteins were extracted from frozen and homogenized seeds according to Poliner *et al.* (2018). To 4 mg seed material, 100 μ L freshly prepared extraction buffer (4 % (w/v) SDS, 2 % (v/v) β -mercaptoethanol, 2 mM phenylmethane sulfonyl fluoride, 0.1 M Tris pH 8.5) were added. Samples were immediately vigorously vortexed for at least 2 min. Afterwards, the samples were incubated at 80 °C for 3 min and centrifuged (10 min, 20810 g, room temperature). The supernatant was transferred to a new tube and was mixed with 4x Lämmli buffer. For SDS-PAGE and western blot analysis, 10 μ L of with 4x Lämmli buffer diluted protein extract was loaded on a SDS gel. For western blot analysis, proteins were detected using an anti-GFP epitope tag antibody (diluted 1:5,000, BioLegend), monoclonal anti-c-MYC antibody (1:5,000, Sigma) and monoclonal anti-FLAG M2 antibody (1:5,000, Merck) followed by the anti-Mouse IgG (whole molecule)—Alkaline Phosphatase (diluted 1:30,000, Merck). The SDS gel serving as loading control was stained with coomassie.

Microscopy

Seedlings were grown on MS agar plates containing 1 % (w/v) sucrose for 3 days under long day condition (16 h light, 8 h darkness, 22 °C) subsequent to 2-3 days of stratification.

Images were recorded using a Zeiss LSM 780 confocal microscope (Carl Zeiss Inc., Jena, Germany). eCFP was excited at 458 nm and detected at a wavelength of 462-520 nm imaged using a T80/R20 beam splitter, or at 463-510 nm using a MBS 458 beam splitter; eYFP was excited at 514 nm and detected at a wavelength of 523-622 nm imaged using a T80/R20 beam splitter, or at 515-551 nm using a MBS 458/514 beam splitter; chlorophyll was excited at 633 nm and detected at a wavelength of 647-722 nm imaged using a T80/R20 beam splitter, or at 647-721 nm using a MBS 488/561/633 beam splitter. Images of 35S::cIMaFAR/35S::cIMaWSD5 lines 18, 19 and 23 (upper image) were recorded with the settings described first. Images of 35S::cIMaFAR/35S::cIMaWSD2 line 21 and 35S::cIMaFAR/35S::cIMaWSD5 line 23 (lower image) were recorded using the settings described second. Pictures were processed with Image J 1.50i (Schneider *et al.*, 2012).

Accession numbers

MaFAR: Accession Number: WP_011785687.1

MaWSD2: Accession Number: ABM20141.1

MaWSD5: Accession Number: ABM20482.1

Author Contributions

KV generated and screened the transgenic plants, performed the GC-FID analysis and data evaluation, prepared the samples for nanoESI-MS/MS measurement, analyzed and evaluated the nanoESI-MS/MS data, performed the western blot analysis and drafted the manuscript. EH participated in cloning the constructs for plant transformation and analyzing the GC-FID data. CH measured WE species by nanoESI-MS/MS. TI recorded the confocal microscopy images. IF designed and supervised the study and edited the drafted manuscript. All authors approved and read the final manuscript.

Acknowledgements

The authors are grateful to Prof. Ed Cahoon for providing us with the seed-specific promoters from soybean and Maria Paulat, Andrea Nickel and Susanne Mester for excellent technical assistance. KV was supported by the GGNB Program Microbiology and Biochemistry. IF acknowledges funding through the German Research Foundation (DFG, INST 186/822-1).

Supporting information

Plastidial localized wax ester biosynthesis results in the formation of shorter and more saturated wax esters

Katharina Vollheyde¹, Ellen Hornung¹, Cornelia Herrfurth^{1,2}, Till Ischebeck^{1,3}, Ivo Feussner^{1,2,3*}

¹University of Goettingen, Albrecht-von-Haller-Institute for Plant Sciences, Department for Plant Biochemistry, D-37077 Goettingen, Germany

²University of Goettingen, Goettingen Center for Molecular Biosciences (GZMB), Service Unit for Metabolomics and Lipidomics, D-37077 Goettingen, Germany

³University of Goettingen, Goettingen Center for Molecular Biosciences (GZMB), Department for Plant Biochemistry, D-37077 Goettingen, Germany

Table S4.1. Primer sequences.

Primer Name	Primer Sequence (5' -> 3')
cl-for- <i>Sall</i>	ACT GTCGAC ATGGCTTCCTCTATGCTCTCTTC
YFP/CFP-for- <i>Sall</i>	ACT GTCGAC ATGGTGAGCAAGGGCGAGGAG
MaFAR-rev- <i>Bam</i> HI	G CGGATCCT CATGCCGCTTTTTTACG
MaWSD2-rev- <i>Bam</i> HI	G CGGATCCT TACTTGCGGGTTCGGGCGCGC
MaWSD2-for- <i>Apal</i>	AG CGGGCC CATGAAACGTCTCGGAACCCTGG
Flag-rev- <i>Apal</i>	AGT GGGCC CCTTATCGTCGTCATCCTTGTAATCC
cl-for- <i>Xho</i> I	ACT CTCGAG ATGGCTTCCTCTATGCTCTCTTC
CFP-for- <i>Xho</i> I	ACT CTCGAG ATGGTGAGCAAGGGCGAGGAG
MaWSD5-rev- <i>Bg</i> III	GC AGATCTT CAGTCCAGCTGATCCAGTTCCGC

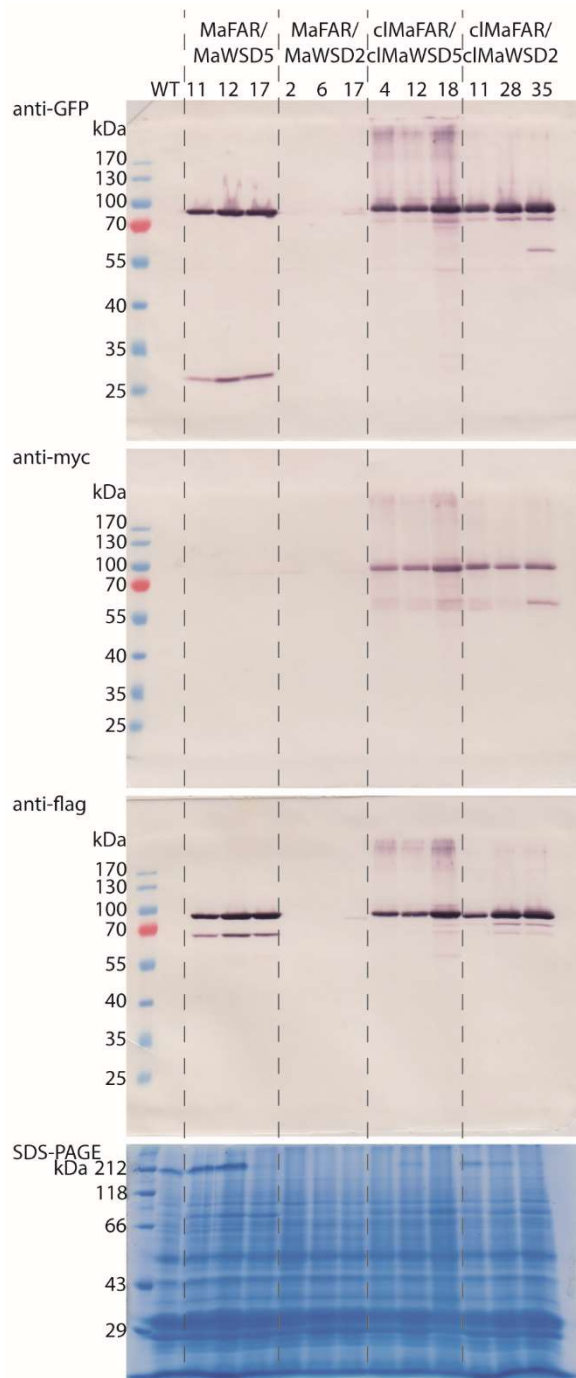


Figure S4.1. Western blot analyses of MaFAR/MaWSD2, cIMaFAR/cIMaWSD2, MaFAR/MaWSD5 and cIMaFAR/cIMaWSD5 seeds.

Equal amounts of total T2 seed protein extracts were loaded on SDS gels for western blot analyses and SDS-PAGE. Protein detection was achieved by anti-GFP, anti-myc and anti-flag IgG antibodies followed by the anti-Mouse IgG (whole molecule)—Alkaline Phosphatase. The SDS-PAGE gel, serving as loading control, was stained with coomassie. The experiment was performed once analyzing three independent plant lines per construct (MaFAR/MaWSD2: β con::YFP-myc-MaFAR/gly::CFP-flag-MaWSD2, cIMaFAR/cIMaWSD2: β con::cl-YFP-myc-MaFAR/gly::cl-CFP-flag-MaWSD2, MaFAR/MaWSD5: β con::YFP-myc-MaFAR/gly::CFP-flag-MaWSD5, cIMaFAR/cIMaWSD5: β con::cl-YFP-myc-MaFAR/gly::cl-CFP-flag-MaWSD5).

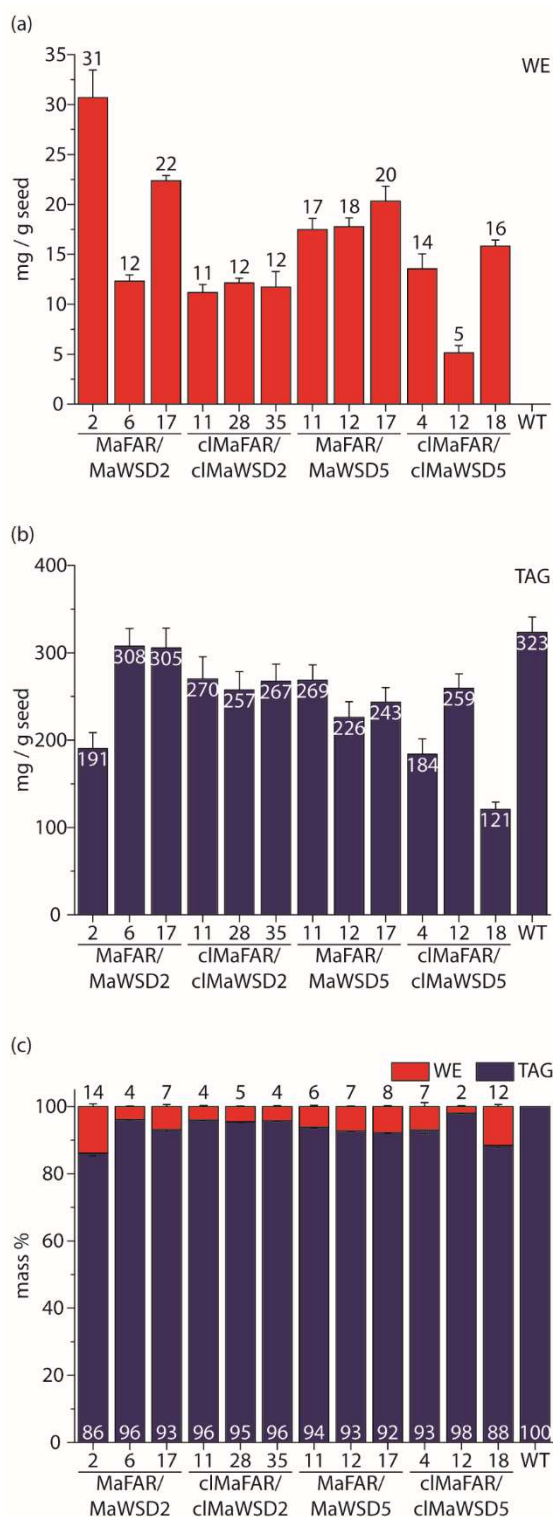


Figure S4.2. WE and TAG content of MaFAR/MaWSD2, cIMaFAR/cIMaWSD2, MaFAR/MaWSD5 and cIMaFAR/cIMaWSD5 seeds.

Absolute WE (a) and TAG (b) amounts in mg/g seed were obtained by GC-FID analysis. Both values were used to calculate their relative portion in mass % (c). Each bar represents the mean of three extraction replicates (+SD).

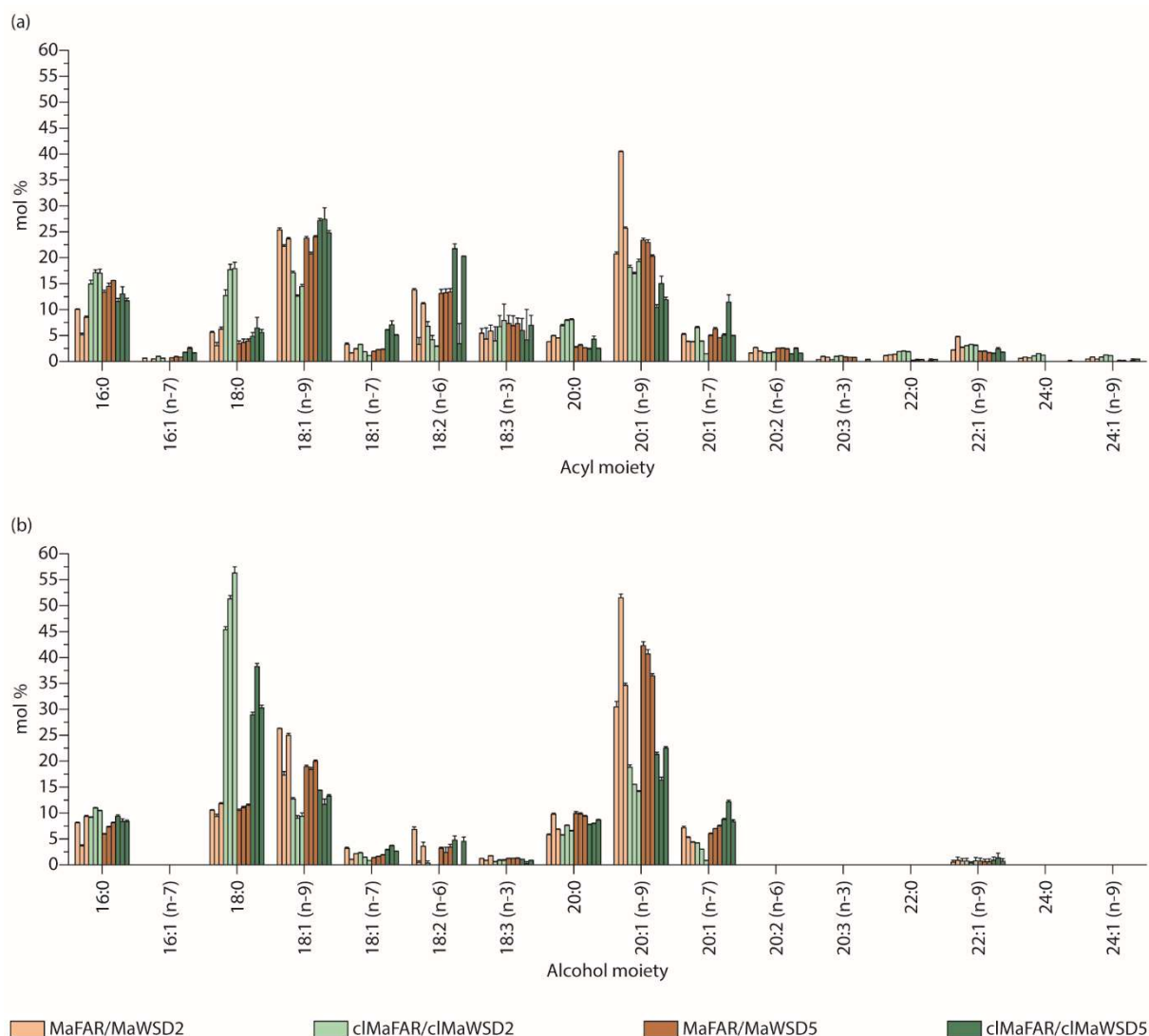


Figure S4.3. Acyl and alcohol moiety profiles of seed WE from MaFAR/MaWSD2, cIMaFAR/cIMaWSD2, MaFAR/MaWSD5 and cIMaFAR/cIMaWSD5.

Acyl (a) and alcohol (b) moiety profiles were obtained by GC-FID analysis. Displayed are relative abundances of WE moieties in mol % of three independent plant lines per construct. Each bar represents the mean of three extraction replicates (+SD).

5 DISCUSSION

5.1 Overview about results obtained in this work

WE are neutral lipids that have diverse physicochemical properties. They are found in nature fulfilling diverse functions such as protection and carbon storage. Furthermore, they are widely used in industry, e.g. as lubricants, in cosmetics or as coating agents. Within the last years, several studies have been published establishing tailor-made WE production for industrial applications in transgenic crop plants. Even though diverse approaches yielded increasing amounts of WE, it emerged, that further work regarding enzyme use, substrate availability and storage capacities is needed to optimize their production.

Goal of this thesis was to contribute solutions to further improve tailor-made WE biosynthesis in two of the three aspects: enzyme use and substrate availability. They were examined by three projects, whose results were combined in three manuscripts being either already published or ready for submission. The first project dealt with the characterization of MaWSD5 in order to study the potential of the enzyme for WE production. Within the second project, a structure-function analysis of AbWSD1 based on its crystal structure was conducted in order to broaden the knowledge about substrate binding sites and catalytic important residues in WSD enzymes. In the third project, the influence of cellular localization of WE biosynthesis on WE formation in transgenic plants was studied and established as a new tool to alter substrate availability.

Within the first project, whose results have been published in Article I, the newly identified fifth WSD of the bacterium *M. aquaeolei* was characterized biochemically. Experiments conducted within the scope of this thesis showed, that MaWSD5 has WS activity but lacks DGAT activity *in vitro*. A DTNB-based activity assay revealed a broad substrate range of the enzyme, accepting acyl-CoA from 6 to 20 carbon chain length, including 16:1 CoA and 18:1 CoA as well as fatty alcohols ranging from 6 carbon chain length to 16 carbon chain length and 16:1 OH and 18:1 OH. Expression of MaWSD5 in combination with MaFAR resulted in WE formation in transgenic *A. thaliana* seeds, producing WE mainly from long chain monoenoic substrates. The obtained results led to the conclusion that MaWSD5 is a promising candidate for transgenic WE biosynthesis consisting of long-chain monoenoic moieties *in planta*. Especially its monofunctionality is advantageous for industrial WE production, as catalyzed TAG formation of WSD is considered as an enzyme's resources wasting side reaction.

The second project, represented by Article II, dealt with the structure-function analysis of AbWSD1, which is the second WSD structure available but the first one with a bound fatty

acid. Based on the crystal structure and identified tunnels within the protein that are connected with the active site, amino acid substitutions were introduced around these cavities. Upon the analysis of the enzyme variants regarding changes in substrate specificities, a cavity involved in DAG binding was identified as well as three amino acids influencing the acyl-CoA specificity of AbWSD1. A detailed comparison of the AbWSD1 structure, containing a bound myristic acid, with the crystal structure of MaWSD1, published while working on this thesis, revealed a structural rearrangement upon substrate binding. Based on these findings it was possible to propose a structural rearrangement upon binding of acyl-CoA/ACP, amino acids involved in binding of the phosphopantetheine moiety and a substrate-binding model for WSD enzymes.

Within the scope of the third project compiled in Article III, the influence of the cellular localization of WE biosynthesis was studied as a new tool to alter substrate availability in WE producing plants. Different MaFAR/MaWSD2 and MaFAR/MaWSD5 constructs, with and without plastidial localization tag, were expressed in *A. thaliana* under the control of either seed specific promoters or the ubiquitous 35S promoter. The experiments conducted here are the first ones showing WE production in plastids of transgenic *A. thaliana* seeds and are the first ones performing a detailed and comprehensive comparison of cytosolic and plastidial WE biosynthesis on formed WE species and WE amounts. Upon plastidial WE biosynthesis a clear shift towards shorter and more saturated WE was observed compared to cytosolic WE biosynthesis. This shift was attributed to the higher availability of mid and long chain acyl substrates in plastids where *de novo* fatty acid synthesis takes place, compared to the cytosol, where acyl-CoA are elongated to very long chain acyl substrates. Interestingly, plastidial WE formation was only detected in seeds upon expression of WSD and FAR controlled by seed specific promoters and no significant WE synthesis was observed in either seeds or leaves, when WSD and FAR enzymes were expressed under the control of the 35S promoter. Furthermore, first localization studies revealed, that FAR and WSD tend to localize to small plastids instead of large plastids. Additionally, both enzymes were detected to co-localize to plastidial micro domains.

5.2 WS(D) catalyze a repertoire of diverse acyl transfer reactions

Which WE species are generated upon transgenic WE biosynthesis is influenced by substrate specificities of WE synthesizing enzymes. Here, not only substrate specificities of WS(D) but also substrate specificities of FAR enzymes have to be taken into consideration, as they influence which fatty alcohols are provided to WS(D) for WE production. Up to now, several WS(D) (Lardizabal *et al.*, 2000; Daniel *et al.*, 2004; Holtzapfle & Schmidt-Dannert, 2007; Kalscheuer *et al.*, 2007; King *et al.*, 2007; Alvarez *et al.*, 2008; Arabolaza *et al.*, 2008; Li *et al.*,

2008; Kaddor *et al.*, 2009; Barney *et al.*, 2012; Shi *et al.*, 2012; Lázaro *et al.*, 2017; Zhang *et al.*, 2017; Shalini & Martin, 2020) and FAR (Aarts *et al.*, 1993; Aarts *et al.*, 1997; Metz *et al.*, 2000; Cheng & Russell, 2004a; Rowland *et al.*, 2006; Doan *et al.*, 2009; Wahlen *et al.*, 2009; Domergue *et al.*, 2010; Chen *et al.*, 2011; Hofvander *et al.*, 2011; Willis *et al.*, 2011) enzymes of different organisms were identified and characterized. *In vitro* analyses revealed in general broad substrate ranges for FAR and WSD enzymes on straight chain acyl substrates. Same was observed for MaWSD5 in this thesis (Article I), making the enzyme a suitable candidate for the synthesis of diverse WE desired for industrial applications.

Broad substrate ranges of WE producing enzymes have the advantage of providing a large repertoire for the catalysis of diverse acyl transfer reactions. Extending the range of applications even more, several WSD were found to accept also isoamyl alcohol, phenyl ethanol, phytol, farnesol, cyclic alcohols, monoacylglycerol and ricinoleoyl alcohol as acyl acceptors and phytanic acid, 3-hydroxybutyryl-CoA, 2-hydroxyisobutyryl-CoA and ricinoleic CoA as acyl donors (Stöveken *et al.*, 2005; Holtzapfle & Schmidt-Dannert, 2007; Barney *et al.*, 2012; Barney *et al.*, 2015; Röttig *et al.*, 2016; Miklaszewska *et al.*, 2018). To analyze, whether MaWSD5 can utilize other substrates beside straight chain acyl molecules, was not within the scope of the thesis and can only be hypothesized. Nevertheless, the probability for that hypothesis is high, as MaWSD5 synthesized an unknown compound when expressed in yeast (Article I) and the enzyme originates from the bacterium *M. aquaeolei*, which can use crude oil components as carbon source (Huu *et al.*, 1999) and MaWSD1/MhWS1 as well as MaWSD2/MhWS2 were already found to utilize other substrates as well (Holtzapfle & Schmidt-Dannert, 2007; Barney *et al.*, 2012; Barney *et al.*, 2015; Miklaszewska *et al.*, 2018).

Reflecting the large number of characterized WS(D) and the broad substrate range of the enzymes, the use of WS(D) for the synthesis of several ester compounds were tested. Whereas some studies studied WS(D) enzymes for the production of long chain monoenoic WE used as lubricants (Heilmann *et al.*, 2012; Iven *et al.*, 2016; Yu *et al.*, 2018), others expressed WS(D) in *S. cerevisiae* or *E. coli* to synthesize fatty acid ethyl esters (FAEE) for their use as biodiesel (Shi *et al.*, 2012; Röttig *et al.*, 2015). Within these studies a variety of WS(D) or FAR/WS(D) combinations was analyzed with the aim to identify the enzymes or enzyme combinations, that produce desired ester compounds in large and mainly exclusive amounts. The use of different enzymes led indeed to the formation of different ester products and different ester amounts. For example, expression of several WS(D) in *E. coli* and *S. cerevisiae* revealed different FAEE production capacities of tested enzymes *in vivo* (Shi *et al.*, 2012; Röttig *et al.*, 2015). And expression of diverse FAR and WS(D) combinations in *A. thaliana* and *C. sativa* in the studies of Heilmann *et al.* (2012), Iven *et al.* (2016) and Yu *et al.* (2018) resulted in the formation of different WE in terms of chain length and desaturation

degree, depending on which enzyme combination was expressed. Consistent with this, different WE were produced as well depending on whether MaWSD2 or MaWSD5 were expressed in *A. thaliana* in this thesis (Article III). However, studying WE biosynthesis in transgenic plants, no analyzed FAR/WS(D) enzyme combination so far was able to produce mainly one desired WE species in larger amounts. As a result of broad substrate specificities and availability of diverse acyl substrates, a large variety of WE was synthesized by FAR/WS(D) combinations in this thesis (Article III) as well as in other studies (Heilmann *et al.*, 2012; Iven *et al.*, 2016; Ruiz-Lopez *et al.*, 2017; Yu *et al.*, 2018). How large the influence of substrate availability is, rather than the influence of substrate specificities of the enzymes themselves, can be seen also by results obtained within the scope of this thesis (Article III). Directing localization of MaFAR/MaWSD2 and MaFAR/MaWSD5 constructs to plastids, a shift towards the formation of shorter and more saturated WE was observed. Strikingly, differences between cytosolic and plastidial WE formation independent from the enzyme combination were more pronounced than differences in WE species produced by MaFAR/MaWSD2 or MaFAR/MaWSD5 combinations. The large influence of substrate availability was also observed in the studies of Heilmann *et al.* (2012), Iven *et al.* (2016) and Yu *et al.* (2018). Expression of diverse FAR/WS(D) combinations in *A. thaliana* and *C. sativa* mutants with high oleic acid levels, resulted in the production of 18:1/18:1 WE of around 60 mol % and 30 mol %, respectively, independent from the enzyme combination used.

Hence, the identification and characterization of new WS(D) and FAR enzymes seems to be more important to increase overall WE formation to synthesize large amounts of industrially favored ester compounds. With the characterization of MaWSD5 as part of this thesis, a new WSD catalyzing diverse ester formations has been added to the list of suitable WS(D) proteins (Article I). However, its overall WE synthesizing capacity did not reach the one obtained with the enzyme of jojoba (Iven *et al.*, 2016). The strategy to improve transgenic WE production should therefore be the identification and characterization of new WS(D) and FAR enzymes in order to broaden the number of proteins with high enzymatic activities in the first place. The regulation of which WE species are produced, however, should be controlled by optimizing the cellular substrate availability. For a detailed discussion about the influence of substrate availability on WE production, see section 5.4. As WE synthesis is dependent on the action of FAR and WS(D) enzymes and studies observed that different FAR/WS(D) combinations also have an influence on WE yield (Iven *et al.*, 2016; Yu *et al.*, 2018), further protein combinations need to be tested in the future in order to identify the ones, that are best adapted to each other as well as to the desired host plant metabolism.

5.3 WS(D) crystal structures as a basis to improve and design enzymes

The availability of crystal structures lifts biochemical characterizations of enzymes to a next level. Having a structure, it is possible to identify substrate-binding sites and unravel catalytic mechanisms of enzymes. Understanding in detail, how a protein catalyzes a specific reaction, it is furthermore possible to generate mutant variants with altered substrate specificities or improved enzymatic activities.

With AbWSD1 (Dr. Karin Kühnel, unpublished data) and MaWSD1 (Petronikolou & Nair, 2018) two crystal structures of WSD proteins are available now, which provide the opportunity for detailed structure-function analyses and the assignment of substrate binding sites and catalytic important residues. The crystallization of MaWSD1 revealed two pockets in the protein. Based on amino acid substitution studies, Petronikolou and Nair (2018) assigned pocket 1 to the acyl-CoA binding site. Considering mutational studies from Barney and co-workers (Barney *et al.*, 2013; Barney *et al.*, 2015), the fatty alcohol binding site was allocated to pocket 2 (Petronikolou & Nair, 2018). The second histidine of the catalytic motif was identified to face the cavity where both pockets meet and was therefore considered to be important for catalysis rather than the first histidine of the motif (Petronikolou & Nair, 2018).

Detailed investigations of the AbWSD1 structure within the scope of this thesis (Article II), provided even further insights into substrate binding sites and amino acid residues involved in catalysis in WSD. Besides the already described two binding sites, a cavity was identified in AbWSD1, which was proven upon mutational studies to be involved in DGAT activity without altering WE formation. Observed structural differences between AbWSD1 and MaWSD1 could be attributed to myristic acid binding in AbWSD1 and led to the proposal of a conformational change upon substrate binding. Modelling of acyl-CoA into the structure of AbWSD1 identified furthermore potential CoA binding amino acids. Additionally, further evidence was provided for the second histidine of the catalytic motif being involved in catalysis, as the carboxyl group of myristic acid is facing towards this residue in AbWSD1.

As a comparison of the AbWSD1 and MaWSD1 crystal structures revealed, that they are almost identical except for the structural rearrangements attributed to substrate binding (Article II), it can be assumed, that other WSD have a similar fold. Thus, structure prediction of other WSD based on AbWSD1 and MaWSD1 is possible and will help to generate specifically mutated enzyme variants of these WSD as well. For engineering WSD enzymes, a huge variety of approaches is possible, altering either substrate specificities, catalytic activities or cellular localization. The different approaches are discussed in the following sections.

5.3.1 Change of substrate specificities

As many WSD were identified to have a broad substrate range, engineering substrate specificities of the proteins will help to narrow substrate preferences of WSD enzymes. This will enable the enzyme variants to use only certain substrates and consequently to produce only desired WE species. However, one has to keep in mind that these mutations may reduce the catalytic efficiency (see below). In order to change substrate specificities of enzymes, the introduction of mutations around substrate cavities is a common tool. Exchanging residues with larger amino acids narrows or closes cavities and leads consequently to a reduced or abolished binding of large substrates. In addition to that, amino acid exchange mutants can also be generated to open or enlarge a tunnel. By the substitution of residues with smaller amino acids, tunnels can be extended or bulges can be flattened to allow the binding of longer or bulkier substrates. Moreover, not only sterical hindrance can be used to alter the shape of a cavity, a change in polarity or the availability of hydrogen bonding partners can be used as well to strengthen or weaken substrate binding.

As part of this thesis, the DAG cavity of AbWSD1 was identified (Article II). Mutations of two the cavity aligning residues towards a larger tryptophan (AbWSD1-V139W-I303W) on opposite sides of the tunnel closed/narrowed the cavity and abolished a proper DAG binding for the formation of TAG. The identification of the DAG binding site and the generation of an enzyme variant, that lacks DGAT activity without influencing WS activity within this thesis now provides the opportunity to generate monofunctional WSD that lack the ability of TAG formation, which is considered as a futile cycle wasting resources in respect to desired WE production.

Examples for amino acid exchanges around the acyl-CoA and the fatty alcohol tunnels of WSD are described as well. MaWSD1-G25 and MaWSD1-A144 are located around the acyl-CoA pocket of MaWSD1 (Petronikolou & Nair, 2018). A substitution of the residues towards larger amino acids (MaWSD1-G25V, MaWSD1-A144F) closed/narrowed the acyl-CoA pocket and led to a preference of both enzyme variants for shorter acyl-CoA compared to wild type enzyme. MaWSD1-A360 and AbWSD1-G355 are located around the fatty alcohol binding site (Barney *et al.*, 2013). Mutations of the residues to larger amino acids resulted in a preference of the enzyme variants to shorter fatty alcohols, too.

In order to predict, which substrates are able to bind to mutated cavities, it is important to know, how substrates are placed within the cavities upon catalysis. The co-crystallized myristic acid in AbWSD1 provides detailed information about the position of the acyl chain within the acyl-CoA pocket and allows to analyze which amino acids of AbWSD1 interact with the acyl chain (Article II). In order to obtain this information also for the DAG and the fatty alcohol cavities,

additional WSD crystal structures with bound substrates or substrate analogs are needed in the future.

In general, to engineer WSD for biotechnological applications, altering substrate preferences of the enzyme should not be on the expense of overall enzymatic activity and should be analyzed conscientiously. That introducing mutations around substrate binding sites is not only restricted to abolish or promote the binding of certain substrates, but also influences the overall enzymatic activity was observed in this thesis for AbWSD1-V23W-G24W and AbWSD1-V350W-V372W (Article II). No WE and TAG formation was observed in the TLC-based enzymatic activity assay for the first enzyme variant, which contains mutations around the acyl-CoA cavity. The second one, in which residues residing opposite to the active site were exchanged, showed a higher preference for shorter acyl-CoA but also an overall lower enzymatic activity compared to wild type AbWSD1. A change in enzymatic activity was also seen for MaWSD1-G25V and MaWSD1-A144F (Petronikolou & Nair, 2018). Although both enzyme variants showed a higher preference for shorter acyl-CoA, MaWSD1-G25V was only half as active on 6:0 CoA as wild type MaWSD1 whereas MaWSD1-A144F was 5.5 fold more active than the wild type enzyme. For AbWSD1-G355I, identified to change the fatty alcohol selectivity of the protein (Barney *et al.*, 2013), a positive effect on catalytic efficiency was also described on *in vitro* WE formation with short chain alcohol moieties and for the production of FAEE in *E. coli* (Röttig *et al.*, 2015; Röttig *et al.*, 2016).

5.3.2 Change in enzymatic activity

For biotechnological WE production, it is favorable to use enzymes with high enzymatic activities in order to produce large WE amounts. Hence, it is also beneficial to improve enzymatic activity of WSD in general. In this case, mutations around the active site are promising. However, for this it is important to know the reaction mechanism of the protein and especially the rate-limiting step of the reaction, as an acceleration of this step accelerates the whole catalytic cycle. WE formation in WSD is proposed to occur within three steps (Stöveken *et al.*, 2009) (Figure 1.4): 1. hydrogen abstraction of the hydroxyl group of the fatty alcohol; 2. nucleophilic attack of the oxyanion; 3. sulfur protonation to generate CoA/ACP-SH as leaving group. In case the hydrogen abstraction is the rate-limiting step in catalysis, an increase in nucleophilicity of the hydrogen abstracting amino acid improves its reactivity and consequently accelerates the hydrogen abstraction. If the formation or dissociation of the transition state is rate limiting, mutations that favor the transition state or that “push” the transition state further into oxoester bond formation are advantageous to be generated.

Although it is proposed, that ester bond formation in WSD is dependent on the action of a histidine of the catalytic motif (HHxxxDG) (Stöveken *et al.*, 2009) and the available data on the AbWSD1 and MaWSD1 structures strongly suggests, that the second histidine of the motif is taking over this task, the reaction mechanism of WSD including all involved amino acid residues has not been fully unraveled so far. Based on findings obtained in this thesis (Article II) and in other publications (Stöveken *et al.*, 2009; Villa *et al.*, 2014; Petronikolou & Nair, 2018), three residues might be important for the reaction mechanism. Based on amino acid counting in AbWSD1, these residues are AbWSD1-H133 as the proposed catalytic histidine, AbWSD1-G138, which is part of the catalytic motif and whose main chain NH group is in hydrogen bonding distance to the carboxyl group of the co-crystallized myristic acid, and AbWSD1-S374. This serine residue is conserved in different WSD (Röttig & Steinbüchel, 2013a; Villa *et al.*, 2014) and a mutation in AbWSD1 towards proline resulted in reduced enzymatic activity (Röttig & Steinbüchel, 2013b). Based on a structural alignment of modeled MaWSD2 with the sorghum hydroxycinnamoyltransferase, Villa *et al.* (2014) discussed, that the serine residue might interact with the oxyanion of acyl-CoA. Assigning various roles to the three residues, three different reaction mechanism scenarios are conceivable (Figure 5.1).

In scenario I, AbWSD1-S374 interacts with the carbonyl oxygen of the fatty acid and stabilizes a generated oxyanion during transition state as suggested by Villa *et al.* (2014). The sulfur of the thioester bond is oriented to the protonated AbWSD1-H133 and the carbonyl carbon is accessible for the nucleophilic attack of the deprotonated fatty alcohol. It can be speculated whether AbWSD1-H133 deprotonates the fatty alcohol beforehand or whether another amino acid is doing this. AbWSD1-G138 has no specific function in this scenario.

In scenario II, AbWSD1-G138 instead of AbWSD1-S374 forms a hydrogen bond with the carbonyl oxygen of the fatty acid via its main chain NH according to the hydrogen bond observed in AbWSD1 between the amino acid and the carboxyl group of myristic acid. AbWSD1-S374 interacts with the sulfur of the thioester bond and hence, provides the hydrogen for the protonation of CoA/ACP. AbWSD1-H133 deprotonates the hydroxyl group of the fatty alcohol to generate the oxyanion needed for the nucleophilic attack as proposed by Stöveken *et al.* (2009).

In scenario III, AbWSD1-G138 is interacting with the carbonyl oxygen as in the previous scenario, stabilizing an oxyanion upon transition state. AbWSD1-H133 interacts with the thioester bond sulfur and protonates CoA/ACP upon catalysis as suggested by Stöveken *et al.* (2009). AbWSD1-S374 is available to deprotonate the fatty alcohol or stabilize the oxyanion of the fatty alcohol after deprotonation.

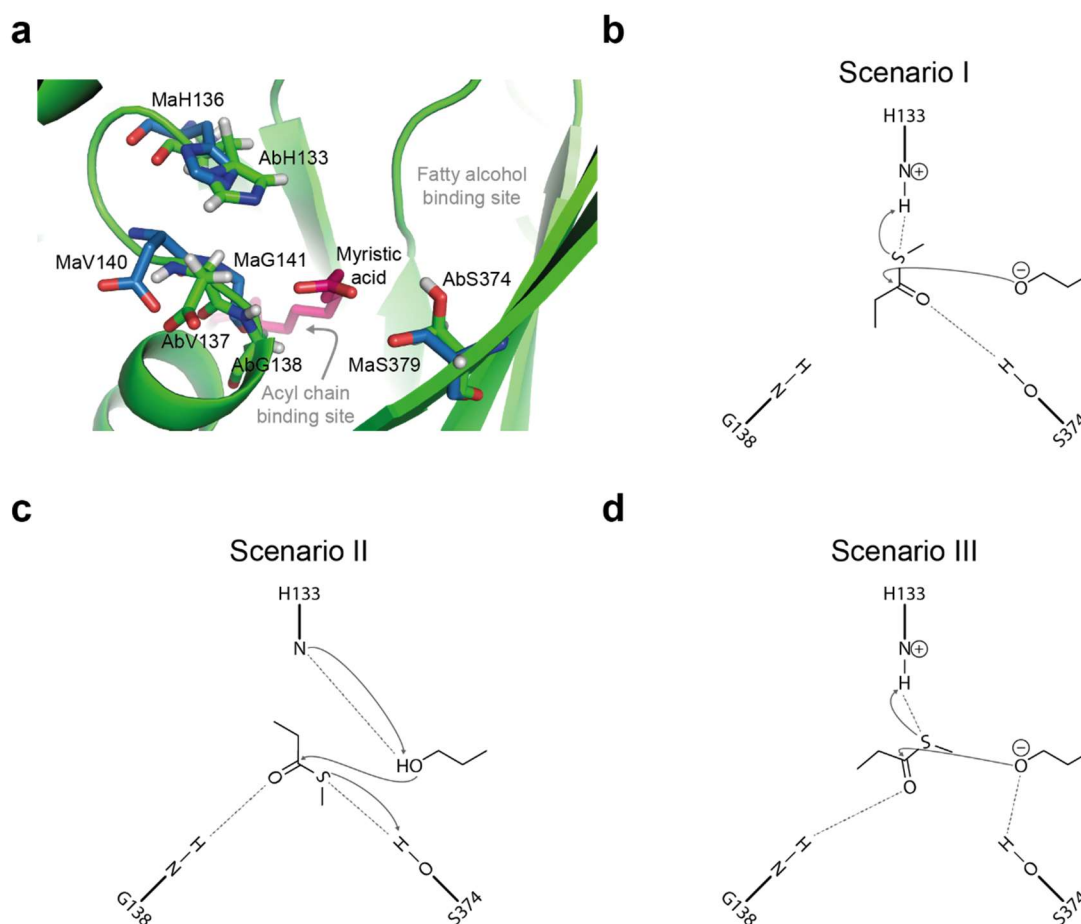


Figure 5.1. Potential WSD reaction mechanisms.

(a) The active site of AbWSD1 (green) is depicted including the co-crystallized myristic acid (pink) and the proposed amino acid residues of AbWSD1 involved in catalysis. The corresponding amino acids of MaWSD1 are depicted in blue. The proposed acyl-chain and fatty alcohol binding sites are marked. The active site is viewed approximately from the direction of the proposed CoA binding site (Article II). Oxygen atoms are displayed in red, nitrogen atoms in blue and hydrogen atoms in white. (b)-(d) Proposed reaction mechanism scenarios regarding the thioester bond of acyl-CoA ($-\text{C}(=\text{O})-\text{S}-$) and the fatty alcohol ($\text{HO}-$) based on the action of the three residues AbWSD1-H133, AbWSD1-G138, AbWSD1-S374. For AbWSD1-H133 the NH group from the side chain ring is proposed to be involved in catalysis, for AbWSD1-G138 the NH group of the main chain and for AbWSD1-S374 the OH group of the side chain. Dashed gray lines illustrate stabilizing interactions, gray arrows mark chemical rearrangements upon catalysis. Distances displayed in the schemes do not correspond to distances within the structure, but were chosen for the purpose of best and comparable visualizations of the reaction mechanisms.

Whether one of the scenarios reflects the actual reaction mechanism of WSD remains elusive. It is also conceivable, that the amino acids fulfill more than one function, e.g. deprotonation of the fatty alcohol and protonation of CoA/ACP as suggested for AbWSD1-H133 by Stöveken *et al.* (2009). Especially, the distances between the amino acids and the substrates during catalysis are important as well as the nucleophilicity of certain amino acids. Petronikolou and Nair (2018) stated that MaWSD1-H136 is not nucleophilic enough for proton abstraction of the

alcohol. They discussed MaWSD1-D8 to change the nucleophilicity of MaWSD1-H136 upon interaction of both, but stated also, that MaWSD1-D8 might be located too far away in the crystal structure. Another possibility might be, that the aspartate of the catalytic motif forms a catalytic diad together with the catalytic histidine. Nevertheless, both AbWSD1-D137 and MaWSD1-D140 are turned away from the histidine in the corresponding structures (Figure 5.1a) and in the former case is proposed to hydrogen bond with CoA of the modelled acyl-CoA (Article II). In order to unravel the reaction mechanism of WSD, further studies are needed. Especially crystal structures with bound substrates in diverse conformations will be helpful. Those crystal structures will furthermore assist to elucidate, which step in substrate binding and/or catalysis induces the in this thesis proposed conformational change of WSD (Article II).

5.3.3 Change in localization

Thinking about metabolic engineering or more specific as one possibility about protein engineering, changes in enzymatic activity or substrate specificity are the most obvious strategies. Apart from this, it is also advantageous to have an enzyme's crystal structure to gain information about the surface of the protein. Influencing its outer appearance, surface properties as hydrophobicity or electrostatic potential can determine the purification efficiency, overall stability, the interaction with other proteins or the cellular localization. Hence, mutations of residues located on the surface of the protein can influence the above stated aspects.

Regarding purification efficiency, protein solubility is a major criterion. For potential biotechnological *in vitro* applications of WSD, economical preparation of the protein is necessary. Although no transmembrane domains were identified in MaWSD5 and AbWSD1, significant amounts of the proteins remained in the pellet after cell lysis and centrifugation, being inaccessible for further purification steps (Article I and II). In order to overcome this, Dr. Felix Lambrecht and Dr. Steffen Kawelke (Kawelke, 2014) generated an AbWSD1 double mutant by substituting the hydrophobic residues AbWSD1-I358 and AbWSD1-I359 with hydrophilic serine residues. Indeed, the protein variant was found to be more stable after purification.

In connection with this, a communicating amino acid network on the surface of a mutated bacterial lipase was observed to influence aggregation propensity, thermostability, as well as stability towards organic solvents (Reetz *et al.*, 2006; Reetz *et al.*, 2009; Reetz *et al.*, 2010). Lipases are biotechnologically used for the cleavage of fatty acids from TAG molecules (Gupta *et al.*, 2004). Due to the hydrophobic character of their substrates and products, lipases catalyze reactions at the lipid-water interface (Gupta *et al.*, 2004). Hence, in order to obtain

high reaction yields, enzymes tolerating the interaction with hydrophobic molecules and solvents are desired. As WSD also catalyze the formation of hydrophobic products, an improved stability towards solvents might be advantageous for biotechnological applications, too.

Surface property is furthermore important for protein-protein-interactions. In terms of WE formation, an ideal cooperation of FAR and WS(D) is aimed for, which was tried to be obtained by testing different FAR/WS(D) combinations or even by generating fusion constructs (Iven *et al.*, 2016; Yu *et al.*, 2018). Altering surface properties of WS(D) and FAR proteins can be achieved in terms of changing the proteins' silhouettes, hydrophobicities or electrostatic potentials. This might allow or improve interactions of the proteins and might result in an efficient substrate channeling from acyl-CoA over fatty alcohols into WE.

The surface of proteins is also important in terms of subcellular localization. Bacterial WE inclusion formation was identified to occur in a plasma membrane associated manner including WSD proteins localizing to the plasma membrane (Wältermann *et al.*, 2005). Membrane surface properties are highly influenced by the head groups of lipids forming the bilayer (Whited & Johs, 2015). Hence, apart from organelle localization signals and transmembrane domains, surface properties, as hydrophobicity or surface charge, determine whether a protein can interact with a certain membrane (Whited & Johs, 2015). Due to this, mutations altering the surface properties of WSD might be used to change the membrane localization of the enzymes and with this, the localization of WE formation. How a change in location can have an influence on generated WE species and amounts is further discussed in section 5.4 and 5.5.

5.3.4 WSD structures as a general WS concept?

AbWSD1 and MaWSD1 are the first WSD structures available. Knowing the substrate binding sites of acyl-CoA, fatty alcohol and DAG as well as amino acids involved in catalysis, it is now possible to engineer WSD enzymes with desired substrate preferences and enzymatic activities as discussed above. This approach is faster and more effective as well as target-oriented than testing a huge number of enzymes for the desired properties. Although DGAT1-like and DGAT2-like WS have a different structure than WSD, structural information obtained from the WSD class might also be transferred to the class of WS enzymes. Only recently, the structures of human DGAT1 (Sui *et al.*, 2020; Wang *et al.*, 2020) and human acyl-CoA:cholesterol acyltransferase (ACAT) 1 (Qian *et al.*, 2020) were published. Due to a similar evolutionary origin of DGAT1-like WS (e.g. ScWS), human DGAT1 and ACAT1, structural predictions and furthermore structure-guided mutations are possible for this WS class now as well. As the identified position of co-crystallized acyl-CoA in the DGAT1 and ACAT1 crystal

structures with the acyl-chain buried in the protein, the thioester bond close to the catalytic histidine and the phosphoadenosin part reaching to the outside of the protein, is similar to the proposed and modeled position of acyl-CoA in WSD (Petronikolou & Nair, 2018) (Article II), a general acyl-CoA binding concept might exist in acyltransferases. Hence, future suggested reaction mechanisms for WSD and DGAT1-like enzymes are worth to compare.

5.4 Influence of substrate availability on WE formation

Article III of this thesis is the first study providing a detailed comparison of cytosolic and plastidial transgenic WE biosynthesis showing that a change in WE biosynthesis localization is a suitable tool to alter substrate availability for FAR and WSD. It was observed in seeds, that with a shift of WE biosynthesis to plastids, the cellular compartment of *de novo* fatty acid synthesis, the formation of shorter and more saturated WE was achieved compared to WE formation in the cytosol, where fatty acid modification like elongation and desaturation takes place.

Therefore it was shown in this thesis, that a change of substrate pool by a change of WE biosynthesis location is an appropriate instrument to modify WE biosynthesis. Other studies available so far altered the substrate pool upon overexpression or knock out/down of fatty acid modifying enzymes causing an alteration in the cytosolic fatty acid pool. Upon expression of diverse enzyme combinations in so-called high oleic plants, Heilmann *et al.* (2012), Iven *et al.* (2016) and Yu *et al.* (2018) obtained 18:1/18:1 WE accounting to around 60 mol % of the total WE content in *A. thaliana* and around 30 mol % of the total WE content in *C. sativa*. In these high oleic plants, the acyl-CoA pool was altered by knocking out genes needed for elongation of fatty acids beyond 18 carbon chain length and desaturation beyond one double bond in seeds. On the contrary, Zhu *et al.* (2016) and Ivarson *et al.* (2017) obtained longer WE by expressing a FAE enzyme. The co-expression of a 14:0 ACP thioesterase, which causes the release of shorter fatty acids to the cytosol, resulted in the formation of shorter WE in the study of Ruiz-Lopez *et al.* (2017). Upon transient inhibition of *KASII* in *N. benthamiana*, Aslan *et al.* (2015a) obtained an increase in 16:0 moieties in WE.

5.4.1 The role of promoter choice on substrate availability

Results of Article III show, that a change in localization of WE biosynthesis is a suitable option to alter substrate availability. In this connection, change in localization can be interpreted quite broadly. This can be on one hand a change of the cellular compartment leading to a different substrate pool, as achieved in this study by expressing enzymes containing signal peptides for

plastidial localization. On the other hand, it can also be a change in spatial or temporal expression denoting a different plant organ or developmental stage with altered metabolic prerequisites, as achieved in this thesis by directing WE synthesis either to seeds or allowing an ubiquitous expression of WE producing enzymes. Whereas for the first case the choice of the appropriate cellular localization signals is important, the choice of an appropriate promoter is important for the second one.

In this thesis, WE formation was detected in the cytosol and in plastids, when seed specific promoters control FAR and WSD expression (Article III). Expression controlled by the 35S promoter however did not result in significant WE amounts upon plastid localized WE synthesis. This demonstrates how the promoter choice influences WE production. The lack of WE might not be explained by insufficient availability of substrates, but rather by insufficient WE storage capacities (see section 5.5) or export to the cuticle, which would however require WE export out of the plastids that has not been described.

An illustration on how important the promotor choice for substrate availability is, appears when comparing which WE were synthesized by the MaFAR/MaWSD2 constructs in this thesis and in the publication of Yu *et al.* (2018). Different WE were synthesized by both constructs although each enzyme combination was expressed in the cytosol of *A. thaliana* seeds. In this thesis (Article III), WE with the main compounds 20:1 (n-9) and 18:1 (n-9) acyl moieties accounting to 20-25 mol % each, and 20:1 (n-9) and 18:1 (n-9) alcohol moieties, accounting to 35-40 mol % and 20-25 mol % respectively, were generated by MaFAR/MaWSD2. In contrast, Yu *et al.* (2018) detected WE species consisting of around 60 mol % 18:0 acyl and 18:1 alcohol moieties synthesized by the same enzyme combination. The observed differences in produced WE species may originate from changes in substrate specificities of MaFAR and MaWSD2 due to the YFP-myc and CFP-flag tags. However, MaFAR/MaWSD2 produced shorter and more saturated WE in this thesis upon localization in plastids (Article III). Due to this, alterations in produced WE species by MaFAR/MaWSD2 in this thesis and the publication of Yu *et al.* (2018) may be caused by the use of diverse promoters resulting in a different temporal expression of the enzymes during seed development. In this work, MaFAR and MaWSD2 expression was controlled by the seed specific promoters β -conglycinin and glycinin, respectively. Yu *et al.* (2018) expressed both proteins under the control of the seed specific napin promoter. The importance of the right time point of enzyme expression for appropriate substrate availability is illustrated by the study of Baud *et al.* (2002). They observed a change in fatty acid composition in *A. thaliana* seeds during seed development. Large amounts of 16:0 and 18:0 fatty acids were detected during early development, accounting together to 40-60 % until torpedo stage. Afterwards, 20:1 and 18:3 fatty acids are increasing up to an amount of 30-40 % in mature and desiccated seeds. Amounts of 18:1 and 18:2 fatty acids remain

relatively stable from triangular stage on, accounting to 40-50 % together. As large amounts of 20:1 (n-9) acyl and alcohol moieties in WE produced by MaFAR/MaWSD2 were detected in this thesis, an activity of β -conglycinin and glycinin during later time points in seed development can be assumed compared to the activity of the napin promoter. However, opposing this assumption, the expression of MaFAR/ScWS constructs controlled by the napin promoter resulted in the formation of WE with high amounts of 20:1 acyl and alcohol moieties (Yu *et al.*, 2018), suggesting, that these substrates are available upon napin promoter controlled expression.

The promoter choice does not only determine the time point of expression and the location, but also strength of expression. A low expression of enzymes results in low protein levels and might result in low amounts of formed WE. Especially when competing with other acyl-CoA consuming reactions, such as TAG production in seeds, the protein level might become relevant. However, an expression at high levels might cause down regulation of protein expression by silencing. Hence, promoters should not only be chosen by their temporal and spatial expression pattern, but also by their expression strength appropriate for the desired application.

5.4.2 The role of metabolic regulation and fatty acid export on substrate availability

Work in this thesis demonstrates that directing WE biosynthesis to plastids is a suitable tool for the production of WE consisting of 18 carbon chain moieties. Upon plastidial WE synthesis, mostly WE species with 18:0 moieties were formed (Article III). Strikingly, WE with 18:1 moieties were not enriched or even decreased upon plastidial WE formation, although 18:1 ACP is generated in the plastids like 16:0 ACP and 18:0 ACP. Plastids contain two types of thioesterases (FatA and FatB), which terminate fatty acid synthesis and prime the export of fatty acids out of the plastid into the cytosol. While FatA thioesterases act on 18:1 ACP (Dörmann *et al.*, 1995), FatB prefers saturated acyl-ACP and mainly 16:0 ACP (Jones *et al.*, 1995). In *A. thaliana* mostly 18:1 fatty acids are exported from the plastids by the action of FatA (Salas & Ohlrogge, 2002; Bonaventure *et al.*, 2003). Thus, although constantly produced, 18:1 ACP might not be available in the plastid in large amounts for WE formation due to an efficient export. Since FatB is mostly active on 16:0 ACP (Salas & Ohlrogge, 2002), mainly 18:0 ACP is available for WE formation as reflected by high content of 18:0 moieties in plastidial produced WE in this work (Article III).

To increase the amount of 18:1 ACP available in the plastid for WE biosynthesis, a reduction of 18:1 ACP export by down regulating either the thioesterase FatA (Dörmann *et al.*, 1995),

the plastidial fatty acid exporter (FAX) 1 (Li *et al.*, 2015) or LACS9, which catalyzes the formation of acyl-CoA from plastid exported fatty acids, (Jessen *et al.*, 2015) is worth trying. However, when introducing new enzymes or knocking down others in order to change the substrate pool available for the WE biosynthesis, it is important to keep in mind, that cell metabolism is a tightly regulated network. Removed, added or altered reactions can lead to - sometimes unpredictable - developmental alterations or unexpected compensating side reactions (Bonaventure *et al.*, 2003; Moreno-Pérez *et al.*, 2012). A suitable mutant plant for the above stated approach is the *A. thaliana fata1 fata2* double mutant generated by Moreno-Pérez *et al.* (2012). The mutant shows a reduced expression of *FatA1* and *FatA2*, resulting in a 40 % reduced 18:1 ACP hydrolyzing activity. In contrast to a reported reduced growth of an *A. thaliana fatb* knockout mutant (Bonaventure *et al.*, 2003), no morphological differences were observed in the *A. thaliana fata1 fata2* double mutant compared to the wild type (Moreno-Pérez *et al.*, 2012). However, upon seed lipid analysis, Moreno-Pérez *et al.* (2012) observed reduced TAG content and altered fatty acid profiles similar to that observed in the *A. thaliana wri1* mutant, which lacks the transcription factor AtWRI1 that regulates fatty acid synthesis (Focks & Benning, 1998; Ma *et al.*, 2013). Due to this, Moreno-Pérez *et al.* (2012) speculated that a reduction in FatA activity leads to temporal increase in the acyl-ACP level, which results finally in a feedback inhibition of fatty acid synthesis. Hence, upon plastidial WE biosynthesis in the *fata1 fata2* double mutant a constant shuttling of 18:1 ACP into WE has to be achieved by efficient FAR and WSD enzymes, preventing an increase of plastidial 18:1 ACP level, that leads to a reduction of fatty acid synthesis.

Fatty acid export is a critical point in terms of substrate availability for high plastidial WE amounts, too, as can be seen in the study of Aslan *et al.* (2014). Transient expression of AtWRI1 in combination with different plastid-localized WE producing enzymes in *N. benthamiana* leaves resulted only for one combination in increased WE amounts although TAG formation was increased upon AtWRI1 expression, suggesting for induced fatty acid synthesis (Aslan *et al.*, 2014). These results show, that increased fatty acid synthesis does not consequently lead to increased plastidial WE synthesis, most probably caused by an efficient export of acyl-ACP from the plastids.

5.5 Influence of WE storage on WE accumulation

Efficient enzymes and appropriate substrate availabilities are useless without sufficient WE storage capacities, needed for high WE contents in transgenic plants. In this thesis, WE amounts of about 20 mg/g seed for cytosolic WE synthesis and 12 mg/g seed for plastidial WE synthesis were obtained, resulting in WE contents of 4-8 mass % (Article III). This is in a

comparable range to what was obtained upon expression of MmFAR/MmWS, MmFAR/ScWS, MaFAR/AbWSD1 or MaFAR/MaWSD2 in *A. thaliana* seeds before (Heilmann *et al.*, 2012; Iven *et al.*, 2016; Yu *et al.*, 2018). Strikingly, in this thesis (Article III) no WE accumulation was detected in seeds or in leaves when plastidial localized MaFAR, MaWSD2 or MaWSD5 were expressed under the control of the 35S promoter.

Major goal for transgenic WE biosynthesis is the generation of plants, producing mainly WE in seeds, as it is the case in jojoba seeds (Miwa, 1971; Busson-Breysse *et al.*, 1994; Sturtevant *et al.*, 2020). Most publications dealing with industrial WE formation in plants analyzed WE formation in seeds of oil seed (crop) plants as their seeds are specialized for neutral lipid accumulation (Lardizabal *et al.*, 2000; Heilmann *et al.*, 2012; Iven *et al.*, 2016; Zhu *et al.*, 2016; Ivarson *et al.*, 2017; Ruiz-Lopez *et al.*, 2017; Yu *et al.*, 2018). High WE contents obtained so far were 43-59 mass % WE upon the expression of MaFAR/ScWS in transgenic *A. thaliana* seeds (Iven *et al.*, 2016), 15-30 % WE in *C. abyssinica*, *B. carinata* and *C. sativa* upon the expression of ScFAR/ScWS with other fatty acid modifying enzymes (Zhu *et al.*, 2016) and 50-65 % WE upon expression of ScFAR/ScWS in *L. campestre* (Ivarson *et al.*, 2017). However, although seeds of these plants are specialized for neutral lipid accumulation, so far no plants could be generated that mainly produce WE as jojoba is doing. Additionally, morphological changes were observed in connection with high WE amounts in the transgenic plants. *C. sativa* plants with high WE levels had white patches on the cotyledons (Iven *et al.*, 2016). White cotyledons were also observed in *A. thaliana* with high WE contents, as well as reduced germination rates for both *A. thaliana* and *C. sativa* lines with WE levels (personal communication Dr. Ellen Hornung). *L. campestre* seeds with high WE amounts were wrinkled, showed disrupted cellular neutral lipid organization and lost the ability to germinate (Ivarson *et al.*, 2017). As reasons for this, high fatty alcohol amounts are discussed as well as insufficient WE storage abilities (Aslan *et al.*, 2015b; Ivarson *et al.*, 2017). In terms of WE storage capacities two main aspects are important, which are the suitability of a plant for proper WE packaging and connected with this, location of WE biosynthesis as it determines the availability of a WE packaging machinery at WE formation sites. The influence of both aspects on WE content is further discussed in the two following sections.

5.5.1 The influence of WE packing on WE accumulation

Neutral lipids, as WE, TAG or sterol esters, are stored in cellular inclusions (Wältermann & Steinbuchel, 2005a; Ischebeck *et al.*, 2020). In plants, lipid droplets originate upon neutral lipid deposition between the two leaflets from the ER membrane and bud off as mature lipid droplets into the cytosol, having a hydrophobic lipid core surrounded by a phospholipid monolayer

(Ischebeck *et al.*, 2020). A second group of lipid inclusions can be found in plastids. They are named plastoglobuli and are most likely formed by similar processes as lipid droplets budding from the thylakoid membrane (van Wijk & Kessler, 2017). Several proteins are known to locate to plastoglobuli or lipid droplets fulfilling functions in neutral lipid synthesis, neutral lipid degradation or having structural functions like preventing their coalescence or regulating their size (Ytterberg *et al.*, 2006; Ischebeck *et al.*, 2020).

Although WE and TAG are both neutral lipids, there are indications, that both require different storage capacities. As mentioned above, Ivarson *et al.* (2017) observed a disruption in neutral lipid organization of seed cells with high WE content. Sturtevant *et al.* (2020) detected a distinct spatial distribution of WE and TAG in jojoba seeds. Whereas WE are mainly present in cotyledons, TAG are mostly found in the embryonic axis. Interestingly, lipid droplets in the cotyledons were also found to be larger. In addition to that, lipid droplet associated proteins were differentially distributed between cotyledons and embryonic axis, too. In cotyledons several oleosins and lipid droplet associated protein (LDAP) 1 are specifically expressed. The authors speculated, that LDAP1, which is homologous to small rubber particle proteins and which is not markedly expressed during TAG formation in other oil seed plants, is needed for correct packaging of WE. Concluding from that, low WE contents in transgenic plants might be a consequence of insufficient WE packaging capacities in these plants. To overcome this, a promising approach would be the generation of transgenic WE producing plants, co-expressing LDAP1 or homologous proteins in order to facilitate proper WE storage.

The publication of Ivarson *et al.* (2017) demonstrates, that wrong WE packaging can lead to severe morphological alterations like wrinkled seeds and reduced germination capacity. A failure in proper WE packaging might also be the reason for no detectable WE formation in plants expressing plastidial localized MaFAR, MaWSD2 or MaWSD5 under the control of the ubiquitous 35S promoter in this thesis (Article III). Functional plastids are needed for proper embryogenesis and seedling establishment (Hsu *et al.*, 2010; Pogson & Albrecht, 2011). High amounts of not properly stored WE in plastids of these lines might cause harmful alterations in the organelle, that are lethal and lead to a counter selection towards lines with low/no WE content. A counter selection towards plants with low plastidial WE content was also discussed by Aslan *et al.* (2015b) when the authors obtained lower WE amounts in stable transformed *N. benthamiana* lines expressing plastidial localized MaFAR/MhWS2 controlled by the 35S promoter compared to leaves in which the construct was only transiently expressed.

Interestingly, although a bit lower, comparable WE amounts were obtained in plastids compared to the cytosol when seed specific promoters controlled the expression of WE producing enzymes instead of the 35S promoter (Article III). This suggests, that plastidial WE accumulation might be tolerated during certain times in seed development and that problems

with high WE content might rather occur during developmental time points, when the two seed specific promoters are not active, either during early times in embryogenesis or during seedling establishment. To investigate how plastid morphology is hampered by WE accumulation during different seed developmental stages, comparison of transmission electron microscopy images taken from plastids at different time points in seed development from seed specific promoter and 35S promoter lines could be helpful.

5.5.2 The influence of WSD localization on WE accumulation

In order to make use of an available WE storage machinery, WE producing enzymes have to localize to the appropriate cellular regions. As described above, in eukaryotes lipid droplets and plastoglobuli form upon deposition of neutral lipids between the two leaflets of the ER membrane or thylakoid membrane, respectively. In order to direct formed neutral lipids into lipid droplets, TAG synthesizing enzymes are located within or at least at the ER membrane in regions of lipid droplet synthesis (Ischebeck *et al.*, 2020). Heilmann *et al.* (2012) described the successful co-localization of MmFAR without a peroxisome target signal and MmWS to lipid droplets in *A. thaliana* and in yeast and detected an increase in WE amounts.

In contrast to lipid droplet formation in eukaryotes, lipid inclusion formation for WE and TAG deposition happens differently in bacteria. Wältermann *et al.* (2005) proposed, that WE and TAG inclusions form upon attachment of WSD proteins to the cytosolic site of the plasma membrane. WSD proteins synthesize WE and TAG molecules, which form small lipid droplets around the proteins. Several of these small lipid droplets build an oleaginous layer on the plasma membrane and start to conglomerate. Subsequently, mature lipid bodies with a phospholipid monolayer are released to the cytosol.

Expressing bacterial WSD in *A. thaliana* seeds, only around 10-20 % of the WE amount detected upon expression of plant ScWS could be obtained so far (Article III, (Iven *et al.*, 2016; Yu *et al.*, 2018). A reason for this might be, that ScWS can use the endogenous lipid droplet machinery to deposit WE in lipid droplets of *A. thaliana*, whereas bacterial WSD cannot. It is conceivable that bacterial WSD might either fail to localize to neutral lipid synthesis sites at the ER or they might not be able to deposit WE between the two membrane leaflets. A targeting of AbWSD1 to the ER by fusion to two transmembrane domains did not lead to a drastic increase in WE amounts in the study of Yu *et al.* (2018). It might be speculated that the failure to synthesize WE between the two leaflets is the reason for lower WE content upon expression of bacterial WSD. Nevertheless, it is also conceivable, that the transmembrane domains reduce enzymatic activity of AbWSD1 by impairing the access of substrates to the active site. Transmission electron microscopy images will help to unravel where WSD proteins localize

within plant cells and where sites of WE biosynthesis are upon expression of bacterial WSD. As confocal microscopy images revealed, that MaFAR and MaWSD5 co-localize to plastidial micro domains (Article III), transmission electron micrographs will furthermore help to analyze to which kind of these subcellular structures the enzymes localize in plastids and whether WE deposition is also occurring at these sites. Additionally, it might be interesting to analyze by confocal microscopy whether MaFAR and MaWSD2/MaWSD5 expressed without plastidial localization tag localize to the ER or other cellular membranes or whether they predominantly localize in the cytosol.

As bacterial WSD have no transmembrane domains (Article I and II) (Petronikolou & Nair, 2018), a correct attachment of the proteins to a membrane is only facilitated by the surface of the enzymes, as discussed in section 5.3.3. Since organelle membranes consist of different phospholipids with diverse head groups, it is advantageous to engineer WSD proteins with adopted surface properties meeting the interaction properties of the target membrane.

5.6 Future strategies for transgenic WE production: summary, conclusions and open research questions

Transgenic WE biosynthesis very likely depends on a tight interplay between substrate availability, substrate specificities of WE producing enzymes and storage capacity (Figure 5.2). Each of the three parts has to be adjusted to optimal conditions, however a change in any of the parameters always has a direct influence on the other ones.

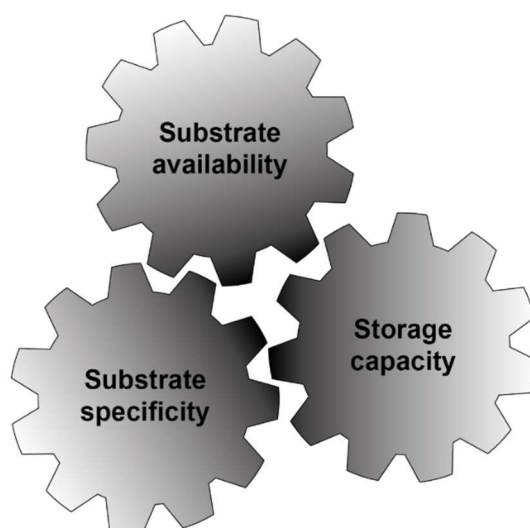


Figure 5.2. Factors influencing transgenic WE biosynthesis.

As WE producing enzymes were found to have a broad substrate range, substrate availability is a powerful tool to regulate which WE species are produced. In former studies, substrate availability was altered by knock out/down or overexpression of acyl-CoA/ACP modifying enzymes. Work conducted in this thesis (Article III) shows, that a change in subcellular localization of WE biosynthesis is a suitable tool, too, to alter the substrate pool available for WE formation. Results from this work display furthermore, that seed plastids are an appropriated cellular compartment for the formation of WE consisting of 18 carbon chain length moieties. In the future, a combination of a changed cellular WE biosynthesis and the overexpression or knock out of acyl chain modifying enzymes will give even more possibilities to fine-tune substrate availability. However, choosing new compartments for WE production, not only the available substrate pool should be considered, but also sufficient product storage capacities.

Enzymatic activities and substrate specificities of WE producing enzymes can influence which and how much WE species are formed. However, as several studies showed, that substrate availability has a major influence on generated WE species (Heilmann *et al.*, 2012; Iven *et al.*, 2016; Yu *et al.*, 2018), future selection criteria for WE producing enzymes should be a high enzymatic activity, cellular localization and the ability to use a desired substrate rather than a perfect specificity for the desired substrate. Furthermore, investigations of novel FAR/WS(D) combinations will aid to identify the combinations, that are adapted best to each other as well as to the host plant metabolism. Ongoing identification and characterization of new WE producing enzymes will help to expand the number of proteins available for transgenic WE formation. The characterization of MaWSD5 as part of this thesis (Article I) adds a new protein to the list of suitable WS(D) enzymes. Besides being able to catalyze the formation of a variety of WE species, MaWSD5 has the advantage to lack DGAT activity and hence does not produce TAG in an undesired side reaction. The availability of WSD crystal structures and the identification of substrate binding sites provide the opportunity to engineer WSD enzymes regarding substrate specificities and enzymatic activity. As the DAG binding pocket and potential CoA binding residues were identified within this thesis (Article II), binding pockets for all WSD substrates are known now. Introduced changes on the surface of the proteins may facilitate furthermore improved or altered binding to cellular membranes, which are the locations of storage lipid synthesis and packaging.

Storage capacities of the host organism determine how much WE are synthesized and stored without causing harmful morphological alterations. As first studies indicate, that WE need a different cellular packaging than TAG do (Ivarson *et al.*, 2017; Sturtevant *et al.*, 2020), it is especially important for the future to identify proteins supporting the correct storage of WE. The LDAP1 protein from jojoba, as suggested by Sturtevant *et al.* (2020), is a promising

candidate. Regarding the usage of bacterial WSD proteins, more work is required to identify how and in which cellular domains these enzymes synthesize and deposit WE. A lack of WE deposition between membrane leaflets might prohibit the use of the endogenous neutral lipid storage machinery and may require the co-expression of proteins aiding in WE storage. An investigation by transmission electron microscopy of the plastidial micro domains to which MaFAR and MaWSD5 co-localized as observed in this thesis (Article III) may provide further information on this.

Apart from WE packaging, WE mobilization is an important aspect to consider. When WE content will be increased in transgenic plants, TAG amounts will get reduced consequently. As TAG are degraded during germination to provide energy and carbon, germination rates might get reduced in plants with high WE levels, when the seeds fail to hydrolyze WE for fatty acid supply. This can lead to a counter-selection towards plants with lower WE and higher TAG levels. Hence, in order to not lose these plants during propagation, the expression of a lipase, suitable to cleave the WE bond, might be helpful to allow the consumption of WE during germination. Nevertheless, besides fatty acids, fatty alcohols are set free upon ester bond cleavage, which themselves or their degradation products can be harmful to plant cells as Aslan *et al.* (2015b) observed chlorotic stems and leaves, as well as stunted growth associated with fatty alcohol accumulation in *N. benthamiana* plants. Therefore, WE breakdown reactions should only be introduced into plant cells, when a complete fatty alcohol degradation yielding harmless products is ensured. Cellular fatty alcohols can also increase upon high FAR and low WS activities, leading to an accumulation of newly synthesized fatty alcohols. Hence, a balanced interplay between FAR and WS activities is needed to prevent this.

REFERENCES

- Aarts MGM, Dirkse WG, Stiekema WJ, Pereira A. 1993. Transposon tagging of a male sterility gene in *Arabidopsis*. *Nature* **363**(6431): 715-717.
- Aarts MGM, Hodge R, Kalantidis K, Florack D, Wilson ZA, Mulligan BJ, Stiekema WJ, Scott R, Pereira A. 1997. The *Arabidopsis* MALE STERILITY 2 protein shares similarity with reductases in elongation/condensation complexes. *The Plant Journal* **12**(3): 615-623.
- Adams PD, Afonine PV, Bunkoczi G, Chen VB, Davis IW, Echols N, Headd JJ, Hung LW, Kapral GJ, Grosse-Kunstleve RW, et al. 2010. PHENIX: a comprehensive Python-based system for macromolecular structure solution. *Acta Cryst.* **D66**(Pt 2): 213-221.
- Aichholz R, Lorbeer E. 2000. Investigation of combwax of honeybees with high-temperature gas chromatography and high-temperature gas chromatography–chemical ionization mass spectrometry: II: High-temperature gas chromatography–chemical ionization mass spectrometry. *Journal of Chromatography A* **883**(1–2): 75-88.
- Al-Obaidi JR, Halabi MF, Alkhalifah NS, Asanar S, Al-Soqeer AA, Attia MF. 2017. A review on plant importance, biotechnological aspects, and cultivation challenges of jojoba plant. *Biological Research* **50**(1): 25.
- Alban C, Baldet P, Douce R. 1994. Localization and characterization of two structurally different forms of acetyl-CoA carboxylase in young pea leaves, of which one is sensitive to aryloxyphenoxypropionate herbicides. *Biochemical Journal* **300**(2): 557-565.
- Alvarez AF, Alvarez HM, Kalscheuer R, Waltermann M, Steinbuchel A. 2008. Cloning and characterization of a gene involved in triacylglycerol biosynthesis and identification of additional homologous genes in the oleaginous bacterium *Rhodococcus opacus* PD630. *Microbiology* **154**(8): 2327-2335.
- Alvarez HM. 2016. Triacylglycerol and wax ester-accumulating machinery in prokaryotes. *Biochimie* **120**: 28-39.
- Arabolaza A, Rodriguez E, Altabe S, Alvarez H, Gramajo H. 2008. Multiple Pathways for Triacylglycerol Biosynthesis in *Streptomyces coelicolor*. *Applied and Environmental Microbiology* **74**(9): 2573-2582.
- Aslan S, Hofvander P, Dutta P, Sitbon F, Sun C. 2015a. Transient silencing of the KASII genes is feasible in *Nicotiana benthamiana* for metabolic engineering of wax ester composition. *Scientific Reports* **5**.
- Aslan S, Hofvander P, Dutta P, Sun C, Sitbon F. 2015b. Increased production of wax esters in transgenic tobacco plants by expression of a fatty acid reductase:wax synthase gene fusion. *Transgenic Research* **24**: 945-953.
- Aslan S, Sun C, Leonova S, Dutta P, Dörmann P, Domergue F, Stymne S, Hofvander P. 2014. Wax esters of different compositions produced via engineering of leaf chloroplast metabolism in *Nicotiana benthamiana*. *Metabolic Engineering* **25**: 103-112.
- Athenstaedt K, Daum G. 2006. The life cycle of neutral lipids: synthesis, storage and degradation. *Cellular and Molecular Life Sciences CMLS* **63**(12): 1355-1369.
- Bacchin P, Robertiello A, Viglia A. 1974. Identification of n-Decane oxidation products in *Corynebacterium* cultures by combined gas chromatography-mass spectrometry. *Applied Microbiology* **28**(5): 737-741.
- Bagge LE, Koopman HN, Rommel SA, McLellan WA, Pabst DA. 2012. Lipid class and depth-specific thermal properties in the blubber of the short-finned pilot whale and the pygmy sperm whale. *The Journal of Experimental Biology* **215**(24): 4330-4339.
- Baker NA, Sept D, Joseph S, Holst MJ, McCammon JA. 2001. Electrostatics of nanosystems: application to microtubules and the ribosome. *Proceedings of the National Academy of Sciences* **98**(18): 10037-10041.
- Barney BM, Mann RL, Ohlert JM. 2013. Identification of a residue affecting fatty alcohol selectivity in wax ester synthase. *Applied and Environmental Microbiology* **79**(1): 396-399.

- Barney BM, Ohlert JM, Timler JG, Lijewski AM. 2015.** Altering small and medium alcohol selectivity in the wax ester synthase. *Applied Microbiology and Biotechnology* **99**(22): 9675-9684.
- Barney BM, Wahlen BD, Garner E, Wei J, Seefeldt LC. 2012.** Differences in substrate specificities of five bacterial wax ester synthases. *Applied and Environmental Microbiology* **78**(16): 5734-5745.
- Baud S, Boutin J-P, Miquel M, Lepiniec L, Rochat C. 2002.** An integrated overview of seed development in *Arabidopsis thaliana* ecotype WS. *Plant Physiology and Biochemistry* **40**(2): 151-160.
- Blomquist GJ, Chu AJ, Remaley S. 1980.** Biosynthesis of wax in the honeybee, *Apis mellifera* L. *Insect Biochemistry* **10**(3): 313-321.
- Blomquist GJ, Soliday CL, Byers BA, Brakke JW, Jackson LL. 1972.** Cuticular lipids of insects: V. Cuticular wax esters of secondary alcohols from the grasshoppers *Melanoplus packardii* and *Melanoplus sanguinipes*. *Lipids* **7**(5): 356-362.
- Bonaventure G, Salas JJ, Pollard MR, Ohlrogge JB. 2003.** Disruption of the *FATB* gene in *Arabidopsis* demonstrates an essential role of saturated fatty acids in plant growth. *The Plant Cell* **15**(4): 1020-1033.
- Bradford MM. 1976.** A rapid and sensitive method for the quantitation of microgram quantities of proteins utilizing the principle of protein-dye binding. *Analytical Biochemistry* **72**: 248-254.
- Bredemeier R, Hulsch R, Metzger JO, Berthe-Corti L. 2003.** Submersed culture production of extracellular wax esters by the marine bacterium *Fundibacter jadensis*. *Marine Biotechnology* **5**(6): 579-583.
- Bryn K, Jantzen E, Bøvre K. 1977.** Occurrence and patterns of waxes in Neisseriaceae. *Microbiology* **102**(1): 33-43.
- Busson-Breyse J, Farines M, Soulier J. 1994.** Jojoba wax: Its esters and some of its minor components. *Journal of the American Oil Chemists' Society* **71**(9): 999-1002.
- Carlsson AS, Yilmaz JL, Green AG, Szymne S, Hofvander P. 2011.** Replacing fossil oil with fresh oil – with what and for what? *European Journal of Lipid Science and Technology* **113**(7): 812-831.
- Challinor CJ, Hamilton RJ, Simpson K. 1969.** Sperm whale head oil: Part I. The ester fraction. *Chemistry and Physics of Lipids* **3**(2): 145-151.
- Chapman KD, Dyer JM, Mullen RT. 2013.** Commentary: Why don't plant leaves get fat? *Plant Science* **207**(0): 128-134.
- Chen W, Yu X-H, Zhang K, Shi J, De Oliveira S, Schreiber L, Shanklin J, Zhang D. 2011.** Male Sterile2 Encodes a Plastid-Localized Fatty Acyl Carrier Protein Reductase Required for Pollen Exine Development in *Arabidopsis*. *Plant Physiology* **157**(2): 842-853.
- Cheng JB, Russell DW. 2004a.** Mammalian wax biosynthesis: I. Identification of two fatty acyl-CoA reductases with different substrate specificities and tissue distributions. *J. Biol. Chem.* **279**(36): 37789-37797.
- Cheng JB, Russell DW. 2004b.** Mammalian wax biosynthesis: II. Expression cloning of wax synthase cDNAs encoding a member of the acyltransferase enzyme family. *Journal of Biological Chemistry* **279**(36): 37798-37807.
- Chovancova E, Pavelka A, Benes P, Strnad O, Brezovsky J, Kozlikova B, Gora A, Sustr V, Klvana M, Medek P, et al. 2012.** CAVER 3.0: a tool for the analysis of transport pathways in dynamic protein structures. *PLOS Computational Biology* **8**(10): e1002708.
- Clarke MR. 1970.** Function of the spermaceti organ of the sperm whale. *Nature* **228**(5274): 873-874.
- Clough RC, Matthis AL, Barnum SR, Jaworski JG. 1992.** Purification and characterization of 3-ketoacyl-acyl carrier protein synthase III from spinach. A condensing enzyme utilizing acetyl-coenzyme A to initiate fatty acid synthesis. *Journal of Biological Chemistry* **267**(29): 20992-20998.
- Craig JP, Tomlinson A. 1997.** Importance of the lipid layer in human tear film stability and evaporation. *Optometry and Vision Science* **74**(1): 8-13.
- Daniel J, Deb C, Dubey VS, Sirakova TD, Abomoelak B, Morbidoni HR, Kolattukudy PE. 2004.** Induction of a novel class of diacylglycerol acyltransferases and triacylglycerol accumulation

- in *Mycobacterium tuberculosis* as it goes into a dormancy-like state in culture. *Journal of Bacteriology* **186**(15): 5017-5030.
- Davies HM. 1993.** Medium chain acyl-ACP hydrolysis activities of developing oilseeds. *Phytochemistry* **33**(6): 1353-1356.
- de Freitas CAS, de Sousa PHM, Soares DJ, da Silva JYG, Benjamin SR, Guedes MIF. 2019.** Carnauba wax uses in food – A review. *Food Chemistry* **291**: 38-48.
- Doan TTP, Carlsson AS, Hamberg M, Bülow L, Stymne S, Olsson P. 2009.** Functional expression of five Arabidopsis fatty acyl-CoA reductase genes in *Escherichia coli*. *Journal of Plant Physiology* **166**(8): 787-796.
- Dolinsky TJ, Nielsen JE, McCammon JA, Baker NA. 2004.** PDB2PQR: an automated pipeline for the setup of Poisson–Boltzmann electrostatics calculations. *Nucleic Acids Research* **32**(suppl_2): W665-W667.
- Domergue F, Vishwanath SJ, Joubes J, Ono J, Lee JA, Bourdon M, Alhattab R, Lowe C, Pascal S, Lessire R, et al. 2010.** Three Arabidopsis fatty acyl-coenzyme A reductases, FAR1, FAR4, and FAR5, generate primary fatty alcohols associated with suberin deposition. *Plant Physiology* **153**(4): 1539-1554.
- Dörmann P, Spener F, Ohlrogge JB. 1993.** Characterization of two acyl-acyl carrier protein thioesterases from developing *Cuphea* seeds specific for medium-chain- and oleoyl-acyl carrier protein. *Planta* **189**(3): 425-432.
- Dörmann P, Voelker TA, Ohlrogge JB. 1995.** Cloning and expression in *Escherichia coli* of a novel thioesterase from *Arabidopsis thaliana* specific for long-chain acyl-acyl carrier proteins. *Archives of Biochemistry and Biophysics* **316**(1): 612-618.
- Duncan CC, Yermanos DM, Kumamoto J, Levesque CS. 1974.** Rapid ethanolysis procedure for jojoba wax analysis by gas liquid chromatography. *Journal of the American Oil Chemists Society* **51**(12): 534-536.
- Emsley P, Cowtan K. 2004.** Coot: model-building tools for molecular graphics. *Acta Crystallogr D Biol Crystallogr* **60**(Pt 12 Pt 1): 2126-2132.
- Fixter LM, Fewson CA. 1974.** The accumulation of waxes by *Acinetobacter calcoaceticus* N.C.I.B. 8250. *Biochemical Society Transactions* **2**(5): 944-945.
- Fixter LM, McCormack JG. 1976.** The effect of growth conditions on the wax content of various strains of *Acinetobacter*. *Biochemical Society Transactions* **4**(3): 504-505.
- Fixter LM, Nagi MN, McCormack JG, Fewson CA. 1986.** Structure, distribution and function of wax esters in *Acinetobacter calcoaceticus*. *Journal of General Microbiology* **132**(11): 3147-3157.
- Focks N, Benning C. 1998.** *wrinkled1*: A novel, low-seed-oil mutant of Arabidopsis with a deficiency in the seed-specific regulation of carbohydrate metabolism. *Plant Physiology* **118**(1): 91-101.
- Gallagher IHC. 1971.** Occurrence of waxes in *Acinetobacter*. *Microbiology* **68**(2): 245-247.
- Gibbs A. 1995.** Physical properties of insect cuticular hydrocarbons: model mixtures and lipid interactions. *Comparative Biochemistry and Physiology Part B: Biochemistry and Molecular Biology* **112**(4): 667-672.
- Gupta R, Gupta N, Rathi P. 2004.** Bacterial lipases: an overview of production, purification and biochemical properties. *Applied Microbiology and Biotechnology* **64**(6): 763-781.
- Hagemann JW, Rothfus JA. 1979.** Oxidative stability of wax Esters by thermogravimetric analysis. *Journal of the American Oil Chemists' Society* **56**(6): 629-631.
- Hedstrom L. 2002.** Serine protease mechanism and specificity. *Chemical Reviews* **102**(12): 4501-4524.
- Heilmann M, Iven T, Ahmann K, Hornung E, Stymne S, Feussner I. 2012.** Production of wax esters in plant seed oils by oleosomal cotargeting of biosynthetic enzymes. *Journal of Lipid Research* **53**(10): 2153-2161.
- Hills G. 2003.** Industrial use of lipases to produce fatty acid esters. *European Journal of Lipid Science and Technology* **105**(10): 601-607.
- Hofvander P, Doan TTP, Hamberg M. 2011.** A prokaryotic acyl-CoA reductase performing reduction of fatty acyl-CoA to fatty alcohol. *FEBS Letters* **585**(22): 3538-3543.

- Holm L. 2020.** DALI and the persistence of protein shape. *Protein Science* **29**(1): 128-140.
- Holtzapple E, Schmidt-Dannert C. 2007.** Biosynthesis of isoprenoid wax ester in *Marinobacter hydrocarbonoclasticus* DSM 8798: Identification and characterization of isoprenoid Coenzyme A synthetase and wax ester synthases. *Journal of Bacteriology* **189**(10): 3804-3812.
- Hölzl G, Dörmann P. 2019.** Chloroplast lipids and their biosynthesis. *Annual Review of Plant Biology* **70**(1): 51-81.
- Hsu S-C, Belmonte MF, Harada JJ, Inoue K. 2010.** Indispensable roles of plastids in *Arabidopsis thaliana* embryogenesis. *Current Genomics* **11**(1875-5488 (Electronic)): 338-349.
- Huu NB, Denner EBM, Ha DTC, Wanner G, Stan-Lotter H. 1999.** *Marinobacter aquaeolei* sp. nov., a halophilic bacterium isolated from a Vietnamese oil-producing well. *International Journal of Systematic and Evolutionary Microbiology* **49**(2): 367-375.
- Ischebeck T, Krawczyk HE, Mullen RT, Dyer JM, Chapman KD. 2020.** Lipid droplets in plants and algae: Distribution, formation, turnover and function. *Seminars in Cell & Developmental Biology*.
- Ishige T, Tani A, Takabe K, Kawasaki K, Sakai Y, Kato N. 2002.** Wax ester production from *n*-alkanes by *Acinetobacter* sp. strain M-1: Ultrastructure of cellular inclusions and role of acyl coenzyme A reductase. *Applied and Environmental Microbiology* **68**(3): 1192-1195.
- Ivarson E, Iven T, Sturtevant D, Ahlman A, Cai Y, Chapman K, Feussner I, Zhu L-H. 2017.** Production of wax esters in the wild oil species *Lepidium campestre*. *Industrial Crops and Products* **108**: 535-542.
- Iven T, Herrfurth C, Hornung E, Heilmann M, Hofvander P, Stymne S, Zhu L-H, Feussner I. 2013.** Wax ester profiling of seed oil by nano-electrospray ionization tandem mass spectrometry. *Plant Methods* **9**(1): 24.
- Iven T, Hornung E, Heilmann M, Feussner I. 2016.** Synthesis of oleyl oleate wax esters in *Arabidopsis thaliana* and *Camelina sativa* seed oil. *Plant Biotechnology Journal* **14**(1): 252–259.
- Jackson LL, Baker GL. 1970.** Cuticular lipids of insects. *Lipids* **5**(2): 239-246.
- Jacobsen E, Billings JK, Frantz RA, Kinney CK, Stewart ME, Downing DT. 1985.** Age-related changes in sebaceous wax ester secretion rates in men and women. *The Journal of Investigative Dermatology* **85**(5): 483-485.
- Jacobson BS, Jaworski JG, Stumpf PK. 1974.** Fat metabolism in higher plants. LXII. Stearyl-acyl carrier protein desaturase from spinach chloroplasts. *Plant Physiology* **54**(4): 484-486.
- Jaworski JG, Post-Beittenmiller D, Ohlrogge JB. 1993.** Acetyl-acyl carrier protein is not a major intermediate in fatty acid biosynthesis in spinach. *European Journal of Biochemistry* **213**(3): 981-987.
- Jessen D, Roth C, Wiermer M, Fulda M. 2015.** Two activities of long-chain acyl-Coenzyme A synthetase are involved in lipid trafficking between the endoplasmic reticulum and the plastid in *Arabidopsis*. *Plant Physiology* **167**(2): 351-366.
- Jones A, Davies HM, Voelker TA. 1995.** Palmitoyl-acyl carrier protein (ACP) thioesterase and the evolutionary origin of plant acyl-ACP thioesterases. *The Plant Cell* **7**(3): 359-371.
- Kabsch W. 1993.** Automatic processing of rotation diffraction data from crystals of initially unknown symmetry and cell constants. *Journal of Applied Crystallography* **26**(6): 795-800.
- Kaddor C, Biermann K, Kalscheuer R, Steinbüchel A. 2009.** Analysis of neutral lipid biosynthesis in *Streptomyces avermitilis* MA-4680 and characterization of an acyltransferase involved herein. *Applied Microbiology and Biotechnology* **84**(1): 143-155.
- Kalscheuer R, Luftmann H, Steinbüchel A. 2004.** Synthesis of novel lipids in *Saccharomyces cerevisiae* by heterologous expression of an unspecific bacterial acyltransferase. *Applied and Environmental Microbiology* **70**(12): 7119-7125.
- Kalscheuer R, Steinbüchel A. 2003.** A novel bifunctional wax ester synthase/acyl-CoA:diacylglycerol acyltransferase mediates wax ester and triacylglycerol biosynthesis in *Acinetobacter calcoaceticus* ADP1. *Journal of Biological Chemistry* **278**(10): 8075-8082.

- Kalscheuer R, Stolting T, Steinbuchel A. 2006a. Microdiesel: *Escherichia coli* engineered for fuel production. *Microbiology* **152**(9): 2529-2536.
- Kalscheuer R, Stoveken T, Luftmann H, Malkus U, Reichelt R, Steinbüchel A. 2006b. Neutral lipid biosynthesis in engineered *Escherichia coli*: Jojoba oil-like wax esters and fatty acid butyl esters. *Appl. Environ. Microbiol.* **72**(2): 1373-1379.
- Kalscheuer R, Stoveken T, Malkus U, Reichelt R, Golyshin PN, Sabirova JS, Ferrer M, Timmis KN, Steinbuchel A. 2007. Analysis of storage lipid accumulation in *Alcanivorax borkumensis*: Evidence for alternative triacylglycerol biosynthesis routes in bacteria. *Journal of Bacteriology* **189**(3): 918-928.
- Kaneshiro T, Nakamura LK, Nicholson JJ, Bagby MO. 1996. Oleyl oleate and homologous wax esters synthesized coordinately from oleic acid by *Acinetobacter* and coryneform strains. *Current Microbiology* **32**(6): 336-342.
- Karmakar G, Ghosh P, Sharma BK. 2017. Chemically modifying vegetable oils to prepare green lubricants. *Lubricants* **5**(4): 44.
- Kawelke SJ. 2014. *Structure-function relationships in wax producing enzymes*. Dissertation, Göttingen.
- King A, Nam J-W, Han J, Hilliard J, Jaworski J. 2007. Cuticular wax biosynthesis in petunia petals: cloning and characterization of an alcohol-acyltransferase that synthesizes wax-esters. *Planta* **226**(2): 381-394.
- Knutson CM, Lenneman EM, Barney BM 2017. *Marinobacter* as a model organism for wax ester accumulation in bacteria. In: Geiger O ed. *Biogenesis of Fatty Acids, Lipids and Membranes*. Cham: Springer International Publishing, 1-22.
- Konishi T, Shinohara K, Yamada K, Sasaki Y. 1996. Acetyl-CoA carboxylase in higher plants: Most plants other than Gramineae have both the prokaryotic and the eukaryotic forms of this enzyme. *Plant and Cell Physiology* **37**(2): 117-122.
- Koshland DE. 1958. Application of a theory of enzyme specificity to protein synthesis. *Proceedings of the National Academy of Sciences of the United States of America* **44**(2): 98-104.
- Kunst L, Samuels AL. 2003. Biosynthesis and secretion of plant cuticular wax. *Progress in Lipid Research* **42**(1): 51-80.
- Kunst L, Taylor DC, Underhill EW. 1992. Fatty acid elongation in developing seeds of *Arabidopsis thaliana*. *Plant Physiology and Biochemistry* **30**(4): 425-434.
- Lardizabal KD, Metz JG, Sakamoto T, Hutton WC, Pollard MR, Lassner MW. 2000. Purification of a Jojoba embryo wax synthase, cloning of its cDNA, and production of high levels of wax in seeds of transgenic *Arabidopsis*. *Plant Physiology* **122**(3): 645-656.
- Lawlor DW 2001. table 4.1 'A semi quantitative analysis of the photosynthetic system in an 'average' C3 plant leaf'. *Photosynthesis: molecular, physiological, and environmental processes*: BIOS scientific publishers limited, p.58.
- Lázaro B, Villa JA, Santín O, Cabezas M, Milagre CDF, de la Cruz F, Moncalián G. 2017. Heterologous expression of a thermophilic diacylglycerol acyltransferase triggers triglyceride accumulation in *Escherichia coli*. *PLOS ONE* **12**(4): e0176520.
- Lee KH, Kim DH, Lee SW, Kim ZH, Hwang I. 2002. *In vivo* Import Experiments in Protoplasts Reveal the Importance of the Overall Context but Not Specific Amino Acid Residues of the Transit Peptide during Import into Chloroplasts. *Molecules & Cells* **14**(3): 388-397.
- Lenneman EM, Ohlert JM, Palani NP, Barney BM. 2013. Fatty alcohols for wax esters in *Marinobacter aquaeolei* VT8: two optional routes in the wax biosynthesis pathway. *Applied Environmental Microbiology* **79**(22): 7055-7062.
- Lerner M, Carlson H 2006. APBS plugin for PyMOL. University of Michigan, Ann Arbor.
- Li F, Wu X, Lam P, Bird D, Zheng H, Samuels L, Jetter R, Kunst L. 2008. Identification of the wax ester synthase/acyl-Coenzyme A:diacylglycerol acyltransferase WSD1 required for stem wax ester biosynthesis in *Arabidopsis*. *Plant Physiology* **148**(1): 97-107.
- Li N, Gügel IL, Giavalisco P, Zeisler V, Schreiber L, Soll J, Philippark K. 2015. FAX1, a novel membrane protein mediating plastid fatty acid export. *PLoS Biology* **13**(2): e1002053.

- Ma W, Kong Q, Arondel V, Kilaru A, Bates PD, Thrower NA, Benning C, Ohlrogge JB. 2013. *WRINKLED1*, A Ubiquitous Regulator in Oil Accumulating Tissues from *Arabidopsis* Embryos to Oil Palm Mesocarp. *PLoS ONE* **8**(7): e68887.
- Madeira F, Park YM, Lee J, Buso N, Gur T, Madhusoodanan N, Basutkar P, Tivey ARN, Potter SC, Finn RD, et al. 2019. The EMBL-EBI search and sequence analysis tools APIs in 2019. *Nucleic Acids Research* **47**(W1): W636-W641.
- Márquez MC, Ventosa A. 2005. *Marinobacter hydrocarbonoclasticus* Gauthier et al. 1992 and *Marinobacter aquaeolei* Nguyen et al. 1999 are heterotypic synonyms. *International Journal of Systematic and Evolutionary Microbiology* **55**(3): 1349-1351.
- Metz JG, Pollard MR, Anderson L, Hayes TR, Lassner MW. 2000. Purification of a Jojoba embryo fatty acyl-Coenzyme A reductase and expression of its cDNA in high erucic acid rapeseed. *Plant Physiology* **122**(3): 635-644.
- Miklaszewska M, Dittrich-Domergue F, Banaś A, Domergue F. 2018. Wax synthase MhWS2 from *Marinobacter hydrocarbonoclasticus*: substrate specificity and biotechnological potential for wax ester production. *Applied Microbiology and Biotechnology* **102**: 4063-4074.
- Miklaszewska M, Kawinski A, Banaś A. 2013. Detailed characterization of the substrate specificity of mouse wax synthase. *Acta Biochimica Polonica* **60**(2): 209-215.
- Miller PJO, Johnson MP, Tyack PL, Terray EA. 2004. Swimming gaits, passive drag and buoyancy of diving sperm whales *Physeter macrocephalus*. *Journal of Experimental Biology* **207**(11): 1953-1967.
- Miwa TK. 1971. Jojoba oil wax esters and derived fatty acids and alcohols - Gas chromatographic analyses. *Journal of the American Oil Chemists Society* **48**(6): 259-264.
- Moreno-Pérez A, Venegas-Calderón M, Vaistij F, Salas J, Larson T, Garcés R, Graham I, Martínez-Force E. 2012. Reduced expression of FatA thioesterases in *Arabidopsis* affects the oil content and fatty acid composition of the seeds. *Planta* **235**(3): 629-639.
- Morris RJ. 1973. The lipid structure of the spermaceti organ of the sperm whale (*Physeter catodon*). *Deep Sea Research and Oceanographic Abstracts* **20**(10): 911-916.
- Murzin AG, Brenner SE, Hubbard T, Chothia C. 1995. SCOP: a structural classification of proteins database for the investigation of sequences and structures. *Journal of Molecular Biology* **247**(4): 536-540.
- Nelson DR, Tissot M, Nelson LJ, Fatland CL, Gordon DM. 2001. Novel wax esters and hydrocarbons in the cuticular surface lipids of the red harvester ant, *Pogonomyrmex barbatus*. *Comparative Biochemistry and Physiology Part B: Biochemistry and Molecular Biology* **128**(3): 575-595.
- Ohlrogge JB, Jaworski JG. 1997. Regulation of fatty acid synthesis. *Annual Review of Plant Physiology and Plant Molecular Biology* **48**: 109-136.
- Okuley J, Lightner J, Feldmann K, Yadav N, Lark E, Browse J. 1994. *Arabidopsis FAD2* gene encodes the enzyme that is essential for polyunsaturated lipid synthesis. *The Plant Cell* **6**(1): 147-158.
- Pape T, Schneider T. 2004. HKL2MAP: a graphical user interface for macromolecular phasing with SHELX programs. *Journal of Applied Crystallography - J APPL CRYST* **37**: 843-844.
- Patel S, Nelson DR, Gibbs AG. 2001. Chemical and physical analyses of wax ester properties. *Journal of Insect Science* **1**(1): 4.
- Pavelka A, Sebestova E, Kozlikova B, Brezovsky J, Sochor J, Damborsky J. 2016. CAVER: algorithms for analyzing dynamics of tunnels in macromolecules. *IEEE/ACM Transactions on Computational Biology and Bioinformatics* **13**(3): 505-517.
- Perrakis A, Morris R, Lamzin VS. 1999. Automated protein model building combined with iterative structure refinement. *Nature Structural & Molecular Biology* **6**(5): 458-463.
- Petronikolou N, Nair S. 2018. Structural and biochemical studies of a biocatalyst for the enzymatic production of wax esters. *ACS Catalysis* **8**(7): 6334-6344.
- Pogson BJ, Albrecht V. 2011. Genetic dissection of chloroplast biogenesis and development: An overview. *Plant Physiology* **155**(4): 1545-1551.
- Poliner E, Pulman JA, Zienkiewicz K, Childs K, Benning C, Farré EM. 2018. A toolkit for *Nannochloropsis oceanica* CCMP1779 enables gene stacking and genetic engineering of the

- icosapentaenoic acid pathway for enhanced long-chain polyunsaturated fatty acid production. *Plant Biotechnology Journal* **16**(1): 298-309.
- Pollard MR, Anderson L, Fan C, Hawkins DJ, Davies HM. 1991.** A specific acyl-ACP thioesterase implicated in medium-chain fatty acid production in immature cotyledons of *Umbellularia californica*. *Archives of Biochemistry and Biophysics* **284**(2): 306-312.
- Post-Beittenmiller D. 1996.** Biochemistry and molecular biology of wax production in plants. *Annual Review of Plant Physiology and Plant Molecular Biology* **47**: 405-430.
- Qian H, Zhao X, Yan R, Yao X, Gao S, Sun X, Du X, Yang H, Wong CCL, Yan N. 2020.** Structural basis for catalysis and substrate specificity of human ACAT1. *Nature* **581**(7808): 333-338.
- Rantamäki AH, Wiedmer SK, Holopainen JM. 2013.** Melting points—The key to the anti-evaporative effect of the tear film wax esters. *Investigative Ophthalmology & Visual Science* **54**(8): 5211-5217.
- Raymond RL, Davis JB. 1960.** *n*-Alkane utilization and lipid formation by a *Nocardia*. *Applied Microbiology* **8**(6): 329-334.
- Razeq FM, Kosma DK, Rowland O, Molina I. 2014.** Extracellular lipids of *Camelina sativa*: Characterization of chloroform-extractable waxes from aerial and subterranean surfaces. *Phytochemistry* **106**(0): 188-196.
- Reetz MT, Carballeira JD, Vogel A. 2006.** Iterative saturation mutagenesis on the basis of B factors as a strategy for increasing protein thermostability. *Angewandte Chemie International Edition* **45**(46): 7745-7751.
- Reetz MT, Soni P, Acevedo JP, Sanchis J. 2009.** Creation of an amino acid network of structurally coupled residues in the directed evolution of a thermostable enzyme. *Angewandte Chemie International Edition* **48**(44): 8268-8272.
- Reetz MT, Soni P, Fernández L, Gumulya Y, Carballeira JD. 2010.** Increasing the stability of an enzyme toward hostile organic solvents by directed evolution based on iterative saturation mutagenesis using the B-FIT method. *Chemical Communications* **46**(45): 8657-8658.
- Reiser S, Somerville C. 1997.** Isolation of mutants of *Acinetobacter calcoaceticus* deficient in wax ester synthesis and complementation of one mutation with a gene encoding a fatty acyl coenzyme A reductase. *Journal of Bacteriology* **179**(9): 2969-2975.
- Roesler KR, Savage LJ, Shintani DK, Shorrosh BS, Ohlrogge JB. 1996.** Co-purification, co-immunoprecipitation, and coordinate expression of acetyl-coenzyme A carboxylase activity, biotin carboxylase, and biotin carboxyl carrier protein of higher plants. *Planta* **198**: 517-525.
- Rontani J-F. 2010.** Production of wax esters by bacteria. In: Timmis KN ed. *Handbook of Hydrocarbon and Lipid Microbiology*. Berlin, Heidelberg: Springer Berlin Heidelberg, 459-470.
- Rontani J-F, Bonin PC, Volkman JK. 1999.** Production of wax esters during aerobic growth of marine bacteria on isoprenoid compounds. *Applied and Environmental Microbiology* **65**(1): 221-230.
- Rontani J-F, Mouzdahir A, Michotey V, Caumette P, Bonin P. 2003.** Production of a polyunsaturated isoprenoid wax ester during aerobic metabolism of squalene by *Marinobacter squalenivorans* sp. nov. *Applied and Environmental Microbiology* **69**(7): 4167-4176.
- Röttig A, Steinbüchel A. 2013a.** Acyltransferases in bacteria. *Microbiology and Molecular Biology Reviews* **77**(2): 277-321.
- Röttig A, Steinbüchel A. 2013b.** Random mutagenesis of *atfA* and screening for *Acinetobacter baylyi* mutants with an altered lipid accumulation. *European Journal of Lipid Science and Technology* **115**(4): 394-404.
- Röttig A, Wolf S, Steinbüchel A. 2016.** In vitro characterization of five bacterial WS/DGAT acyltransferases regarding the synthesis of biotechnologically relevant short-chain-length esters. *European Journal of Lipid Science and Technology* **118**(1): 124-132.
- Röttig A, Zurek PJ, Steinbüchel A. 2015.** Assessment of bacterial acyltransferases for an efficient lipid production in metabolically engineered strains of *E. coli*. *Metabolic Engineering* **32**: 195-206.
- Rottler A-M, Schulz S, Ayasse M. 2013.** Wax lipids signal nest identity in bumblebee colonies. *Journal of Chemical Ecology* **39**(1): 67-75.

- Rowland O, Domergue F. 2012. Plant fatty acyl reductases: Enzymes generating fatty alcohols for protective layers with potential for industrial applications. *Plant Science* **193-194**(0): 28-38.
- Rowland O, Zheng H, Hepworth SR, Lam P, Jetter R, Kunst L. 2006. *CER4* encodes an alcohol-forming fatty acyl-Coenzyme A reductase involved in cuticular wax production in Arabidopsis. *Plant Physiology* **142**(3): 866-877.
- Ruiz-Lopez N, Broughton R, Usher S, Salas JJ, Haslam RP, Napier JA, Beaudoin F. 2017. Tailoring the composition of novel wax esters in the seeds of transgenic *Camelina sativa* through systematic metabolic engineering. *Plant Biotechnology Journal* **15**(7): 837-849.
- Russell NJ, Volkman JK. 1980. The effect of growth temperature on wax ester composition in the psychrophilic bacterium *Micrococcus cryophilus* ATCC 15174. *Microbiology* **118**(1): 131-141.
- Salas JnJ, Ohlrogge JB. 2002. Characterization of substrate specificity of plant FatA and FatB acyl-ACP thioesterases. *Archives of Biochemistry and Biophysics* **403**(1): 25-34.
- Samuels L, Kunst L, Jetter R. 2008. Sealing plant surfaces: Cuticular wax formation by epidermal cells. *Annual Review of Plant Biology* **59**(1): 683-707.
- Santala S, Efimova E, Koskinen P, Karp MT, Santala V. 2014. Rewiring the wax ester production pathway of *Acinetobacter baylyi* ADP1. *ACS Synthetic Biology* **3**(3): 145-151.
- Santín O, Galié S, Moncalián G. 2019a. Directed evolution of a bacterial WS/DGAT acyltransferase: improving tDGAT from *Thermomonospora curvata*. *Protein Engineering, Design and Selection*.
- Santín O, Galié S, Moncalián G. 2019b. Directed evolution of a bacterial WS/DGAT acyltransferase: improving tDGAT from *Thermomonospora curvata*. *Protein Engineering, Design and Selection* **32**(1): 25-32.
- Schneider CA, Rasband WS, Eliceiri KW. 2012. NIH Image to ImageJ: 25 years of image analysis. *Nature Methods* **9**(7): 671-675.
- Schrödinger L 2006. The PyMOL molecular graphics system, version 0.99rc6.
- Schrödinger L 2010. The PyMOL molecular graphics system, version 1.3r1.
- Schrödinger L 2015. The PyMOL molecular graphics system, version 2.2.0a0.
- Scott CC, Finnerty WR. 1976. Characterization of intracytoplasmic hydrocarbon inclusions from the hydrocarbon-oxidizing *Acinetobacter* species HO1-N. *Journal of Bacteriology* **127**(1): 481-489.
- Shalini T, Martin A. 2020. Identification, isolation, and heterologous expression of Sunflower wax synthase for the synthesis of tailored wax esters. *Journal of Food Biochemistry* n/a(n/a): e13433.
- Shanklin J, Somerville C. 1991. Stearoyl-acyl-carrier-protein desaturase from higher plants is structurally unrelated to the animal and fungal homologs. *Proceedings of the National Academy of Sciences USA* **88**(6): 2510-2514.
- Sheldrick G. 2008. A short history of SHELX. *Acta crystallographica. Section A, Foundations of crystallography* **64**: 112-122.
- Shi S, Octavio Valle-Rodríguez J, Khoomrung S, Siewers V, Nielsen J. 2012. Functional expression and characterization of five wax ester synthases in *Saccharomyces cerevisiae* and their utility for biodiesel production. *Biotechnology for Biofuels* **5**(1): 7.
- Shimakata T, Stumpf PK. 1982. Isolation and function of spinach leaf β -ketoacyl-[acyl-carrier-protein] synthases. *Proceedings of the National Academy of Sciences USA* **79**(19): 5808-5812.
- Silva RA, Grossi V, Alvarez HM. 2007. Biodegradation of phytane (2,6,10,14-tetramethylhexadecane) and accumulation of related isoprenoid wax esters by *Mycobacterium ratisbonense* strain SD4 under nitrogen-starved conditions. *FEMS Microbiology Letters* **272**(2): 220-228.
- Singer ME, Tyler SM, Finnerty WR. 1985. Growth of *Acinetobacter* sp. strain HO1-N on n-hexadecanol: physiological and ultrastructural characteristics. *Journal of Bacteriology* **162**(1): 162-169.
- Smith MA, Dauk M, Ramadan H, Yang H, Seamons LE, Haslam RP, Beaudoin FP, Ramirez-Erosa I, Forseille L. 2013. Involvement of Arabidopsis ACYL-COENZYME A DESATURASE-LIKE2 (At2g31360) in the biosynthesis of the very-long-chain monounsaturated fatty acid components of membrane lipids. *Plant Physiology* **161**(1): 81-96.

- Stöveken T, Kalscheuer R, Malkus U, Reichelt R, Steinbüchel A. 2005.** The wax ester synthase/acyl coenzyme A:diacylglycerol acyltransferase from *Acinetobacter* sp. strain ADP1: Characterization of a novel type of acyltransferase. *Journal of Bacteriology* **187**(4): 1369-1376.
- Stöveken T, Kalscheuer R, Steinbüchel A. 2009.** Both histidine residues of the conserved HHXXXDG motif are essential for wax ester synthase/acyl-CoA:diacylglycerol acyltransferase catalysis. *European Journal of Lipid Science and Technology* **111**(2): 112-119.
- Stubbs CD, Smith AD. 1984.** The modification of mammalian membrane polyunsaturated fatty acid composition in relation to membrane fluidity and function. *Biochimica et Biophysica Acta* **779**(1): 89-137.
- Studier FW. 2005.** Protein production by auto-induction in high-density shaking cultures. *Protein Expression and Purification* **41**(1): 207-234.
- Sturtevant D, Lu S, Zhou Z-W, Shen Y, Wang S, Song J-M, Zhong J, Burks DJ, Yang Z-Q, Yang Q-Y, et al. 2020.** The genome of jojoba (*Simmondsia chinensis*): A taxonomically isolated species that directs wax ester accumulation in its seeds. *Science Advances* **6**(11): eaay3240.
- Sui X, Wang K, Gluchowski NL, Elliott SD, Liao M, Walther TC, Farese RV. 2020.** Structure and catalytic mechanism of a human triacylglycerol-synthesis enzyme. *Nature*.
- Tada A, Ishizuki K, Yamazaki T, Sugimoto N, Akiyama H. 2014.** Method for the determination of natural ester-type gum bases used as food additives via direct analysis of their constituent wax esters using high-temperature GC/MS. *Food Science & Nutrition* **2**(4): 417-425.
- Tulloch AP. 1970.** The composition of beeswax and other waxes secreted by insects. *Lipids* **5**(2): 247-258.
- Uthoff S, Stoveken T, Weber N, Vosmann K, Klein E, Kalscheuer R, Steinbuchel A. 2005.** Thio Wax Ester Biosynthesis Utilizing the Unspecific Bifunctional Wax Ester Synthase/Acyl Coenzyme A:Diacylglycerol Acyltransferase of *Acinetobacter* sp. Strain ADP1. *Appl. Environ. Microbiol.* **71**(2): 790-796.
- Van Duyne GD, Standaert RF, Karplus PA, Schreiber SL, Clardy J. 1993.** Atomic structures of the human immunophilin FKBP-12 complexes with FK506 and rapamycin. *Journal of Molecular Biology* **229**(1): 105-124.
- van Wijk KJ, Kessler F. 2017.** Plastoglobuli: Plastid microcompartments with integrated functions in metabolism, plastid developmental transitions, and environmental adaptation. *Annu. Rev. Plant Biol.* **68**: 253-289.
- Vanhercke T, Wood CC, Stymne S, Singh SP, Green AG. 2013.** Metabolic engineering of plant oils and waxes for use as industrial feedstocks. *Plant Biotechnology Journal* **11**(2): 197-210.
- Villa JA, Cabezas M, de la Cruz F, Moncalián G. 2014.** Use of limited proteolysis and mutagenesis to identify folding domains and sequence motifs critical for wax ester synthase/acyl Coenzyme A:diacylglycerol acyltransferase activity. *Applied and Environmental Microbiology* **80**(3): 1132-1141.
- Vioque J, Kolattukudy PE. 1997.** Resolution and purification of an aldehyde-generating and an alcohol-generating fatty acyl-CoA reductase from pea leaves (*Pisum sativum* L.). *Archives of Biochemistry and Biophysics* **340**(1): 64-72.
- Vollheyde K, Yu D, Hornung E, Herrfurth C, Feussner I. 2020.** The fifth WS/DGAT enzyme of the bacterium *Marinobacter aquaeolei* VT8. *Lipids* **55**(5): 479-949.
- Wahlen BD, Oswald WS, Seefeldt LC, Barney BM. 2009.** Purification, Characterization, and Potential Bacterial Wax Production Role of an NADPH-Dependent Fatty Aldehyde Reductase from *Marinobacter aquaeolei* VT8. *Applied Environmental Microbiology* **75**(9): 2758-2764.
- Wallace AC, Laskowski RA, Thornton JM. 1995.** LIGPLOT: a program to generate schematic diagrams of protein-ligand interactions. *Protein Engineering, Design and Selection* **8**(2): 127-134.
- Wältermann M, Hinz A, Robenek H, Troyer D, Reichelt R, Malkus U, Galla H-J, Kalscheuer R, Stöveken T, von Landenberg P, et al. 2005.** Mechanism of lipid-body formation in prokaryotes: how bacteria fatten up. *Molecular Microbiology* **55**(3): 750 - 763.

- Wältermann M, Steinbuchel A. 2005a.** Neutral Lipid Bodies in Prokaryotes: Recent Insights into Structure, Formation, and Relationship to Eukaryotic Lipid Depots. *J. Bacteriol.* **187**(11): 3607-3619.
- Wältermann M, Steinbuchel A. 2005b.** Neutral lipid bodies in prokaryotes: Recent insights into structure, formation, and relationship to eukaryotic lipid depots. *Journal of Bacteriology* **187**(11): 3607-3619.
- Wältermann M, Stöveken T, Steinbüchel A. 2007.** Key enzymes for biosynthesis of neutral lipid storage compounds in prokaryotes: Properties, function and occurrence of wax ester synthases/acyl-CoA:diacylglycerol acyltransferases. *Biochimie* **89**(2): 230-242.
- Wang L, Qian H, Nian Y, Han Y, Ren Z, Zhang H, Hu L, Prasad BVV, Laganowsky A, Yan N, et al. 2020.** Structure and mechanism of human diacylglycerol *O*-acyltransferase 1. *Nature* **581**(7808): 329-332.
- Wang L, Takayama K, Goldman DS, Schnoes HK. 1972.** Synthesis of alcohol and wax ester by a cell-free system in *Mycobacterium tuberculosis*. *Biochimica et Biophysica Acta* **260**(1): 41-48.
- Wei H. 2012.** An overview of wax production, requirement and supply in the world market. *European Chemical Bulletin* **1**(7): 266-268.
- Whited AM, Johns A. 2015.** The interactions of peripheral membrane proteins with biological membranes. *Chemistry and Physics of Lipids* **192**: 51-59.
- Willis RM, Wahlen BD, Seefeldt LC, Barney BM. 2011.** Characterization of a Fatty Acyl-CoA Reductase from *Marinobacter aquaeolei* VT8: A Bacterial Enzyme Catalyzing the Reduction of Fatty Acyl-CoA to Fatty Alcohol. *Biochemistry* **50**(48): 10550-10558.
- Yeats TH, Rose JKC. 2013.** The formation and function of plant cuticles. *Plant Physiology* **163**(1): 5-20.
- Ytterberg AJ, Peltier J-B, van Wijk KJ. 2006.** Protein Profiling of Plastoglobules in Chloroplasts and Chromoplasts. A Surprising Site for Differential Accumulation of Metabolic Enzymes. *Plant Physiology* **140**(3): 984-997.
- Yu D. 2016.** *Production of wax esters in Camelina sativa*. PhD thesis, University of Goettingen.
- Yu D, Hornung E, Iven T, Feussner I. 2018.** High-level accumulation of oleyl oleate in plant seed oil by abundant supply of oleic acid substrates to efficient wax ester synthesis enzymes. *Biotechnology for Biofuels* **11**(1): 53.
- Zhang N, Mao Z, Luo L, Wan X, Huang F, Gong Y. 2017.** Two bifunctional enzymes from the marine protist *Thraustochytrium roseum*: biochemical characterization of wax ester synthase/acyl-CoA:diacylglycerol acyltransferase activity catalyzing wax ester and triacylglycerol synthesis. *Biotechnology for Biofuels* **10**(1): 185.
- Zhu L-H, Krens F, Smith MA, Li X, Qi W, van Loo EN, Iven T, Feussner I, Nazarens TJ, Huai D, et al. 2016.** Dedicated industrial oilseed crops as metabolic engineering platforms for sustainable industrial feedstock production. *Scientific Reports* **6**: 22181.

ACKNOWLEDGEMENTS

First of all, I would like to thank Prof. Dr. Ivo Feußner for providing me with this fascinating project. During my time in his department, I enjoyed working on the diverse topics of WE biosynthesis. I am grateful to Prof. Feußner for all his guidance and support as well as for many discussions we had advancing the project.

I want to thank the members of my thesis advisory committee, Prof. Dr. Andrea Polle and Prof. Dr. Ralf Ficner. I appreciated all advices they gave and the discussions we had during the TAC meetings.

I am thankful to Prof. Dr. Christiane Gatz, PD Dr. Till Ischebeck and PD Dr. Thomas Teichmann for serving as members of my examination board.

I am grateful to all members of the GGNB Office, that do a great job supporting the doctoral students regarding all official issues in connection with doctoral studies in GGNB/GAUSS.

For her fantastic and excellent supervision in the lab, Dr. Ellen Hornung deserves a huge Thank-you. I am grateful, Ellen, for all your guidance and support, for your help and instructions during every day lab work. I am also thankful for your help with the cloning of the plant constructs, for providing me with the different expression vectors, for teaching me GC-FID analyses as well as for proofreading my thesis. With your experience and knowledge, you always came up with solutions solving smaller and larger problems. Apart from the scientific work, thanks a lot for several cooking recipes, lunch meals and especially delicious cakes and cookies, that sweetened many coffee breaks.

I am grateful to Dr. Karin Kühnel, Dr. Steffen Kawelke and Dr. Felix Lambrecht, who made a lot of effort to crystallize AbWSD1. Furthermore, I want to thank Dr. Dan Yu, who identified MaWSD5 and started the purification and characterization of the protein. I could not have worked on my project without the excellent pre-work of these four persons.

I am thankful to Dr. Cornelia Herrfurth for measuring the nanoESI-MS/MS samples of the enzyme activity assays as well as of the *A. thaliana* WE samples. Thank you, Conny, also for your effort and help regarding lipid analysis for the establishment of enzymatic competition assays.

I want to thank Dr. Viktor Sautner from the Department for Molecular Enzymology for recording the CD spectra. Thank you for your advice regarding potential assays to study the proposed conformational change. I also want to thank Dr. Fabian Rabe von Pappenheim for providing me with the instrument settings and measuring parameters after Viktor left the department.

I am furthermore thankful to Dr. Achim Dickmanns, Dr. Piotr Neumann and Dr. Alaa Shaikhqasem from the Department for Molecular Structural Biology. Dr. Achim Dickmanns and Dr. Alaa Shaikhqasem performed the DLS measurement and provided helpful suggestions on how to study the proposed conformational change. Dr. Piotr Neumann also provided advice on this topic. He furthermore explained me how to model acyl-CoA into the structure and helped me whenever I had questions regarding PDB deposition.

I want to thank PD Dr. Till Ischebeck for recording the confocal microscopy images, introducing me to our fluorescence microscope and for helpful discussions regarding potential microscopic analyses of the transgenic *A. thaliana* plants.

Prof. Dr. Agnieszka Zienkiewicz provided me with the fast and easy protein extraction protocol and recorded confocal microscopy images during the first plant screening process. I am grateful to her and her husband, Prof. Dr. Krzysztof Zienkiewicz, for helpful discussions about my project and also for their scientific and personal support.

I would like to thank Dr. Amelie Kelly and Dr. Tegan Haslam for several scientific discussions and suggestions. I am also grateful for their scientific and personal advices regarding future carrier planning.

I owe many thanks to Susanne Mester for taking care of my plants, Andrea Nickel and Maria Paulat for their help with cloning and seed harvesting, as well as Kalina Wolf for seed harvesting and a first WE screening. Furthermore, I would like to thank Sabine Freitag for answering all technical handling questions in terms of lipid analysis.

I want to thank all former and current members of the Department for Plant Biochemistry. I enjoyed the supportive and collaborative working atmosphere and I am grateful to say that several friendships arose from that. I enjoyed the large number of activities we did apart from scientific work: barbecue events, Christmas movie nights and various PhD hat handcraft sessions. All of this made the last years special.

Many thanks to all former and current members of the “AG Ellen” for the supportive and encouraging working atmosphere in our lab. Working and laughing with you was and is great.

Many thanks to my “PhD girls” Franzi, Anna, Milena, Yi-Tse, Elisa and Jasmin. You made my PhD time unforgettable. Jasmin and Elisa deserve a large hug: starting together, working together, cheering together, suffering together, crying together, laughing together and successfully finishing together. Thanks a lot to you two, that we went through the past years together.

I also want to thank Carina and Nina for our long-lasting friendship. I enjoy our regular phone calls, keeping us updated despite we do not live in the same place anymore.

And last but not least, I want to thank my parents and my sister. You are always by my side, supporting and encouraging me in all what I am doing and planning to do. I am grateful for all your help, your guidance and your advices. I am more than thankful for all your motivation and your support especially during the last days before submission. Thank you for all your love and that I can always rely on you.

CURRICULUM VITAE

Katharina Vollheyde

Date of birth: 16.10.1992

Place of birth: Salzgitter (Germany)

Nationality: German

Education

- | | |
|-------------------|--|
| Since 02/2017 | <p>Doctoral Studies
 Göttingen Graduate Center for Neuroscience, Biophysics, and Molecular Bioscience, Göttingen University, Doctoral program: Microbiology and Biochemistry
 Thesis: Department for Plant Biochemistry
 Title: "Characterization of acyltransferases in neutral lipid synthesis"</p> |
| 10/2014 – 12/2016 | <p>Master Studies
 M.Sc. Microbiology and Biochemistry, Göttingen University
 Master Thesis: Department for Plant Biochemistry
 Title: "Biochemical characterization of bacterial wax synthases"</p> |
| 10/2011 – 07/2014 | <p>Bachelor Studies
 B.Sc. Biochemistry, Göttingen University
 Bachelor Thesis: Department for Plant Molecular Biology and Physiology
 Title: "Establishment of a method to identify cysteine modifications using the SCL14 protein from <i>Arabidopsis thaliana</i> roots as an example"</p> |
| 2011 | <p>University Entrance Qualification
 Christian-von-Dohm Gymnasium Goslar, Graduation: Abitur</p> |

Publications

- Vollheyde K***, Yu D*, Hornung E, Herrfurth C, Feussner I. **2020**. The fifth WS/DGAT enzyme of the bacterium *Marinobacter aquaeolei* VT8. *Lipids* 55(5): 479-494.
- Zulu NN, Zienkiewicz K, **Vollheyde K**, Feussner I. **2018**. Current trends to comprehend lipid metabolism in diatoms. *Progress in Lipid Research* 70: 1-16.
- Zienkiewicz K, Zienkiewicz A, Poliner E, Du Z-Y, **Vollheyde K**, Herrfurth C, Marmon S, Farré EM, Feussner I, Benning C. **2017**. Nannochloropsis, a rich source of diacylglycerol acyltransferases for engineering of triacylglycerol content in different hosts. *Biotechnology for Biofuels* 10(1): 8.
- Zienkiewicz K, Du Z-Y, Ma W, **Vollheyde K**, Benning C. **2016**. Stress-induced neutral lipid biosynthesis in microalgae — Molecular, cellular and physiological insights. *Biochimica et Biophysica Acta (BBA) - Molecular and Cell Biology of Lipids* 1861(9, Part B): 1269-1281.
- Voget S, Díaz Valerio SM, von Hoyningen-Huene AJE, Natramilarasu PK, **Vollheyde K**, Xiao S, Daniel R. **2015**. Genome sequence of *Jannaschia aquimarina* GSW-M26, a member of the Roseobacter clade. *Genome announcements* 3(2): e00353-00315.

* shared first authors